THE POLYMERIZATION OF LACTIC ACID ANHYDROSULPHITE BY ANIONIC INITIATORS

LUKE RICHARD ADAMS

Doctor of Philosophy

THE UNIVERSITY OF ASTON IN BIRMINGHAM

August 1994

SUMMARY

The University of Aston in Birmingham

THE POLYMERIZATION OF LACTIC ACID ANHYDROSULPHITE BY ANIONIC INITIATORS

Luke Richard Adams

A thesis submitted for the degree of Doctor of Philosophy

1994

This thesis is primarily concerned with the synthesis and polymerization of 5-methyl-1, 3, 2-dioxathiolan-4-one-2-oxide (lactic acid anhydrosulphite (LAAS)) using anionic initiators under various conditions. Poly(lactic acid) is a biodegradable polymer which finds many uses in biomedical applications such as drug-delivery and wound-support systems. For such applications it is desirable to produce polymers having predictable molecular weight distributions and crystallinity. The use of anionic initiators offers a potential route to the creation of living polymers.

The synthesis of LAAS was achieved by means of an established route though the procedure was modified to some extent and a new method of purification of the monomer using copper oxides was introduced. Chromatographic purification methods were also examined but found to be ineffective. An unusual impurity was discovered in some syntheses and this was identified by means of ^{1}H and ^{13}C NMR, elemental analysis and GC-MS.

Since poly-α-esters having hydroxyl -bearing substituents might be expected to have high equilibrium water contents and hence low surface tension characteristics which might aid bio-compatibility, synthesis of gluconic acid anhydrosulphite was also attempted and the product characterised by ^{1}H and ^{13}C NMR.

The kinetics of the decomposition of lactic acid anhydrosulphite by lithium *tert*-butoxide in nitrobenzene has been examined by means of gas evolution measurements. The kinetics of the reaction with potassium *tert*-butoxide (and also *sec*-butyl lithium) in tetrahydrofuran has been studied using calorimetric techniques.

LAAS was block co-polymerized with styrene and also with 1,3-butadiene in tetrahydrofuran (in the latter case a statistical co-polymer was also produced).

Keywords

α-HYDROXY ACID, ANIONIC POLYMERIZATION, BIODEGRADABLE, POLY(LACTIC ACID), ANHYDROSULPHITE

DEDICATION

to Elaine.

ACKNOWLEDGEMENTS

My thanks go to Dr. Allan Amass for his advice and encouragement during the work

Also, the rest of the team:-
Val, Monali, Karine, Fred, Wendy, Robert and Dr's Dav and Marcia.
(may your solvents be dry and your glasses wet !)

my sponsors at DRA Dr.Eammon Colclough, Niall Shepherd and Hemant Desai.

the support staff at Aston, especially Roger, Lynne and Steve, Mike & Dave, Denise and Mike, and Dr.Mike Perry.

And the guys next door - Phil, Mike, Andy, Mark and Babs.

CONTENTS

CHAPTER ONE

INTRODUCTION

CHAPTER TWO

EXPERIMENTAL TECHNIQUES

CHAPTER THREE

MONOMER SYNTHESIS

CHAPTER FOUR

PRELIMINARY EXPERIMENTS

CHAPTER FIVE

DECOMPOSITION OF LACTIC ACID ANHYDROSULPHITE BY GROUP I METAL ALKOXIDES

CHAPTER SIX

COPOLYMERIZATION OF LACTIC ACID ANHYDROSULPHITE WITH STYRENE AND BUTADIENE INITIATED BY BUTYL LITHIUM

CHAPTER SEVEN

CONCLUSIONS

LIST OF FIGURES

LIST OF TABLES

CHAPTER ONE

INTRODUCTION

1.1 SYNTHETIC ROUTES TO α-HYDROXY ACID POLYMERS

1.1.1 Poly(lactic acid)

In recent years there has been great interest in the use of polymeric materials for specialist medical applications. Of particular value are biodegradable polymers, having found use as wound support and drug delivery systems. It is important that materials in such sensitive applications do not cause adverse tissue reactions (such as calcification) and so the choice of polymer is restricted to those with a high degree of biocompatibility. Since many of the materials still used as biomedical polymers were not originally designed for this application, they exhibit relatively low biocompatibility (e.g. methyl methacrylate). Therefore, by designing polymers for particular applications by modification of molecular architecture, copolymerization and blending, etc., there is considerable scope for improvements in the performance characteristics of biomaterials. Poly(lactic acid) is a well-known biodegradable polymer, its great advantage (as with other poly(α-hydroxy acids) being easy hydrolysis of the ester backbone in aqueous environments such as body fluids.

Despite the interest in poly(lactic acid) as a biodegradable polymer, there are comparatively few synthetic routes to poly-α-esters available (i.e. linear aliphatic structured polyesters having an ester repeat unit separated by only one main chain carbon atom). Under acid catalysis, lactic acid undergoes self-esterification to form a di-lactone, or lactide. The lactide may be polymerized in the melt with stannous octoate[1] (tin (II)-ethyl hexanoate), zinc[2], or zinc oxide[3] as catalyst, or by poly-condensation under nitrogen at 200°C for 8 - 12 hours[4]. A recent patent describes a variation on the latter technique for producing high molecular weight poly(lactic acid). Low molecular weight material is heated (under vacuum) to a temperature between the glass transition and melting temperatures of the polymer.[5]

Whilst these methods may be used to produce polymers based on lactic and glycolic acids, optimum conditions for polymerization have only briefly been studied.[6] Thus control is limited, yielding products of unpredictable molecular weights which may be discoloured and contaminated with degradation products.[7] Also, the techniques cannot be extended to di-substituted α-hydroxy acids, which will not undergo similar reaction (it is possible

to produce a co-polymer from mono-substituted and a symmetrically di-substituted glycollide, but at least fifty per cent must be of the former).[8]

Anhydrosulphites (and the related compounds, anhydrocarboxylates) are convenient intermediates to those polymers of α-hydroxy acids which might not otherwise be prepared. With suitable catalyst systems, it may be possible, under relatively mild conditions, to exert a high degree of control over the molecular architecture of the resultant products. In this way, the properties of poly(α-hydroxy acid) polymers might be tailored to suit the requirements of specific applications.

1.1.2 Development of Anhydrosulphite Chemistry

Anhydrosulphites (1,3,2-dioxathiolan-4-one 2-oxides) are moisture-sensitive, thermally-unstable, five-membered heterocyclics based upon α-hydroxy acids and prepared by the reaction of thionyl chloride in dry etheric solvent with either the parent acid (see figure 1.1) or its corresponding copper (II) salt.

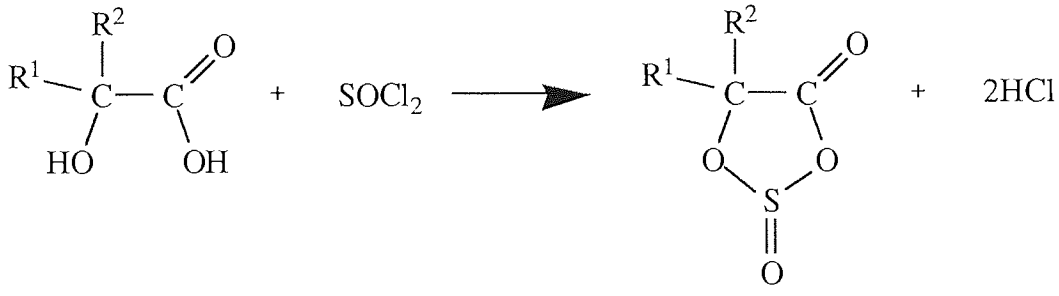

Figure 1.1 General synthesis of anhydrosulphite.

The first such compounds were prepared in 1922 by Blaise and Montagne, who were attempting the synthesis of the chlorosulphinate of hydroxy iso-butyric acid (R^1 = H, R^2 = CH_3). They found that when heated, the product released sulphur dioxide, leaving a polymeric residue.[9]

No further work was published until 1957 when Du Pont published a patent which showed that high molecular weight polymer might be produced when an anhydrosulphite (HBAS) is refluxed in a dry aromatic solvent.[10]

Rose and Warren[11] attempted to extend the range of anhydrosulphites for which synthetic routes were available with syntheses of anhydrosulphites with alkyl, chlorinated and

cyclo-alkyl α-substituents. They were only successful in obtaining high molecular weight polymer from the α-hydroxy iso-butyric anhydrosulphite, probably because this member of the class is one of the few which may be rendered sufficiently pure for polymerization, by means of distillation alone.

1.1.2.1 Monomer Synthesis

Ballard and Tighe[12] developed the use of α-hydroxy acid copper (II) salts as a means of producing anhydrosulphites, thereby increasing the number of monomers which might be prepared considerably. However, some α-hydroxy acids (especially those with functionalised substituents) have been found to be unsuitable for conversion to the relevant anhydrosulphite.

It has not been possible to prepare the malic acid anhydrosulphite due to a preferential dehydration which occurs under (anhydrous) reaction conditions[13] (see figure 1.2). The alternative synthetic route was not utilised due to the difficulty of leaving one carboxyl selectively unreacted when preparing the copper (II) salt.

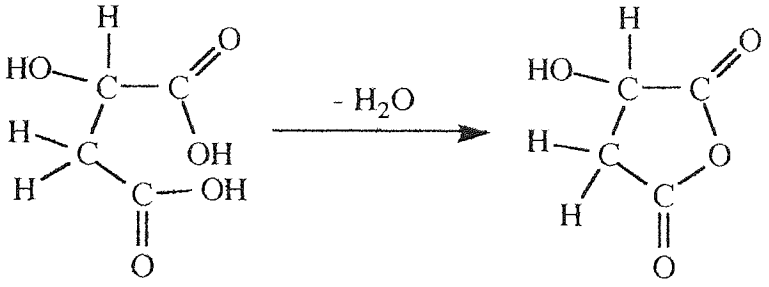

Figure 1.2 Preferential dehydration reaction of malic acid.

Al-Mesfer showed that carboxyl-functionalised polymers might be produced from anhydrosulphites using tartronic acid as a starting material.[14] Synthesis of lactobionic acid anhydrosulphite has also been attempted using the silver salt but the product was difficult to purify and only an ester carbonyl at 1740 cm^{-1} was observed.[33] This was perhaps due to the reaction of substituent hydroxyl groups with the ring.

Table 1.1 shows the range of anhydrosulphites which have been prepared to date, using either the parent α-hydroxy acid or its copper (II) salt. R^1 and R^2 refer to the α-substituents on the acid (as shown in figure 1.1).

Table 1.1 Anhydrosulphites for which a synthetic route exists.

R^1	R^2	parent α-hydroxy acid	ref.
H	H	glycolic	15
H	CH_3	lactic	12
CH_3	CH_3	α-hydroxy iso-butyric	16
CH_3	C_2H_5	α-methyl α-hydroxy-butanoic	17
C_2H_5	C_2H_5	α-ethyl α-hydroxy-butanoic	18
n-C_3H_7	*n*-C_3H_7	α-propyl α-hydroxy-valeric	18
n-C_4H_9	*n*-C_4H_9	α-butyl α-hydroxy-hexanoic	18
CH_3	*n*-C_3H_7	α-methyl α-hydroxy-valeric	19
CH_3	*n*-C_4H_9	α-methyl α-hydroxy-hexanoic	17
CH_3	*n*-C_6H_{13}	α-methyl α-hydroxy-octanoic	17
CH_3	*n*-C_8H_{17}	α-methyl α-hydroxy-decanoic	17
CH_3	*sec*-C_3H_7	α-hydroxy iso-valeric	19
CH_3	CH_2Cl	α-hydroxy chloro-iso-butyric	20
CH_2Cl	CH_2Cl	α-bis-chloromethyl α-hydroxy acetic	21
H	C_6H_5	benzilic	22
CH_3	C_6H_5	α-phenyl α-hydroxy-propanoic	24
C_6H_5	C_6H_5	mandelic	22
--(--CH_2--)3--		cyclobutane α-hydroxy-carboxylic	23
--(--CH_2--)4--		cyclopentane α-hydroxy-carboxylic	23
--(--CH_2--)5--		cyclohexane α-hydroxy-carboxylic	23
--(--CH_2--)6--		cycloheptane α-hydroxy-carboxylic	23
H	COOH	tartronic	14
CH_3	C_6F_5	α-pentafluorophenylα-hydroxy-propanoic	24

A general synthetic procedure based on that proposed by Rose and Warren[11] is described by Blackbourn and Tighe.[25]

1.1.2.1 Initiator Systems

Tighe *et al* published a series of papers studying the effects of structural factors (such as the nature of the α-substituents) upon anhydrosulphite reactivity.[12,15-19,22,23] The

mechanisms of thermally-induced polymerizations were studied, along with those of polymerizations initiated by tertiary amines and hydroxylic compounds.

Inoue[26] *et al* published evidence that asymmetrically-selective polymerization was possible using brucine (an optically-active tertiary amine). The same researchers[27] also briefly tested a number of organometallic initiators including aluminium, lithium, magnesium and zinc compounds but found that only *n*-butyl lithium or diethyl zinc/water caused even partial conversion of HBAS to polymer. The effectiveness of the latter initiator system must be queried as anhydrosulphites are readily hydrolysed by water.

In a further paper[28], the co-polymerization of HBAS in acrylonitrile and methacrylonitrile at 80°C in the presence of a free radical source, is described. In similar reactions with styrene, vinyl chloride and methyl methacrylate, however, only homo-polymers were formed.

Anhydrosulphites have been co-polymerized with the structurally similar N-carboxy-anhydrides to produce poly(depsi-peptides), an interesting class of polymer with potential applications as a biocompatible material[29]. Other synthetic routes are available to these co-polymers but require rather severe reaction conditions.[30] A recent paper describing a preparation of a poly(depsi-peptide) with lactic acid anhydrocarboxylate reports that only low molecular weight material was obtained.[31]

Several previous theses have included work using alkoxides[32,33] and bimetallic oxo-alkoxides[34] as initiators. However, in the latter case, no evidence of 'living' character was observed when LAAS (lactic acid anhydrosulphite) or GAAS (glycolic acid anhydrosulphite)were polymerized and experiments with simple alkoxides have not been performed using these monomers.

1.2 RING-OPENING POLYMERIZATION

1.2.1 Factors Governing Ring-opening Polymerizations

Whilst external influences such as reaction temperature, the presence of initiators and solvent type affect the polymerization of heterocyclics considerably, there is an inherent thermodynamic 'driving-force' toward ring-opening due to the additional rotational degree of freedom possessed by the chain form. The intrinsic 'polymerizability' of a particular heterocyclic molecule is affected by a number of factors:-

(1) the ability to replicate the attacking species,
(2) the ring size, strain and stability,
(3) the nature, size and number of substituents, and
(4) the nature and reactivity of hetero-atom(s) and functional groups.

It is well-known that ring-strain plays a considerably important role in the polymerization of heterocyclic monomers. Ring-strain exists for a number of reasons. In a ring composed of a certain number of atoms, a finite number of conformations will be available, which places a restriction upon the bond angles which can be adopted. The ring sizes with lowest energy will be those which allow the bond angles of the constituent atoms to be closest to their 'ideal' values, hence five- and six-membered rings will tend to be more stable than three- or four-membered.

The size and nature of the hetero-groups present also affects the bond angles and lengths, which in turn, contribute to ring-strain, the number of possible conformations being restricted by the presence of substituents on the ring, which interact sterically with one another. Small[35] suggests that the contribution from hetero-groups such as -C-O-C- or -C-NH-C- is not significant, since their bond angles and lengths are little different to those of a methylene group. However, if functionalised groups are present, the effect becomes much more marked, as such species as carbonyl or sulphoxide groups will tend toward bond angles significantly different from those of a methylene group. Altogether, these effects create a situation in which the ring is unable to adopt the most thermodynamically-stable position. Instead, the conformations which minimise the contributions of bond-strain, non-bonded interactions and angle-strain will be adopted, increasing the internal energy of the system.

In the case of the cyclic ethers, the five-membered ring will polymerize where the six-membered will not, since this is the ring-size which allows the ring-members to adopt the most 'comfortable' angular conformations. If a functional group is introduced into the ring, the stability of the ring is affected such that, in the case of lactones, the six-membered ring will polymerize where the five-membered ring will not.[36]

In most ring-opening polymerizations (e.g. lactones, lactams, epoxides, etc.) an equilibrium exists between the ring and chain forms (as shown in figure 1.3). This has the effect of making complete conversion to polymer difficult and sets a 'ceiling temperature'[37] above which the equilibrium shifts toward the left and de-polymerization predominates.

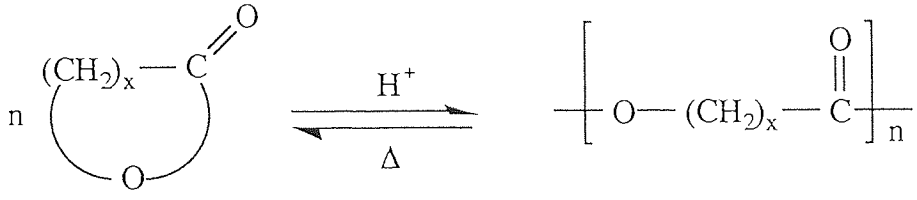

Figure 1.3 Ring-chain equilibrium.

Dainton and Ivin[38] explained the existence of a ceiling temperature in thermodynamic terms, relating it to the free energy of polymerization for the reaction. For reaction to occur, the free energy must be negative. The free energy of a reaction can be related to entropy and enthalpy as :-

$$\Delta G = \Delta H - T_C.\Delta S \qquad (1)$$

where :-

ΔG = free energy of reaction,

ΔH = enthalpy of reaction,

T_C = ceiling temperature, and

ΔS = entropy of reaction.

From equation (1) it may be shown that for ΔG to be negative, the following condition must be satisfied :-

$$|\Delta H| > |T_C.\Delta S| \qquad (2)$$

Therefore, polymerization will be favoured where the enthalpy and entropy are negative and positive, respectively. Also, the ceiling temperature can be defined as that temperature at which the free energy of polymerization, ΔG, passes from negative to positive. Thus the equation may be rearranged to define the ceiling temperature as :-

$$T_C = \Delta H/\Delta S \qquad (3)$$

It should be understood, however, that the anhydrosulphites belong to a class of ring-opening polymerizations in which such equilibria do not occur. Reactions which fall into this class are termed 'Extrusion' polymerizations[39] and their particular characteristics are discussed in section 1.2.2.

1.2.2 Extrusion Polymerizations

Extrusion polymerizations are irreversible and consequently there can be no ring-chain equilibrium, and thus no tendency toward depolymerization to the monomer (though other forms of depolymerization may not be excluded e.g. hydrolysis to parent acid). Because of this, complete conversion from monomer to polymer is possible, even at elevated temperatures.

These reactions are unusual in that they exhibit features common to both 'condensation' and 'addition' polymerizations. They are defined as ring-opening polymerizations where a small molecule is eliminated from the ring (as in a 'condensation' polymerization) but the reaction proceeds by successive additions of repeat units (as in an 'addition' polymerization).

Many of the compounds that undergo 'extrusion' polymerization have a characteristic structure and may be prepared by means of the reaction shown in figure 1.4.

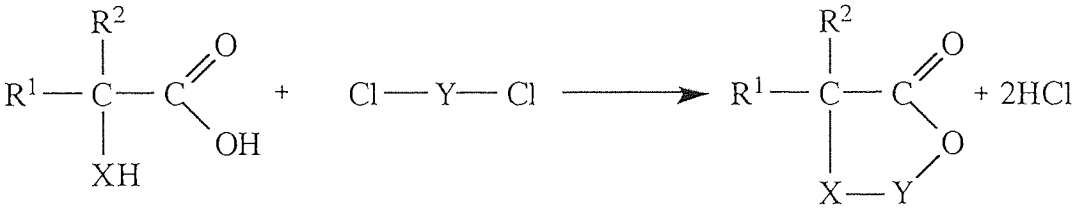

where:-

X	= CH_2, NH, O, S, Se, NR_3
Y	= CO, SO, SeO, CS, CSe
R^1 and R^2	= H, alkyl, aryl, chloro-alkyl, etc.

Figure 1.4 General synthesis of heterocyclics undergoing 'extrusion'.

Based on this scheme, compounds such as anhydrocarboxylates, anhydrosulphites and thio-α-hydroxy acid variants have been prepared, and used to produce numerous poly-α-

esters and poly-α-thio-esters, etc. The reactivity of the compounds comprising this group obey certain general rules regarding their reactivity but there are distinct differences due to the hetero-atoms in the ring and α–substituents. One member of this class of monomers, the N-carboxy anhydrides, has been studied extensively and is valuable as it offers a route to the synthesis of poly-peptides, which may be used to produce artificial silk fibres.

1.2.3 Anionic Polymerization

Monomers with strong electronegative groups or highly de-localised double bonds e.g. styrene, methyl methacrylate can be polymerized by initiators such as metal alkyls and amides. The initiation reaction is a nucleophilic addition across the carbon-carbon double bond, creating a carbanion, which subsequently attacks other monomer molecules in a similar manner. The reaction is termed anionic because the propagating species is negatively charged, thus it will undergo all the typical reactions of anions. This means that all traces of reactive species such as water must be removed from the reaction medium as they will destroy the propagating centre.

Figure 1.5 shows the potassium amide-initiated polymerization of styrene, one of the first anionic polymerizations to be studied in detail.[40] The reaction is conducted at low temperature in liquid ammonia, a highly polar solvent. Potassium amide dissociates into its constituent ions and the anion formed adds to the monomer carbon-carbon double bond, creating an propagating chain.

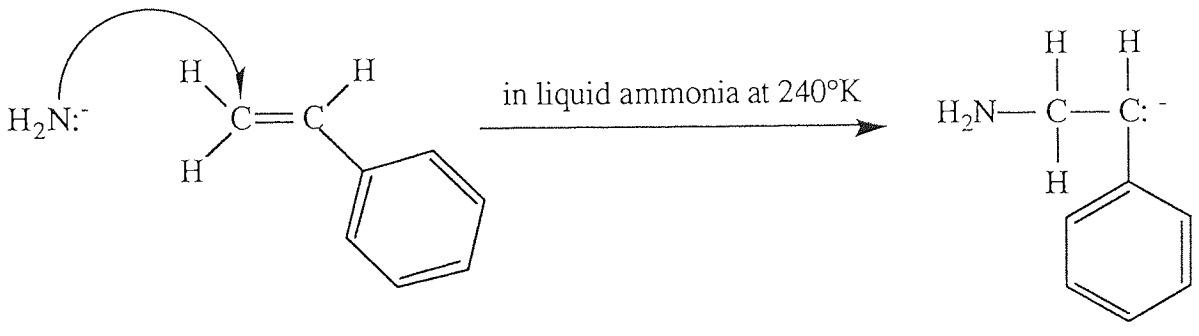

Figure 1.5 Initiation of styrene polymerization by potassium amide.

Ziegler *et al* [41] identified that anionic polymerizations have no intrinsic termination step. The absence of this stage in a polymerization mechanism has significant implications for the synthetic utility of such reactions. Polymerizations in which there is no termination

step may be described as 'living'.[42] If external terminating agents are excluded from the reaction, the propagating species will remain active after all the monomer present is consumed. If additional monomer is added, propagation will continue. If that monomer is of a different type to the original, block copolymers can be created. Addition of specially selected terminating agents to living polymers can be used in order to prepare terminally functionalised polymers e.g. carbon dioxide creates carboxyl groups.

Anionic polymerization reaction rates are less affected by temperature than those of cationic polymerizations, but the rates also depend upon :-

(1) the dielectric constant of the solvent,
(2) the degree of solvation of the counter-ion,
(3) the electronegativity of the counter-ion, and
(4) the nature of the carbanion.

Unlike free-radical polymerizations (in which the solvent's dielectric constant has little effect on the rate of propagation) the propagating chains in an anionic polymerization may exist in a number of forms. These range from aggregated molecules to free solvated ions (see figure 1.6) depending upon the nature of the medium. In a polar solvent (e.g. tetrahydrofuran, dielectric constant = 7.6) the equilibrium is shifted toward the right, favouring dissociated species. In a non-polar solvent (e.g. hexane, dielectric constant = 1.9) the formation of contact ion pairs and aggregates of covalent structures is favoured (e.g. lithium *tert*-butoxide is thought to be hexameric in hexane[43] and benzene).[44]

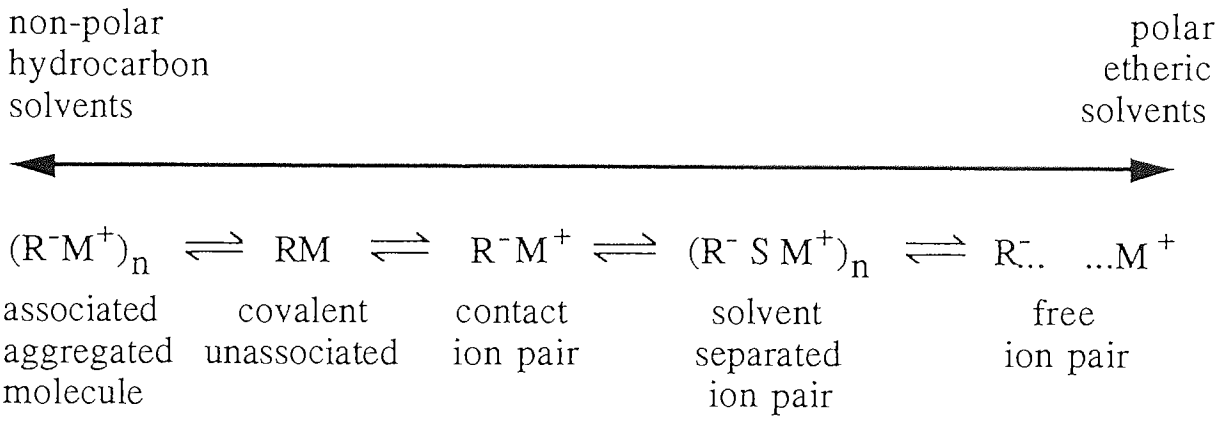

Figure 1.6 Effect of solvent polarity on nature of propagating species.

Since free ions react with the monomer much faster than ion pairs and covalent structures, rates of propagation may differ greatly depending upon the nature of the solvent used. Interconversion between the contact ion pairs, solvent-separated ion pairs and free ions is

very rapid and this means that, statistically, each propagating chain must exist in all forms at different times during its lifetime, resulting in an 'averaging-out' of the rate of propagation and the production of a narrow molecular weight distribution polymer. In fact, there will be a tendency for the polydispersity to become closer to unity as chain-length increases.

If, in a reaction with no termination reactions, initiation is fast relative to propagation, then the molecular weight distribution of the polymeric product will be narrow. This is because the formation of propagating species occurs over a short period of time. There is an equal chance of adding monomer to each propagating end and so they grow at the same rate (nb. this also means that the number average molecular weight will increase linearly with conversion of monomer to polymer).

In a polar solvent, the initiator may exist predominantly as free ions and solvent-separated ion pairs, causing rapid initiation and consequently a low polydispersity. In a non-polar solvent, the initiator will tend to exist as an aggregate, therefore initiation may be very slow and the build-up of living ends may take a significant period of time. This means that in such a reaction, the polymer will have a broader molecular weight distribution than the product of a similar reaction in a polar solvent.

The degree of dissociation is also affected by the nature of the counter-ion. The polymerization of styrene in tetrahydrofuran is faster with lithium rather than potassium as the counter-ion. The small lithium ion can be solvated to a greater extent than the larger potassium and the propagation rate is increased because of the higher proportion of living ends existing as free ions rather than ion pairs.

The initiation of styrene by *sec*-butyl lithium in benzene is ten times faster than by *n*-butyl lithium in the same solvent.[45] There may be some contribution to this effect from intrinsic differences in reactivity but it is likely that steric factors are most important. The *sec*-isomer is more bulky than the *n*-isomer so aggregation of initiator molecules is inhibited and the equilibrium concentration of monomeric initiator increased.

1.3 REACTIVITY OF ANHYDROSULPHITES

1.3.1 Thermal Polymerization

Anhydrosulphites decompose thermally more easily than the structurally-similar anhydrocarboxylates because of the added ring-strain imposed by the sulphur atom. Being much larger than a carbonyl, the sulphoxide group is forced out of the plane of the

ring distorting it into a non-planar form (this also affects the nuclear magnetic resonance spectra, as discussed in section 3.1.6.2).

Thermal decomposition occurs by means of an initial ring-contraction, with simultaneous expulsion of sulphur dioxide, to form the α-lactone. This unstable intermediate reacts rapidly with trace nucleophiles to produce a propagating species, as shown in figure 1.7.

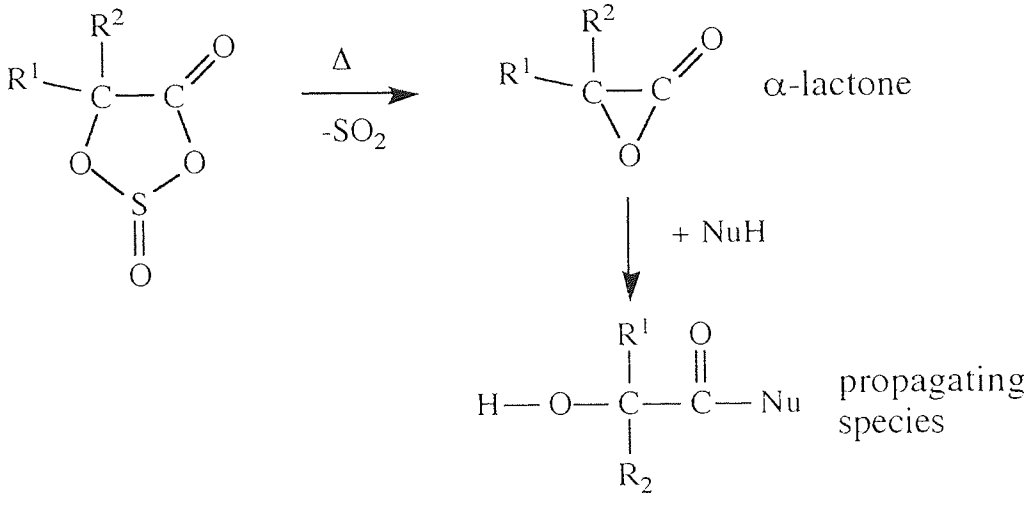

(where NuH = trace nucleophile e.g. moisture).

Figure 1.7 Thermal polymerization mechanism.

The decomposed α-lactone continues chain-growth by attack on other α-lactones by way of the terminal hydroxyl.

1.3.2 Effects of α–Substituents on Thermal Decomposition

The thermal decomposition rates of a number of di-alkyl substituted anhydrosulphites were studied by Blackbourn (see figure 1.8).[18]

It was found that the effect of increasing the chain length of the *n*-alkyl α-substituents was to increase the rate of thermal decomposition up to a plateau after the di-ethyl substituted anhydrosulphite. This is thought to be due to the Thorpe-Ingold effect, whereby, as the bond-angle between the substituents is increased by repulsion between them, a compressive strain is transmitted to the ring, reducing its stability. The effect of

increasing chain length becomes less marked as the increase in bond angle reaches a maximum.

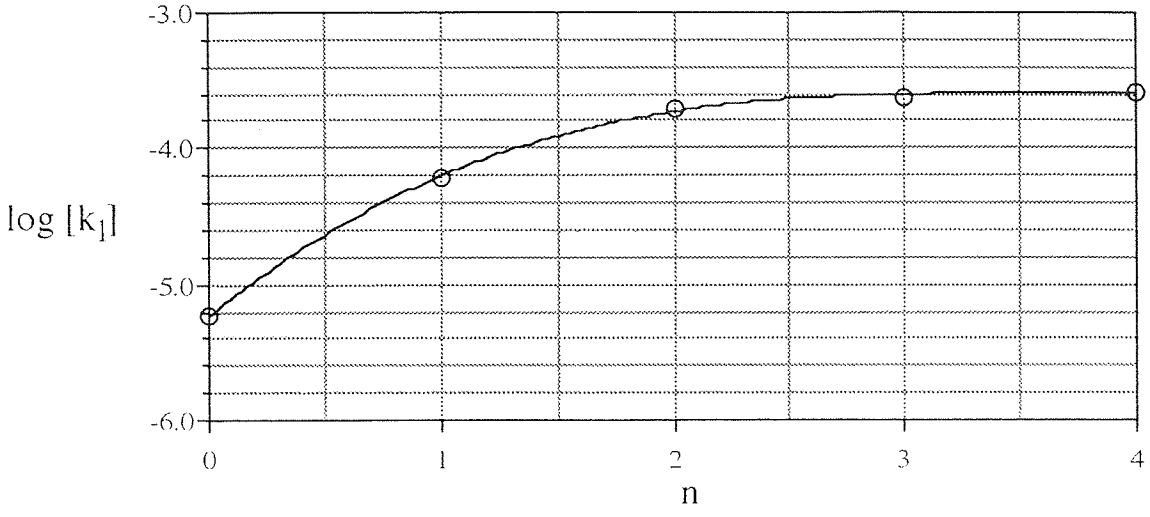

Figure 1.8 Effects of di-alkyl substitution (where R^1=R^2=C_nH_{2n+1}) on rates of thermal decomposition of anhydrosulphites.

In a similar study, Crowe[17] studied the effect of changing the size of only one of the substituents, while holding the other constant (i.e. R^1 = Me, R^2 = Me, Et, *n*-Prop, *n*-But, *n*-Pent). A similar trend to that of the symmetrically-substituted series was observed up to the R^1 = Me, R^2 = *n*-But substituted anhydrosulphite (see figure 1.9). Higher members of this series exhibited greater thermal stability.

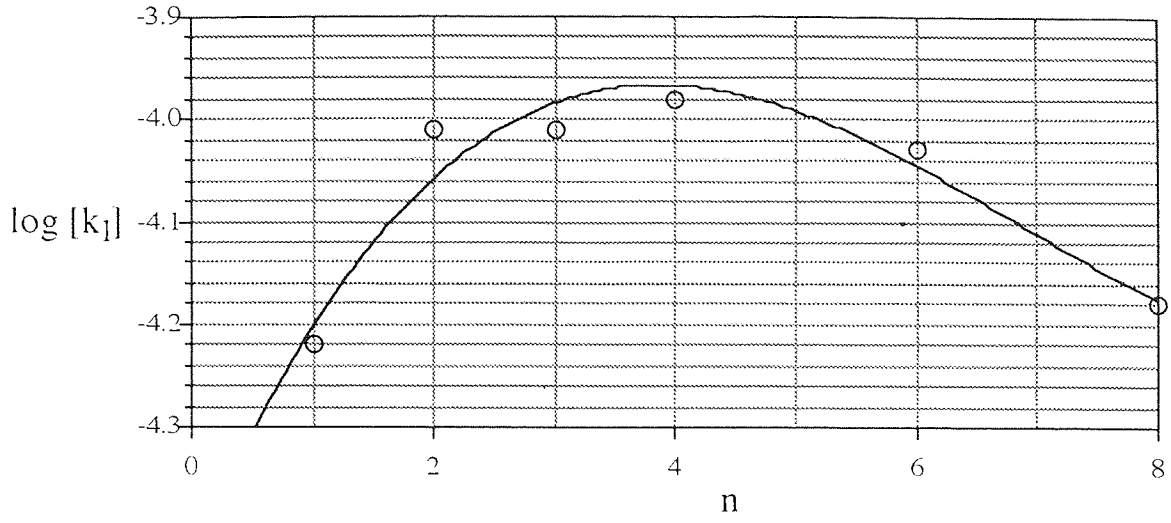

Figure 1.9 Effects of mono-alkyl substitution (where $R^1 = CH_3$ and $R^2 = C_nH_{2n+1}$) on rates of thermal decomposition of anhydrosulphites.

It was suggested that this effect is caused by the longer chains 'doubling-back' over the ring (as shown in figure 1.10), thereby restricting the sulphur dioxide from leaving.

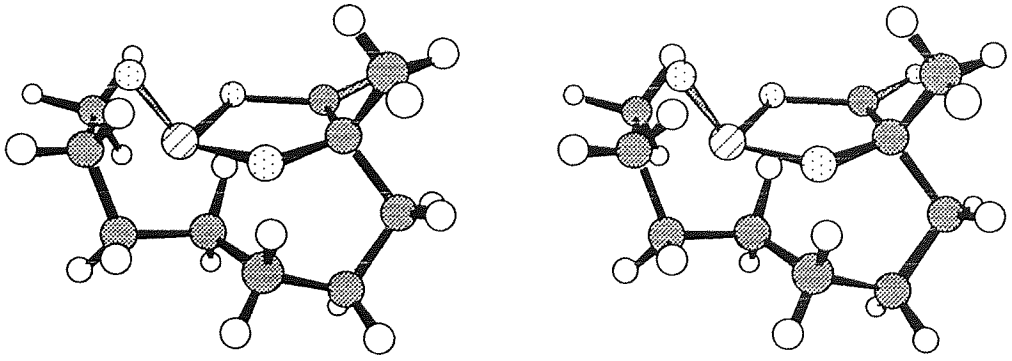

Carbon Hydrogen Oxygen Sulphur

(where the α-substituents are $R^1 = CH_3$ and $R^2 = C_7H_{15}$)

Figure 1.10 Stereo plot showing sulphoxide obstruction by long alkyl side chain.

In the case of spiro-alkyl substituents,[2 3] steric and ring-strain effects again provide the main contributions to thermal stability. A minimum is observed (see figure 1.11) with the cyclopentyl-substituted anhydrosulphite being the most stable. By analogy with

cyclohexane, the six-membered ring provides the most energetically-favourable bond-angle.

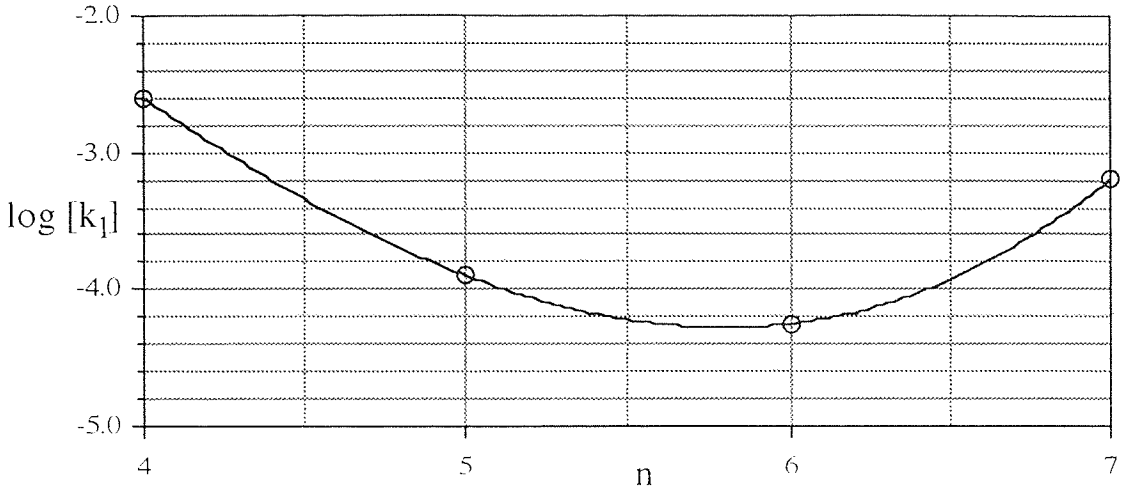

Figure 1.11 Effects of spiro-alkyl substitution (where the α-substituent is -(-CH_2-)$_n$-) on rates of thermal decomposition of anhydrosulphites.

The thermal polymerization (and distillation) of some anhydrosulphites is complicated by a competitive decomposition process leading to non-polymeric products (see figure 1.12). This secondary process is favoured by bulky or electron-withdrawing α-substituents.[22] The products of this reaction are a ketone, carbon monoxide and sulphur dioxide.

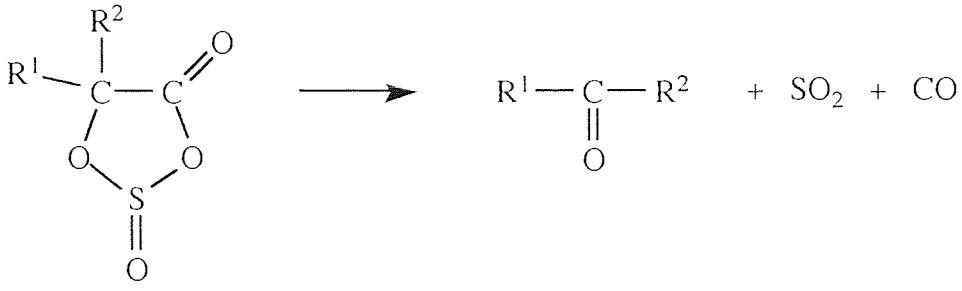

Figure 1.12 Non-polymer forming thermal decomposition.

1.3.3 Protonic Nucleophile initiated Polymerization

The reaction of anhydrosulphites with protonic nucleophiles e.g. primary and secondary amines and alcohols, is analogous to the situation with N-carboxy anhydrides. The mechanism proposed by Tighe *et al* [12] is shown in figure 1.13.

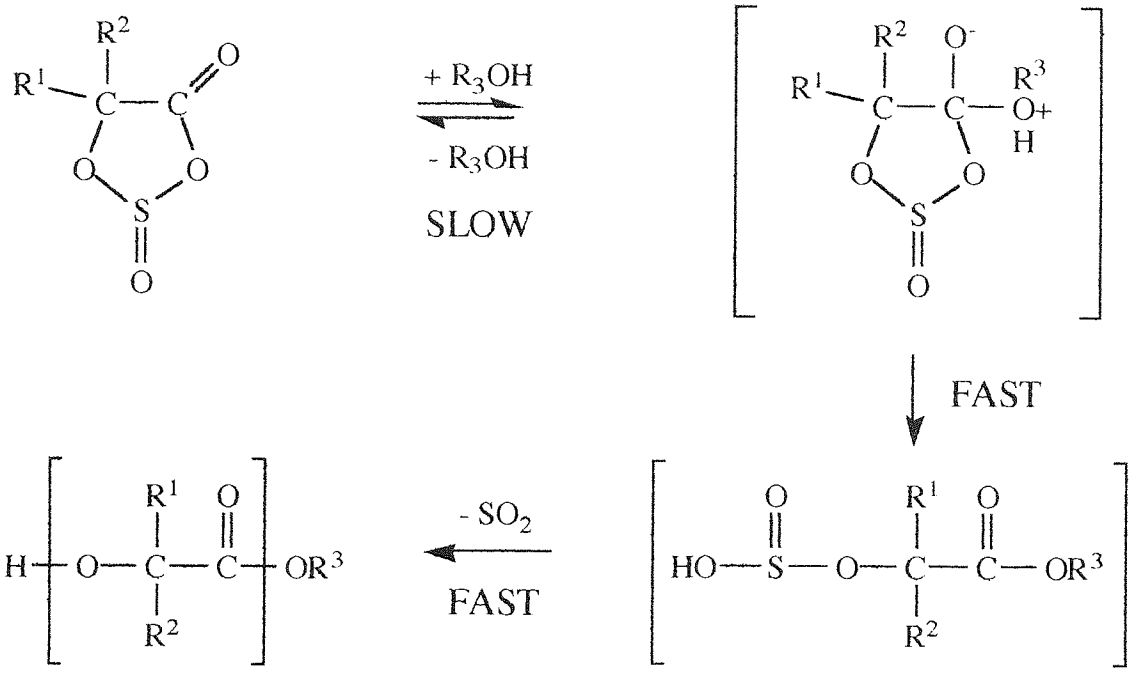

(Where R3OH = tertiary alcohol).

Figure 1.13 Hydroxylic nucleophile-initiated decomposition.

Initiation occurs by direct nucleophilic attack on the C-4 carbonyl, forming a polar transition state which decomposes rapidly with evolution of sulphur dioxide. Propagation occurs via further attack on anhydrosulphite by the nucleophilic chain end. As attack on the carbonyl is the slowest (and therefore rate-determining) step, the rate of polymerization depends greatly upon the nucleophilicity of the attacking group and steric hindrance by the C-5 substituents. As the nucleophilicity of the terminal hydroxy group is low compared to that of an amine, rates of propagation will be slower than those of N-carboxy anhydrides.

1.3.4 Aprotic Nucleophile initiated Polymerization

Anhydrosulphite polymerization may also be initiated by aprotic bases. Initiators which have been studied include tertiary amines e.g. pyridine and strong bases e.g. alkoxides. A

mechanism for polymerization by tertiary amines has been suggested where attack occurs upon the C-5 carbonyl, forming an unstable complex (see figure 1.14).

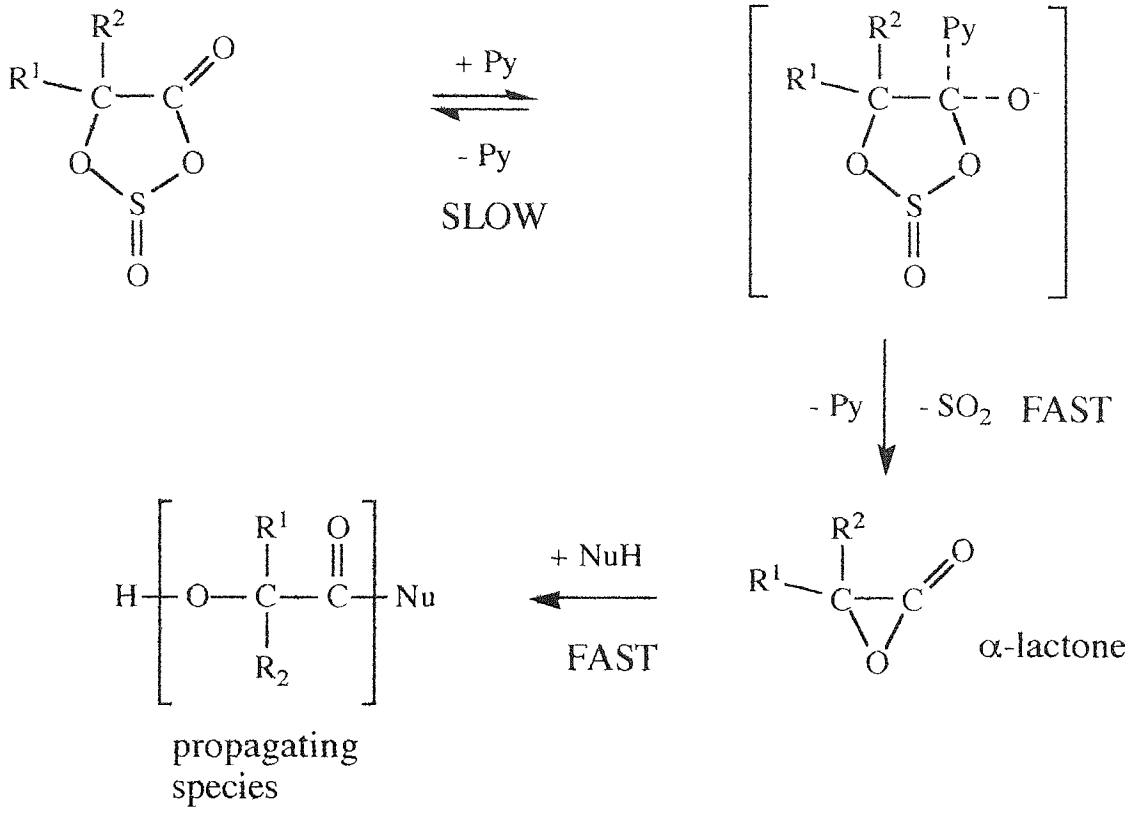

(Where Py = pyridine and NuH = available nucleophiles).

Figure 1.14 Tertiary base-initiated decomposition.

This complex rapidly decomposes, forming a reactive α-lactone by expulsion of sulphur dioxide. Whilst this route has been of some utility in polymerizing anhydrocarboxylates, products of anhydrosulphite decomposition tend to be of lower molecular weight. Other aprotic tertiary bases which have been used to polymerize anhydrosulphites and related heterocyclics include triethylamine, dimethyl-formamide and dimethyl-acetamide.[20]

Alkoxides have been seen to be effective in polymerizing a number of ring systems. The polymerization of lactones, which proceeds by nucleophilic attack, results in cleavage of the ring at an acyl oxygen. However, such polymerizations require relatively high temperatures for reactions to occur at reasonable rates. In the case of alkoxide-initiated decomposition, the situation is more complex than the mechanisms previously discussed. The mechanism is thought to be a multi-stage process involving a number of routes (some

of which are non-polymer-forming). The subject is discussed in greater detail in chapter five.

1.3.5 Effects of α-Substituents on Rates of Initiated Decomposition

The nature of the α-substituents exerts a marked effect upon the mechanism of polymerization of an anhydrosulphite. In the absence of suitable initiator species, decomposition via the thermal mechanism will occur at a rate dependent upon substituents and temperature. However, if both substituents are bulky, the thermal route may predominate even when initiators are present. This is due to steric interference, as the large α-substituents hinder attack on the carbonyl whilst increasing ring-strain and thereby promoting thermal decomposition.

This effect is illustrated by comparison of the rates of initiated decomposition of un-, singly- and di-substituted anhydrosulphites (see table 1.2).

Table 1.2 Steric and electronic effects on rates of initiated decomposition.

Anhydrosulphite	R^1	R^2	rate x 10^6/l.mol^{-1}.s^{-1}
GAAS	H	H	370
LAAS	H	CH_3	85
HBAS	CH_3	CH_3	<0.05
-	CH_2Cl	CH_2Cl	2
MAAS	H	C_6H_5	1100
BAAS	C_6H_5	C_6H_5	<0.02

(measured in benzyl alcohol at 90°C. source: ref.**46**).

Table 1.2 also shows the effect of electron-withdrawing substituents on the rate of initiated decomposition. Electron-withdrawing substituents activate the carbonyl group, increasing the rate of decomposition. The rate of initiated decomposition of the chloro-methyl di-substituted anhydrosulphite is much greater than that of HBAS. However, while the rate of thermal decomposition of benzyl-substituted MAAS is greater than that of the alkyl-substituted anhydrosulphites, the rate at which BAAS decomposes is comparatively low. This is due to the fact that while the benzene rings activate the carbonyl, they are also bulky and hinder attack. In conclusion, it seems that while

electronic effects are observed, steric considerations have most influence on rates of initiated decomposition.

1.4 APPLICATIONS OF POLY(LACTIC ACID)

Apart from the limited number of synthetic routes, one of the reasons poly-α-esters are not so widely used as other polyesters is that they are relatively easily hydrolysed. However, this property makes them increasingly useful in certain applications.

It has been mentioned that poly(lactic acid) is a 'biodegradable' polymer. Two of the main areas where such materials may be valuable are those of biomedicine and disposable packaging.

1.4.1 Biodegradable Packaging

In the UK alone, 2 million tonnes of plastic products were consumed in 1990, of which over half was packaging material. In that year, only 2% of post-use waste plastic was re-cycled.[47] The time required for decomposition of most commodity plastics greatly exceeds their useful lifetimes as packaging materials but incineration is expensive and creates pollutant by-products, so thousands of tons are committed to landfill sites every year. It is theoretically possible for a single tonne of landfill waste to produce over 200 cubic metres of methane which may be collected and used to generate electricity.[48]

The need for degradable plastic materials is clear; whilst poly(lactic acid) and similar biodegradable plastics are far too expensive to completely replace less environmentally-friendly materials, and indeed may not meet performance requirements anyway, they do have a place in reducing the environmental impact of waste polymeric materials. Such polymers may be incorporated into plastics by means of copolymerization or blending so that even in very low concentration they might increase significantly the rate of degradation.

1.4.2 Biomedical Applications

In the sixties, poly(lactic acid) began to be used as a material for the manufacture of absorbable sutures, either on its own or in combination with poly(glycolic acid). It was found to be more biocompatible than catgut, causing less tissue reaction. Since then, it

has been used in many similar biomedical applications e.g. wound supports, ligating clips and bone-plates and screws.[49] In such applications, the main considerations are that the material used should remain intact and functional long enough to perform its intended task; once this is done, the material should decompose, producing only substances which may be processed by the body's metabolic system.

Poly(lactic acid) is well-suited to this task as it degrades to lactic acid, which is a natural product of muscle contraction in the presence of an inadequate supply of oxygen and is easily converted into carbon dioxide and water by the body via the tricarboxylic acid cycle, or is excreted by the kidneys.[50]

For wound-support applications, a highly-porous polymer matrix is necessary for rapid tissue regeneration. A large surface area of adhesive polymer substrate is needed for adequate cell seeding and growth. Such materials can be created using poly(lactic acid) treated with super-critical fluids to produce foams[51] which may be treated with growth-promoting pharmaceuticals or shaped to the dimensions required for implantation.[52]

If the aim is to produce a drug delivery system, rather than simply a wound fixation/support system, the situation is much more complex: When a conventional drug delivery method is used (i.e. tablet, injection, etc.) plasma levels of the drug are initially raised but decrease rapidly as the drug is metabolised. The aim of a polymeric drug delivery system is (usually) to administer a more even dose over a long period of time, keeping plasma levels of administered pharmaceutical within an optimum range. In order to fulfil this objective, the delivery system must be reliable, releasing the drug constantly at a pre-determined rate. poly(lactic acid) has been used successfully for a wide range of drug delivery applications, including systems designed to aid individuals in withdrawal from nicotine addiction.[53]

poly(lactic acid) is an ideal material for use in novel drug delivery systems: when used as a coating film for a granular drug combined with a swelling agent e.g. gelatin, the polymer allows moisture to diffuse into the core of the coated particles so that the swelling agent can burst the coating, releasing the drug. The quantity of swelling agent can be varied in order to burst the coating after a specific period of time.[54] Another novel system combines poly(lactic acid)/poly(glycolic acid) copolymer with a biocompatible solvent to produce a syringeable, in-situ forming solid implant for animals.[55]

Drug 'targetting' is another objective which may be achieved by polymeric systems. This may be done by simply inserting a polymer 'slug' containing the drug into the site (this method has been used successfully in the treatment of certain cancers).[56] The medication simply diffuses out of the implant over a period of time, as the polymer binder

decomposes. Alternatively, a more sophisticated system might involve attaching drug molecules to a polymer back-bone via side-groups. The bonds would only be cleaved, releasing the drug under certain conditions, e.g. by a certain enzyme present in one part of the body.

Poly(α-hydroxy acids) can be used to combine wound-support and drug delivery/targetting functions in one implant. Such systems have potential for promotion of osseous regeneration *in vivo*, by impregnating the polymer bone-plate with a bone-derived growth factor.[57]

It is worthwhile noting that price represents little obstacle to the use of biodegradable polymers in biomedical devices, as the expenditure upon the surgical procedure alone, far outweighs the cost of the polymeric device implanted. This has been shown to be the case in the field of contact lens manufacture, as gas-permeable hard lens materials replace conventional poly(methyl methacrylate) despite vastly higher basic costs.[58]

1.4.3 Influences on Rates of Polymer Degradation

Obviously, control over factors which influence rates of degradation *in vivo* is vital in order to produce reliable products with consistently predictable characteristics. The mechanism by which poly(α-hydroxy acids) like poly(lactic acid) and poly(glycolic acid) degrade can be seen as a simple hydrolysis of the ester back-bone in aqueous media such as body fluids but the mode *in vivo* is certainly complex as decomposition is affected by a number of variables.

The factors which affect the rate of polymer degradation are inter-dependent to a certain extent, e.g. stereo-regularity and crystallinity, but they may be summarised as:-

(1) molecular weight, structure and distribution,
(2) stereo-regularity and crystallinity,
(3) processing effects (melt pressing, annealing, sterilisation, etc.),
(4) physical conditions (pH, temperature, tonicity, etc.), and
(5) biochemical environment (exposure to enzymes, fungi, etc.).

There is some evidence to suggest that degradation *in vivo* of low molecular weight poly(lactic acid) material is more rapid than of equivalent high molecular weight polymer.[1,2]

The chirality of lactic acid leads to an inherent high stereo-regularity in the corresponding polymer chain. However, if poly(lactic acid) is subjected to a thermal process, e.g. melt-

pressing, the resulting product solidifies on cooling to an amorphous, glassy substance. Crystallisation may be induced by nucleation or annealing but is nonetheless very slow. Pistner[1] *et al* found that hydrolysis occurs by random scission of ester bonds along the chain in the amorphous polymer, leading to a uniform decay of molecular weight distribution but in partially-crystalline samples, the amorphous regions are degraded preferentially because of their higher hydrophilicity. This gives rise to a multi-modal molecular weight distribution and an overall increase in crystallinity.

While the hydrophobicity of amorphous poly(lactic acid) has the effect of retarding decomposition, the situation is complicated by the nature of the polymer surface. It is known that 'as-polymerized' poly(lactic acid) is micro-porous,[49] allowing water to penetrate, and degradation products to leave the polymer more easily than through the relatively sealed surface and tight internal structure of thermally-treated polymer.

Reed and Gilding[59] studied the effects of pH on the *in vitro* degradation of poly(glycolic) and poly(lactic acid) homo- and co-polymers, finding that, in contrast to homo-poly(glycolic acid), decomposition rates of poly(lactic acid) and co-polymers were not significantly different in the range of pH 5 to pH 9. Rates of decomposition were considered to be more dependent on hydrophobic/hydrophilic balance and crystallinity of the polymers. By co-polymerizing the (hydrophilic) glycolic acid with between 25 and 70% (hydrophobic) lactic acid it was possible to produce amorphous materials with a range of hydrophilicities. It was found that if the l-lactic acid polymer was replaced by the dl- equivalent (which is amorphous as homo-polymer) the range was extended to between 0 and 70%.

A number of studies have been made of the rates of biodegradation of copolymers composed of lactic acid and benzene-substituted α-hydroxy acids repeat units.[60,61] Where the aromatic content was low, the pattern of decomposition *in vivo* followed a parabolic pattern. In co-polymers with a low aromatic content the pattern changed to an S-shaped curve. This latter mode of decomposition is thought to be characterised by a slow initial induction period where swelling occurs at the surface, followed by degradation of the swollen polymer and subsequent loss of oligomers produced by decomposition of the main chain.[62]

It has been shown that rates of degradation of copolymers of poly(lactic acid) can be altered by varying the composition of monomers. A similar effect can also be achieved by blending poly(lactic acid) with suitable homo-polymers e.g. blending with poly(sebacic acid) enhances release of bupivicaine hydrochloride.[63]

For enzymes to have an effect upon decomposition it is necessary for the polymer chain to be able to fit into the active enzyme site. Therefore a degree of flexibility is required, making aliphatic more degradable than aromatic polyesters. In a 5% solution of hydroxylase, poly(lactic acid) membranes decomposed at a rate three times faster than when no enzyme was present.[64] A copolymer of poly(lactic acid) and β-phenyl-lactic acid has been shown to be decomposed by chymotrypsin.[65] It should be noted that residual metallic initiators and catalysts present in the polymer may act as biocides and retard degradation by this route.

In order to use polymers in surgery, sterilisation is necessary and this is often achieved by irradiation. The effects of γ-rays have been studied by Gupta and Deshmukh.[66] They found that the melting temperatures of poly(lactic acid) samples decreased with increasing radiation doses, due to chain scission and cross-linking. This suggests an increase in chain flexibility and a decrease in crystallinity, having obvious implications for biodegradation behaviour.

CHAPTER TWO

EXPERIMENTAL TECHNIQUES

2.1 PURIFICATION OF MATERIALS

As anhydrosulphites are easily decomposed by water, it is essential that materials brought into contact with the monomer be free of moisture. Therefore the use of scrupulously dry solvents, reactants and initiators, etc. is of prime importance.

2.1.1 Solvents

2.1.1.1 Nitrobenzene

Analytical grade nitrobenzene (supplied by BDH) was extracted with 2 M aqueous sodium hydroxide, water, dilute hydrochloric acid and again, three times with water.[67] After drying over calcium chloride or barium oxide it was distilled onto calcium or sodium hydride. Before use, the solvent was fractionally distilled, the first fraction being discarded and the fraction boiling at 130-135 °C/3 mmHg collected in a vessel fitted with a vacuum tap. This was closed at reduced pressure and re-opened in the dry box.

2.1.1.2 Tetrahydrofuran

HPLC grade tetrahydrofuran was supplied by Fisons. After standing over calcium hydride overnight it was vacuum distilled onto sodium metal and benzophenone. The indigo-colour of the resulting solution was taken as an indication of dryness and the absence of peroxides. The solvent was re-distilled into a reaction vessel immediately prior to use.

2.1.1.3 Diethyl Ether

Diethyl ether was supplied pre-dried (<0.01 % H_2O) by BDH or Fisons. Sodium wire was added to act as an indicator for dryness (the solvent was not used if tarnishing was observed).

2.1.1.4 Decalin

Decalin (*cis*- and *trans*-decahydronaphthalene) was supplied by Fluka and dried initially by standing over calcium hydride. It was then distilled onto sodium metal and redistilled, at reduced pressure, into a suitable vessel immediately prior to use.

2.1.1.5 Other Solvents

Acetone and cyclohexane were supplied by BDH and dried over calcium sulphate and calcium hydride, respectively. Acetone was filtered from the drying agent before use whilst cyclohexane was distilled into a suitable vessel.

Methanol was used as supplied by BDH, except when used for termination of polymerizations, when argon was bubbled through to remove dissolved oxygen.

2.1.2 Drying Agents

2.1.2.1 Barium Oxide

Barium oxide was obtained from Griffin and George Ltd as a powder. It was dried at 130 °C overnight and cooled under dry argon.

2.1.2.2 Sodium Hydride

Sodium hydride was obtained from BDH as a powder in mineral oil and stored in the glove box. It was washed with dry tetrahydrofuran before use, in order to remove the oil.

2.1.2.3 Sodium Metal

Sodium metal was supplied in paraffin oil by BDH. The oil was removed by washing with dry tetrahydrofuran and tarnished surfaces cut away before use.

2.1.2.4 Other Drying Agents

Calcium chloride and calcium hydride were both obtained as anhydrous powder from BDH and used as supplied.

Benzophenone and phosphorus pentoxide were used as supplied by Janssen Chimica and Fisons, respectively.

2.1.3 Initiators

2.1.3.1 Aluminium iso-Propoxide

Aluminium iso-propoxide was obtained from Fluka with a purity of 99 % and used without further treatment. Attempts to purify by vacuum sublimation and distillation simply liquefied the powder, producing a super-cool liquid which only solidified after several days refrigeration and was not easily manipulated.

2.1.3.2 Ethyl (5,10,15,20-tetraphenylporphinato) Aluminium

Ethyl (5,10,15,20-tetraphenyl porphinato) aluminium, was supplied by Dr.D.S.Riat. It was prepared by the reaction of 5,10,15,20-tetraphenyl-porphine and trimethyl aluminium in dichloromethane under a nitrogen atmosphere. The solvent was removed under reduced pressure and the purple powder re-dissolved in nitrobenzene.

2.1.3.3 *n*- and *sec*-Butyl Lithium

n- and *sec*-butyl lithium were obtained from Aldrich as 1.6 M and 1.3 M cyclohexane solutions, respectively. Ingress of moisture to the 'sure-seal' bottles was prevented by transferring initiator solution within the glove box or by adopting Schlenk techniques i.e. connecting the bottle to an argon line whilst solution is removed. Whilst in storage, the bottles were refrigerated to reduce decomposition but were allowed to warm to room temperature for one hour prior to use.

2.1.3.4 Dibenzo-18-crown-6

Dibenzo-18-crown-6 (2,3,11,12-dibenzo-1,4,7,10,13,16-hexaoxacyclooctadeca-2,11-diene) was obtained as a 98 % pure solid from Aldrich, dried at 100 °C under vacuum and cooled under argon.

2.1.3.5 Lithium *tert*-Butoxide and Sodium Ethoxide

Lithium *tert*-butoxide and sodium ethoxide were supplied as solid powders by Fluka and BDH, respectively. The solids were stored and used under argon, with no further purification.

2.1.3.6 Potassium *tert*-Butoxide

Potassium *tert*-butoxide was supplied by Aldrich, both as a solid and as a 1.0 M solution in tetrahydrofuran. The powder was sublimed under vacuum before use and stored under argon. The solution was treated as described for butyl lithium.

2.2 MANIPULATION TECHNIQUES

2.2.1 Inert Gas Techniques

Many of the products and reactants used in synthesis were sensitive to the presence of atmospheric moisture. Anhydrosulphites in particular, are hydrolysed rapidly by moisture. A number of inert gas techniques were used to prevent decomposition, though in each case the inert gas used was argon. Since argon is denser than nitrogen, it provides a 'blanket' of inert gas, effectively displacing air from reaction vessels. Dry argon was supplied by BOC with a purity of <3 vpm moisture and <3 vpm oxygen and no further purification carried-out.

2.2.1.1 Glove Box Techniques

Glove box techniques were used for manipulation (and in some cases storage) of air- and moisture-sensitive reagents such as initiators and polymerization solvents. For the very early part of the project the system used was a simple box with two glove-ports,

manufactured by Slee. While the box was purged with dry argon, the only means of further desiccation was a dish of phosphorus pentoxide placed inside.

The latter part of the work was performed using a far superior Miller-Howe box, complete with a recirculation drying system. The box was operated under positive pressure with a constant argon flow of 45 litres per minute through a series of columns containing 3 Å molecular sieves, BASF R311 catalyst and BDH activated charcoal. These columns were reformed periodically in order to attain moisture levels below 5 ppm and oxygen below 1 ppm (as confirmed by the manufacturer). An indication of dryness was given by measuring the length of time required for freshly-exposed sodium metal to become tarnished or for sodium benzophenone solution in tetrahydrofuran to lose its indigo colour[68]. Samples and equipment etc. were introduced to the box by means of a port which was evacuated and purged with dry argon three times before opening to the main box. The port was evacuated using an Edwards rotary vacuum pump which was vented to a fume cupboard in order to remove potentially harmful vapours.

It was not possible to use a glove-box for anhydrosulphite synthesis or purification, since it is necessary to cool the monomer to 0-5 °C using ice baths, etc. Such procedures were performed in large polythene glove-bags supplied by Aldrich as 'Atmosbags'. Apparatus and materials were placed in the bag which was attached to an argon-line and flushed with dry gas for 20 - 30 minutes before work was begun.

2.2.1.2 Schlenk Techniques

For certain operations (e.g. the polymerization of anhydrosulphite in tetrahydrofuran under argon at atmospheric pressure) Schlenk techniques were used. For example, an oven-dried vessel was fitted with rubber septa, connected to a vacuum line and evacuated. When cooled, the vessel was filled with dry argon via an argon line connected to the manifold and removed. An argon line was connected to the vessel by means of a wide bore syringe needle as shown in figure 2.1 so that a slight positive pressure of inert gas might be maintained. Dry solvents, reactants, etc. were then introduced from a syringe via the septum.

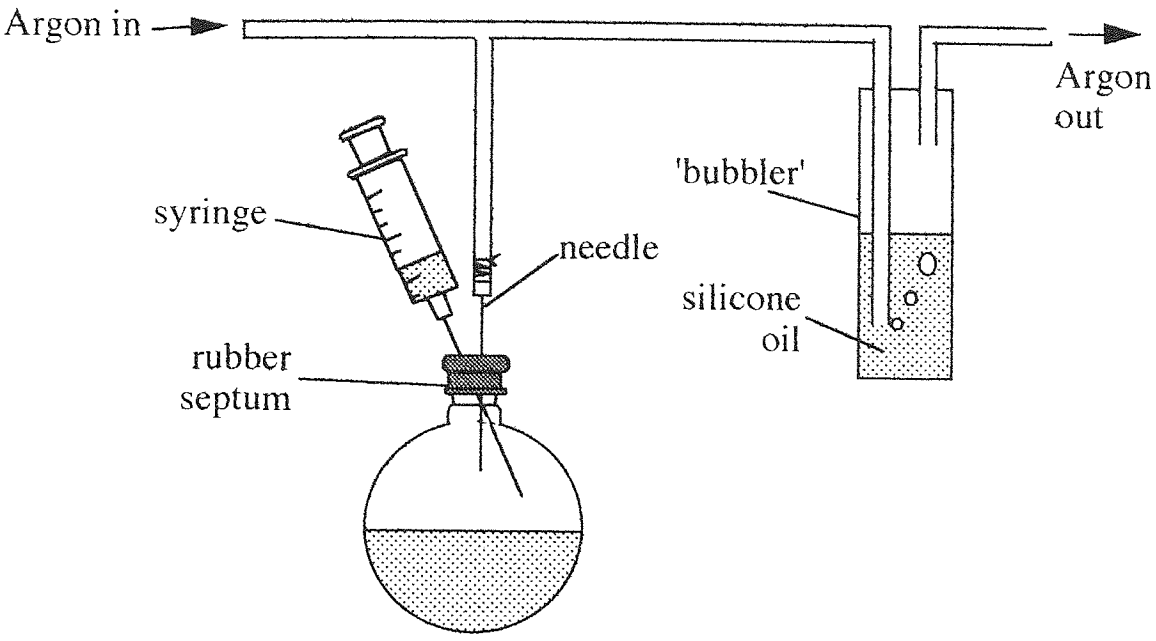

Figure 2.1 The argon line.

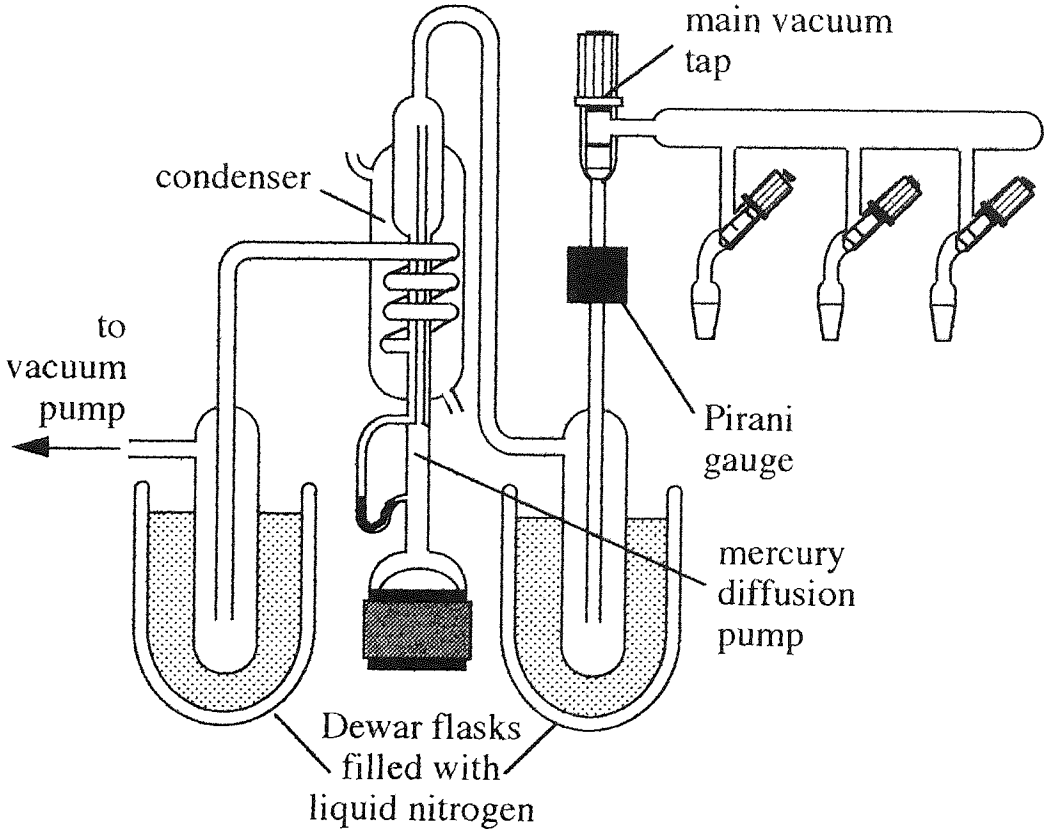

Figure 2.2 The high vacuum line.

2.2.2 Vacuum Line Techniques

Vacuum line techniques were used to dry solvents such as tetrahydrofuran and diethyl ether, and to evacuate reaction vessels before use. The vacuum line manifold was fitted with PTFE taps and connected to a mercury diffusion pump via a liquid nitrogen trap. A second trap connected the mercury diffusion pump outlet to an Edwards rotary vacuum pump. The function of the traps is to condense harmful solvent vapours, which damage the rotary vacuum pump. A Pirani gauge was used to determine when a 'hard' vacuum (10^{-4} mmHg) was achieved. Attached to the vacuum manifold via a PTFE tap, an argon line allowed the manifold to be filled directly with inert gas. Reaction vessels were either dried at 130 °C overnight and attached to the vacuum line to cool whilst evacuated, or evacuated and 'flamed-out' with a bunsen burner before use.

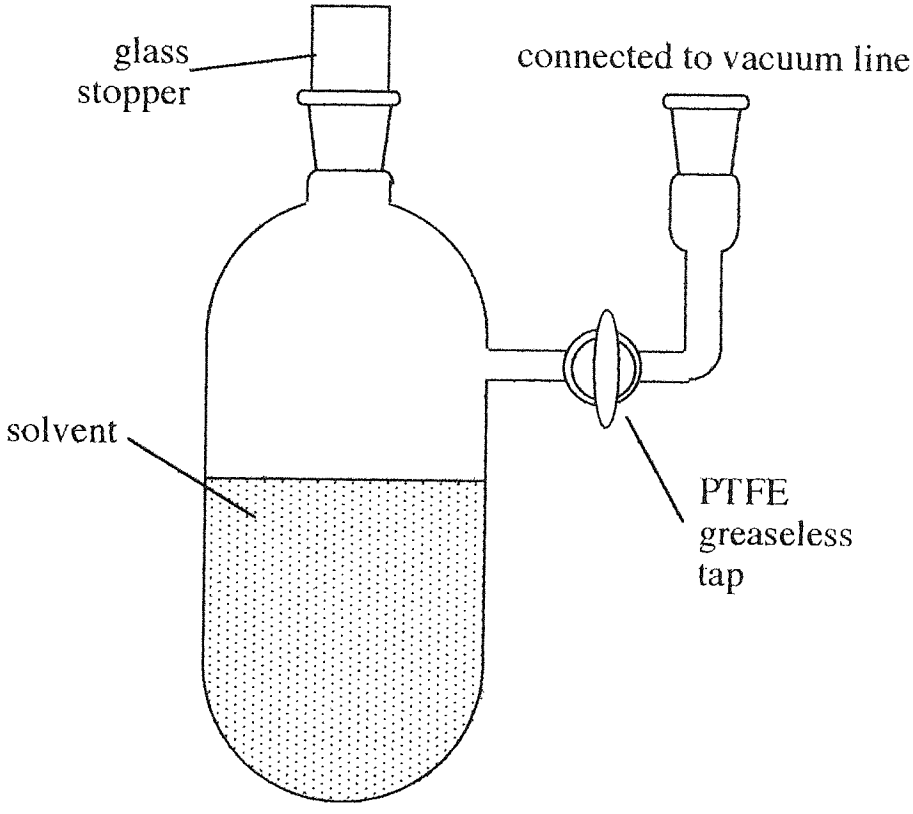

Figure 2.3 Solvent vessel for use with vacuum line.

2.2.2.1 De-gassing of Solvents

Gasses dissolved in the solvent at atmospheric pressure were removed from the solvents by the 'freeze-thaw' technique. The solvent was placed in a vessel (as shown in figure 3) and attached to the vacuum line with the tap closed. Immersion in a Dewar flask

containing liquid nitrogen froze the solvent completely within 10-20 minutes, after which the tap was carefully opened to the evacuated manifold. Once the pressures in the vessel and manifold were equilibrated, tap of the vessel was closed and the manifold re-evacuated. The Dewar flask was removed and the vessel allowed to warm to room temperature, melting the frozen solvent and further releasing dissolved gas. The process was then repeated twice. This procedure prevented 'bumping' and 'flashing-over' during distillation.

After de-gassing, solvents were dried by distillation onto a suitable drying agent. Distillation was achieved by connection of an empty solvent vessel to the manifold, alongside the vessel containing de-gassed solvent. The empty vessel was evacuated and a liquid nitrogen-filled Dewar flask placed around it. The main vacuum tap connecting the manifold was closed, isolating the manifold from the vacuum pump system and the tap on the vessel containing solvent opened carefully. When the liquid began to bubble steadily as solvent evaporated, the tap was left until a sufficient volume of solvent was condensed in the other vessel, at which time the taps were closed and the Dewar flask removed, allowing the solvent to reach room temperature. Occasionally it was necessary to open the tap further or to apply gentle heating.

In the case of tetrahydrofuran and diethyl ether, the solvent was first de-gassed, then distilled into a solvent vessel containing calcium hydride. After 24 hours, it was distilled from the calcium hydride onto sodium metal and benzophenone. The latter reagents effectively remove both residual moisture and peroxides, colouring the solvent a deep indigo (if too much moisture is present the solution will become green). The solvent was distilled from the flask before use in reactions, etc.

2.2.3 Spinning-Band Column Distillation

The spinning-band column (SBC) offers several advantages over a conventional column distillation where moisture-sensitive, thermally-unstable compounds are concerned.

2.2.3.1 Experimental

The spinning-band column used for distillation of LAAS was the Nester-Faust model[69] (see figure 2.4) as supplied by Perkin-Elmer Ltd. When used for reduced pressure distillation of LAAS it was connected to an Edwards rotary vacuum pump. The pressure of the system was monitored with a Drück DPI 140 digital pressure indicator and

controlled by alteration of a Fairchild valve fitted between the pump and the SBC. Also connected between the pump and the SBC, was a potassium hydroxide 'U' tube and dry ice/acetone cold trap (in order to prevent damage to the pump by acidic gases evolved during cyclisation of the anhydrosulphite).

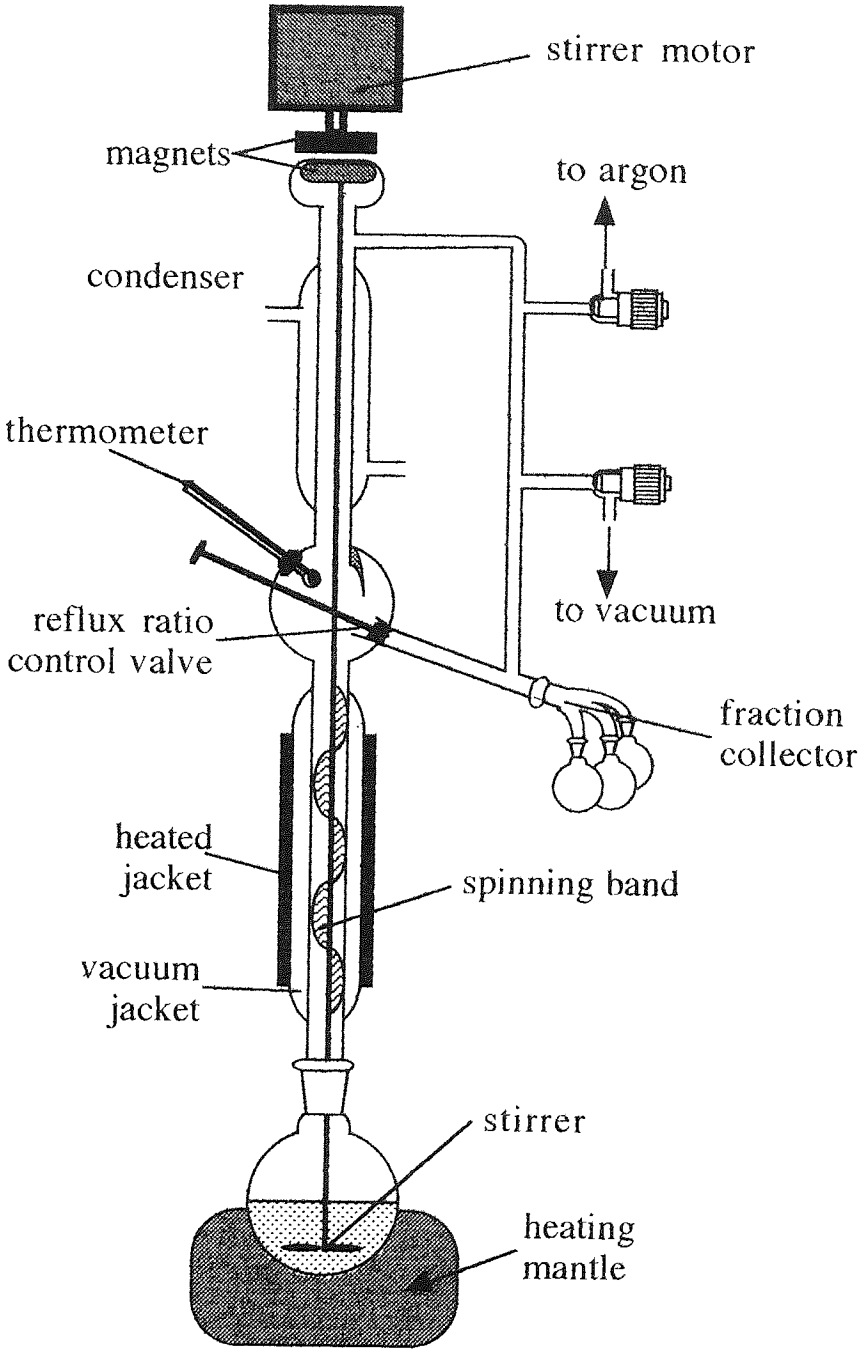

Figure 2.4 The spinning-band column.

2.2.3.2 Discussion

The spinning-band column operates by means of a spiral of metal gauze rotating rapidly (up to 4000 r.p.m.) inside the inner distillation column. This has a significant advantage over conventional distillation columns since contact between gas and liquid is greatly increased. The band throws vapour onto the walls of the column to mix with the condensate flowing downward, which has the effect of greatly increasing column efficiency and reduces the pressure differential between the top and bottom regions of the column. The level of heating needed at the distillation flask is consequently reduced.

In the case of anhydrosulphite, it is desirable to achieve maximum separation of the monomer and α-chloro-acid chloride but two considerations affect the conditions of distillation: the process must be performed rapidly but heating should be minimised in order to reduce decomposition. These conflicting objectives may be reconciled by heating the round-bottomed flask only mildly and using the column heater to promote cyclisation and distillation. The reflux-ratio and rotation speed are adjusted to achieve maximum separation with minimal decomposition. In addition, spinning-band systems typically have very low hold-up volumes compared with conventional fractionating columns. This is an important factor as the quantity of monomer produced by a typical synthesis is not great, being of the order of 50 - 100 g.

2.3 POLYMERIZATION TECHNIQUES

2.3.1 Monitoring of Gas Pressure

The decomposition of the anhydrosulphite ring is accompanied by the expulsion of sulphur dioxide. As this occurs concurrently with ring-opening, measurement of the increase in gas pressure may be used to follow the progress of the reaction and hence calculate the rate of decomposition. The apparatus used for many kinetic experiments is shown in figure 2.10. It is a modified version of a design by Ballard and Bamford[70] which was subsequently used by a number of workers in this area.

Since reactions are conducted at very low pressure, certain restrictions apply to the variety of experiments that may be conducted. Not only must the solvents used be compatible with the monomer and initiator systems, they must be of high boiling point in order that their vapour pressures do not interfere with the measurement of gas evolution). Also, as the pressure of gas evolved is measured by a mercury column of finite length (~350 mm), the range of measurement is limited, so that the quantities of monomer must be very small (typically 0.1 - 0.2g).

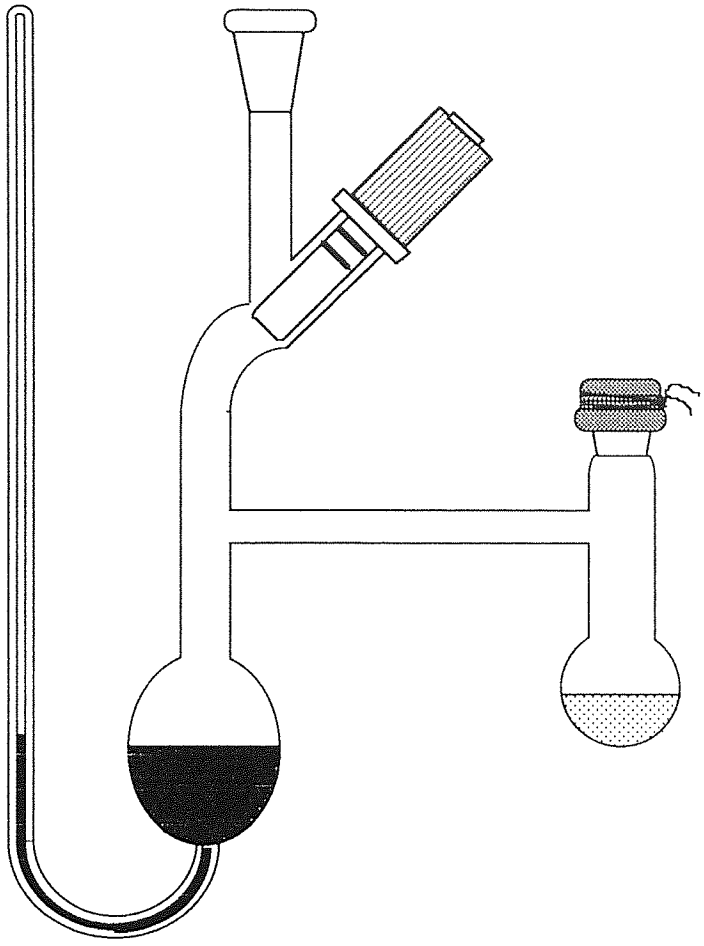

Figure 2.5 Mercury manometer polymerization vessel.

2.3.1.1 Experimental

Prior to use, the mercury was removed from the vessel, which was then rinsed with dilute nitric acid to remove residual traces. After cleaning with 'Decon 90' solution followed by rinsing thoroughly with distilled water, the vessel was dried at 130 °C for several hours. Approximately 50g mercury was added to the reservoir, a PTFE tap and rubber septum were fitted and the septum wired tight. The vessel was attached to the vacuum line by means of the B19 socket and evacuated carefully to avoid 'breaking-up' the mercury in the manometer column. The vessel was then 'flamed-out'. After allowing the vessel to cool, the tap was closed and the vessel removed from the line. By tilting the vessel, the pressure either side of the mercury was equalised and residual air in the manometer column removed. The vessel was then re-attached to the vacuum line and completely evacuated.

Monomer and initiator solutions were prepared in the glove box. Re-distilled monomer and purified initiators were weighed out into volumetric flasks, and the flasks filled with

dry solvent up to the mark. In the case of initiators which were not readily soluble, the vessels were stoppered, sealed with 'parafilm' and PVC tape, and placed in an ultrasound bath for 30 - 60 minutes.

Initiator solution was injected into the vessel by means of a Luer syringe and the vessel clamped to a rigid frame in a thermostatted water bath for 15 minutes to reach the required temperature. The bath used was a Bridge control series II, manufactured by Townson and Mercer Ltd. Set temperatures were maintained ±0.5 °C between 35 and 70 °C.

The height of the mercury in the column was measured relative to the reservoir and the vessel removed from the bath. The monomer solution was then injected and a timer started simultaneously. After 'swirling' the reaction mixture rapidly to mix the reactants, the vessel was replaced in the bath and the height of the mercury in the manometer column measured using a bench cathetometer. The heights of mercury both in the manometer column and in the reservoir bulb were measured at suitable intervals so that the pressure of gas might be calculated by the difference between the two in millimetres. It should be noted that a correction was applied by subtracting the value for the height of the mercury determined before injection of monomer from all subsequent measurements. In this way, the (slight) contribution to the gas pressure due to the solvent vapour from the initiator solution was eliminated.

Before a reading was taken, the vessel was agitated by vibration of the frame using a Pifco 'massager' clamped to it. This is necessary in order to equilibrate the concentration of sulphur dioxide between the vapour phase and that dissolved in solution. When readings were taken every 15 seconds it was necessary to maintain almost constant agitation.

2.3.1.2 Discussion

Assuming ideal gas behaviour and constant temperature and volume, the pressure of the gas evolved, P, can be used to derive the concentration of monomer, $[M]_t$, remaining at time, t, where $[M]_0$ is the monomer concentration at t = 0 :-

$$P_t \propto [M]_0 - [M]_t \qquad (1)$$

and at the end of the reaction,

$$P_\infty \propto [M]_0 \qquad (2)$$

The concentration of monomer can be related directly to the pressure of gas evolved at time, t :-

$$\frac{[M]_o - [M]_t}{[M]_o} = \frac{P_t}{P_\infty} \qquad (3)$$

Rearranging gives an expression relating the gas pressure to the proportion of monomer remaining (i.e. fractional monomer) at time, t :-

$$\frac{[M]_t}{[M]_o} = \frac{P_\infty - P_t}{P_\infty} \qquad (4)$$

Since the pressure of gas in this system is directly proportional to the height of mercury in the manometer column, H, then :-

$$\frac{P_\infty - P_t}{P_\infty} = \frac{H_\infty - H_t}{H_\infty - H_o} \qquad (5)$$

and hence :-

$$\frac{[M]_t}{[M]_o} = \frac{H_\infty - H_t}{H_\infty - H_o} \qquad (6)$$

For equation (6) to be true, three conditions must be satisfied :-

(1) the temperature of the bath must remain constant throughout the reaction,
(2) the volume of the vessel must not change, and
(3) the behaviour of the evolved gas must be near to ideal.

It has already been mentioned that the temperature of the bath was maintained to ±0.5 °C. Since the vessel is allowed to reach bath temperature before experiments are started, its volume can be considered to be constant (in fact the volume change over the course of an experiment has been estimated as being as low as 0.01 %).[71] Sulphur dioxide will tend towards ideal behaviour at low pressure, so it may be assumed that the associated laws will apply and the pressure of the system will be directly related to the number of moles of gas present. The vapour pressure of the anhydrosulphite and solvent may have some influence but this is only likely to be significant during the initial period where little sulphur dioxide is present in the gas phase. The evolved gas may be quite soluble in the reaction solvent, but according to Henry's law, the concentration of the vapour in the vapour phase will be directly proportional to that in solution.

The progress of a particular reaction may be studied by plotting the concentration of monomer against time. In the case of a reaction in which the consumption of monomer follows first order kinetics, then :-

$$[M]_t = [M]_o.e^{-k_1.t} \qquad (7)$$

where k_1 is the rate constant for the reaction. This rate constant may incorporate a dependence on the concentration of initiator.

A plot of $\ln[(P_\infty-P_t)/P_\infty]$ against t, will give a straight line, the slope of which is $-k_1$. Alternatively, the half-life method may be used i.e. measuring the time when half the monomer is consumed and calculating the result of the equation :-

$$k_1 = \frac{0.693}{t_{\frac{1}{2}}} \qquad (8)$$

If the reaction is first order with respect to both monomer and initiator, the rate constant, k_1, will be proportional to the initiator concentration, and the second order rate constant, k, may be obtained by comparison of the values of k_1 obtained at different concentrations of initiator. If the relationship between the rate constants is defined as:-

$$k_1 = k.[I]_o \qquad (9)$$

where $[I]_o$ is the initial concentration of initiator, then a plot of k_1 against $[I]_o$ should produce a straight line of slope k.

If the rate constant, k is determined for identical reactions at different temperatures, the activation energy, frequency factor and entropy of activation can be calculated using the Arrhenius equation[72]:-

$$k = -A.e^{-E_a/RT} \qquad (10)$$

where :-

A = frequency factor/s^{-1},
E_a = activation energy/ $J.mole^{-1}$,
R = the gas constant (8.3145 $J.K^{-1}.mol^{-1}$),
T = temperature/K.

If ln[k] is plotted against the reciprocal of the absolute temperature, the gradient of the line will give the activation energy :-

$$E_a = -\text{gradient} \times R \qquad (11)$$

The entropy of activation, ΔS, may then be calculated by means of the expression :-

$$A = \left(\frac{KT}{h}\right).e^{\Delta S/R} \qquad (12)$$

where :-

A = frequency factor/s^{-1},
ΔS = entropy of activation/$J.mole^{-1}.K^{-1}$,
K = Boltzmann constant (1.381×10^{-23} $J.K^{-1}$),
h = Planck's constant (6.626×10^{-34} J.s), and
T = temperature/K.

2.3.2 Infra-Red Spectroscopic Techniques

An alternative means to gas pressure measurement for observing monomer decomposition/polymer formation is the use of infra-red spectroscopic techniques. The strained ring system present in anhydrosulphites gives rise to a relatively high carbonyl absorption frequency (1823 cm^{-1} in LAAS) while the absorption frequency of the lactic acid polymer carbonyl is much lower at 1758 cm^{-1}. Since these absorptions occur at wavenumbers differing by over 50 cm^{-1}, their intensities may be measured independently.

Either the disappearance of monomer carbonyl or appearance of polymer carbonyl (or both) may be followed if several conditions are satisfied. The solvent used must exhibit no strong absorptions in the region of the observed carbonyls since the greater concentration of solvent would mask the contributions from the monomer and/or polymer. The reaction must also be homogenous throughout because the presence of solid would cause a rapid decrease in percentage transmission. Nitrobenzene and tetrahydrofuran are both suitable solvents as neither possess strong absorptions in the carbonyl region and solubilise monomer and polymer effectively.

2.3.2.1 Experimental

For experiments followed by means of infra-red spectroscopy, a solution cell having polished sodium chloride windows separated by a PTFE spacer was used. The spectrum of the purified, dried solvent used was recorded prior to reaction and stored on computer disc. Spectra recorded during the progress of the reaction were processed using the on-board infra-red data manager by subtraction of the pre-recorded solvent spectrum from each of the experimentally-recorded spectra. This was done to remove the (slight) contributions from solvent in the carbonyl region. Spectra may be recorded by taking samples at intervals from a reaction mixture or by allowing the reaction to occur inside a closed cell. In either case, it is important to exclude moisture by the use of scrupulously dry equipment and blanketing with dry inert gas.

2.3.2.2 Discussion

The Beer-Lambert law relates the intensity of absorbance to a number of variables:-

$$\log\left(\frac{I_0}{I}\right) = \varepsilon.c.l \qquad (1)$$

where :-

I_0 = intensity of incident light,

I = intensity of transmitted light,

ε = molar absorptivity coefficient,

c = concentration of absorbing species/mole.litre^{-1}, and

l = path length of cell/cm.

Since E and l are both constant for a particular system, absorbance may be related directly to the concentration of the absorbing species, c, which may be either monomer or polymer. The experimental techniques of reaction monitoring by FTIR solvent cell are described in detail by Braterman.[73]

The possibility of using ultra-violet spectroscopy to follow reactions in a similar manner to infra-red was investigated. Unfortunately, as the λ_{max} of LAAS is quite low at 291.5nm,[25] the peak is masked by most suitable solvents e.g. a 4 x 10^{-4} M solution of LAAS in tetrahydrofuran (quartz cell) produced a tetrahydrofuran absorption with only a slight shoulder at 250 nm (tetrahydrofuran has a λ_{max} of 220 nm).[66] Also, as ultra-violet spectroscopy normally requires the use of very dilute solutions, this would restrict the range of reactions which might be followed. Reactions at low concentration would also increase the likelihood of contamination by moisture, etc. over time.

2.3.3 Calorimetric Techniques

Following the decomposition of anhydrosulphites by measuring the pressure of evolved sulphur dioxide is a useful technique but there are certain limitations to its use. The quantities of monomer which may be used are small ($\sim$ 0.1g) and it is difficult to remove the high boiling solvents from the products at the end of the reaction.

Use of calorimetric methods allows the high boiling solvent to be replaced by a relatively volatile one which may be easily removed from the product by evaporation. Rapid reactions of less than one minute duration may be followed by measuring the heat evolved during the process of polymerization.

2.3.3.1 Experimental

The system used was a modified form of that used successfully for monitoring the cationic polymerization of cyclic ethers,[74] developed by Biddulph and Plesch.[75] The rise in temperature associated with the ring-opening reaction was measured using a GL23 2kΩ thermistor (supplied by RS components Ltd.). The change in resistance as a function of temperature was measured by Knauer auto potentiometer bridge. The output from the bridge was sent to a Serviscribe 'IS' chart recorder which recorded the change in temperature as a deflection. Calibration was carried out by noting the deflection on the chart recorder at different temperatures so that a curve of deflection against temperature was obtained. The apparatus was found to have approximately linear sensitivity to increases in temperature, with some deviation at the extremes.

The reaction vessel was connected to an argon line (see section 2.2.1.2) by means of a wide-bore needle and polythene tubing. This ensured both that the reaction took place under a blanket of inert gas, and that the pressure of sulphur dioxide evolved was released safely. Monomer, solvent and initiator solution were introduced to the reaction vessel by injection through a rubber septum. The syringes used were weighed before and after injection so that volumes of reactants and hence concentrations could be obtained.

The reaction vessel containing monomer in solution was suspended in a water bath in order to stabilise the initial temperature of the reactions. Magnetic stirrers were used in both the water bath and the reaction vessel, to ensure homogeneity of temperature and chemical composition, respectively. Before injection of initiator, the bridge was adjusted to a convenient setting and the chart recorder zeroed. The solution in the reaction vessel

was then allowed to reach equilibrium so that a stable base-line might be obtained. The temperature of the water bath was recorded and the chart recorder set running before the start time was marked on the trace when initiator was injected.

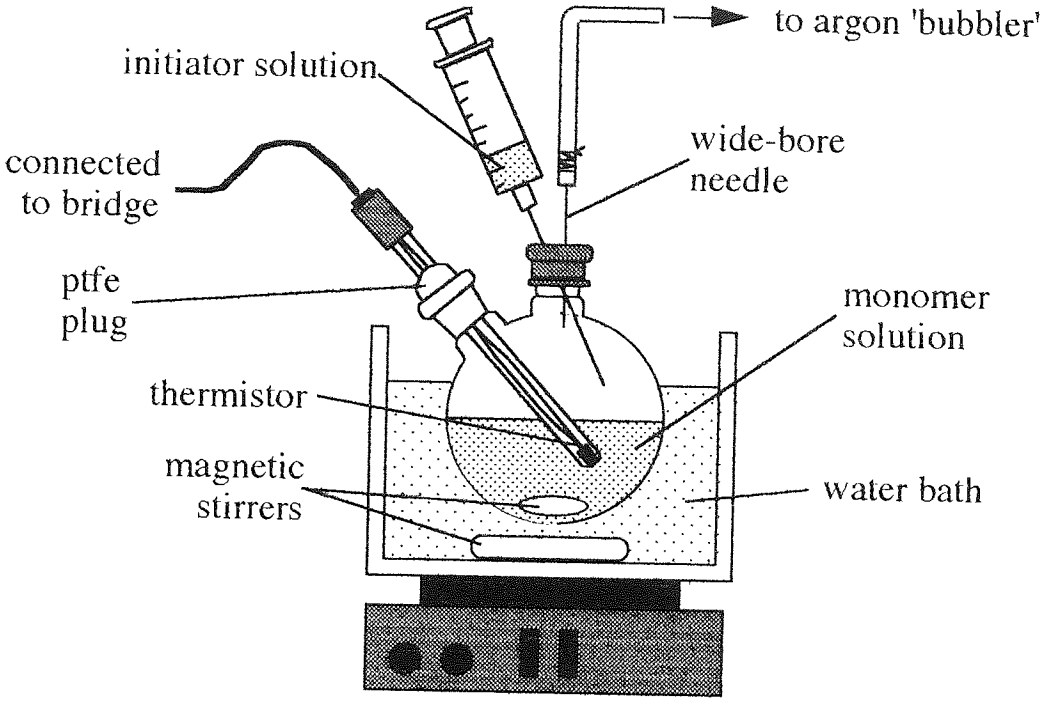

Figure 2.6 Calorimetry apparatus.

2.3.3.2 Discussion

The trace of deflection against time was converted to °C against time by means of the calibration curve described in section 2.3.3.1. The rate of increase in temperature during polymerization, measured in $°C.s^{1}$, could then be used to estimate therates of reaction from the slopes of the line obtained. The rates measured in $°C.s^{1}$ were converted to the more conventional units of $mol.dm^{3}.s^{-1}$, by measuring the maximum deflection of each experiment and converting to °C using the calibration curve. A linear relationship between the maximum temperatureincrease and the concentration of monomer used in that experiment was observed. Thus the rateof change in temperature already calculated may be converted to a rate of change in monomer concentration. A typical trace is shown in figure 2.7.

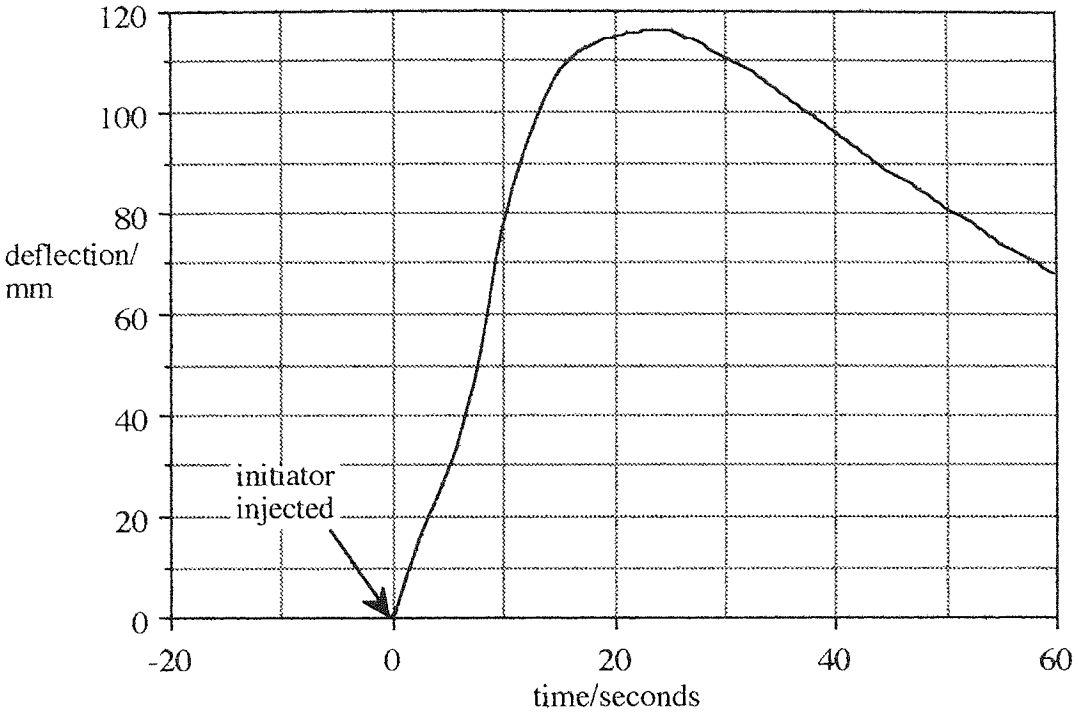

Figure 2.7 A typical calorimeter trace.

2.4 ANALYTICAL TECHNIQUES

2.4.1 Determination of Chlorine Content

The purity of the anhydrosulphite was determined by potentiometric titration using a method based on that of Ingram[76] and modified by Tighe et al.[77]

2.4.1.1 Experimental

Between 0.1 and 0.2 grams of crude anhydrosulphite was weighed accurately into a 5 cm^3 beaker. This was rinsed into a 100 cm^3 beaker with 10 cm^3 'Analar' grade acetone. 20 - 30 cm^3 distilled water and a few drops of 1.0 M nitric acid were then added. The solution was covered with a watch-glass and heated to boiling point for several minutes. On cooling to room temperature, the solution was titrated against 0.1 M silver (I) nitrate solution (made up from 99+ % pure solid supplied by Aldrich and standardised against sodium chloride solution) using the apparatus shown in figure 2.8.

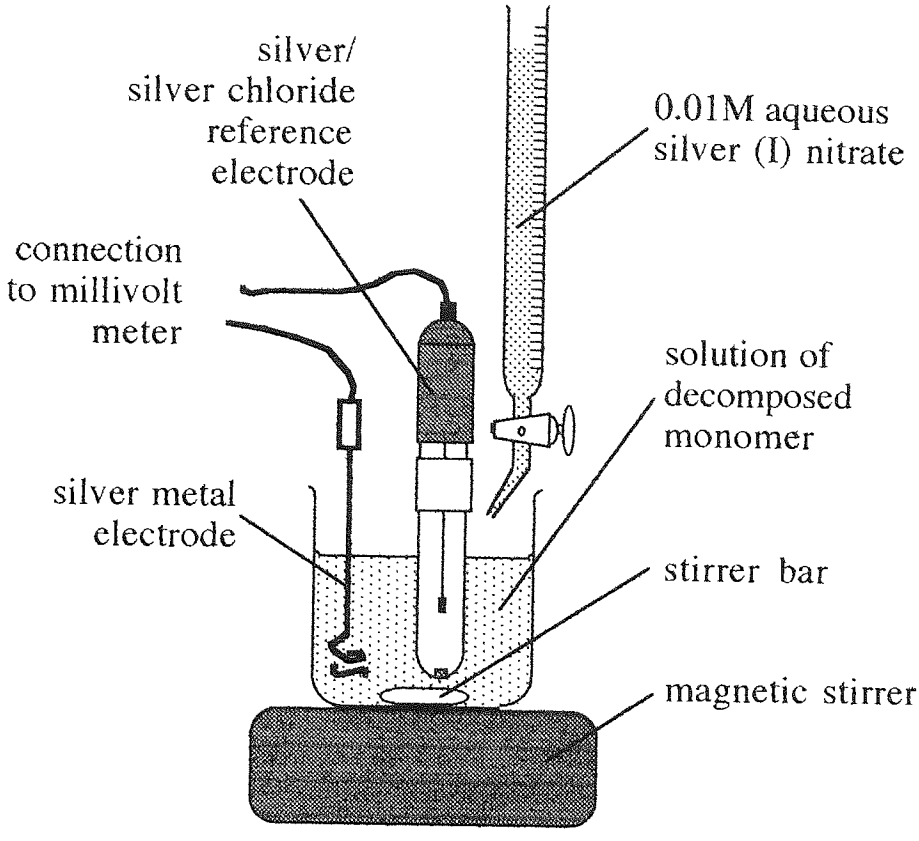

Figure 2.8 Potentiometric titration apparatus.

A Corning 220 millivolt meter was used to followed the potential difference of the half-cell created using against a combination electrode constructed from silver wire (supplied by Fisons) and a Gallenkamp silver/silver chloride reference electrode. The voltage was plotted against the volume of silver (I) nitrate solution added, to produce a curve with a sharp inflection at the equivalence point as shown in figure 2.9. The system was tested using standard solutions of sodium chloride and titrations were performed in duplicate to ensure an accuracy of ±0.5 % (based on moles of anhydrosulphite).

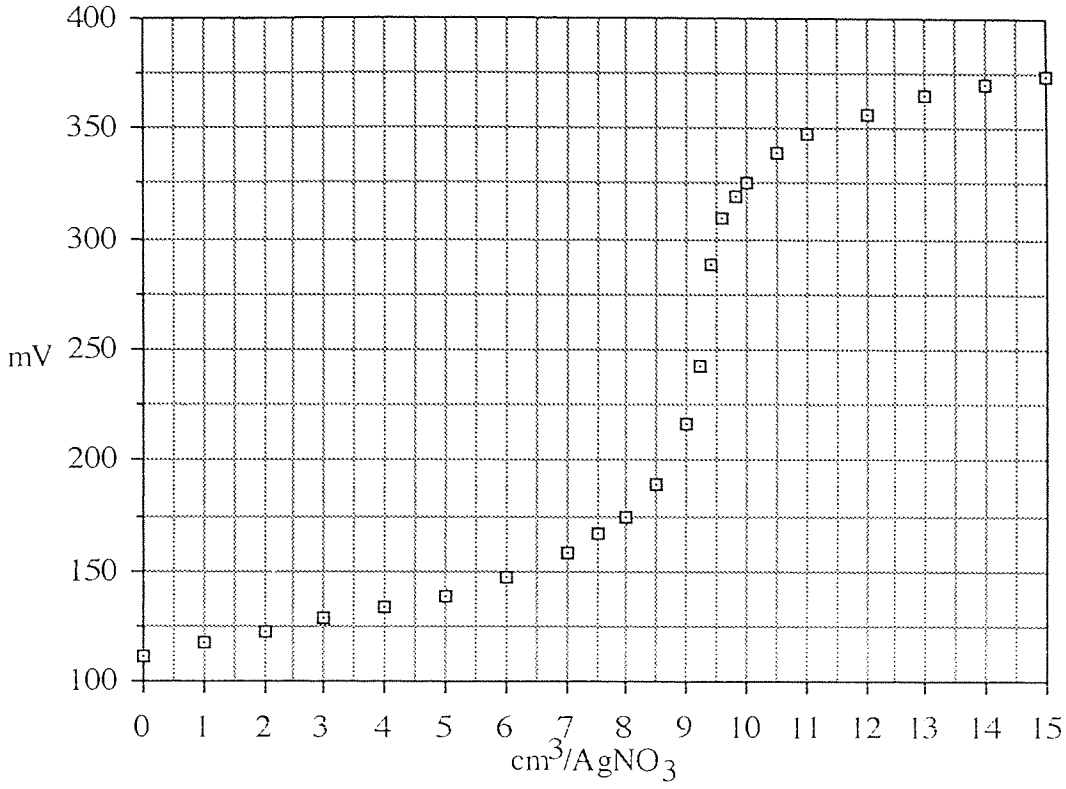

Figure 2.9 Plot of voltage against volume of silver (I) nitrate.

2.4.2 Infra-Red Spectrography

Fourier Transform Infra-red (FTIR) spectra were obtained using a Perkin Elmer FT1710 instrument. Data was obtained as a set of 10 scans at a resolution of 4 cm^{-1}. The spectra were recorded and manipulated using a Perkin-Elmer infra-red data manager (run on an Inmac PC), converted to Lotus 1-2-3 format and transferred to an Apple Macintosh Classic computer via PC exchange into Excel v3. The spectra were finally collated and printed using Cricketgraph III.

2.4.3 Nuclear Magnetic Resonance Spectrography

Nuclear Magnetic Resonance (NMR) spectra were obtained on a Bruker Spectrospin AC300 instrument operating at 300Mhz. Samples for analysis by NMR were made up as 10 % w/v solutions in deuterated chloroform, except where otherwise stated.

2.4.4 Gel Permeation Chromatography

Gel Permeation Chromatography (GPC) is also known as Size Exclusion Chromatography (SEC) and used to determine the molecular weight distribution of polymers. The determination depends upon fractionation of a polymer sample, according to its hydrodynamic volume. This is achieved by passing the sample through a series of columns containing swollen cross-linked polystyrene beads. This stationary phase is constructed so that when swelling occurs, pores appear in the beads, which are of different sizes and each pore allows only polymer chains of sufficiently small volume to enter it. This effectively slows down the passage of small molecules since they will occupy a larger pore volume, permeating the gel structures and taking a longer path through the column than larger polymer chains which are excluded from the gel and elute more rapidly.

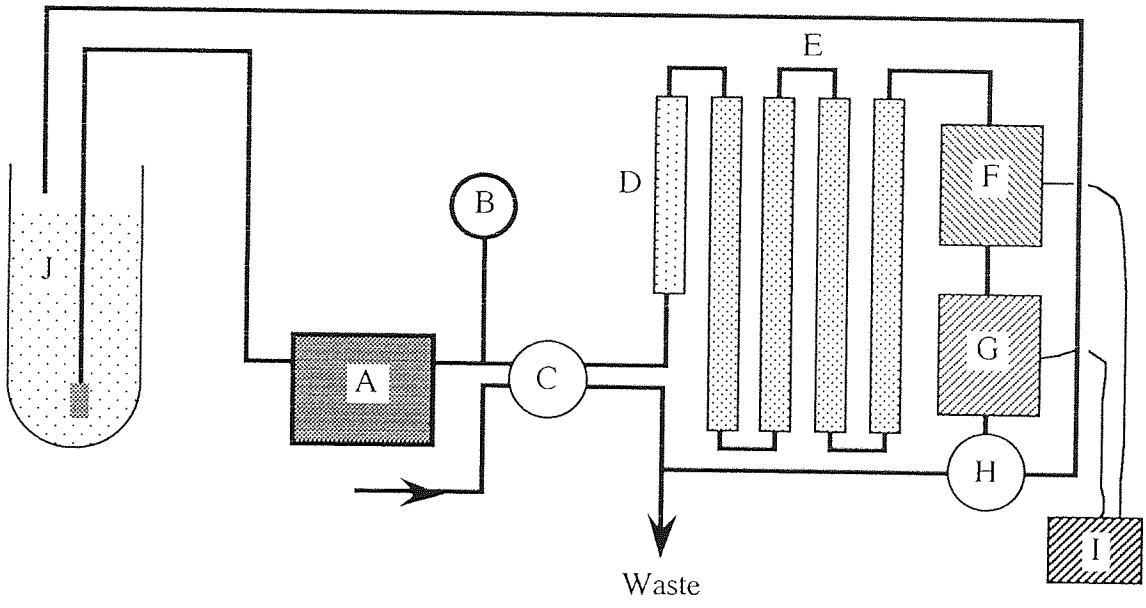

A	HPLC pump	B	Pressure gauge	C	Valve and loop injector
D	Pre-column	E	PL-Gel columns	F	RI detector
G	UV detector	H	2-way tap	I	Chart recorder
J	Solvent reservoir				

Figure 2.10 The Gel Permeation Chromatography system.

2.4.4.1 Experimental

A sample of polymer was dissolved in a suitable solvent (in this case tetrahydrofuran) to produce a solution having a concentration of 1 - 2 % w/v.

This solution was then introduced to the column via a 100 µL valve and loop injector system (C in figure 2.10). A Knauer HPLC pump (A) was used to deliver HPLC grade tetrahydrofuran to the system at 1 cm^3 per minute. The solution passed first through a short pre-column (D) designed to removed suspended solids. Connected to this column are five μ-PL gel columns (E) (supplied by Polymer Laboratories) having exclusion limits of 10^5, 10^4, 10^3 and 10^2 Å. These columns contain mechanically stable, highly cross-linked gels having progressively smaller pore sizes. As selective permeation occurred, the polymer was separated into a continuous range of molecular weight fractions which were detected as the outflow from the last column passes through a refractometer (F) and ultra-violet spectrometer (G) (both supplied by Polymer Laboratories), the output from these being recorded on a dual-pen chart recorder (J). While samples were passing through the column, solvent was run to waste but when not in use it was re-routed back to the solvent reservoir (I) via the two-way tap (H).

The R.I. detector continuously compares the refractive index of the solution with that of the pure eluent. Any difference will be proportional to the concentration of polymer present in the solution. The U.V. detector only responds polymers containing chromophoric groups (which absorb at a given wavelength) either attached to, or part of the polymer back-bone (e.g. polystyrene). A trace of intensity against elution volume is obtained which may be converted to molecular weight distribution parameters by means of calibration data.

2.4.4.2 Calibration of GPC columns

In order to interpret the trace of intensity against elution volume to molecular weight distribution data it is necessary to determine how the molecular weight of a given polymer varies over the range of elution volumes. In the case of lactic acid polymers, there are no reference samples of known molecular weight available so it is not possible to calibrate the column directly. Polystyrene samples of known peak molecular weight and narrow distribution were used instead. The peak molecular weights of these samples may be plotted against elution volumes to create a simple calibration curve as shown in figure 2.11.

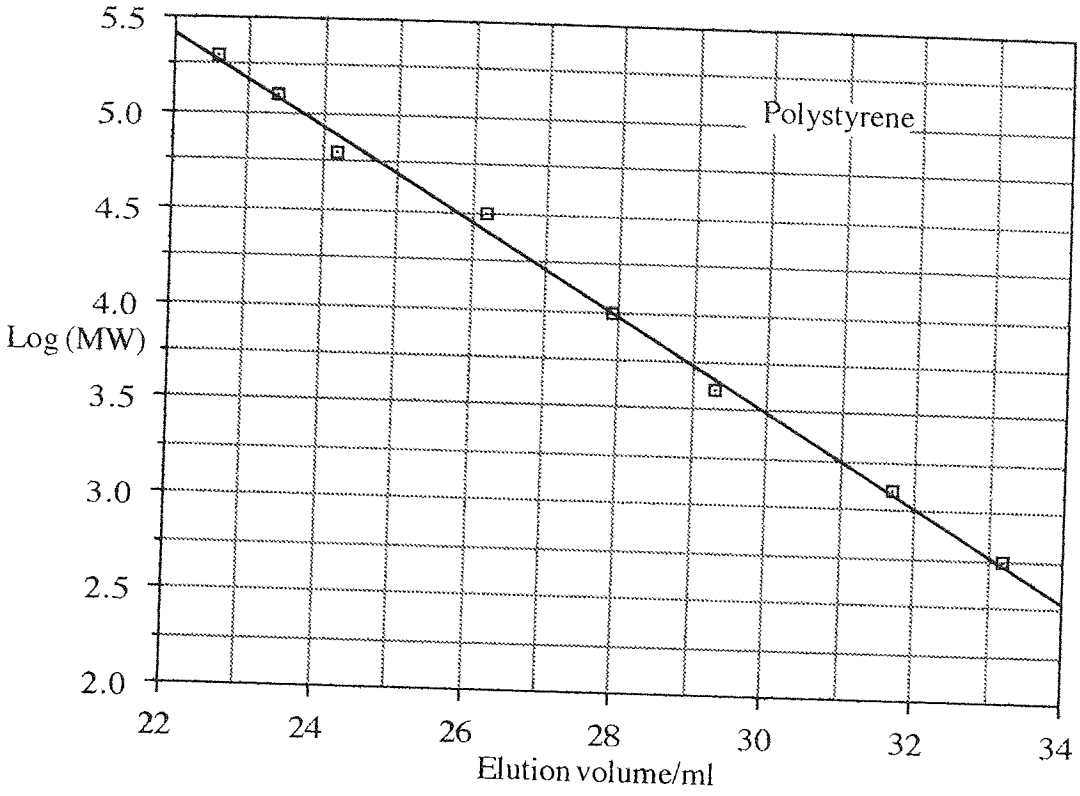

Figure 2.11 GPC calibration curve (polystyrene)

The system was calibrated with Polymer Laboratories polystyrene samples of known peak molecular weights ranging from 580 to 1,400,000 and though it is possible to convert a calibration curve for one type of polymer to that of another, the Mark-Houwink data is only available for poly(lactic acid) in chloroform.[7,8] Since the system used tetrahydrofuran as solvent it was not possible to convert the poly(styrene) calibration data to poly(lactic acid). Molecular weights quoted are therefore polystyrene equivalents unless otherwise stated.

The data obtained from the chromatograph may be used to calculate number and weight average molecular weights (and thus polydispersities). Average molecular weights are calculated by the following equations:-

$$\overline{M}_n = \frac{\sum w_i}{\sum \frac{w_i}{M_i}} \qquad (1)$$

$$\overline{M}_w = \frac{\sum w_i M_i}{\sum w_i} \qquad (2)$$

where :-

$\overline{M}_n$ = number average molecular weight,
$\overline{M}_w$ = weight average molecular weight,
w_i = weight fraction of polymer of molecular weight M_i in a given sample, and
M_i = molecular weight of a given sample.

Since the detector response is proportional to the concentration of polymer in solution, W_i may be replaced by h_i, the height (or deflection) of the trace at a given elution volume (and hence molecular weight) as shown in figure 2.12.

$$\overline{M}_n = \frac{\sum h_i}{\sum \frac{h_i}{M_i}} \qquad (3)$$

$$\overline{M}_w = \frac{\sum h_i M_i}{\sum h_i} \qquad (4)$$

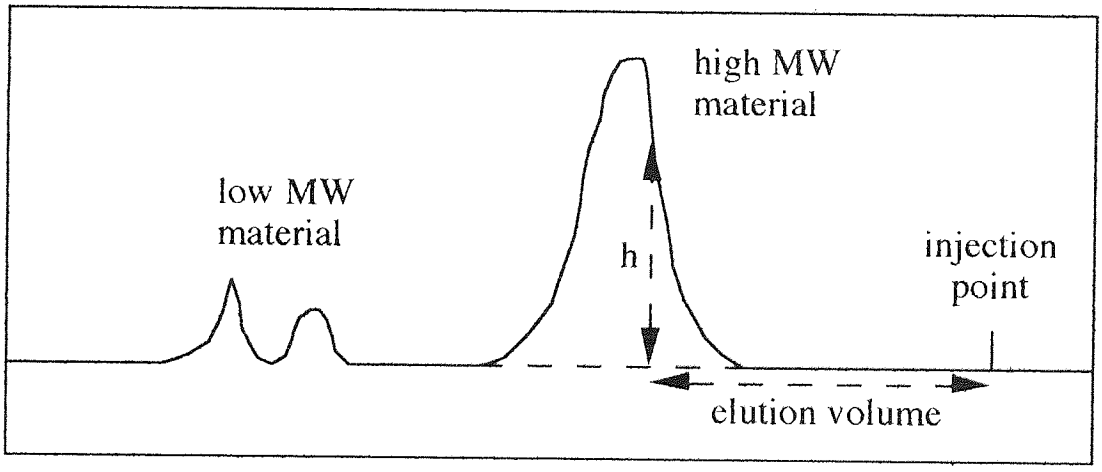

Figure 2.12 A typical GPC trace.

If the deflections obtained for apolymer sample across a range of elution volumes are measured and these elution volumes converted to molecular weight data by reference to a calibration curve, number and weight average molecular weights maybe calculated. In practice, this data was processed using Excel 3, a spreadsheet package run on a Macintosh 'Classic' 40Mb computer.

Some samples were processed using different gel permeation chromatography equipment to that described above. Samples were processed by RAPRA Technology Ltd. using a gel permeation chromatography system having two 30 cm mixed bed PL gel columns operating with a flow rate of 1.0 ml/minute. A refractive index detector was used and molecular weights calculated using a GPC PRO computer package. Solutions of polymer were produced by dissolving 20 mg of sample in 10 cm^3 solvent. A trace amount of ortho-dichlorobenzene was added as an internal marker and the solution filtered through a 0.2 micron polyamide or PTFE membrane. Where chloroform was used as eluent (at ambient temperature) the column was calibrated using polystyrene standards. Since some samples of poly(lactic acid) apparently gave no detector response in chloroform, dimethyl formamide was used (at 80 °C) and the columns calibrated against poly(ethylene oxide) and poly(ethylene glycol).

Some samples were also processed using a gel permeation chromatograph located at the DRA site in Fort Halstead. This sytem consisted of a Waters 510 pump passing tetrahydrofuran through an ERC 3522 degasser and into PL gel columns having exclusion limits of 10^5, 10^4, 10^3 and 10^2 Å. Samples were introduced to the column by a Waters 717 autosampler and the output from the columns was detected by a Viscotek differential refractometer/viscometer. The column was calibrated with polystyrene standards and molecular weights were calculated using a similar method to that described in section 2.4.4.1.

2.4.5 Differential Scanning Calorimetry

Differential Scanning Calorimetry (DSC) is a useful technique for identifying the thermal transitions of a polymer e.g. melting temperatures, glass transitions, etc.

2.4.5.1 Experimental

Polymer samples were characterised by Differential Scanning Calorimetry using a Polymer Laboratories Thermal Sciences PL-DSC instrument, the output from which was manipulated by an Epson AX2 personal computer. A temperature programme was followed whereby samples were heated from -100 to +180 °C under an atmosphere of nitrogen gas at 20 psi pressure.

2.4.5.2 Discussion

In this technique, a sample is sealed in a small aluminium pan and placed in a heating block. A reference sample (either alumina or an empty pan) is placed in a separate block. Both the sample and reference are heated and their temperatures measured by thermocouples so that the heat input to the sample may be automatically adjusted so that the increase in temperature is the same for each. When a transition occurs in the sample, more or less heat will be necessary in order to maintain parity between the temperatures of the sample and reference and the heat input to the sample is adjusted accordingly. In this way both endothermic and exothermic transitions may be identified and the area under the peaks will be proportional to the change in enthalpy occurring.

CHAPTER THREE

MONOMER SYNTHESIS

3.1 SYNTHESIS OF LACTIC ACID ANHYDROSULPHITE

The preparation of an anhydrosulphite is a multi-stage process, which is outlined in figure 3.1. Although the same general procedure may be used to prepare a range of anhydrosulphites, the process must be adapted for different products. Though the procedure described below is based upon the general synthesis outlined in earlier publications, it has been optimised for the preparation of lactic acid anhydrosulphite and has been modified in certain respects.

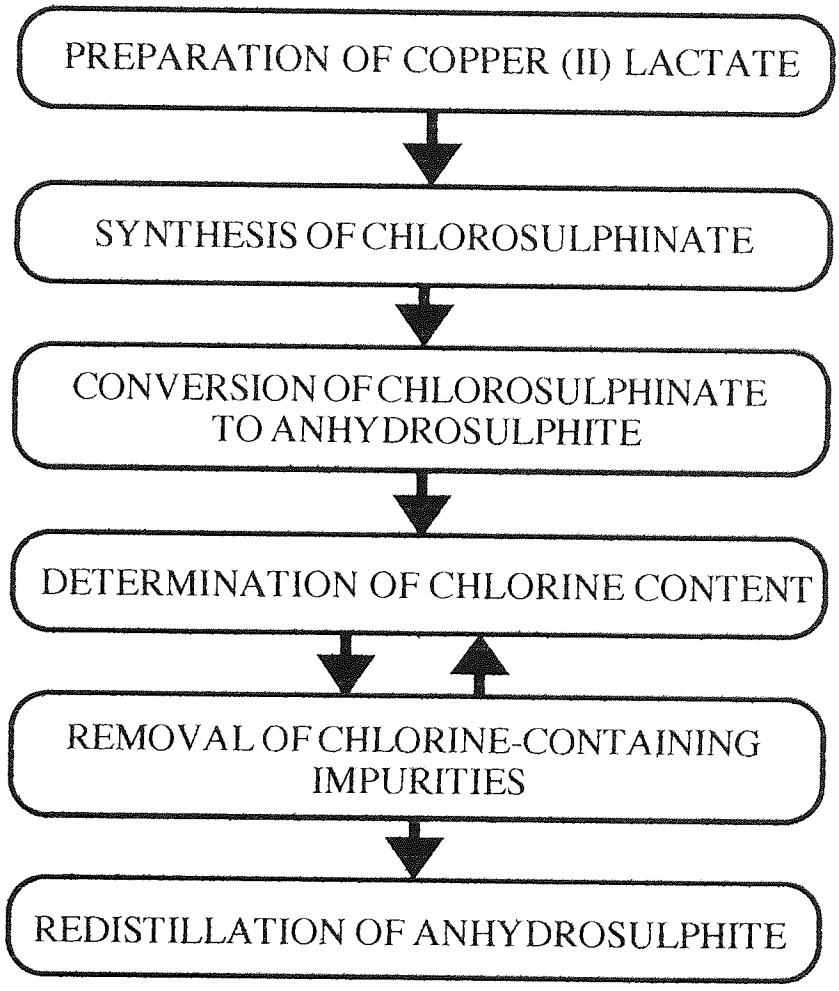

Figure 3.1 Schematic diagram of LAAS synthesis.

3.1.1 Preparation of Copper (II) Lactate

3.1.1.1 Experimental

In a typical synthesis, 400cm^3 (4 moles) of a 90% w/v solution of L(+) lactic acid (supplied by Aldrich) was neutralised by concentrated ammonia solution, and excess ammonia removed by heating the solution to boiling. After the solution was cooled to 0-5 °C, 341g (2 moles) of copper (II) chloride (supplied by BDH as the di-hydrate) dissolved in a minimum of methanol was added with stirring. A bright blue precipitate formed which was filtered off and washed with ethanol and diethyl ether. After drying in a vacuum oven at 30°C for 24 hours, the solid was powdered and drying continued at 90°C.

The yields were between 60-70% (based on lactic acid). An FT-IR spectrum of the salt was obtained (see figure 3.2) and compared with that of a small sample of copper (II) lactate supplied by BDH some years previously (production has since been suspended).

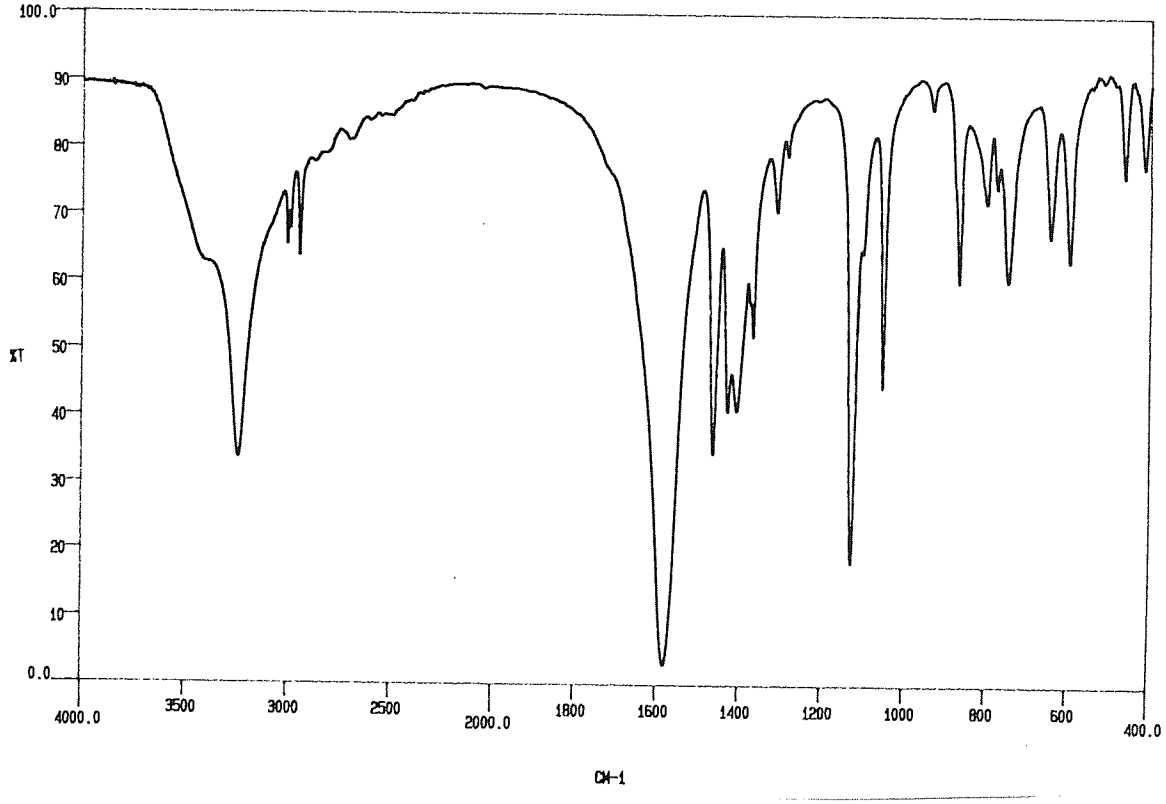

Figure 3.2 FT-IR spectrum of copper (II) lactate.

3.1.1.2 Discussion

The FT-IR spectrum of the product shows a carboxylate peak at 1581cm^{-1} and a C-H at 3239cm^{-1}. For comparison, lactic acid exhibits an intense carboxylate peak at 1787cm^{-1} and a hydroxyl at 3578cm^{-1}.[79]

In some experiments, an excess of copper (II) chloride was added in order to ensure maximum precipitation of the lactate. This tended to produce a greener product, contaminated by the copper (II) chloride. Washing with solvents (e.g. water, ethanol, ether, etc.) decreased the yield considerably as copper (II) chloride is not significantly more soluble than copper (II) lactate.

Direct reaction of lactic acid with copper (II) chloride does not produce copper (II) lactate. If the ammonium salt is first prepared, the desired product may be obtained. However, attempts to prepare the copper salt following the general procedure for α-hydroxy acid salt preparation described by Al-Mesfer[80] failed to produce a precipitate. This is probably because the lactate is more soluble than the mandelate prepared by Al-Mesfer from a 1M aqueous solution of mandelic acid. Modifying the procedure by using concentrated lactic acid and methanol as solvent successfully produced copper (II) lactate every time.

3.1.2 Synthesis of Lactic Acid Chlorosulphinate

3.1.2.1 Experimental

In a typical synthesis of lactic acid anhydrosulphite, 240g of dry copper (II) lactate was placed in a dry 1 dm^3 round-bottomed flask. The flask and contents were further dried at 70°C for 72 hours in a vacuum oven, then allowed to cool and released to atmospheric pressure by admitting dry argon. The apparatus shown in figure 3.3 was assembled in a glove bag, flushed with argon and 400cm^3 dry ether added to the copper (II) lactate to form a slurry. This mixture was cooled to 0-5° C by lowering the round-bottomed flask into an acetone/dry ice bath outside the bag. When cooled, 220cm^3 of thionyl chloride (supplied by BDH and re-distilled under argon immediately prior to use) was added dropwise, maintaining the reaction temperature between 0 and 5°C. The mixture was agitated by swirling and a glass stirring-rod used to break up aggregated solid. An exothermic reaction was observed as a colour change from blue-green to a dark reddish-brown accompanied the formation of anhydrous copper (II) chloride. After the addition was completed, the mixture was further agitated for 30-60 minutes.

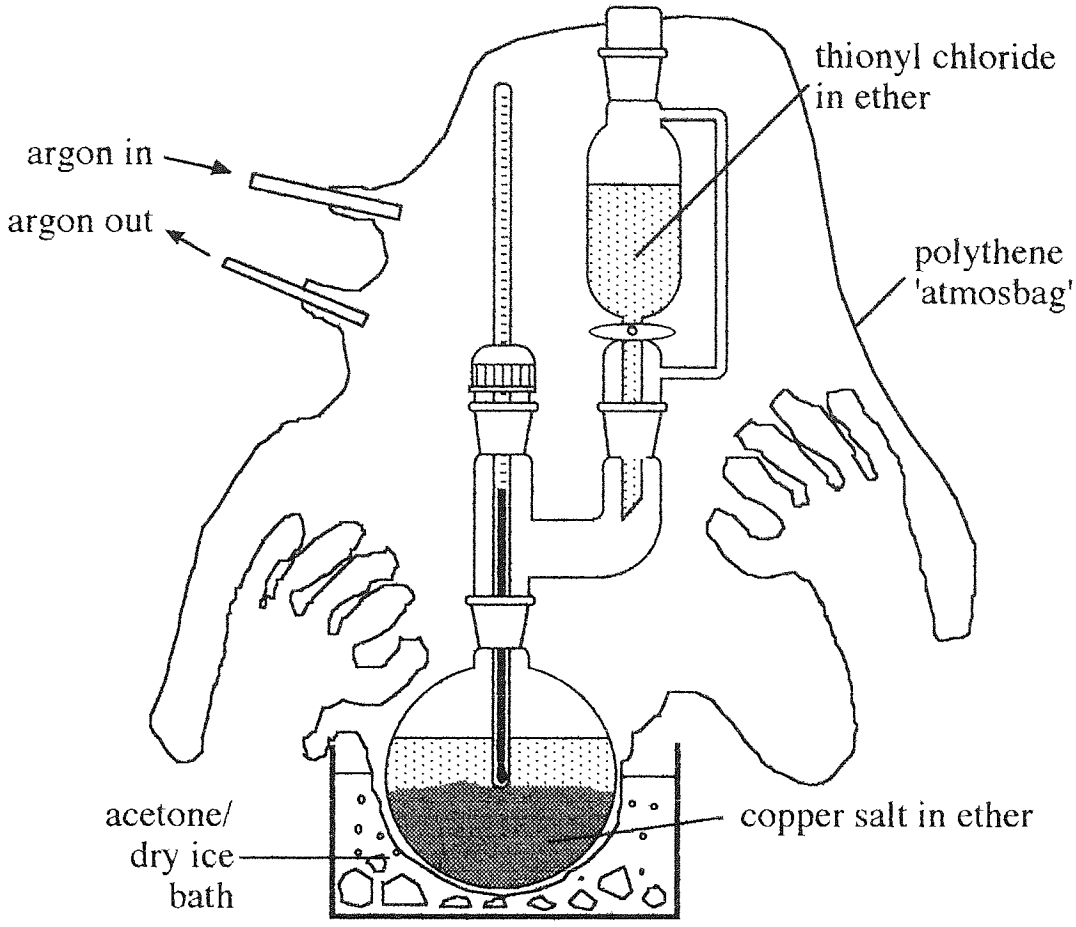

Figure 3.3 Apparatus for synthesis of lactic acid chlorosulphinate.

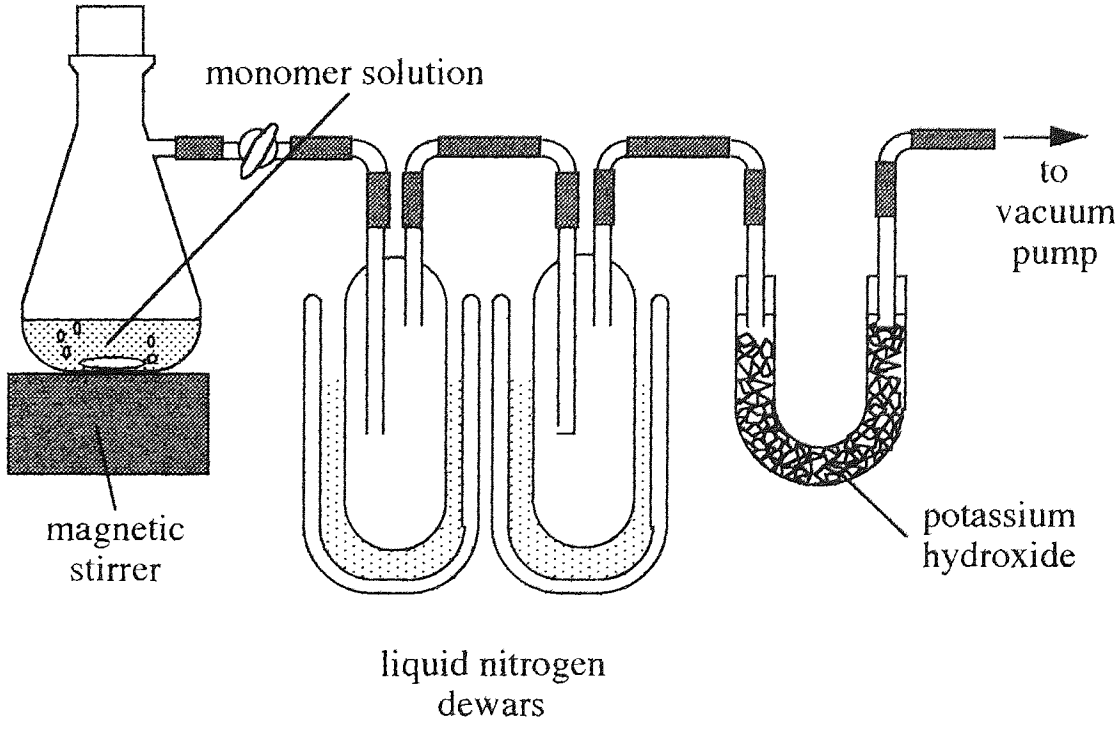

Figure 3.4 Apparatus for removal of volatiles.

The mixture was then filtered through a grade 4 porosity 'Quickfit'-jointed sintered glass Buchner funnel using a rotary vacuum pump. The pump was separated from the 'Quickfit' Buchner flask by an acetone/dry ice cold-trap and a potassium hydroxide 'U'-tube. The solid was rinsed with more dry ether before a magnetic follower was added and the stoppered flask removed from the bag and connected to the apparatus in figure 3.4. The solvent and unreacted thionyl chloride were removed by evaporation while the flask was cooled in an ice-water bath.

3.1.2.2 Discussion

The reaction of thionyl chloride with a hydroxyl substituent is normally used to replace the hydroxyl group with a chlorine atom. The anhydrosulphite synthesis takes advantage of this but traps the reactive intermediate precursor in the chlorination reaction. This precursor subsequently decomposes by thermal decomposition. Consequently, in preparation of the anhydrosulphite, the temperature of the reaction mixture is kept at 0-5°C in order to limit the production of impurities.

It is possible to prepare most anhydrosulphites by direct reaction of the parent α-hydroxy acid with thionyl chloride but it can be advantageous to use the copper (II) salt instead. Tighe suggests that aryl-substituted anhydrosulphites are best prepared by the latter route.[25]

The synthesis proceeds by way of a chlorosulphinate intermediate, which cyclises, eliminating hydrogen chloride to form the anhydrosulphite. A number of side-reactions may be observed, in which chlorinated by-products are formed by thermal decomposition reactions. Similar reactions are observed when thionyl chloride is reacted 'directly' with the parent α-hydroxy acid. Whether parent acid or salt are used, it is possible for thionyl chloride to react with either one or both the acyl C(1) and alkyl C(2) hydroxyl groups. However, using the copper (II) salt in place of the acid is thought to reduce the level of impurities for a number of reasons.

The mechanism for the reaction between copper (II) lactate and thionyl chloride is shown in figure 3.5.

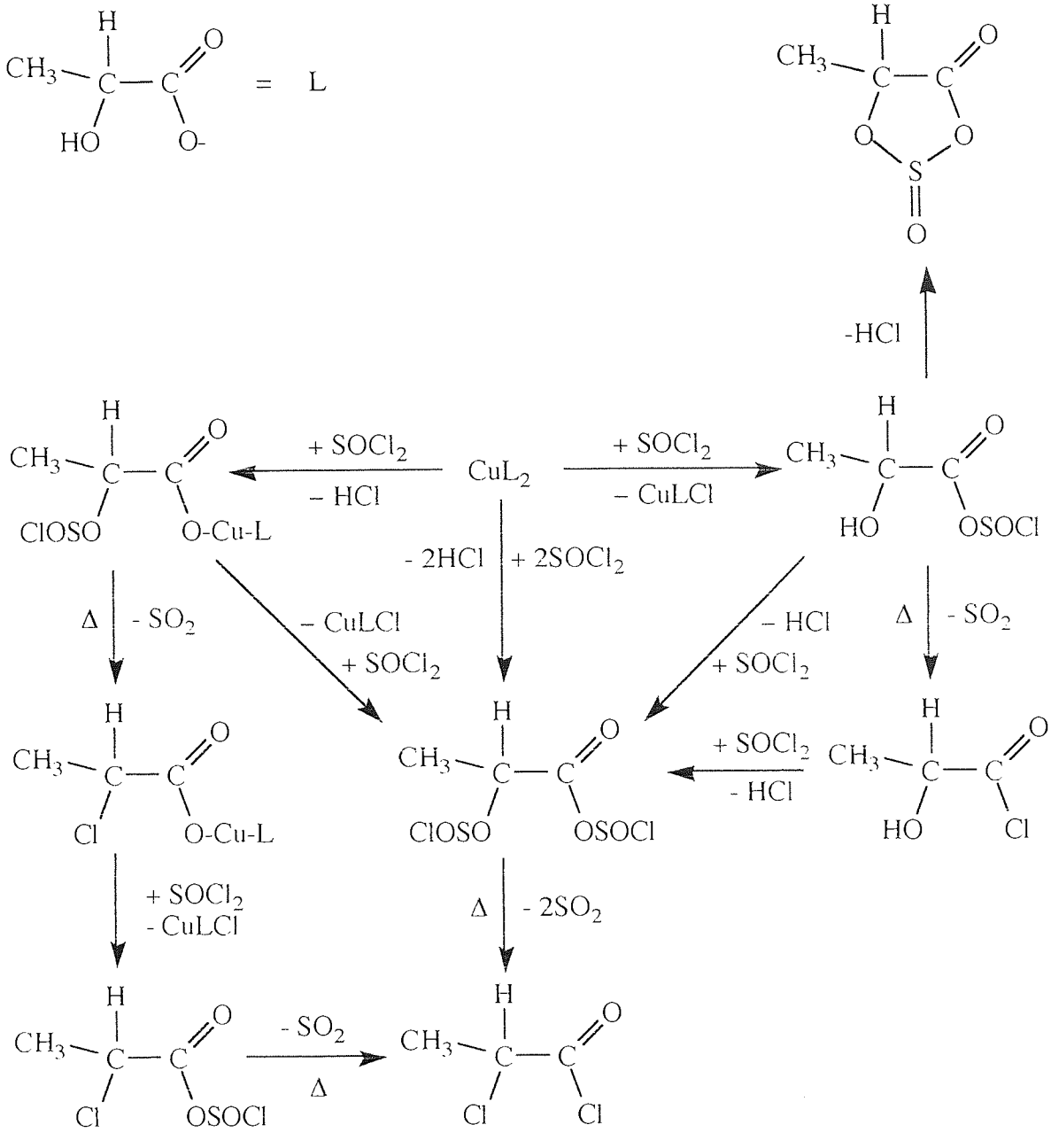

Figure 3.5 Reaction of copper (II) salt with thionyl chloride.

The thermal decomposition reaction affects both acyl and alkyl chlorosulphinates, resulting in the formation of chlorine-containing impurities. It occurs via an internal S_N2 mechanism involving nucleophilic attack on the carbon by the chlorine (as shown in figure 3.6). The acyl chlorosulphinate is thought to be more stable than the alkyl form and therefore less likely to eliminate sulphur dioxide, producing undesirable by-products.

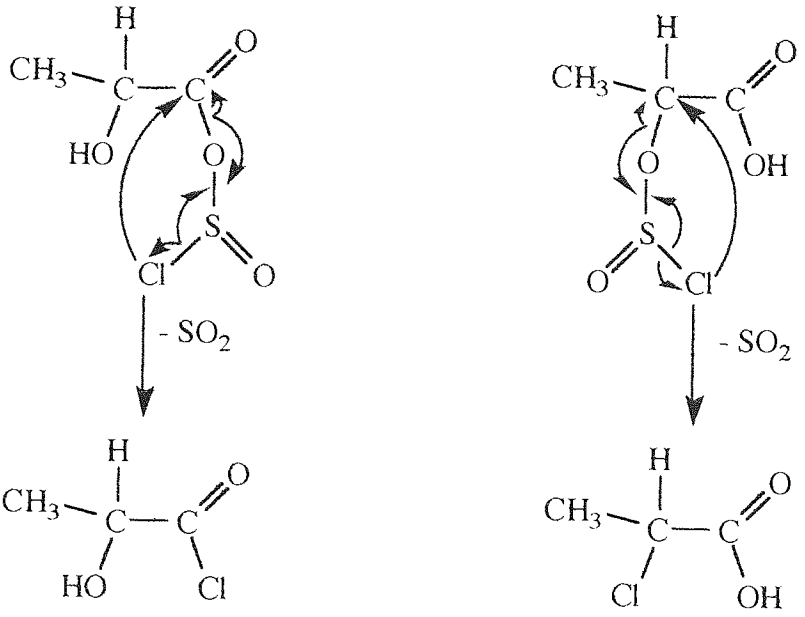

Figure 3.6 Elimination of sulphur dioxide from lactic acid chlorosulphinates.

If the copper (II) salt is used, the carboxylate anion attacks thionyl chloride preferentially to form the acyl chlorosulphinate. While attack by the α-hydroxy group is possible, it is likely to be appreciably slower than by the acyl group, since the hydroxyl is co-ordinated to the central copper ion (see figure 3.7), reducing electron density at the oxygen atom.

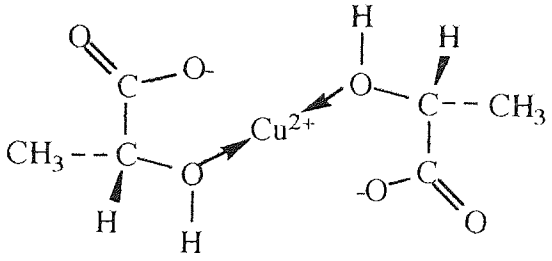

Figure 3.7 Structure of copper (II) lactate.

In contrast, a carboxyl group is more ionic in character, and reaction therefore likely to be more rapid. Since using the copper (II) salt promotes the formation of the more stable acyl chlorosulphinate, the level of thermal decomposition, and consequently the proportion of impurity present in the crude product, will be reduced.

The use of the copper (II) salt also offers other benefits. Firstly, such salts may be dried at a higher temperature than the parent α-hydroxy acid, creating a reactant which is more easily dried. This is particularly important in the case of lactic acid, where the parent acid

is very hygroscopic and only conveniently available as an aqueous syrup. Secondly, the chlorine-containing by-products of anhydrosulphite synthesis are more easily removed. Half the chlorine will be present as copper (II) chloride, which is insoluble in diethyl ether, and easily filtered-off as a reddish-brown precipitate. The precipitation of the by-product, effectively removing it from the system, should provide an additional 'driving force' for the reaction. This is also the reason for using a half-molar excess of thionyl chloride. It has been found that if too much thionyl chloride is used the level of chlorinated impurities produced is high. If too little is used, then yields are low.

It is possible that the benefits of using a metal salt might be greater still if copper was replaced with other metals. Use of lithium salts has been reported but appears to offer no great advantage over copper.[3 4] In fact, as no colour change in the white salt occurs, the reaction cannot be followed visually. Thomas attempted to produce glycolic acid anhydrosulphite (GAAS) using the sodium salt, with dimethyl sulphoxide as solvent, but results were not encouraging, with little (if any) product formed.[8 3]

3.1.3 Conversion of Lactic Acid Chlorosulphinate to LAAS

Cyclisation of the chlorosulphinate is achieved by rapid distillation at reduced pressure. A spinning-band column is particularly useful for this procedure as it allows the conditions of reflux and distillation to be controlled accurately. The use of the spinning band column is described in more detail in section 2.2.3.

3.1.3.1 Experimental

The flask containing the chlorosulphinate was opened under argon and the yellow liquid poured into a round-bottomed flask, from which it was distilled at reduced pressure (2-10mm Hg) using the spinning-band column. The fraction boiling at 41-44°C/5.5mmHg was collected. After distillation, the column was released to atmospheric pressure using dry argon.

3.1.4 Estimation of Chlorine Content

The chlorine content of the distilled anhydrosulphite was estimated by means of the potentiometric titration described previously (see section 2.3.5). Typical values for the crude product were between 5 and 15 % g.atom Cl/g.mol product. The chlorinated

impurities had to be removed before use in polymerization experiments since they are known to reduce the molecular weight of products significantly.

3.1.5 Removal of Chlorinated Impurities

Chlorine-containing impurities may be removed from some anhydrosulphites (e.g. HBAS) simply by distillation. However, under conditions of distillation, the boiling point of the impurity in LAAS is within a few degrees of the monomer, so this is impractical because rapid thermal decomposition of LAAS also occurs at these temperatures. Treatment with copper (I) oxide provides an alternative method of purification.

3.1.5.1 Experimental

50 g of anhydrosulphite was weighed under argon, into a 100 cm^3 conical flask and diluted with 50 cm^3 of dry tetrahydrofuran (or acetone). The solution was cooled by an ice/salt bath and a two molar excess, based on chloride content, of copper (I) oxide added. The mixture was kept cool, stirred for several hours and then left in a refrigerator overnight. The copper (I) oxide was removed by filtration through a grade 4 sintered-glass filter and the solvent removed as described previously. After re-distillation, the chloride content was determined by potentiometric titration, and if necessary, the treatment repeated.

3.1.5.2 Discussion

Copper (I) oxide was studied alongside other reagents for removal of chlorine-containing impurities from anhydrosulphite and found to be most effective. The results of this study are described and discussed more fully in section 3.3.1.

3.1.6 Characterisation of Product

The anhydrosulphite product was characterised by FTIR and NMR spectroscopy, before and after purification. Other methods of characterisation of the monomer are discussed in section 3.3.

3.1.6.1 Infra-Red Spectral Analysis

Figure 3.8 shows the FT-IR spectrum of the crude product, LAAS, before removal of the chlorine-containing impurities. 2-chloro-propionyl chloride is the most likely impurity and the intense carbonyl absorption at 1800cm^{-1} typical of acyl halides[81], is evidence of the α-chloro-acid chloride being present. The anhydrosulphite carbonyl absorbs at a slightly higher frequency.

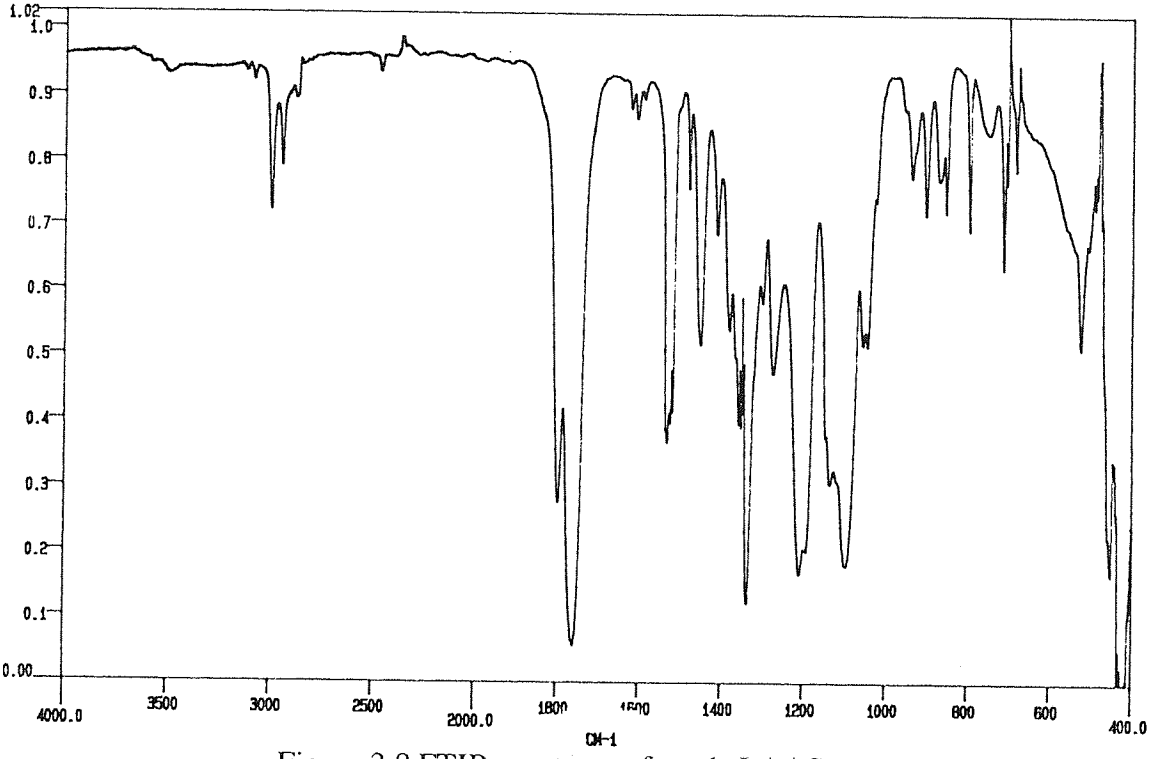

Figure 3.8 FTIR spectrum of crude LAAS

After removal of the chlorine-containing compounds, the characteristic strong anhydrosulphite carbonyl peak at 1824cm^{-1} can be seen, along with a less intense peak at 1241cm^{-1} due to the sulphoxide group and weak C-H stretching absorptions at 2946cm^{-1} and 2999cm^{-1}.

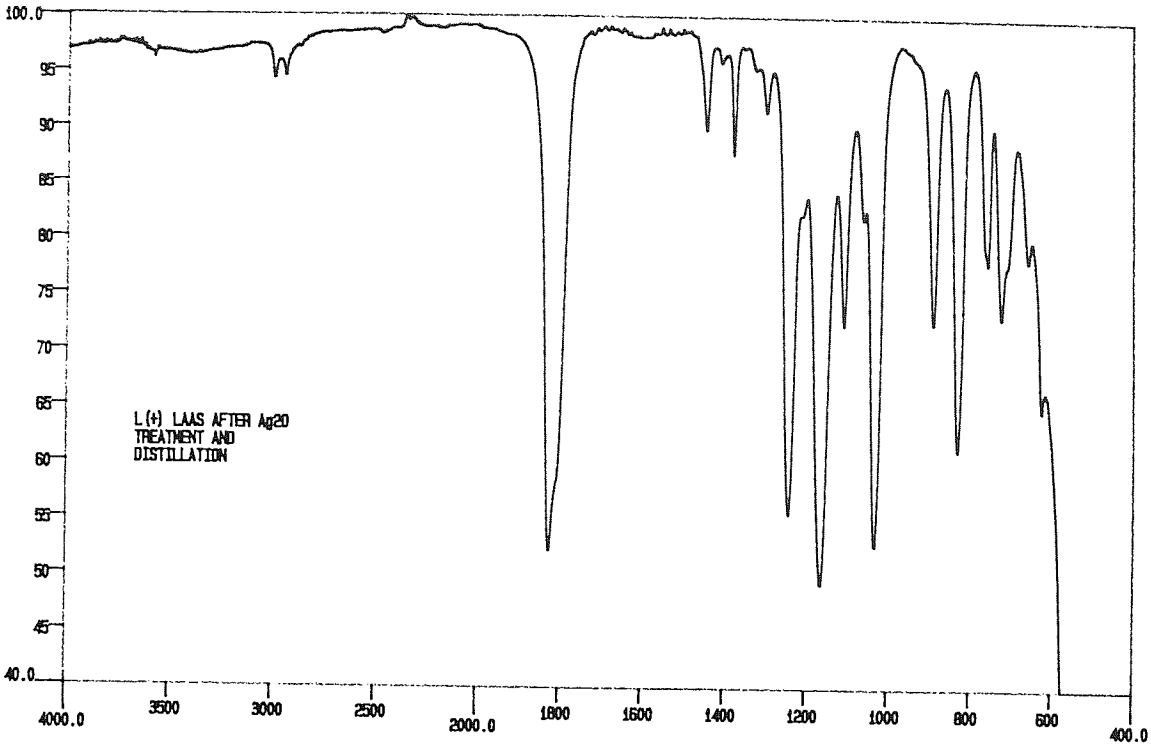

Figure 3.9 FTIR spectrum of pure LAAS.

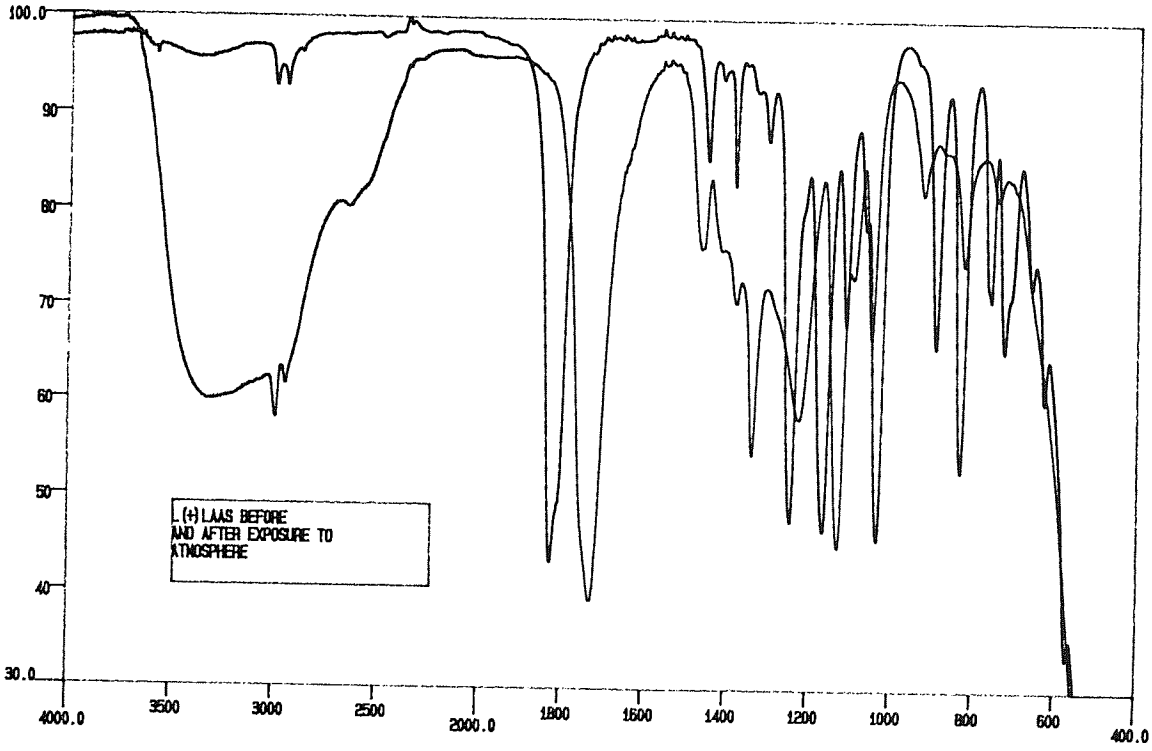

Figure 3.10 FTIR spectral overlay of pure and hydrolysed LAAS.

Figure 3.10 shows the FT-IR spectra of LAAS, both before and after exposure to atmospheric moisture for several minutes. After exposure, the anhydrosulphite carbonyl and sulphoxide disappeared, being replaced by a strong peak at 1728cm^{-1} and a broad strong absorption around 3000-3500cm^{-1}. These peaks are due to the lactic acid

carbonyl and hydroxyls, respectively, because the anhydrosulphite is rapidly hydrolysed to its parent acid.

3.1.6.2 NMR Spectral Analysis

Figures 3.12 and 3.13 respectively, show the ^{1}H and ^{13}C NMR spectra of purified LAAS. In both ^{1}H and ^{13}C NMR spectra LAAS exhibits more peaks than would be expected. This is probably because LAAS, in common with other anhydrosulphites, can exist in two conformations. The sulphoxide group is larger than a carbonyl and is forced out of the plane of the ring, distorting it as shown in figure 3.11. Since it can bend either above or below the plane of the ring, two orientations are possible. At temperatures where the rate of exchange between the two forms is slow, the magnetically non-equivalent environments of the carbons and hydrogens would give rise to double absorptions in the NMR spectra.

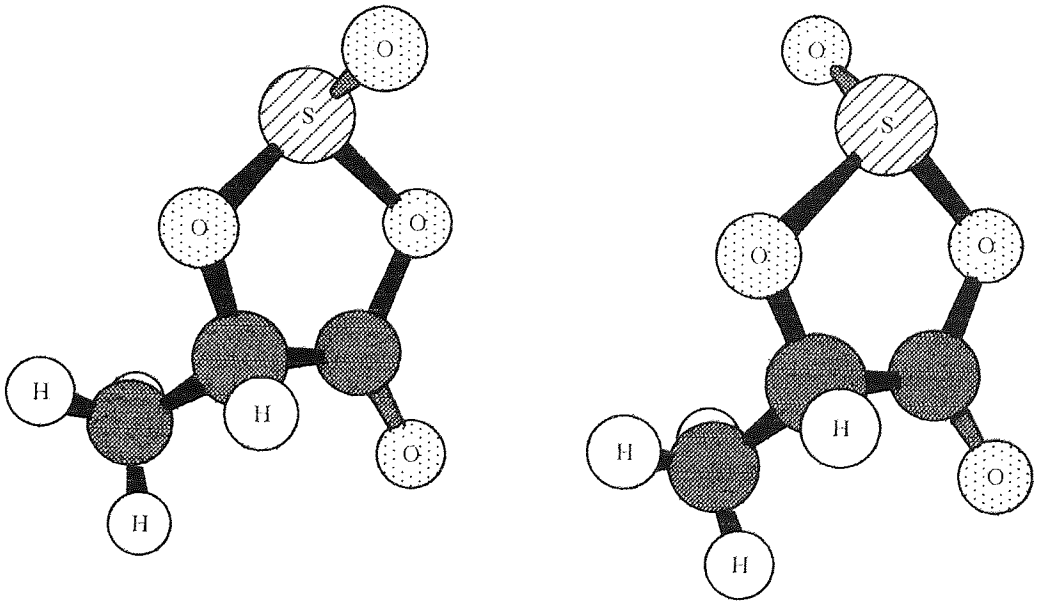

Figure 3.11 Alternative conformers of LAAS.

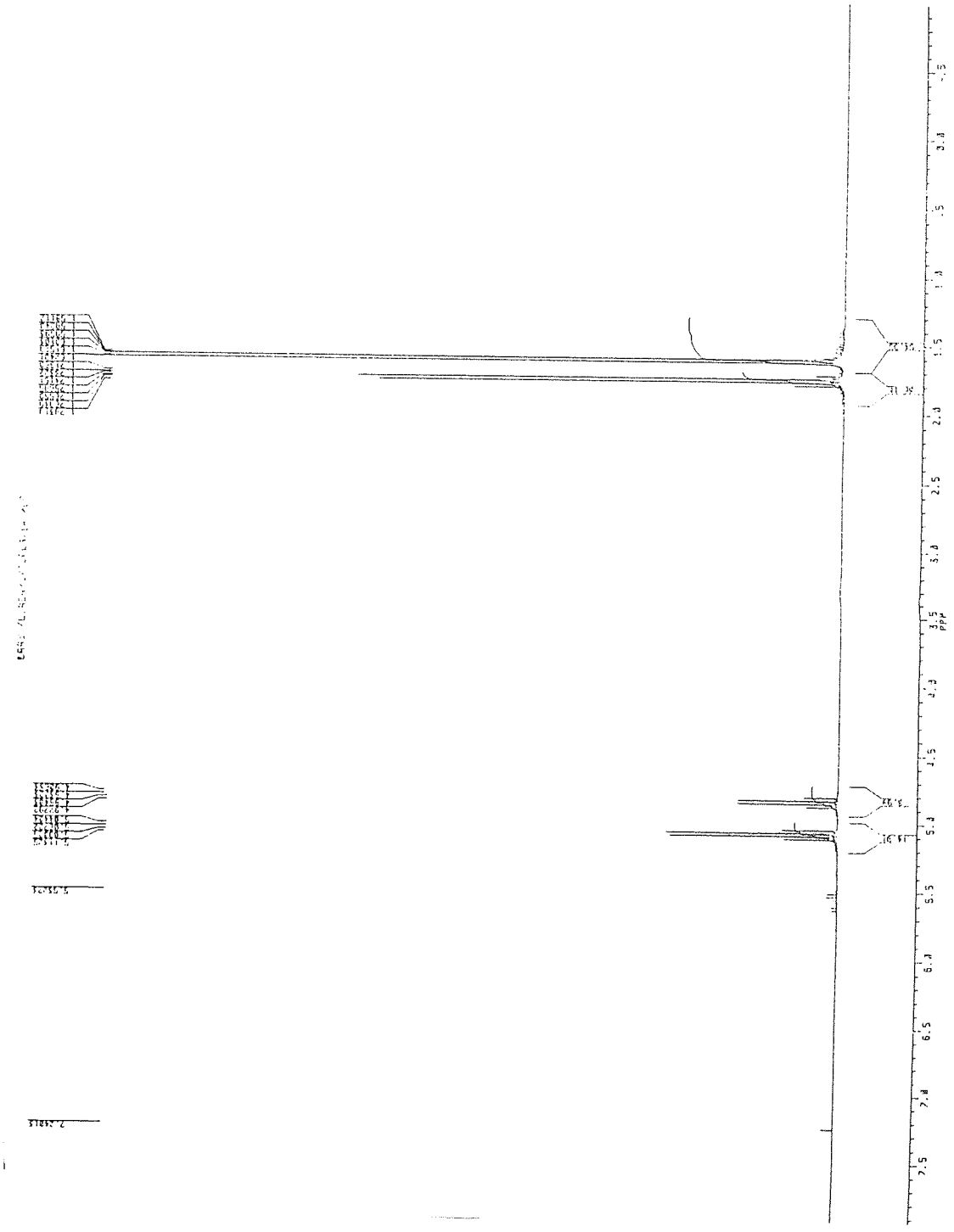

Figure 3.12 ^{1}H NMR spectrum of purified LAAS.

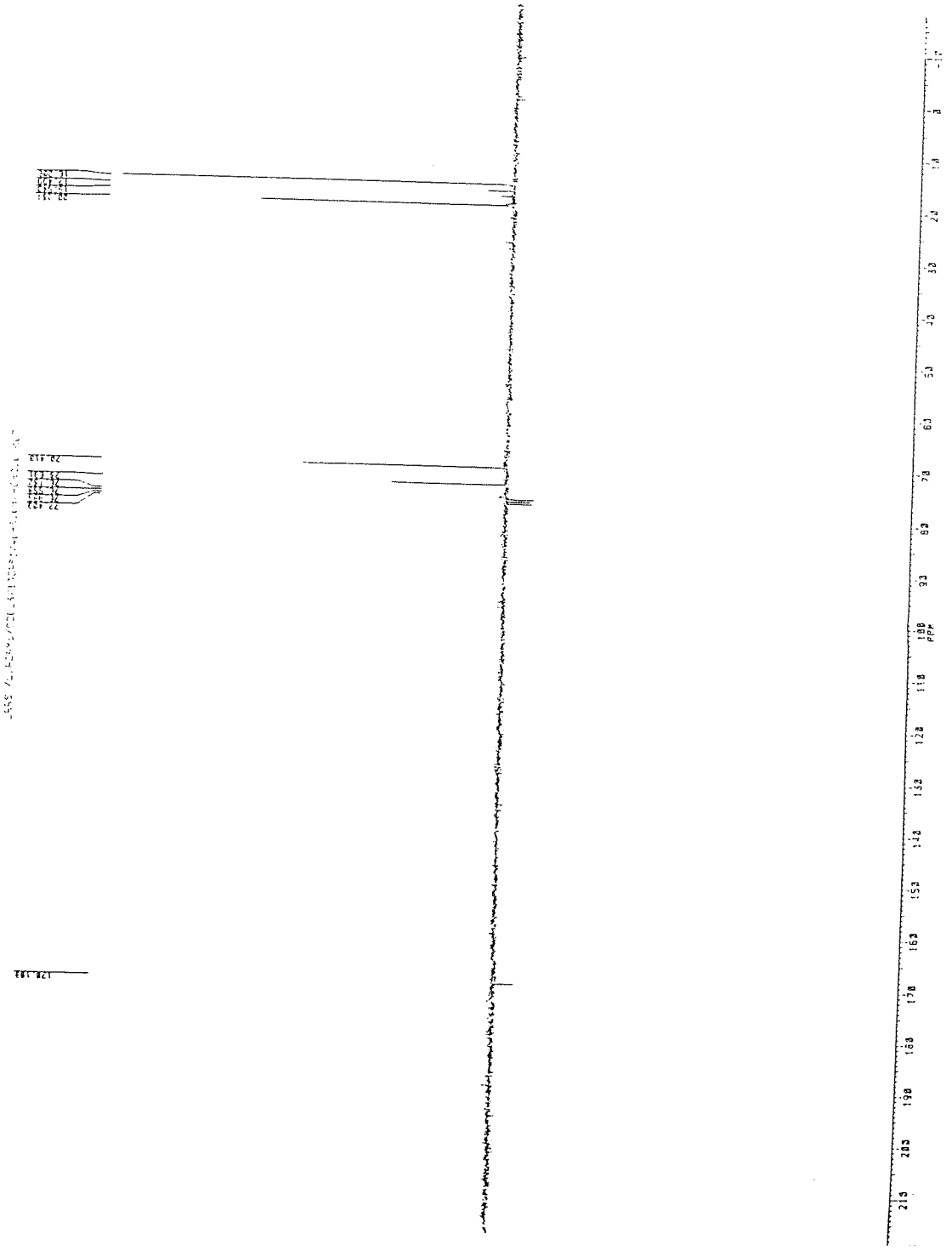

Figure 3.13 ^{13}C NMR spectrum of purified LAAS.

The NMR spectral data for LAAS is summarised in the peak tables below :-

Table 3.1 ^{1}H NMR spectrum of purified LAAS.

ppm	multiplicity	assignment	relative peak areas
1.60 - 1.62	doublet	CH_3	6.1
1.74 - 1.77	doublet	CH_3	4.0
4.81 - 4.88	quartet	C-H	1.0
5.04 - 5.11	quartet	C-H	1.7

Though the peak areas do not correspond exactly to the 3:1 ratio expected for the methyl and methine protons, respectively, the relative molar concentrations of each conformer, at the temperature the spectra is obtained, may be estimated from the relative peak areas due to the -CH and -CH_3 absorptions of the two conformers. From the data in table 3.1, the ratio of one conformer to another is calculated as approximately 3:2. It is reasonable to assume that the higher proportion is from the conformer where the sulphoxide is angled away from the methyl group, because this would be the less sterically-hindered, and thus energetically more favourable, conformation. This is consistent with the C-H chemical shift being displaced more than CH_3 by spatial coupling.

A spin decoupling experiment was performed by irradiating the LAAS sample with a strong radio frequency signal corresponding to the resonance frequency of the doublet at 1.74-1.77ppm. Only the quartet at 4.81-4.88ppm collapsed, proving that these absorptions were derived from protons attached to a common carbon i.e. from a -$CH(CH_3)$- group. It is reasonable to assume that the remaining methyl and methine absorptions are similarly associated with one another, being due to the alternative conformer.

Table 3.2 ^{13}C NMR spectrum of purified LAAS.

ppm	+/- intensity	assignment
16.21	12.2	CH_3
20.23	7.8	CH_3
70.42	6.2	C-H
73.69	3.7	C-H
170.11	-0.7	C=O

(Note. the three peaks at 73.7-77.4 ppm are due to the deuterated chloroform used as solvent).

The intensities of the methyl and methine carbon peaks are high and in the expected range. Two carbonyl absorptions (one due to each conformer) might be expected, but as carbonyls characteristically give a low intensity peak, that due to the less energetically favourable conformer may be masked by noise.

3.1.7 Redistillation of Lactic Acid Anhydrosulphite

3.1.7.1 Experimental

Before use in polymerization, the purified anhydrosulphite was redistilled at reduced pressure through a 10 cm column filled with 3 mm diameter raschig rings, into a Liebig condenser and the distillate collected in a weighed 10 cm^3 flask. B10 micro-distillation apparatus was used rather than the SBC since the volumes used were small. After the required volume was distilled (typically at 39 °C/2 mmHg), the apparatus was filled with dry argon and the flask stoppered rapidly. The flask was then re-weighed in order to determine the mass of anhydrosulphite and transferred to the glove box.

3.2 METHODS OF PURIFICATION AND ANALYSIS

Whilst distillation is effective in removing parent acid and oligomers from the monomer, it is only of limited usefulness in separating anhydrosulphite from chlorinated by-products. This is due to the thermal decomposition of anhydrosulphite and the close proximity of monomer and impurity boiling points. For this reason, the α-chloro-acid chloride is best removed by reaction with an added reagent to which the anhydrosulphite is insensitive. Thomas[82] investigated the use of mercury, copper (II) glycollate, triethylamine and silver (I) oxide in purifying glycolic acid anhydrosulphite. However,

only the latter two reagents were effective. Tighe[25] recommends the use of silver (I) oxide for aryl-substituted anhydrosulphites.

3.2.1 Effectiveness of Metal Oxides as Purifying Agents for LAAS

Qualitative experiments suggested that copper (I) oxide might be at least as effective as silver (I) oxide in removing chlorinated impurities from LAAS so parallel experiments were conducted using copper (I) and (II) oxides and silver (I) oxide, to assess their use in chlorine removal.

3.2.1.1 Experimental

Silver (I) oxide, copper (I) and (II) oxides were supplied by Johnson Matthey Materials Technology, Fisons and BDH, respectively, dried under vacuum at 130 °C overnight and allowed to cool under argon before use.

A sample of distilled anhydrosulphite of known chloride content was divided into three portions of 10 g each in 150 cm^3 conical flasks. Each sample was diluted with dry tetrahydrofuran and cooled in an ice bath before the addition of two molar excess of silver (I) oxide, copper (I) oxide or copper (II) oxide, based on moles of chloride ions present. The conical flasks were then stoppered and the stoppers sealed with plastic film and placed in a Camlab 'Transsonic' T310 ultrasound bath for 15 minutes. The flasks were removed from the bath, the stoppers checked and the flasks left overnight at -18 °C, in a freezer. After filtration to remove the oxides, evaporation of the solvent and distillation as described previously, the products were weighed to estimate yield, and purity determined by potentiometric titration, as described in section 2.4.1.

3.2.1.2 Results

Table 3.3 shows the percentage product (based on original mass of anhydrosulphite) remaining and chloride content after a single treatment with metal oxide. Each of the samples contained 6.6 % g.atom Cl/g.mol before treatment with metal oxide.

Table 3.3 Effectiveness of silver and copper oxides as purifying agents.

Oxide used	yield /% initial mass	chloride content/ % g.atom $Cl.g^{-1}.mol^{-1}$
Silver (I)	64.5	3.2
Copper (I)	89.0	1.1
Copper (II)	86.8	1.9

3.2.1.3 Discussion

Clearly, the copper oxides are considerably more effective at removing chlorinated compounds both in terms of the residual chlorine content and the amount of monomer lost during the purification process. However, it seems that the effectiveness of all oxides is limited to removing only a limited amount of impurity in a single experiment. In other experiments where the chlorine content was higher than about 10%, chlorine-containing impurities were only reduced to around 5% in a single treatment. In this case the monomer was best purified by fractional distillation initially, as oxide treatment will not be completely effective unless repeated.

Ultrasound treatment was used in all three experiments to disperse the solid and expose unreacted oxide by breaking down the surface and thereby increasing the effectiveness of the reagent. No apparent effect upon the anhydrosulphite was observed, which was kept at a reduced temperature in order to minimise decomposition.

While the use of copper (I) oxide was consistently found to be effective in purifying LAAS, there is an additional economic benefit in that copper oxides are obviously much cheaper than the silver equivalents.

3.2.2 Thin Layer Chromatography (TLC) Experiments

In the case of monomers such as gluconic acid anhydrosulphite, it is not possible to use distillation as a means of removing unwanted by-products. For this reason, the development of a means of removing chlorinated impurities, parent acid and oligomers, etc. without heating is vital. Chromatographic separation of LAAS from impurities has been attempted under anhydrous conditions. By performing the process in this way it was hoped that decomposition of monomer to parent acid could be avoided.

Thin layer chromatography was first used to assess the suitability of possible stationary phase and solvent combinations.

3.2.2.1 Experimental

Co-solvent systems were made up from dry tetrahydrofuran and cyclohexane in a range of proportions. Both aluminium oxide and silica gel TLC plates were investigated as separation media, supplied by Polygram and BDH respectively. Each plate was dried in an oven at 130°C before use and allowed to cool under argon. A sample was introduced to the TLC plate by means of capillary tube and the plate placed in a beaker containing a volume of solvent, so that the sample was above the liquid level. When the solvent front had reached a point approximately 1 cm away from the top, the plate was removed from the beaker and the solvent front marked. The plate was then removed from the glove box, sprayed with a 10% aqueous solution of silver (I) nitrate and exposed to ultra-violet light for 10 minutes. This developing agent caused the monomer and chlorine-containing impurities to show up as dark grey and brown regions, respectively. If observed under the ultra-violet light itself, these regions appeared orange and black, respectively. The nature of each spot was determined by performing TLC experiments using pure materials.

3.2.2.2 Results

Figure 3.14 shows a simple sketch of a typical TLC plate after development. The TLC traces all tended to have similar patterns with a long trailing trace for the anhydrosulphite and a smaller 'tear-drop' for the chlorine-containing impurities.

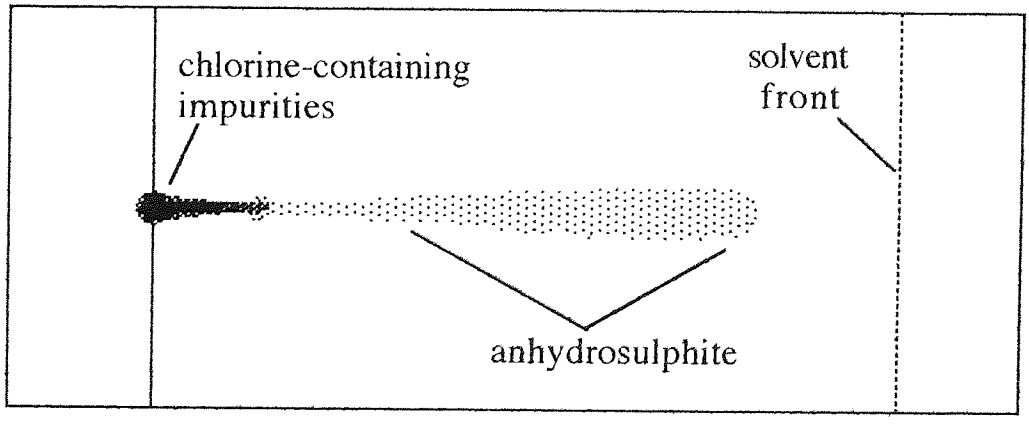

Figure 3.14 Sketch of a typical LAAS TLC.

R_f values, such as can be made when the components produce distinct spots, could not be determined in this case. Instead, the maximum distances travelled by the substances were measured and plotted to produce the chart shown in figure 3.15. The chart has been 'normalised' so that the solvent fronts are all equal and distances travelled by substances altered accordingly.

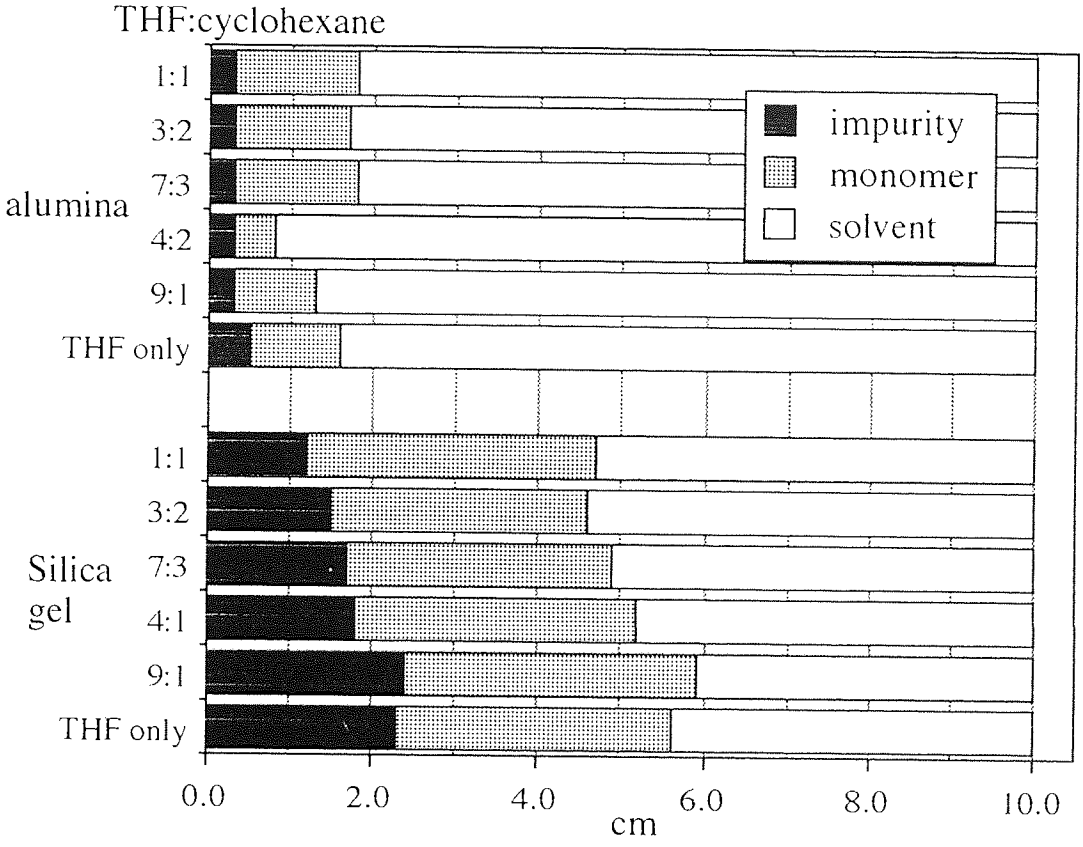

Figure 3.15 'Normalised' plot of TLC results.

3.2.2.3 Discussion

As neither anhydrosulphite, α-chloro-acid chloride, nor parent acid, are strongly coloured, a means of visualising the TLC plates was necessary. A 5 % m/v aqueous solution of palladium (II) chloride is often used as a developing agent for sulphur-containing compounds.[83] However, while this technique produced a yellow spot, the solution also turned the background pale orange making the spot unclear. Spraying with 5 % m/v alcoholic sulphuric acid solution followed by heating was more effective in producing a dark brown spot but it was not possible to distinguish between monomer and impurities. Exposure to bromine vapour in a developing tank was ineffective for the same reason. Spraying with silver nitrate solution followed by exposure to ultra-violet

light developed the plates most effectively, allowing monomer and impurities to be distinguished with a high contrast between spots and background.

Silica gel appears to be a better substrate than alumina as the distance travelled by the spots is generally further. Also, in more polar solvent blends, the solutes travelled further. While the impurity has a greater affinity for the adsorbant than the monomer, both appear to stick to the substrate, hence the long trace. This effect may be caused by decomposition of the monomer, though rigorous drying procedures were used. It is possible that H^+ ions on the surface of the stationary phase react with the monomer, causing it to decompose as it travels up the plate.

3.2.3 Two-Dimensional Thin Layer Chromatography Experiments

3.2.3.1 Experimental

Two-dimensional TLC (2-D TLC) experiments were also performed. In this technique, samples are spotted in the normal way, but onto a square plate. After the solvent front was marked, the square was turned through 90° and placed in a different solvent tray until the second front was marked and the plate removed for development.

3.2.3.2 Results

Two-dimensional TLCs were performed for both LAAS and lactic acid and these developed as shown by the sketches in figure 3.16.

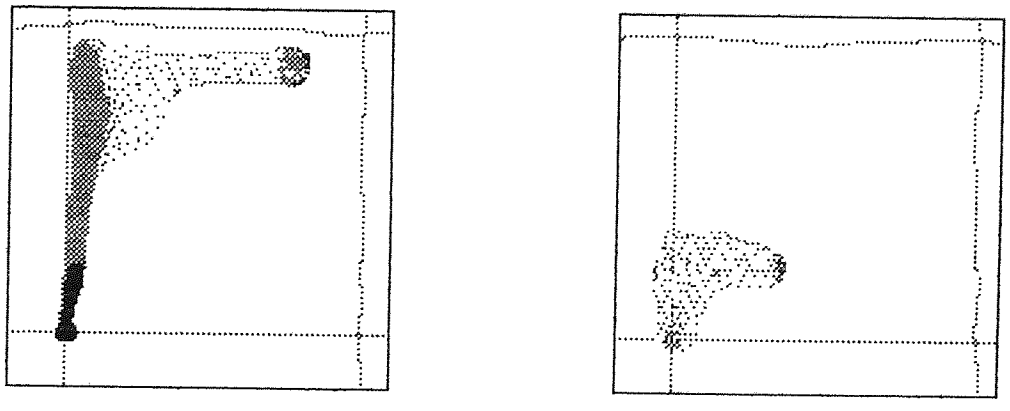

A. impure monomer

B. lactic acid

Figure 3.16 Sketches of 2-D TLC plates.

3.2.3.3 Discussion

The 2-D TLC of lactic acid shows a 'spot' which has travelled a shorter distance than in the case of LAAS, though it is just as blurred. This blurring might have been because lactic acid is a weak acid with an equilibrium existing between the covalent molecule to ion forms, each of which travel at a different rate. Alternatively, it may be simply adhering to the substrate but there is a distinct difference between the acid and anhydrosulphite. The 2-D TLC of the anhydrosulphite shows a distinctly 'L'-shaped trace, indicating that a single substance is being eluted and not a mixture, which would produce a number of spots in a diagonal formation.

The 2-D TLCs seem to show that all the substances present in impure LAAS have a strong attraction for the substrate to a greater or lesser degree. 'Dry Flash' chromatography was used to see whether it was possible to elute the monomer while leaving the impurities adsorbed on the column.

3.2.4 'Dry Flash' Chromatography

This is a form of column chromatography that uses suction rather than percolation or pressure, to force solvent through the column. This reduces the risk of bursting glassware and means that the procedure may be carried out rapidly in a glove-box using a hand-pump. It is also faster than percolation chromatography, and hence may help to reduce decomposition of monomer on the support.

3.2.4.1 Experimental

A grade 4 porosity sintered glass funnel (diameter 30 cm), with a 'Quickfit' joint was fitted to a Buchner flask, as shown in figure 3.17, and filled with a slurry of around 30 g of TLC grade silica gel in dry tetrahydrofuran. Suction was applied using a hand pump until the column was dry. It was then pressed down with a large stopper to ensure good packing and provide a smooth, flat surface. The column was loaded carefully with 10 g of LAAS dissolved in 25 cm^3 of a 3:7 tetrahydrofuran:cyclohexane (v/v) solution and sucked dry. This fraction was set aside and the column washed with 50 cm^3 portions of solvent systems of increasing polarity. 1:1 and 7:3 (v/v) tetrahydrofuran:cyclohexane solutions were used and finally pure tetrahydrofuran. The fractions collected were removed from the glove box and solvent removed from each in turn using the evaporation apparatus described in section 3.1.2.1.

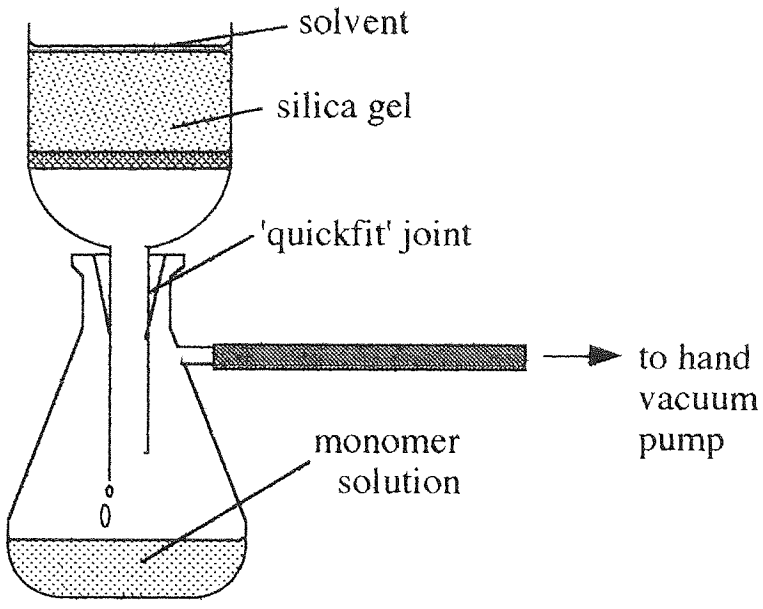

Figure 3.17 Dry-flash chromatography apparatus.

3.2.4.2 Results

After evaporation of solvent from each solvent in turn only very slight traces of a sticky residue remained in the Buchner flask.

3.2.4.3 Discussion

It appears that the affinity of the anhydrosulphite for the silica gel is too great for it to be removed from the column, even by pure tetrahydrofuran. Though some separation was observed in the TLC experiments the long traces would seem to confirm this conclusion. If an alternative substrate/solvent combination could be found chromatographic separation could prove a useful method of purification for anhydrosulphites.

3.2.5 GLC Assessment of Anhydrosulphite Purity

Gas-Liquid Chromatography (GLC) was examined as a possible means of conveniently and rapidly assessing monomer purity with sufficient accuracy to allow treatment with purifying agents e.g. copper oxides.

3.2.5.1 Experimental

Gas-Liquid Chromatography (GLC) of samples was performed using a Pye GCD chromatograph with a 'Chromosorb' column and nitrogen as carrier gas. The output from the flame-ionization detector was printed-out on a Hewlett Packard integrator.

Samples of undiluted LAAS containing different quantities of chlorinated impurities were injected at a constant column temperature of 130 °C with nitrogen as carrier gas.

3.2.5.2 Results

Figure 3.18 shows the GLC traces of three samples of LAAS containing:-

A 13% chloride,
B 8% chloride, and
C 2% chloride.

These results are also recorded in table 3.4 below.

Table 3.4 GLC analysis of impure LAAS - Peak areas.

Retention time	13% Cl	8% Cl	2% Cl	Assignment
0.67	23.6	0.3	0.3	diethyl ether
0.81	-	11.5	-	acetone
1.2-1.3	38.8	13.7	-	chlorinated impurities
3.0-3.3	37.5	74.5	99.7	LAAS

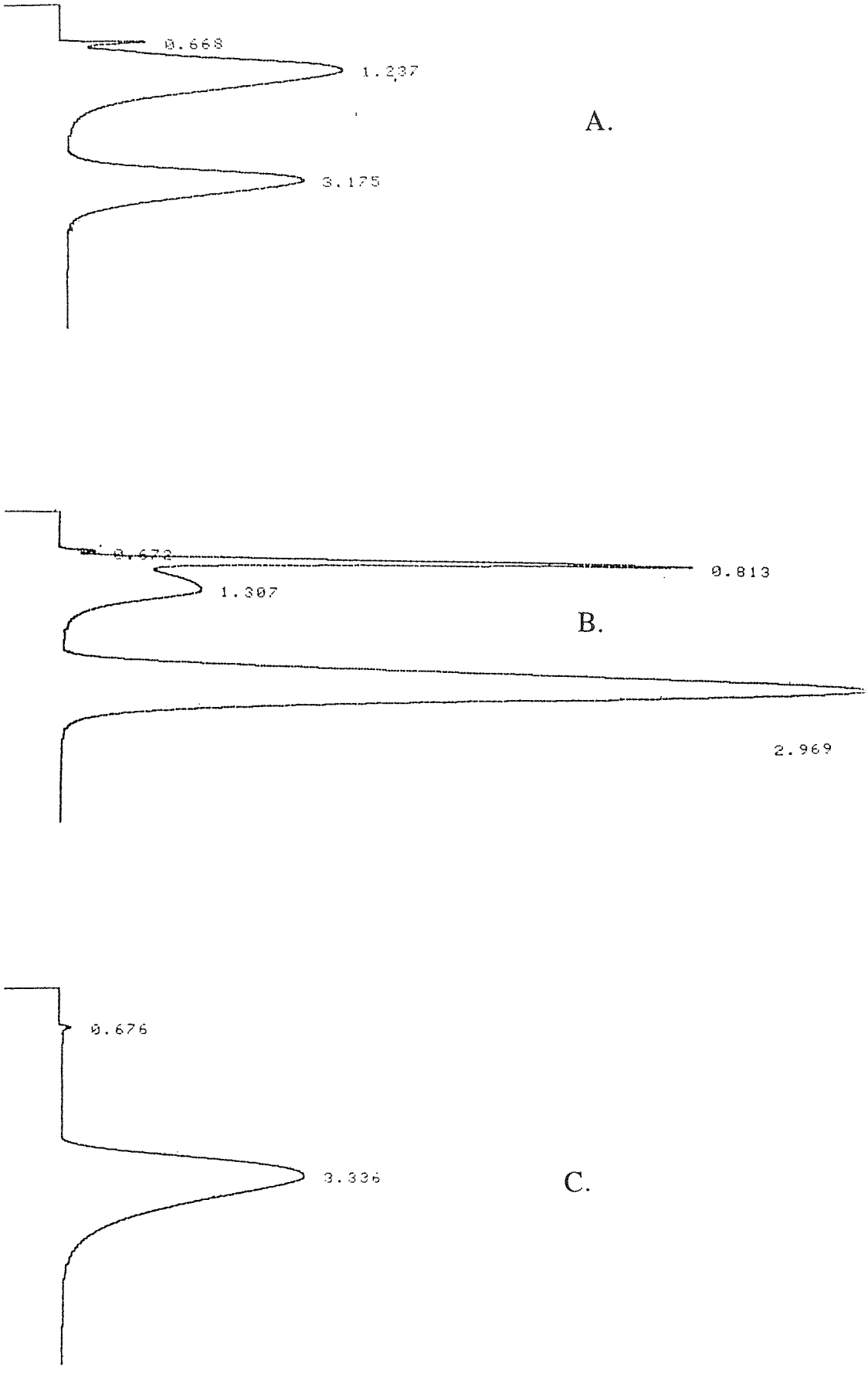

Figure 3.18 GLC traces of impure LAAS.

3.2.5.3 Discussion

The GLC traces (see figure 3.18) all show a small, sharp peak at 0.67 minutes. This is simply slight traces of the diethyl ether which is used to rinse the syringe between injections and may be disregarded. The broad peak centred at around 3.0 - 3.3 appears to be due to anhydrosulphite (it is probably broad due to decomposition occurring on the column). The peak at around 1.2 - 1.3 minutes appears to be due to the impurity. This is easily proved by comparison of the relative areas of the two peaks. While more convenient than potentiometric titration, GLC is less sensitive and was not used further.

3.3 SYNTHESIS OF GLUCONIC ACID ANHYDROSULPHITE

Biodegradable polymers with functionalised pendant groups are potentially very valuable as the side-chains could be used to attach drug molecules to the polymer backbone. Such a polymer would be useful as drug-release would be completely dependant upon the rate of polymer hydrolysis and largely unaffected by other factors such as mechanical breakdown of the polymeric drug-coating.

If the pendant chains contain a number of hydroxyl groups the poly-α-ester might behave like a 'hydrogel'. These soft elastic gel-like materials swell in water and are used in a variety of biological applications due to their high degree of biocompatibility. In the absence of water, hydrogels such as poly(hydroxy-ethyl methacrylate) are hard and glassy, but the hydroxyl groups present in this polymer will take up large quantities of water (even up to 80%[84]), creating a clear elastomeric gel. Hydrogels are able to mimic the surface properties of body tissue due to their high degree of hydrophilicity (which also causes high gas permeability). The surface structure of cells is complex, containing many chemical groups (including carbohydrates and proteins), unlike most polymers which are relatively simple. The presence of hydroxyl-bearing side-chains goes some way toward replicating the cell surface, making hydrogels valuable in applications where biocompatibility and gas-permeability is required, such as extended-wear contact lenses, artificial liver support systems and haemodialysis.[57]

Gluconic acid is an α-hydroxy acid in which one of the α-substituents is a hydroxyl-bearing alkyl group (R^1 = -$(CHOH)_3CH_2OH$, R^2 = H; see fig.1.1, p.18 for general structure of α-hydroxy acids). If it could be used to produce a linear poly-α-ester the polymer would have hydroxylated side-chains (as shown in figure 3.19, thus its surface properties might bear similarities to the hydrogels, whilst also being biodegradable.

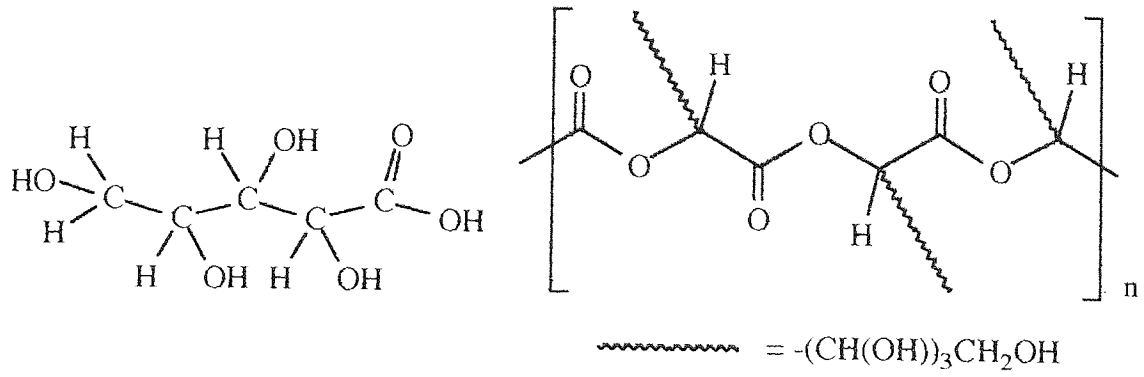

gluconic acid poly(gluconic acid)

Figure 3.19 Structure of gluconic acid and linear poly(gluconic acid).

Since gluconic acid is an α-hydroxy acid it may be possible to adapt the techniques used to prepare lactic acid anhydrosulphite to prepare the analogous gluconic acid anhydrosulphite.

3.3.1 Experimental

Initial experiments were performed using dry ether as solvent. In this case there was no colour change in the copper (II) gluconate, even after several days. After filtration and evaporation of the solvent, no product was found. Synthesis of LAAS had shown tetrahydrofuran to be a viable alternative to diethyl ether, and the copper salt seemed more soluble in this solvent, so the experiment was repeated, with the results described below.

177 g of sodium gluconate (0.81 M) (supplied by BDH) was dissolved in a minimum of distilled water and a solution of 68g of copper (II) chloride (0.4 M) in 400 cm^3 methanol added carefully. The resulting solution was stirred thoroughly and added dropwise, with stirring, to an excess of cold methanol. The pale blue-green precipitate was filtered-off and washed with fresh methanol. After drying under vacuum at 50 °C for 72 hours the product was found to weigh 111 g (0.24 g copper (II) gluconate), a yield of 60 %.

59 g (0.13 moles) of the dried, powdered copper (II) gluconate was placed in a 250 cm^3 round-bottomed flask and dried at 40 °C, under vacuum overnight. After the vessel was cooled and filled with dry argon, 100 cm^3 of dry tetrahydrofuran was added by distillation (from sodium metal and benzophenone). The slurry produced was placed into an ultrasound bath for 30 minutes and cooled to 0 - 5 °C by means of an ice bath.

25 cm^3 (0.26 moles) of re-distilled thionyl chloride was diluted by the addition of 50 cm^3 of tetrahydrofuran and the resulting solution added carefully to the copper salt, whilst the temperature was monitored. On addition of thionyl chloride, the slurry began

to change colour from pale blue-green to a brighter green and the temperature rose to about 15 °C. The vessel was stoppered and sealed with 'Parafilm' and left overnight in a refrigerator.

The next morning, the liquid had turned orange-red in colour but the bulk of the solid was still green. The flask was subjected to 30 minutes ultrasound, after which all of the solid had turned the reddish-brown characteristic of anhydrous copper (II) chloride. The solid was filtered-off by vacuum filtration through a grade 4 sintered-glass funnel and washed with dry ether. Addition of the ether caused a fine orange precipitate to appear in the filtrate. The yellow solution was re-filtered to remove this precipitate and solvent removed using the evaporation system described previously.

After one hour, the manometer reading on the evaporation system was <1 mm Hg, indicating that the greater part of the solvent had been removed. The bright yellow viscous liquid foamed easily under vacuum when warmed slightly. The 26 g of product was collected under argon and stored at -18 °C.

3.3.2 Product Analysis

The nature of the blue-green copper (II) gluconate prepared for use in synthesis of anhydrosulphite was confirmed by FT-IR. This spectrum was identical to that obtained from a small sample of copper (II) gluconate supplied by Aldrich, both having broad, strong carbonyl and hydroxyl absorptions at 1609 cm^{-1} and 3380 cm^{-1}, respectively (as shown in figure 3.20).

The sticky yellow product had a sweet ester-like smell that was less sharp than that of the lactic acid anhydrosulphite. A drop of benzylamine added (under argon) to a sample of the material caused the evolution of white fumes. The product's chlorine content was determined as 9.5 % based upon moles of GlucAS (gluconic acid anhydrosulphite), i.e. assuming no other impurities. Attempts to distil the product at reduced pressure failed, causing rapid decomposition but the 26 g of product was treated with a 2 molar excess of silver (I) oxide in dry acetone (it was found to be insufficiently soluble in ether). After treatment, the chlorine content was only 0.5 %. 12 g of product remained as a viscous, sticky, lime-green substance which foamed easily.

After evaporation of tetrahydrofuran and thionyl chloride, a sample of the product was subjected to FT-IR spectral analysis (see figure 3.21). A carbonyl at 1752 cm^{-1} with a strong shoulder around 1800 cm^{-1} was observed along with characteristic absorptions at 1216 cm^{-1} (sulphoxide), 2879 cm^{-1} and 2962 cm^{-1} (C-H), and 3471 cm^{-1} (hydroxyl).

After treatment with silver (I) oxide, the peak at 1752 cm^{-1} (and shoulder) were still present, but a peak at 1708 cm^{-1} was also visible (see figure 3.22). When exposed to atmospheric moisture, a carbonyl at 1633 cm^{-1} appeared and the hydroxyl absorption intensified (see figure 3.23).

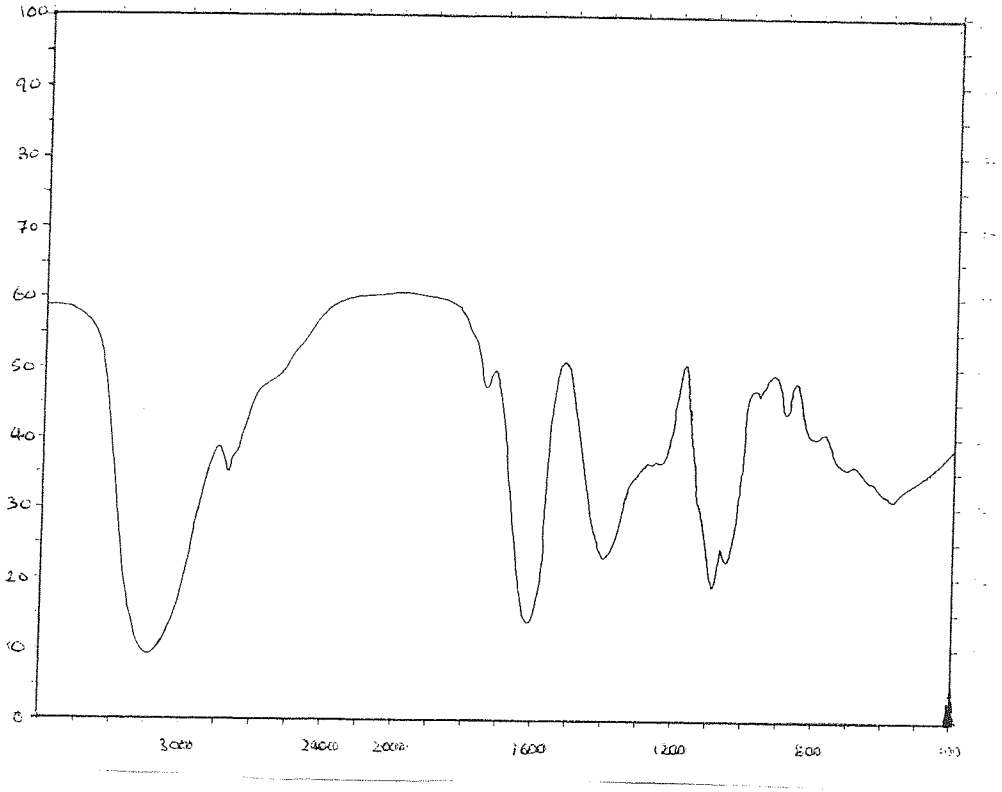

Figure 3.20 FT-IR spectrum of copper (II) gluconate.

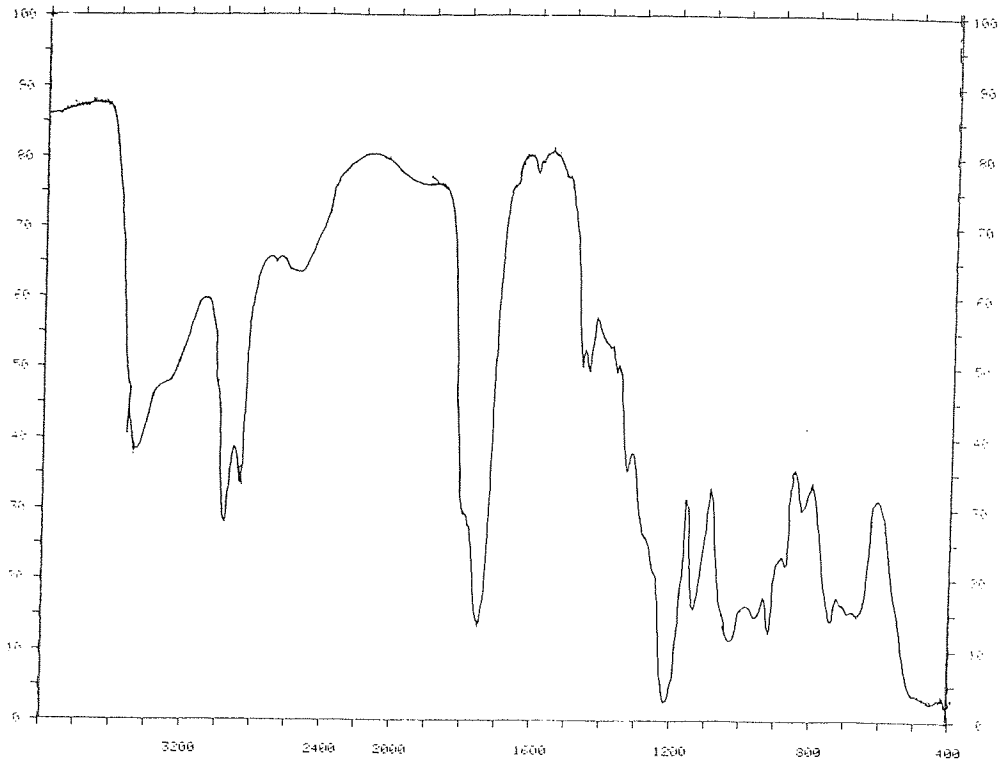

Figure 3.21 FT-IR spectrum of crude product of GlucAS synthesis.

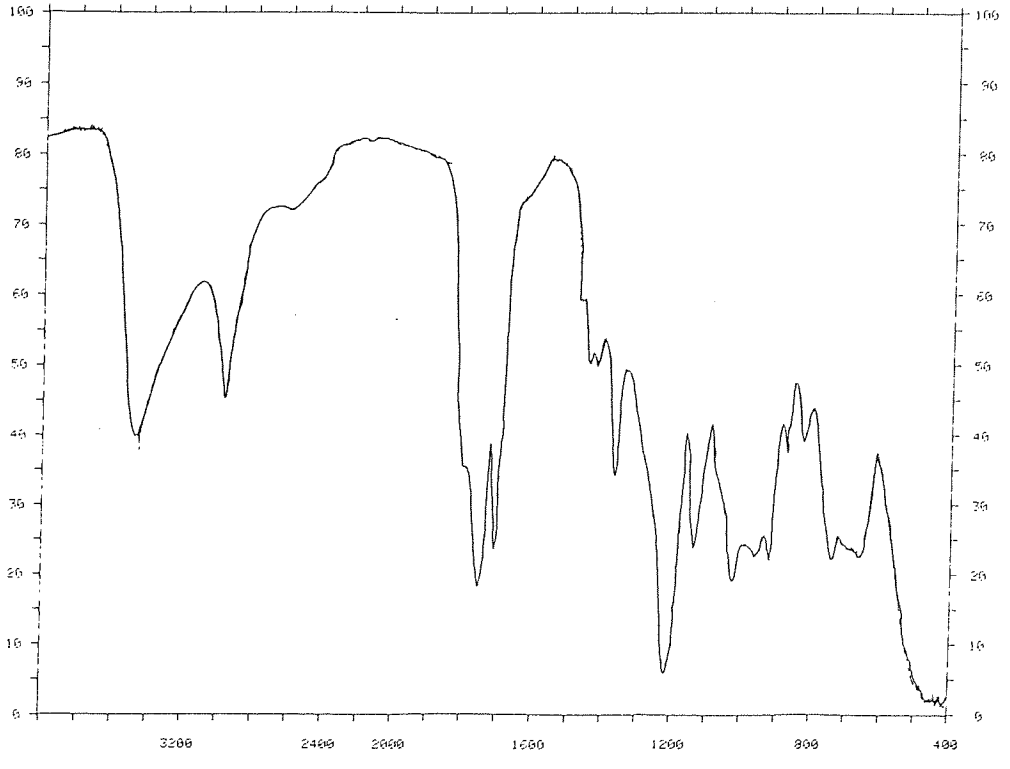

Figure 3.22 FT-IR spectrum of product of GlucAS synthesis after removal of chlorine-containing impurities.

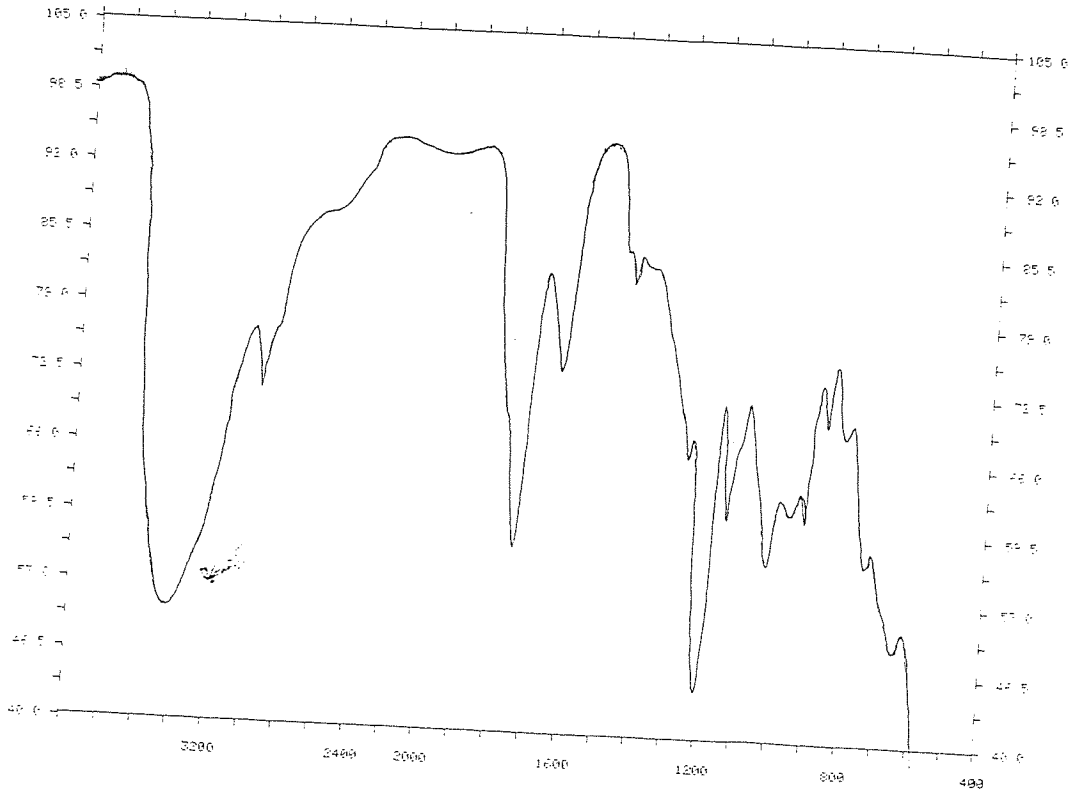

Figure 3.23 FT-IR spectrum of product of GlucAS synthesis after exposure to atmospheric moisture.

A second experiment was conducted in order to provide a sample for rapid NMR analysis (i.e. directly after isolation of the product, in order to minimise decomposition). This time the reaction occurred more rapidly, with the solid copper salt turning completely brown within 4 hours of addition of thionyl chloride (this may be because the second sample of copper (II) gluconate was powdered more finely). The product was purified as described previously. The sticky material produced was found to be insoluble in chloroform, so deuterated acetone was used to solvate the sample used for NMR analysis.

The ^{1}H NMR spectrum shown in figure 3.24 contains several very intense peaks which have been identified as deriving from tetrahydrofuran (1.82 ppm, 3.6 - 3.7 ppm) and acetone (2.02 - 2.08ppm), indicating a high concentration of the solvents still present in the product even after a number of hours evaporation at low pressure. A complex set of multiple hydroxyl absorptions (from the product mixture) can be seen overlapping in the region between 4.0 and 5.5 ppm.

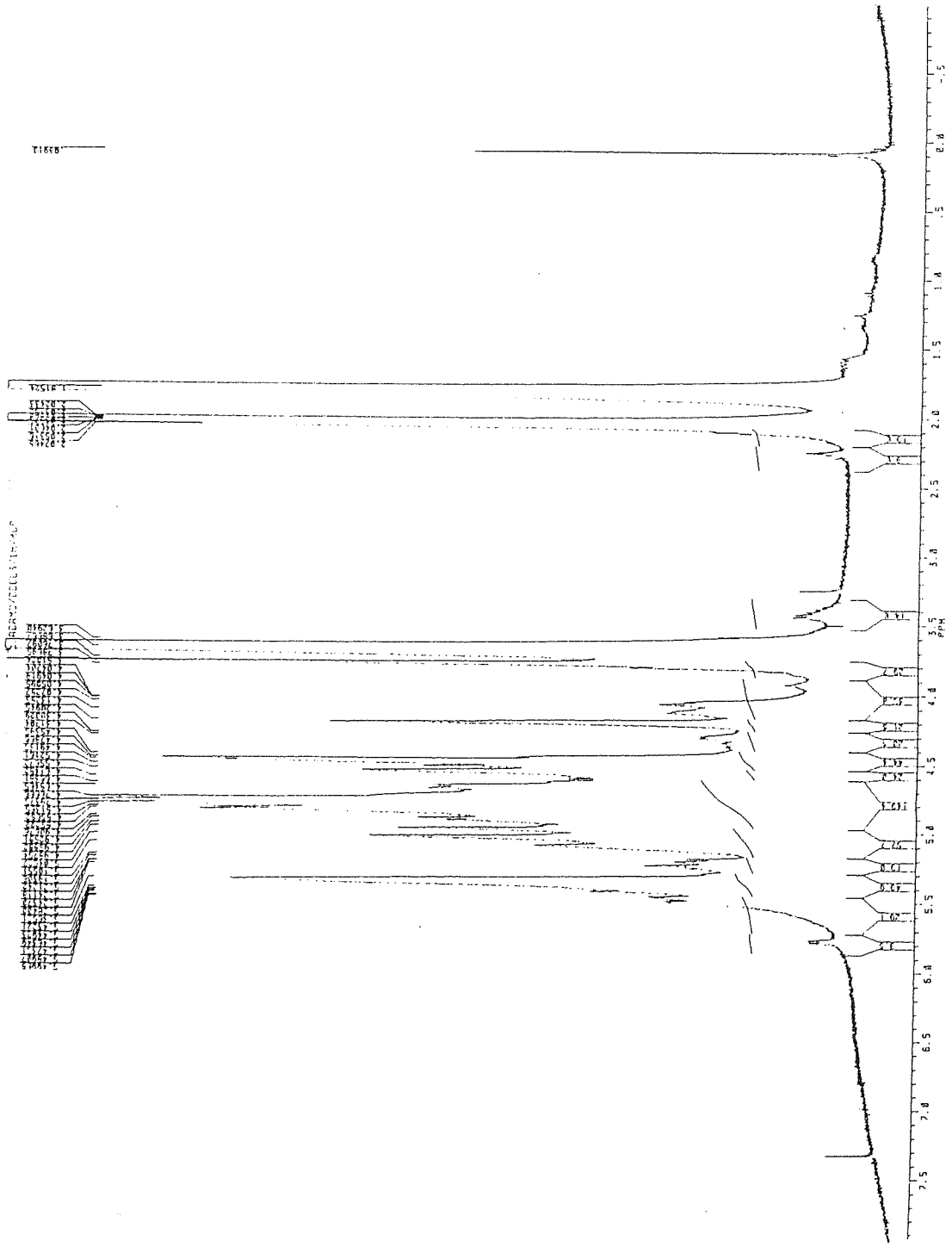

Figure 3.24 ^{1}H NMR spectrum of product of GlucAS synthesis.

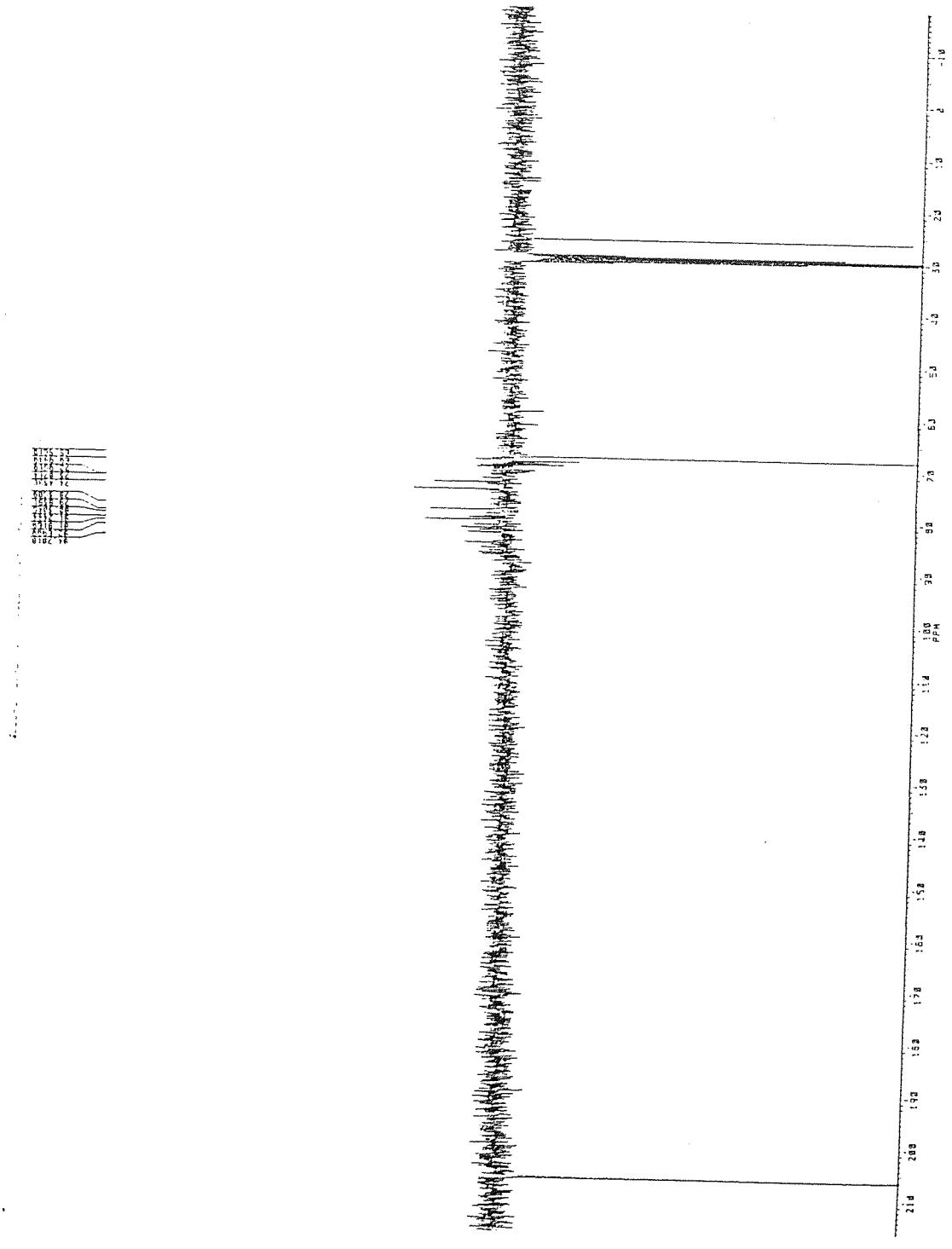

Figure 3.25 ^{13}C NMR spectrum of product of GlucAS synthesis.

The ^{13}C NMR spectrum (see figure 3.25) shows a strong set of peaks around 30 ppm from tetrahydrofuran and at 26 ppm and 208 ppm from acetone. The complex arrangement of peaks at 68 - 85ppm are from the product but as resolution is not good and the most intense peaks will be from parent acid, it is not possible to assign specific identities. The procedure for evaporation of volatiles was repeated but a second NMR spectral analysis showed that very little further solvent had been removed.

3.3.3 Discussion

The reddish precipitate of anhydrous copper (II) chloride indicates that the gluconate anion has been replaced by chloride. The copper (II) gluconate is probably more soluble in tetrahydrofuran than diethyl ether, bring both reactants into the same phase and allowing reaction to occur more easily. However, copper (II) chloride is also more soluble in tetrahydrofuran than in diethyl ether. The dissolved copper (II) chloride was precipitated on adding a small volume of diethyl ether to the product solution and re-filtering to remove the fine orange precipitate. The application of ultrasound has the effect of breaking up solid material, thereby reducing the particle size and exposing un-reacted copper (II) gluconate.

The crude product was contaminated with a high proportion of the parent acid, probably due to hydrolysis occurring after anhydrosulphite is formed. It seems likely that gluconic acid anhydrosulphite was formed by the reaction, since the characteristic carbonyl absorption was present as a 'shoulder' in the FT-IR spectrum of the crude product. Although the anhydrosulphite carbonyl often produces a peak close to that of the corresponding chlorinated α-hydroxy acid, the shoulder can assigned to anhydrosulphite with some certainty. This is because the shoulder's intensity is not diminished by removal of chlorine-containing compounds.

The additional carbonyl absorption observed after silver (I) oxide treatment is probably caused by the presence of acetone (used as a solvent during the treatment). Acetone has a carbonyl which appears at 1714 cm^{-1}. The viscous, sticky product was subjected to several hours further evaporation under vacuum, however residual solvent was still present. This is confirmed by the NMR spectra which also show the presence of tetrahydrofuran.

The strong carbonyl absorption around 1746 - 1752 cm^{-1} is derived from the parent acid and remains even after exposure of the product to atmospheric moisture.

The product's reaction with benzylamine is typical of that of an anhydrosulphite.[83] The product's sweet, ester-like odour however, is not. It is possible that this is due to the

product of a reaction between an anhydrosulphite carbonyl and a hydroxyl group from a second anhydrosulphite see figure 3.26.

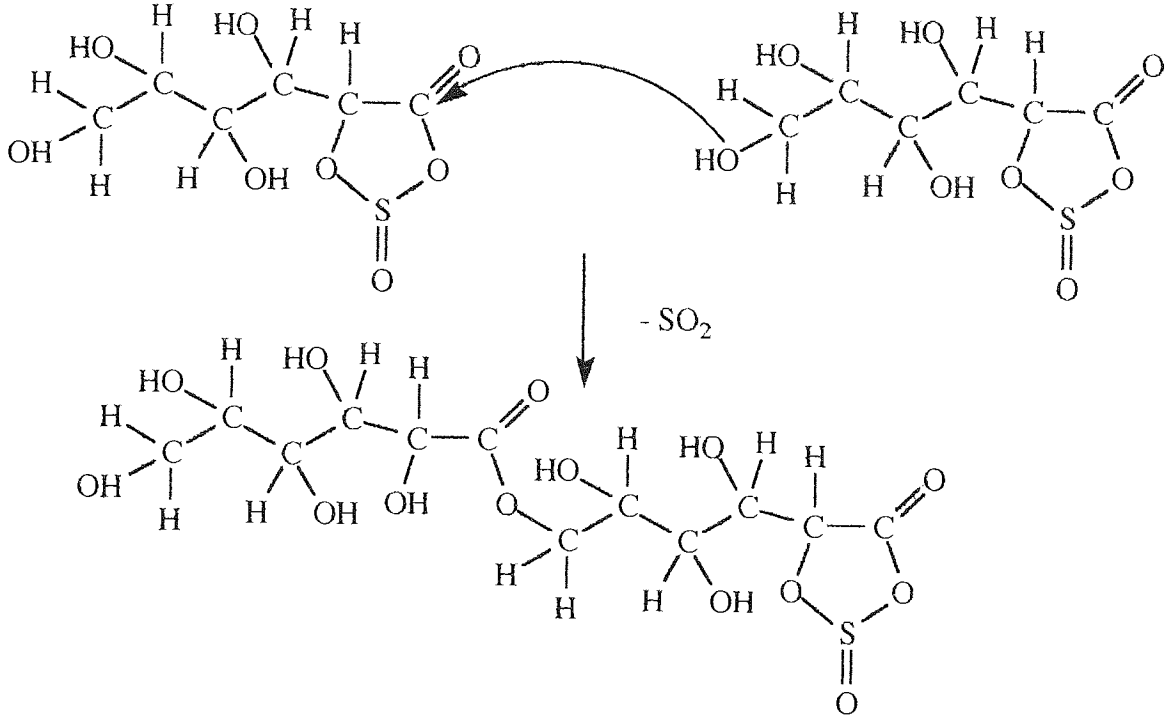

Figure 3.26 Possible reaction of gluconic acid anhydrosulphite.

In conclusion, it seems it is possible to produce an anhydrosulphite based on gluconic acid via this route but there are some difficulties to be overcome. There is a much greater tendency for hydrolysis to occur than is the case with LAAS so that the product is contaminated with significant quantities of the parent acid. Whilst treatment with silver (I) oxide was effective in removing chlorinated compounds, it was not possible to distil the anhydrosulphite, so an alternative means of separating the anhydrosulphite from parent acid and oligomers, etc. is needed. Chromatography has been investigated (using LAAS) with a view toward solving this problem and found to be unsuccessful as the monomer adhered to the column. It is not likely that an anhydrosulphite based on gluconic acid would yield a better result as the hydroxyl groups would probably have an even greater affinity for the chromatographic stationary phase.

CHAPTER FOUR

PRELIMINARY EXPERIMENTS

4.1 COMPARISON OF POTENTIAL ANIONIC INITIATORS

A number of known anionic initiators were selected for preliminary trials with LAAS, in order to identify a suitable initiator for further study. The initiators were as follows:-

(1) Aluminium *iso*-propoxide, (Al(Oi-Prop)3),
(2) Ethyl (5,10,15,20-tetraphenyl porphinato) aluminium, (Et(TPP)Al),
(3) Lithium *tert*-butoxide, (LiOt-But),
(4) Potassium *tert*-butoxide, (KOt-But),
(5) Sodium ethoxide, (NaOEt) and,
(6) Aluminium *iso*-propoxide/potassium *tert*-butoxide, (Al(Oi-Prop)3/KOt-But).

4.1.1 Experimental

An initial LAAS concentration of 1.46 M was used for each reaction. All monomer and initiator solutions were made up in nitrobenzene except those of lithium *tert*-butoxide, for which dry decalin was used. Previous studies have shown that lithium alkoxides are relatively insoluble in polar solvents such as nitrobenzene[85]. All of the initiator solutions contained undissolved solid and were subjected to ultrasound treatment in order to decrease particle size and hence improve homogeneity. This procedure caused the alkoxide solutions to become progressively darker, turning from yellow to brown over a period of 2 - 3 hours. Since the white alkoxide powder rapidly turned reddish-brown on contact with the solvent, it would appear that the colour change is associated with the formation of a charge transfer complex. This colour change was also observed over a period of several weeks in solutions of lithium *tert*-butoxide which were not subjected to ultrasound treatment.

The reactions were carried out in a water bath at 52 °C using the mercury manometer polymerization vessels described in section 2.3.1 and followed by measuring the height of the mercury in the manometer column with a bench cathetometer. When gas evolution had ceased, the reactions were terminated by injection of de-oxygenated methanol and the vessels opened. The product solutions were removed by syringe and left in a vacuum oven at 70 °C for several days, in order to remove the solvent prior to GPC analysis. All

of the experiments yielded glassy yellow solids except for Ethyl (TPP)Aluminium which produced a sticky purple liquid.

4.1.2 Results

4.1.2.1 Gas Evolution Data

Figure 4.1. shows the progress of the different reactions of LAAS with anionic initiator systems (as measured by gas evolution). Since the quantity of monomer used for each reaction was the same, the reactions may be compared by assuming that the final pressures of gas evolved would be identical. The reaction times are adjusted so that time, t, is taken as zero at the time when initiator was injected.

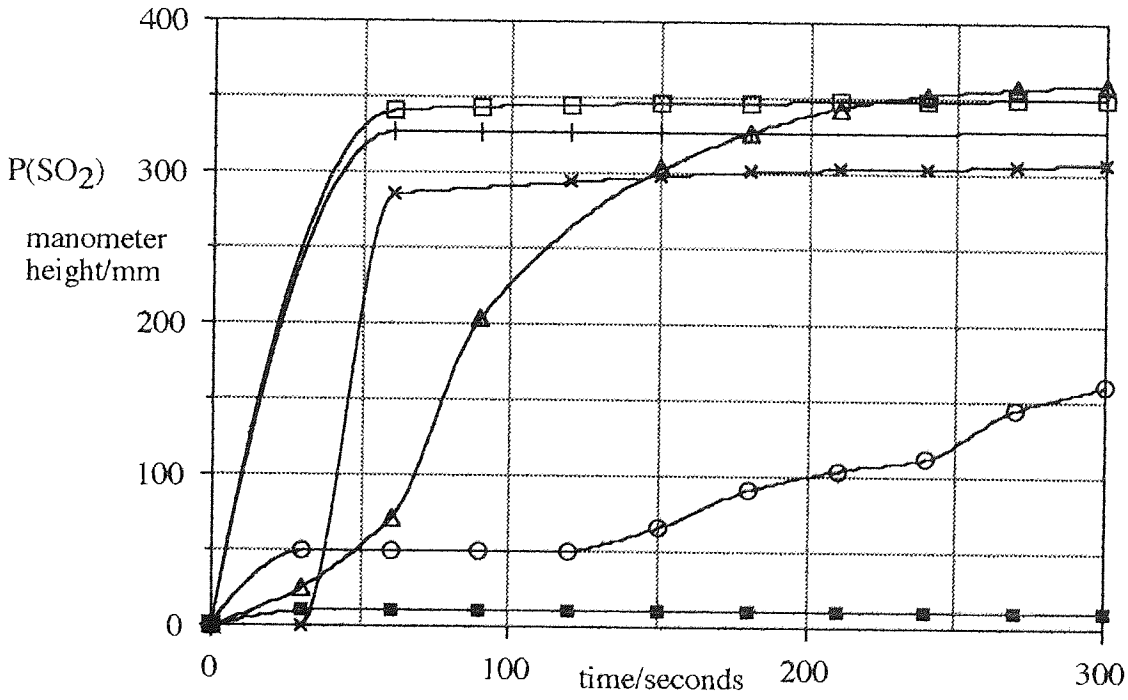

□ KOt-But, 0.041M,
× NaOEt, 0.047M,
○ Et(TPP)Al, 0.027M,
+ Al(Oi-Prop)3/KOt-But, 0.02.2/0.020M,
△ LiOt-But, 0.039M,
■ Al(Oi-Prop)3, 0.043M,

Figure 4.1 Decomposition of LAAS by anionic initiators - gas evolution graph.

4.1.2.2 GPC Analysis

The GPC analyses of the products were carried out in tetrahydrofuran as described in section 2.4.4. Weight and number average molecular weights, $\overline{M}_W$ and $\overline{M}_n$, and polydispersities, P_d, are recorded in table 4.1 as polystyrene equivalents, together with the complexity of the molecular weight distribution.

Table 4.1 Comparison of anionic initiators - GPC analysis of products.

Initiator system	[M]/[I]	Type of distribution	$\overline{M}_W$	$\overline{M}_n$	Pd
Et(TPP)Al	54	multi-modal broad	170	140	1.19
LiOt-But	37	narrow, high mw shoulder	2050	1450	1.42
KOt-But	36	narrow, high mw shoulder	2760	1970	1.40
NaOEth	31	multi-modal broad	540	320	1.70
Al(Oi-Prop)3/ KOt-But	73/66	bi-modal, equal intensity	660	450	1.46

(Note. No product was obtained from the reaction using aluminium iso-propoxide only).

4.1.3 Discussion

Ethyl (TPP) aluminium caused relatively slow decomposition of LAAS to produce material of low molecular weight and complex distribution. It was not possible to purify the product significantly, making it unsuitable as an initiator since such a highly coloured and contaminated product was obtained.

Lithium and potassium *tert*-butoxides both caused decomposition at reasonable rates and appeared from GPC analyses to be the most promising initiators. While sodium ethoxide caused rapid decomposition, the product was of lower molecular weight and greater polydispersity.

Decomposition of the monomer was most rapid in the case of the potassium *tert*-butoxide initiator systems, both with and without aluminium iso-propoxide. Aluminium *iso*-propoxide alone caused no gas evolution, even though monitoring was continued for 72 hours. Polymerization of LAAS initiated by a 1:1 ratio of potassium *tert*-butoxide and aluminium iso-propoxide was attempted, since bi-metallic alkoxides have been shown

previously to decompose anhydrosulphites, including that derived from lactic acid.[34] In Penny's work zinc and aluminium bi-metallic oxo-alkoxides, having the general formula $(RO)_2Al\text{-}O\text{-}Zn\text{-}O\text{-}Al(OR)_2$, where R is an alkyl group, were synthesised by the reaction of zinc acetate and aluminium *tert*-butoxide in dry decalin. However it is possible to prepare various μ-metallic alkoxides by direct reaction of the individual alkoxides (see figure 4.2).[86]

$$MOR + M'(OR')_3 \longrightarrow M[M'(OR')_3OR]$$

where M and M' = metallic counter-ions
and R and R' = alkyl groups

Figure 4.2 Synthesis of μ-metallic alkoxide.

The combination initiator system contained only half the concentration of potassium *tert*-butoxide compared with the potassium *tert*-butoxide only system. This is significant since the combination system decomposes LAAS at a rate which is at least equivalent to that of potassium *tert*-butoxide alone. It may be that the aluminium *iso*-propoxide activates the potassium *tert*-butoxide by increasing its solubilisation, however it may be that any difference between the rates of reaction was not detectable in such rapid reactions. The molecular weight of the product of the combination system-initiated decomposition is certainly of lower molecular weight than that from pure potassium *tert*-butoxide.

4.2 EFFECTS OF DIFFERENT COUNTER-IONS ON RATES OF POLYMERIZATION

Since the alkoxides seemed to be the most promising initiators, further experiments were performed in order to compare the effects of different counter-ions upon the decomposition of LAAS.

4.2.1 Experimental

Initiator and monomer solutions were prepared as described in the previous experiment. Since sodium *tert*-butoxide was not readily available in sufficient purity, the ethoxide was

used instead. The polymerization reactions were conducted as before, using mercury manometer polymerization vessels in a water bath at 48.5 °C. After decomposition had stopped, a sample was removed by syringe, injected into an FT-IR solution cell and analysed by infra-red spectrography. De-oxygenated methanol was added to the remaining portion of the reaction mixture and solvent removed as described previously.

4.2.2 Results

Figure 4.3 shows the effects of different alkoxides on the rate of evolution of sulphur dioxide.

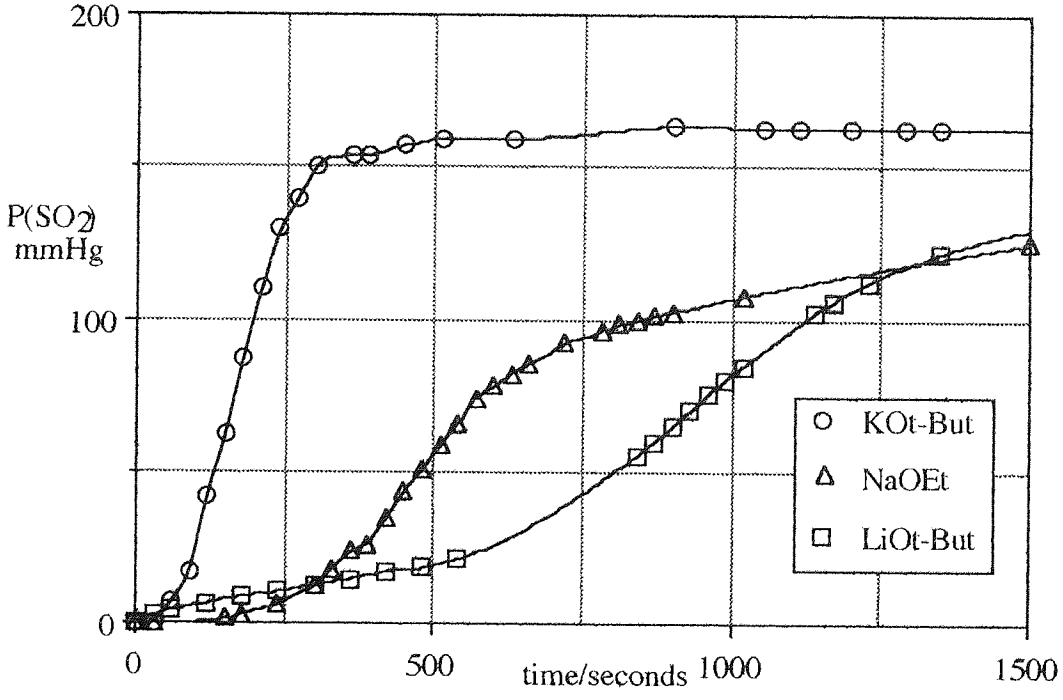

Figure 4.3 Decomposition of LAAS by alkali metal alkoxides - gas evolution graph.

4.2.3 Discussion

The potassium salt appears to cause the most rapid decomposition of LAAS. In the experiments using the lithium and sodium salts a higher concentration of initiator was used, yet the rate of decomposition was still slower than that caused by the potassium salt. The polarity of the counter-ion exerts a significant influence on the reactivity of the initiator and propagation species towards monomer because a more electropositive

counter-ion will cause the metal-alkoxide bond to become more polarised. This can be seen as a shift in the equilibrium of the initiator in solution towards more reactive, dissociated species.

4.3 EFFECT OF CROWN ETHER ON THE POTASSIUM *tert*-BUTOXIDE INITIATED DECOMPOSITION OF LAAS.

Crown ethers are known to be effective as solubilising agents for alkali metal cations in organic solvents.[87,88] Owing to the difficulty of dissolving the initiator completely, the effect of a crown ether upon the solubility and reactivity of an alkoxide was examined.

4.3.1 Experimental

Two solutions containing equal concentrations of potassium *tert*-butoxide were prepared using nitrobenzene as solvent. To one of these di-benzo-18-crown-6 solution was added such that the molar ratio di-benzo-18-crown-6 : potassium *tert*-butoxide was 2:1. To the other, a volume of nitrobenzene equivalent to that of the di-benzo-18-crown-6 solution was added. The solutions were then used as initiators for LAAS polymerizations at 50.0 °C. Before injection of methanol, samples of the polymerizate were taken for infra red analysis. The spectra obtained confirmed that no monomer remained since only polymer carbonyl peaks at 1760 cm^{-1} were present.

4.3.2 Results

The effectiveness of the initiator systems were determined by a comparison of the rates of evolution of sulphur dioxide as determined by the gas pressure (see figure 4.4).

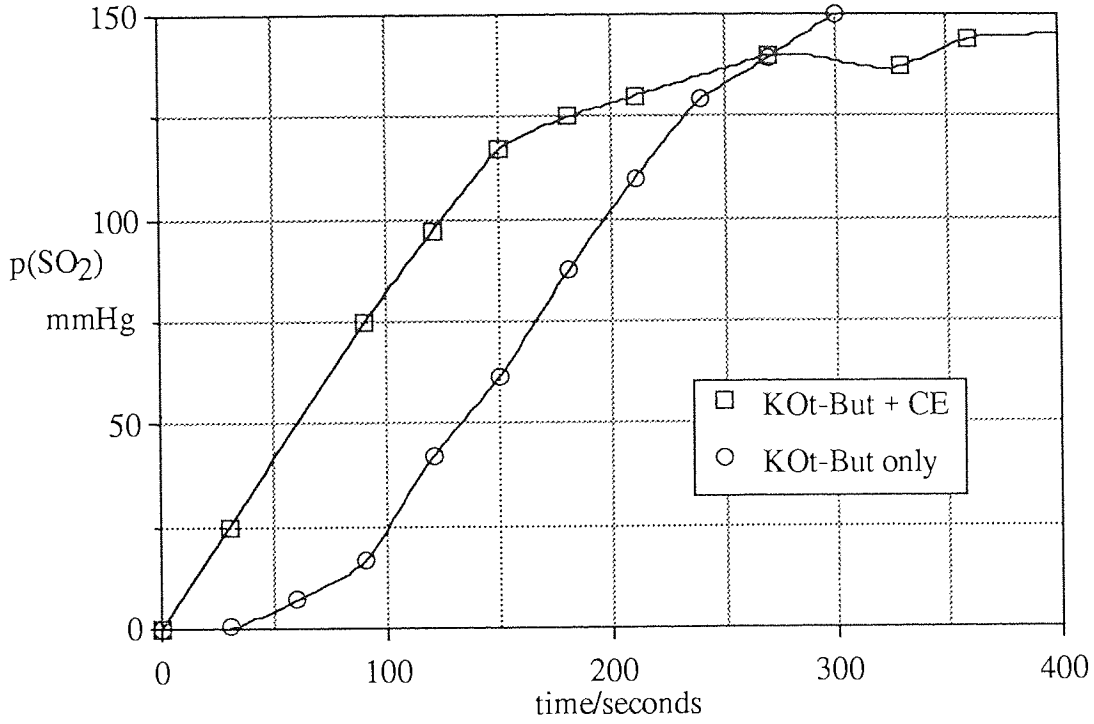

Figure 4.4 Decomposition of LAAS by potassium *tert*-butoxide with/without crown ether - gas evolution graph.

4.3.3 Discussion

When crown ether is present in the initiator system, decomposition of LAAS by potassium *tert*-butoxide is significantly more rapid in the initial stages, i.e. when the first 10 - 20 % of monomer is consumed. After this initial period, there is little difference between the rates and both reactions appear to go to completion. The FT-IR spectra showed no anhydrosulphite carbonyl.

It is believed that the solubising effect of the crown ether, in co-ordinating to the potassium ion, increased the rate of decomposition of the anhydrosulphite ring but did not affect the maximum rate of decomposition. It may be that the addition of a crown ether to the initiator could prove useful in reducing heterogeneity of the initiator. In this way, the reaction might be simplified and smooth decomposition of the anhydrosulphite could be more easily achieved.

4.4 COMPARISON OF INFRA-RED SPECTROSCOPY AND GAS EVOLUTION AS METHODS OF FOLLOWING LAAS DECOMPOSITION

An experiment was performed in order to confirm that the technique of following LAAS decomposition by monitoring the pressure of sulphur dioxide evolved was accurately recording the rate at which ring-opening occurred. Infra-red spectroscopy was used to determine the intensities of monomer and polymer carbonyl absorptions in parallel with gas pressure measurements.

4.4.1 Experimental

Monomer and initiator solutions were mixed rapidly in a small round-bottomed flask under dry argon and separate portions injected by syringe into an FT-IR solution cell and the low pressure gas evolution vessel. The polymerization was followed using both techniques. The temperature in the FT-IR sample chamber was measured and found to vary from 23 - 25°C during the course of the experiments (ambient temperature was 19 - 20 °C). Concentrations of monomer and lithium *tert*-butoxide initiator in the polymerization were 2.21 and 0.12 M, respectively.

4.4.2 Results

For this reaction, the monomer conversion could be calculated by three methods:-

(1) The sulphur dioxide pressure recorded by the mercury manometer was extrapolated back to the value at t = 0 and the value at the end of the reaction was assumed to be representative of the total quantity of monomer decomposed. The fraction of monomer was then calculated simply by assuming a linear relationship between gas pressure and number of moles of monomer decomposed.

(2) A plot of infra-red absorption at 1823 cm^{-1} (monomer carbonyl) could be extrapolated back to the value at t = 0. The difference between this value and the value at the end of the reaction was assumed to be equivalent to the change in absorption due to the complete decomposition of monomer. If expressed as a fraction, this value represents the fractional conversion of monomer.

(3) The infra-red absorption at 1757 cm^{-1} (polymer carbonyl) could be monitored. However, the value calculated is the 'polymer fraction' i.e. the fraction of total polymer

produced at time, t. If it is assumed that one mole of monomer gives rise to one mole of polymer repeat units, this is easily converted to the monomer fraction.

The fractional conversion of monomer as determined by these methods is plotted in figure 4.5.

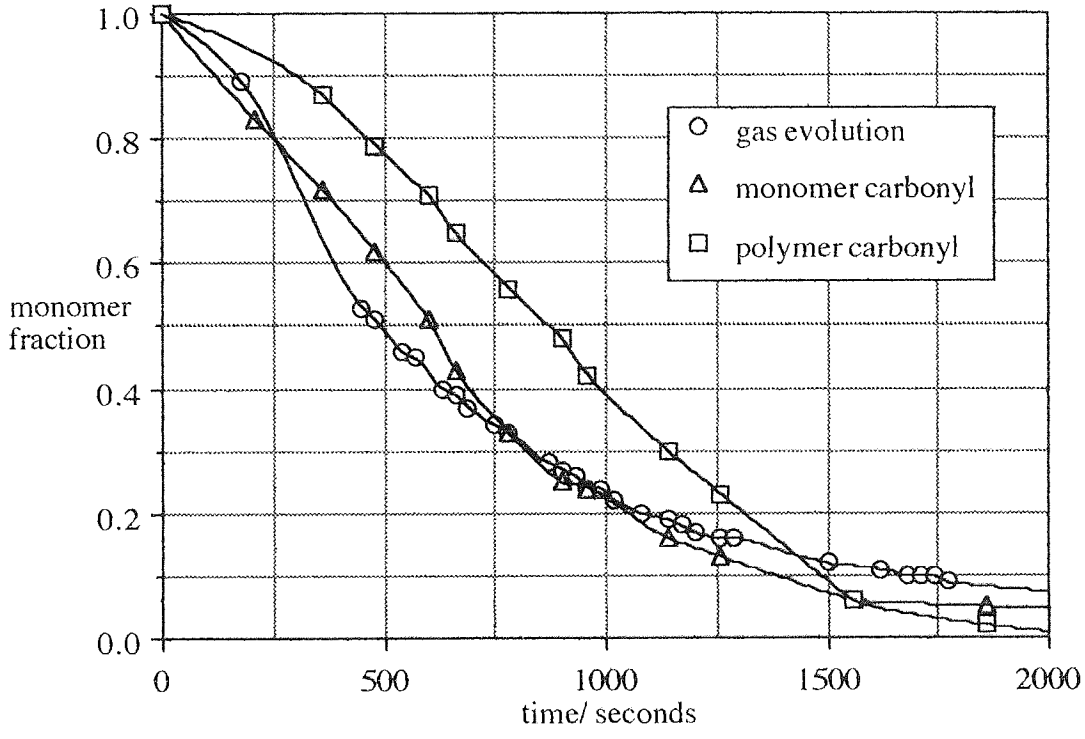

Figure 4.5 Comparison of gas pressure and infra-red spectroscopy as methods of following LAAS decomposition - fractional conversion of monomer plotted against time.

4.4.3 Discussion

Figure 4.5 shows good correlation between the monomer fraction curves derived from gas pressure and the monomer carbonyl at 1823 cm^{-1}. The curve derived from the polymer carbonyl at 1757 cm^{-1} indicates a slower reaction but is not greatly different to the other curves. This may indicate that not all monomer is converted into polymer, though some error is expected due to the difficulty of eliminating completely the contribution from solvent peaks.

Figure 4.6 provides additional information, showing that an extra carbonyl absorption is present. This absorption is initially masked by the monomer carbonyl, causing only a very slight 'shoulder' which could have simply been a feature of the particular peak (this

explains why it was not observed during the process of monomer synthesis and purification). As monomer decomposes and the LAAS carbonyl intensity decreases, a peak at 1800 cm^{-1} becomes visible.

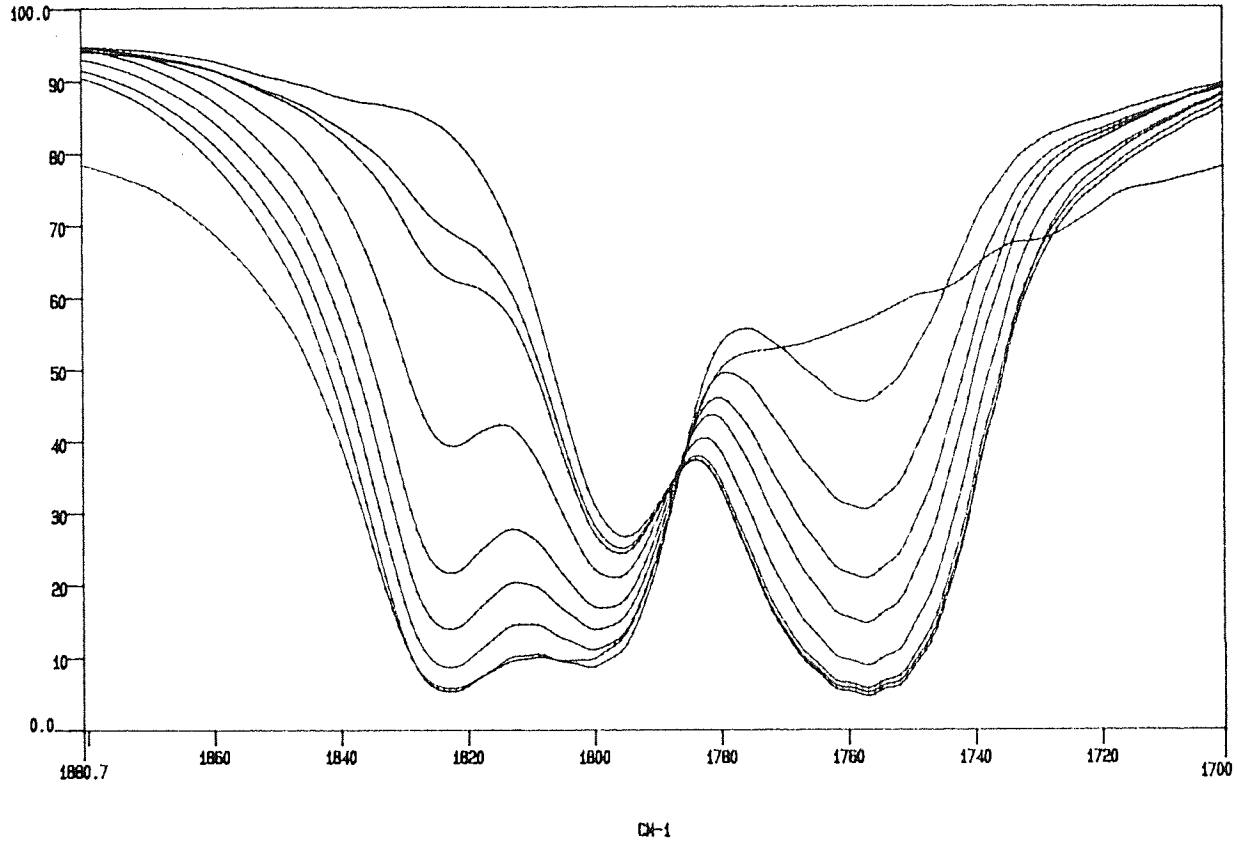

Figure 4.6 Comparison of gas pressure and infra-red spectroscopy as methods of following LAAS decomposition - FT-IR spectra recorded during reaction.

As this is the region in which the α-chloro-acid chloride would be expected to appear, the monomer was re-tested for chlorine content (by potentiometric titration and gas chromatography) but this was found to be negligible. Further work was done to identify the nature of this unknown contaminant and this is described fully in section 4.4.

4.4 CHARACTERISATION OF UNUSUAL IMPURITY IN LAAS

Section 4.3 describes a polymerization experiment during which an unusual impurity was found to be present in the lactic acid anhydrosulphite. Despite initial analyses indicating a pure product, when used in FTIR-followed polymerization it became apparent that an unusual impurity was present (i.e. neither parent acid, oligomer or a chlorinated by-product). This impurity was also subsequently discovered in the LAAS used in the experiment described in section 5.1.

The impurity was detected as a carbonyl absorption at 1796 cm^{-1}, after the anhydrosulphite was completely reacted. Initially, it was assumed that the potentiometric titration technique had failed, but repeated titrations determined the chlorine content as being negligible.

Fractional distillation of the impure monomer using the SBC showed that the fraction boiling at 36 - 40 °C/5 mmHg contained slightly more of the impurity than that boiling at 42 - 46 °C/5 mmHg. It was not possible to achieve good separation by this means since the boiling points were too close. Repeated distillation was not possible because the monomer is prone to thermal decomposition during distillation and no benefit was gained by repeated treatment.

The fraction containing the greater proportion of impurity was subjected to further analysis in order to determine the nature of the unusual contaminant.

4.4.1 Nuclear Magnetic Resonance Spectral Analysis

4.4.1.1 Experimental

The impure monomer was re-distilled and made up into a 10 % solution in deuterated chloroform in order to obtain ^{1}H and ^{13}C nuclear magnetic resonance spectra.

4.4.1.2 Results

The ^{1}H and ^{13}C spectra of the anhydrosulphite containing the impurity are shown in figures 4.7 and 4.8. The data is summarised in tables 4.2 and 4.3.

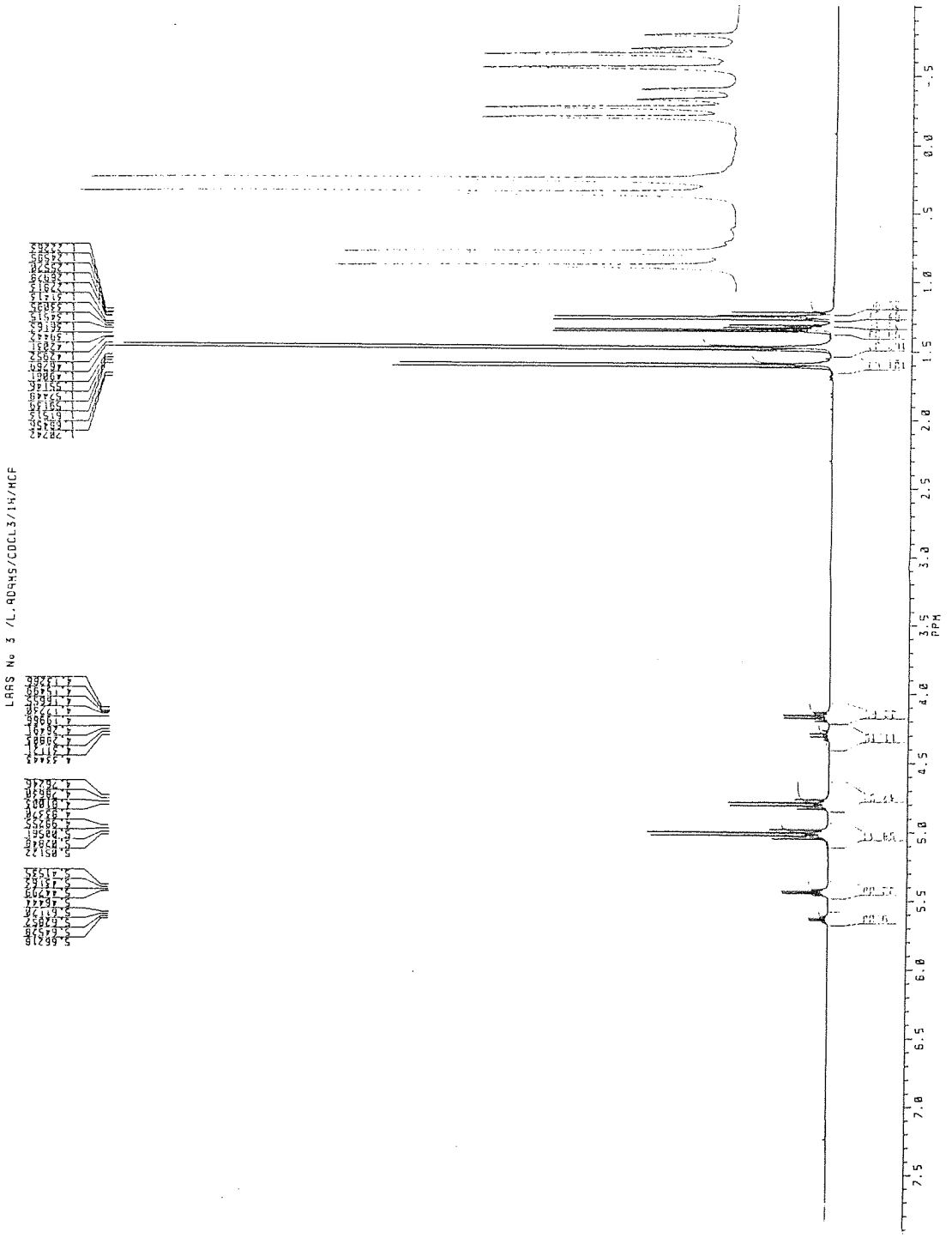

Figure 4.7 ^{1}H NMR spectrum of LAAS containing unusual impurity.

Table 4.2 ^{1}H NMR spectrum of LAAS containing unusual impurity.

ppm	multiplicity	assignment	relative peak areas
1.22 - 1.25	doublet	CH_3	2.9
1.26 - 1.28	doublet	CH_3	6.4
1.31 - 1.33	doublet	CH_3	2.7
1.34 - 1.36	doublet	CH_3	6.5
1.47 - 1.49	doublet	CH_3 - LAAS	18.5
1.59 - 1.62	doublet	CH_3 - LAAS	11.3
4.13 - 4.18	quartet	CH	2.5
4.27 - 4.33	quartet	CH	1.2
4.76 - 4.83	quartet	CH -LAAS	4.2
4.98 - 5.05	quartet	CH -LAAS	6.5
5.41 - 5.46	quartet	CH	2.4
5.61 - 5.66	quartet	CH	1.0

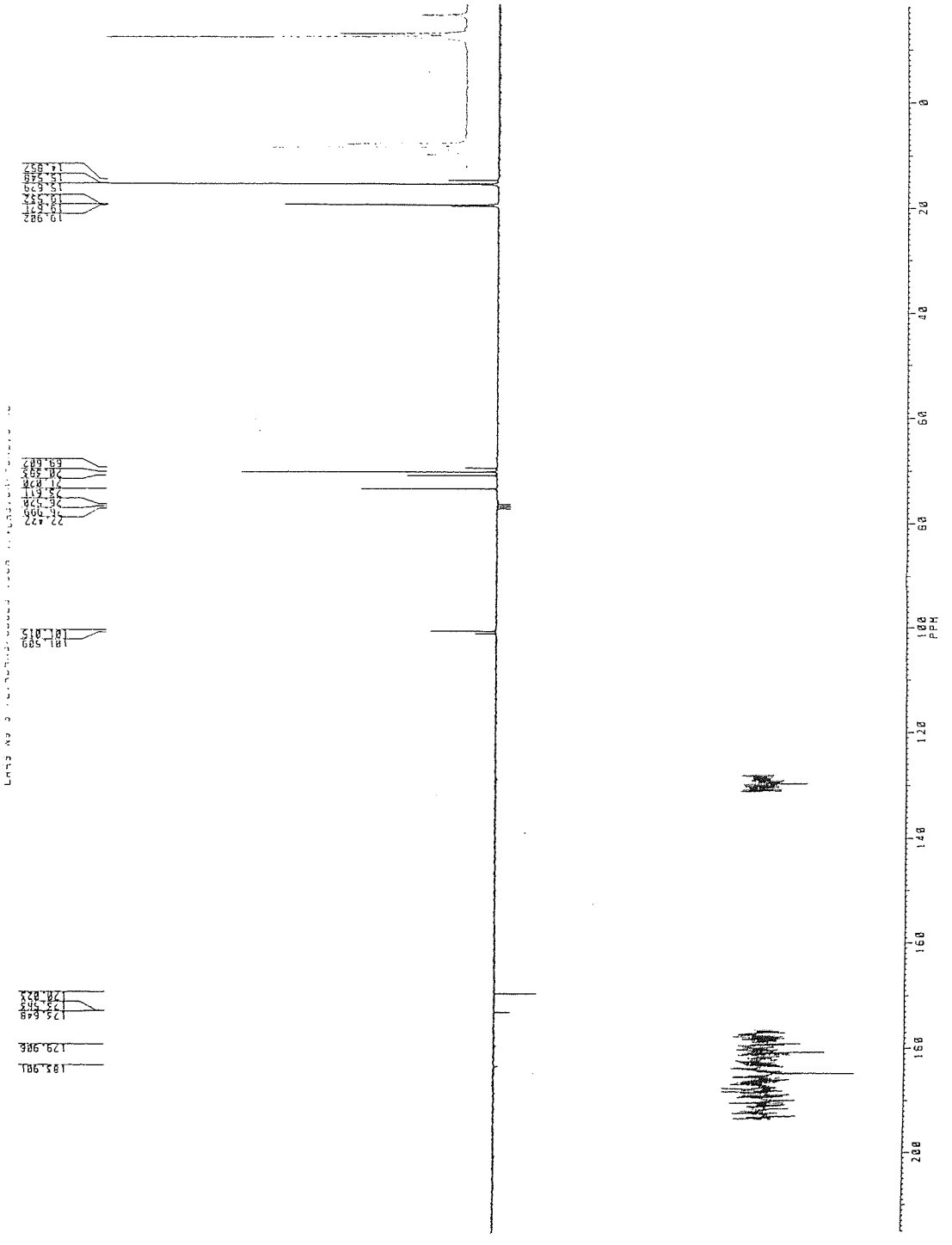

Figure 4.8 ^{13}C NMR spectrum of LAAS containing unusual impurity.

Table 4.3 ^{13}C NMR spectrum of LAAS containing unusual impurity.

ppm	assignment	+/- intensity
14.9	CH_3	+1.5
15.6	CH_3	+4.3
15.7	CH_3 - LAAS	+12.0
19.5	CH_3	+4.2
19.6	CH_3 - LAAS	+6.8
19.9	CH_3	+1.5
69.6	H	+1.0
70.4	H - LAAS	+7.9
71.1	H	+2.9
73.6	H - LAAS	+4.3
101.0	H	+2.0
101.5	H	+0.7
170.0	C=O - LAAS	-1.3
173.6	C=O	-0.2
173.7	C=O - LAAS ?	-0.5
179.9	C=O	-0.1
183.9	C=O	-0.1

4.4.1.3 Discussion

From peak area data, the proportion of the methyl and methine hydrogens which are derived from the unknown impurity (compared to LAAS methyls and methines) may be calculated as 62 % and 60 %, respectively. From the methyl and methine splitting patterns, it can be seen that they must be present as a -CH(CH_3)- group in the impurity. Furthermore, this group must exist in four different magnetic environments, due to the different chemical shifts observed. The methyl and methine absorptions shown in the ^1H spectrum appear to be in pairs of equal intensities. This could indicate two methyls and two methines all present in a single molecule existing as two magnetically non-equivalent isomers.

The absence of ^1H NMR hydroxyl proton or ^{13}C NMR carboxyl absorptions shows that the parent acid is not present. The ^{13}C spectrum confirms the presence of 4 different methines and 4 different methyls along with several absorptions in the region

characteristic of carbonyl groups. This indicates that the impurity may be an ester or lactone containing 2 each of methyls and methines.

4.4.2 Elemental analysis

4.4.2.1 Experimental

A sample of the impure LAAS was submitted to Medac Ltd at Brunel University for elemental analysis. This was done in order to confirm the potentiometric titration results and also to determine whether or not the impurity contained nitrogen.

4.4.2.2 Results

Table 4.4 shows the results of the elemental analysis of the sample of anhydrosulphite containing the unusual impurity.

Table 4.4 Elemental analysis of impure LAAS.

	Carbon	Hydrogen	Nitrogen	Chlorine
First run/ % mass	30.24	3.63	undetected	<0.05
Second run/ % mass	30.23	3.53	undetected	<0.05

4.4.2.3 Discussion

It is not possible to calculate of the empirical formula of the unknown from the elemental analysis results since the material tested was a mixture of the unknown impurity, LAAS, and its decomposition products i.e. lactic acid and oligomers. However, conversion of LAAS to lactic acid will not significantly affect the presence of chlorine in the sample, which is shown to be very low indeed, approaching the limits of detection. This rules out the possibility that the impurity might be 2-chloro-propionyl chloride, 2-chloro-propionic acid or simply propionyl chloride. Since no nitrogen was detected, the possibility of the unknown being an amine, amide etc. can also be dismissed.

4.4.3 Gas Chromatographic-Mass Spectral Analysis (GC-MS)

As it was not possible to separate the unknown impurity completely from LAAS, gas-chromatographic mass spectrometry (GC-MS) was used to isolate and analyse the two components of the mixture. In this technique, a sample is passed through a gas chromatography column before being transferred to a mass spectrometer. Scans are repeated at intervals in order to isolate the contributions to the mass spectrum from individual components of the mixture.

4.4.3.1 Experimental

GC-MS work was performed at Birmingham University using equipment operated by Dr.J.Riches and Dr.R.Lehrle. The GC-MS equipment was operated with an accuracy of ±1 a.m.u. for fragment ions and a scanning range of 45 - 300 a.m.u.. A sample of anhydrosulphite was fractionally distilled using the SBC in order to increase the concentration of the unknown impurity and this sample re-distilled immediately prior to use in the experiment. A dichloromethane blank was run prior to the anhydrosulphite sample in order to calibrate the column. The sample was diluted in dichloromethane and introduced to the chromatographic column at an injection temperature of 140 °C. The column temperature was held at this temperature for one minute before increasing to 150 °C at a rate of 5 °C/min., then to 250 °C at a rate of 15 °C/min. The temperature was then held until the experiment was completed. Ionisation voltage was 70eV.

Mass spectral experiments were also performed under chemical ionization conditions in order to identify the molecular weights of the two compounds. Methane at a pressure of 2×10^{-4} mbar was used as the reagent gas, with an electron energy of 50 eV and a source temperature of 150 °C. Otherwise, the gas chromatographic conditions were identical to those used for the electron ionization work. Calibration of the mass range was carried out using amyl acetate in order to ensure that the molecular masses calculated were accurate.

4.4.3.2 Results

Figure 4.9 shows the total ion current chromatogram. At retention times between 145 and 230 seconds, two peaks are visible with some degree of overlap. Using the GC-MS data manipulation software it was possible to identify mass spectral peaks which were unique to each of the chromatogram peaks and thereby identify suitable points on the chromatogram where there was little overlap.

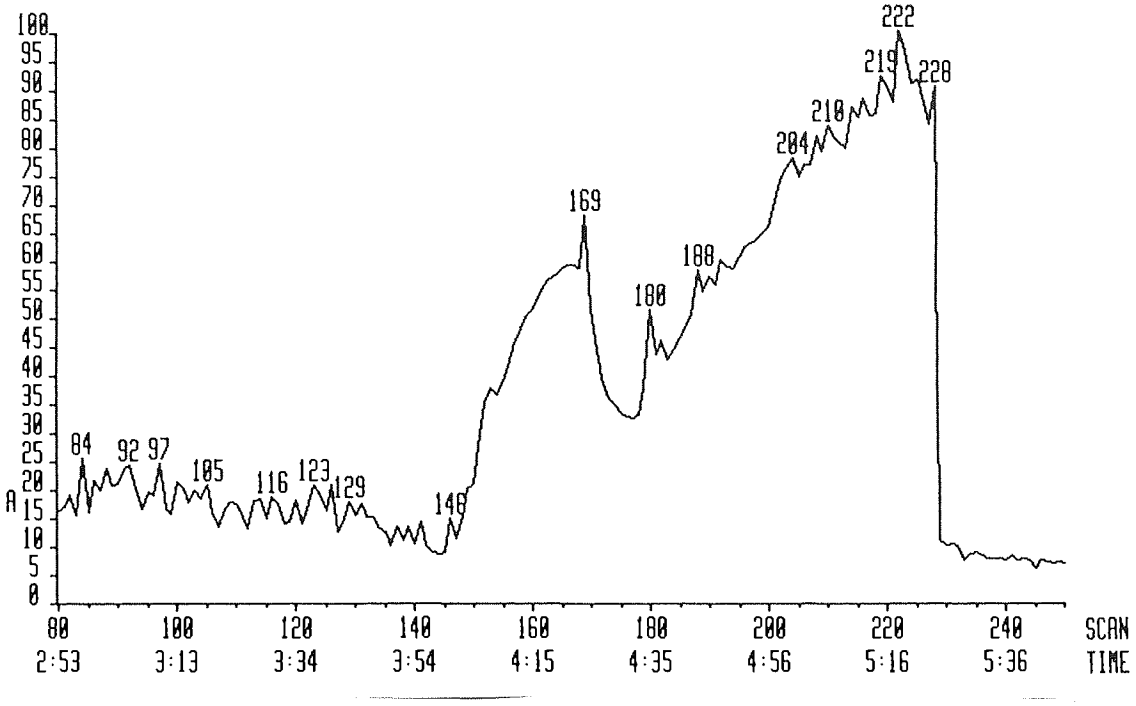

Figure 4.9 Total ion current chromatogram of impure anhydrosulphite.

Scan numbers 169 and 220 were taken as being representative of each compound (labelled A and B, respectively). This achieved the objective of obtaining an effectively separate mass spectrum for each compound (as shown in figures 4.10 and 4.11).

Chemical ionization experiments confirmed that there were indeed only two compounds under examination. Compound A was found to have a molecular weight of 116 and compound B, 136.

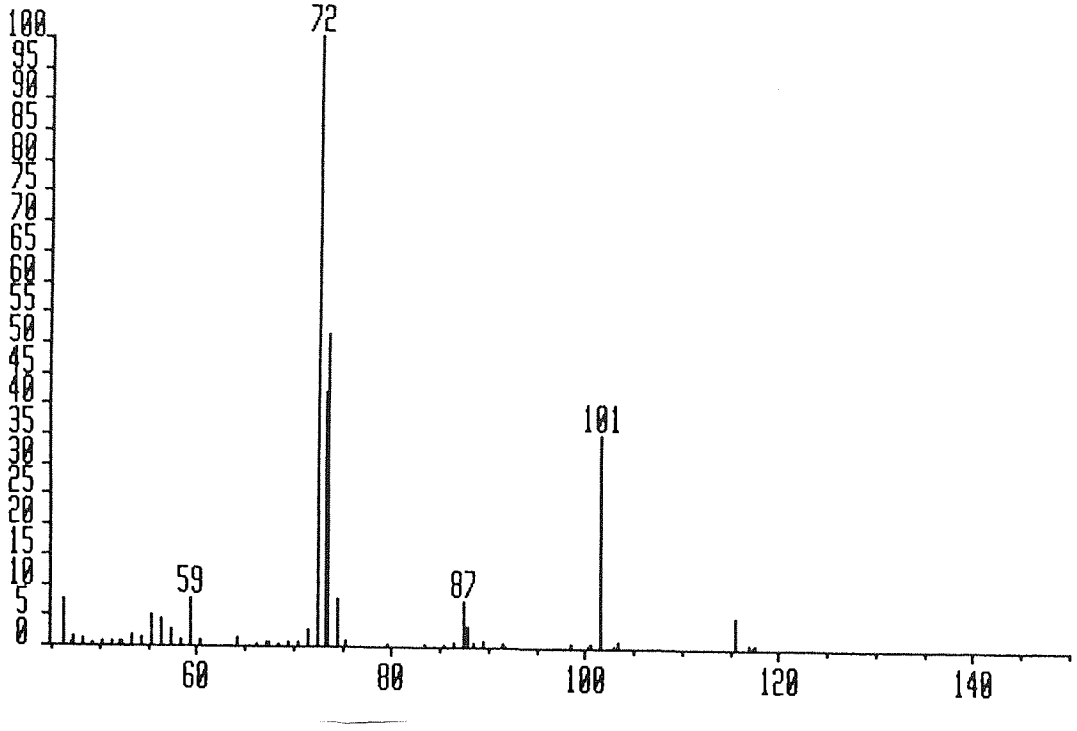

Figure 4.10 GC-MS scan 169 (compound A).

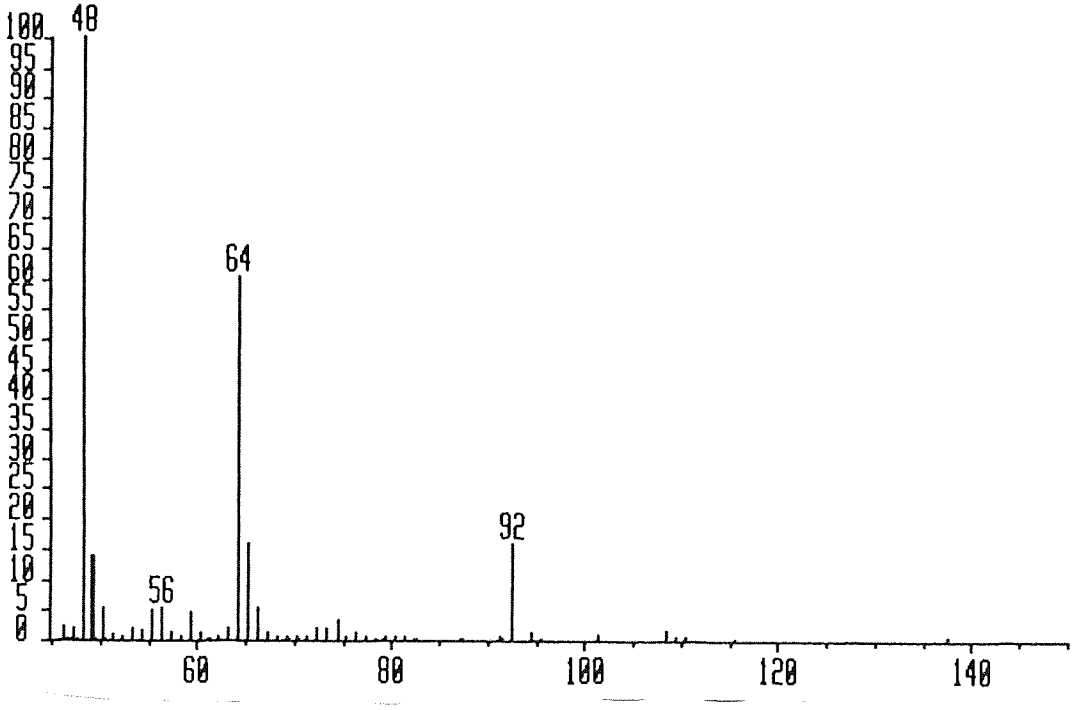

Figure 4.11 GC-MS scan 220 (compound B).

4.4.3.3 Discussion

It would seem reasonable to assume that compound B is LAAS with a molecular weight of 136. The electron ionization spectrum of B features four main peaks at m/z = 48, 56, 64 and 92, which partly matches values obtained by Blackbourn for other anhydrosulphites (64, 80(weak), 92 and 108).[89]

A theoretical fragmentation pattern which fits the observed results for LAAS is suggested in figure 4.12.

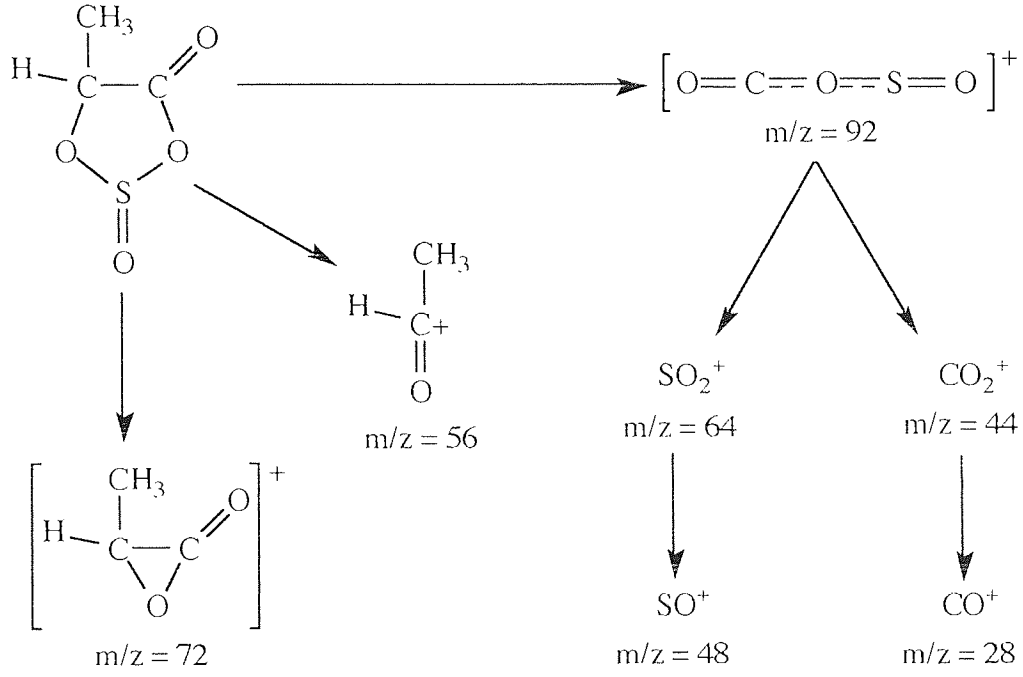

(Note. carbon monoxide and dioxide were not detected due to limitations of the equipment. under the conditions of operation).

Figure 4.12 Theoretical mass-spectral fragmentation pattern for LAAS.

Since the molecular weight compound of A has been determined by chemical ionization as being even, it must contain either an odd number of nitrogen atoms or none at all.[90] This is as would be expected based on the results of elemental analysis.

Since the two chlorine isotopes ^{35}Cl and ^{37}Cl occur naturally in the ratio 3:1, compounds containing chlorine exhibit characteristic fragmentation patterns which are not exhibited by compound A. This confirms the absence of chlorine-containing impurities. Sulphur also exhibits a isotopic pattern, derived from the ^{32}S and ^{34}S isotopes, in the ratio 24:1. This

pattern can be seen in the spectrum of compound B (but not A) as peaks at 48/50, 64/66, and 92/94. Therefore it may be assumed that compound A contains no sulphur.

There is no strong molecular ion peak in its electron ionization spectrum, scan 169, therefore compound A must be relatively unstable e.g. a cyclic compound with some degree of ring strain. Scan 169 shows a principal peak at 72 and less intense peaks at 101, 87 and 59. The peak at 72 may represent a positively charged α-lactone and, if the molecular weight of this compound is 116, the peak at 101 may correspond to the loss of a methyl. Assuming an error of ±1 a.m.u. for the electron ionization experiments, a peak at 88 may indicate the loss of -CH(CH3)- group. A theoretical fragmentation pattern for a compound which may fit observed results is suggested in figure 4.13.

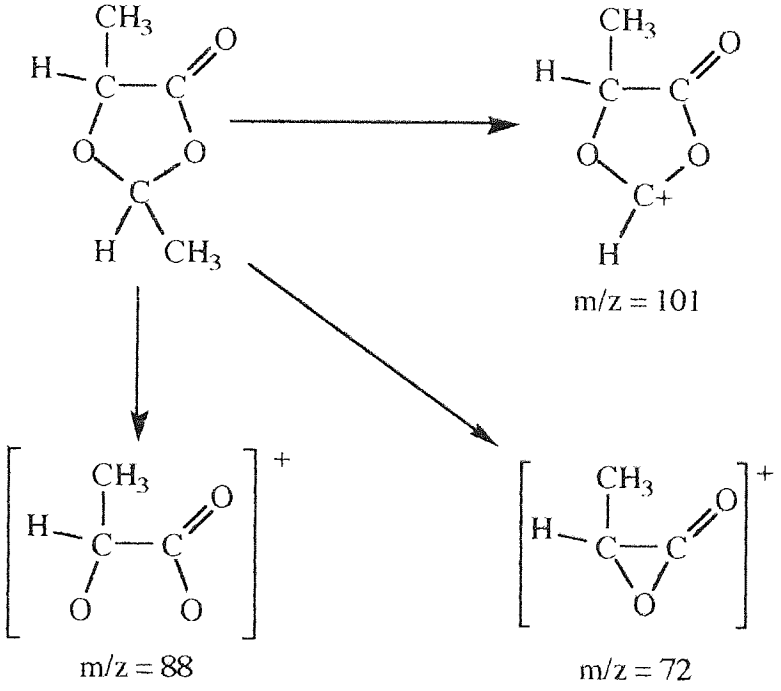

Figure 4.13 Theoretical fragmentation pattern for unusual impurity.

4.4.4 Conclusions

The anhydrocarboxylate of lactic acid has a molecular weight of 116, however if this were the unknown compound, two carbonyl absorptions would be observed in the IR spectrum. Furthermore, only 1 methyl and 1 methine peak would be observed in the ^{1}H NMR spectrum of the impurity since the anhydrocarboxylate is known to be planar, existing in one conformation only.

The fragmentation pattern suggested in figure 4.13 is based upon a molecule which has a single carbonyl group but two methyls and methines, both in the form of -$CH(CH_3)$- groups. This means that two magnetically non-equivalent isomeric forms are possible, as shown in figure 4.14, which would fit the observations made regarding its nuclear magnetic resonance spectra.

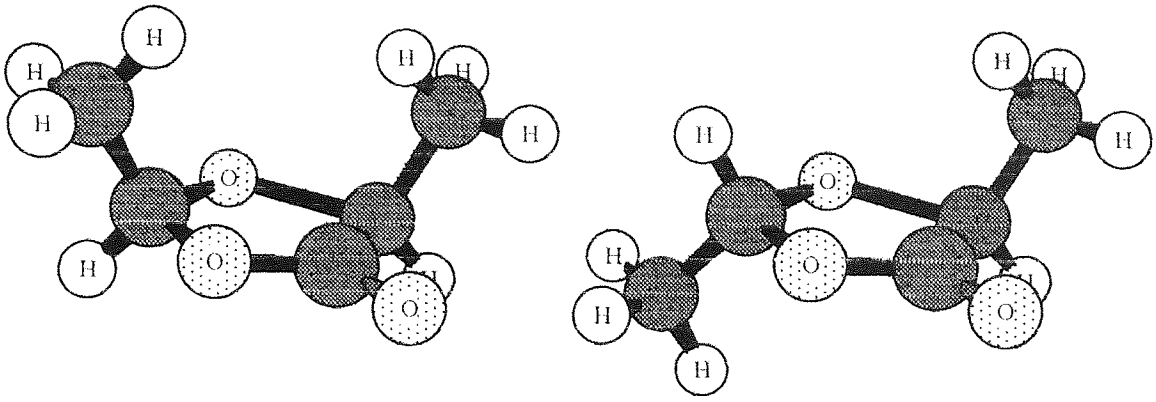

Figure 4.14 Possible structures of isomeric contaminants in LAAS prepared from commercial copper (II) lactate.

If this heterocyclic compound is the impurity present in the anhydrosulphite, the mechanism of its formation is uncertain. It was found that the only samples of LAAS which contained the impurity were those in which commercially supplied copper (II) lactate was used. This reagent was manufactured by Strem Chemicals Inc., USA. and supplied by Fluorochem Ltd as a hydrate, having the formula $Cu(CH_3.CHOH.COO)_2.xH_2O$. It was dried overnight at 90°C under vacuum and allowed to cool over dry argon before use.

Since the samples purchased were the last available, and no alternative supplier could be found, more effort was devoted to the preparation of reasonable quantities of usable copper (II) lactate in the laboratory (initial experiments had only produced the salt in low yields and contaminated by copper (II) chloride). As has been described in section 3.1.1, these attempts were successful and the copper (II) lactate subsequently used in LAAS synthesis was that prepared in the lab direct from the parent acid. As the impurity was never observed in any monomer prepared from 'lab' copper (II) lactate, it seems reasonable to conclude that a contaminant present in the commercially-prepared salt was responsible. It should however, be noted that infra-red spectra of the commercial salt were indistinguishable from those of lab-prepared samples.

CHAPTER FIVE

DECOMPOSITION OF LACTIC ACID ANHYDROSULPHITE BY GROUP I METAL ALKOXIDES

5.1 DETERMINATION OF THE KINETIC AND THERMODYNAMIC PARAMETERS OF LITHIUM *tert*-BUTOXIDE INITIATED DECOMPOSITION OF LAAS IN NITROBENZENE

A series of experiments designed to accurately measure the rates of reaction of LAAS with an alkali metal alkoxide was conducted. Since preliminary experiments had indicated that both reaction temperature and the addition of a crown ether to the initiator might affect the rate of reaction, these factors were also studied.

5.1.1 Experimental

Three sets of experiments were carried out at 34.5, 50.0 and 69.0 °C, using quantities of the same batch of initiator solutions for each, but newly-distilled monomer and nitrobenzene as solvent.

Initiator solutions were prepared as described in section 2.3.1.1. Three concentrations of lithium *tert*-butoxide dissolved in nitrobenzene were used, both with and without di-benzo-18-crown-6 in a 1:1 molar ratio, making six initiator systems in total. Attempts were made to ensure that the concentration of monomer was constant at 1.4 M but because of the difficulty of distilling a specific mass of monomer, the concentrations in solution at the start of the reactions were 1.42 M, 1.27 M and 1.59 M for 34.5, 50.0 and 69.0 °C runs, respectively.

Initiator was injected into manometer vessels and the vessels suspended in the water bath for 20 minutes before injection of monomer. During this time, monomer solution was stored in the vessel shown in figure 5.1. This vessel was suspended in the water bath, with dry argon passing slowly over it.

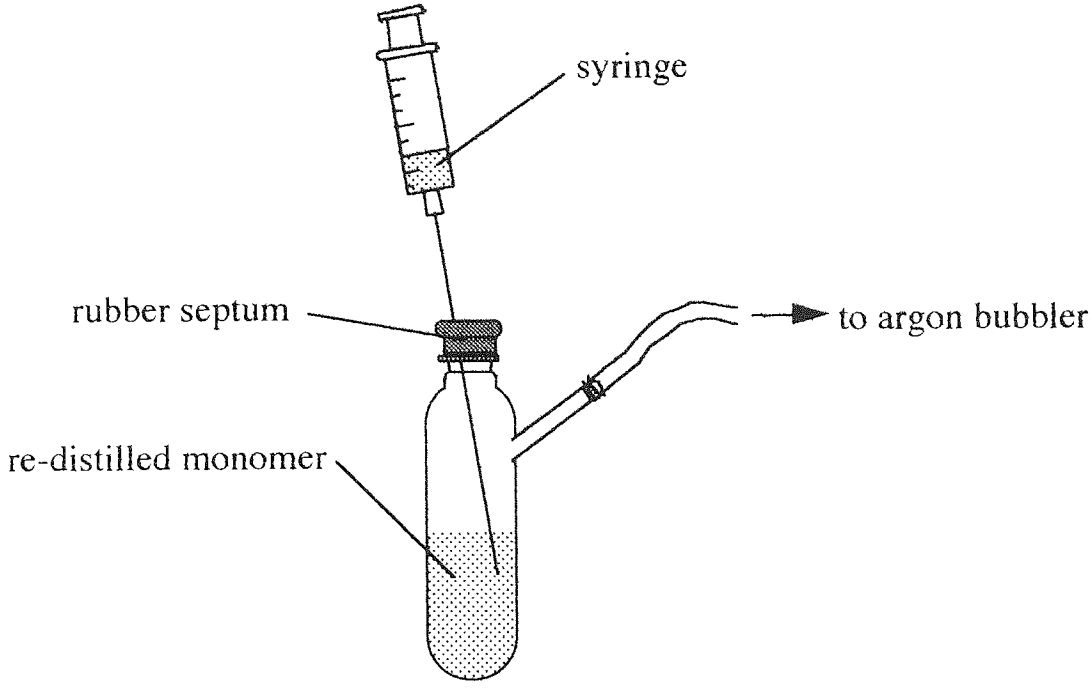

Figure 5.1 Vessel used for storage of LAAS prior to use in polymerization reactions.

After addition of the monomer solution to the manometer vessel, each experiment was left in the water bath until gasevolution had slowed to such a rate as to be undetectable over several days. A sample of the reaction mixture was removed for infra-red spectral analysis and de-oxygenated methanol added to the remaining solution.Solvent was then removed by evaporation at 70 °C in a vacuum oven, yielding small quantities of brittle yellow-green glassy solids. These materials were dissolved in tetrahydrofuran and analysed by GPC.

5.1.2 Results

5.1.2.1 Gas Evolution Data

The fraction of monomer remaining at time, t, was calculated by fitting gas pressure data into the equations described in section 2.3.1.2. The gas evolution data obtained for the three sets of reactions are plotted as monomer fraction remaining against time in figures 5.2 through to 5.7.

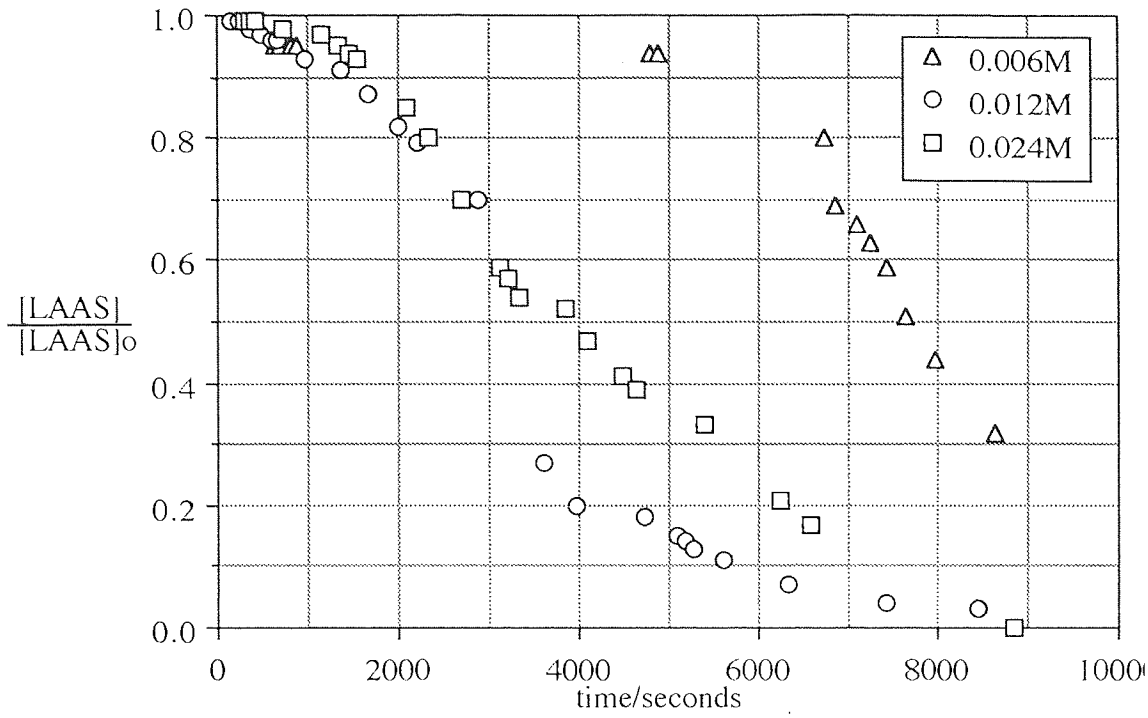

Figure 5.2 Decomposition of LAAS initiated by lithium *tert*-butoxide in nitrobenzene at 34.5°C - gas evolution graph.

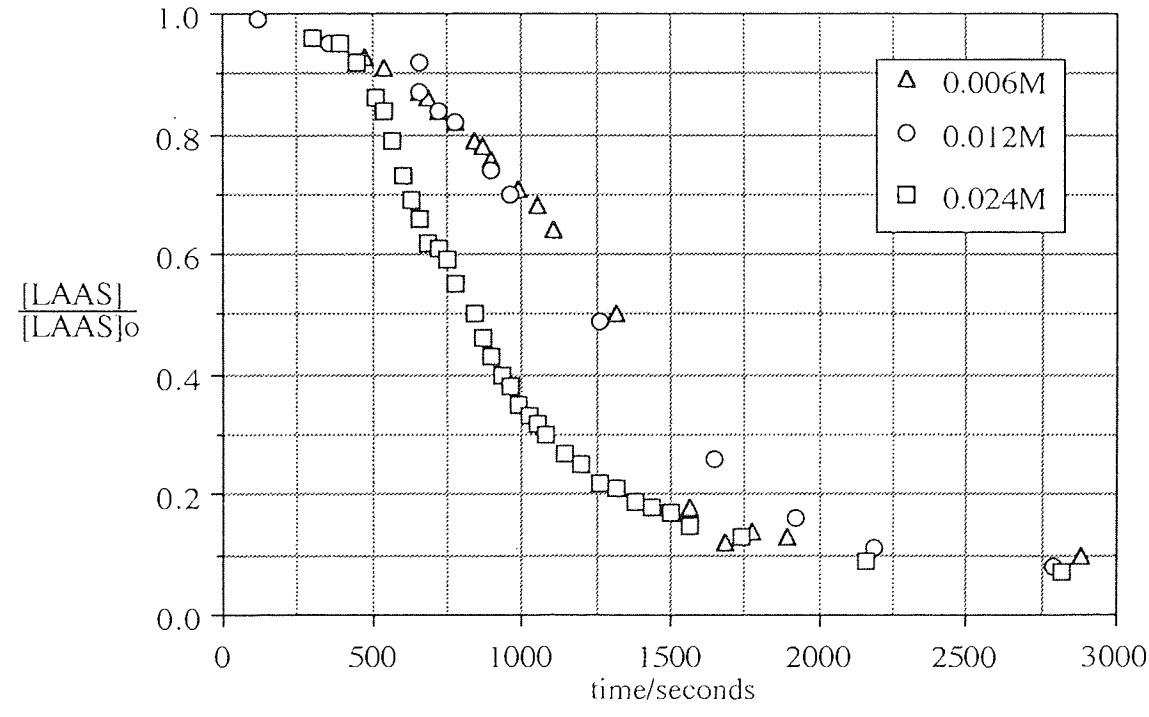

Figure 5.3 Decomposition of LAAS initiated by lithium *tert*-butoxide with crown ether in nitrobenzene at 34.5°C - gas evolution graph.

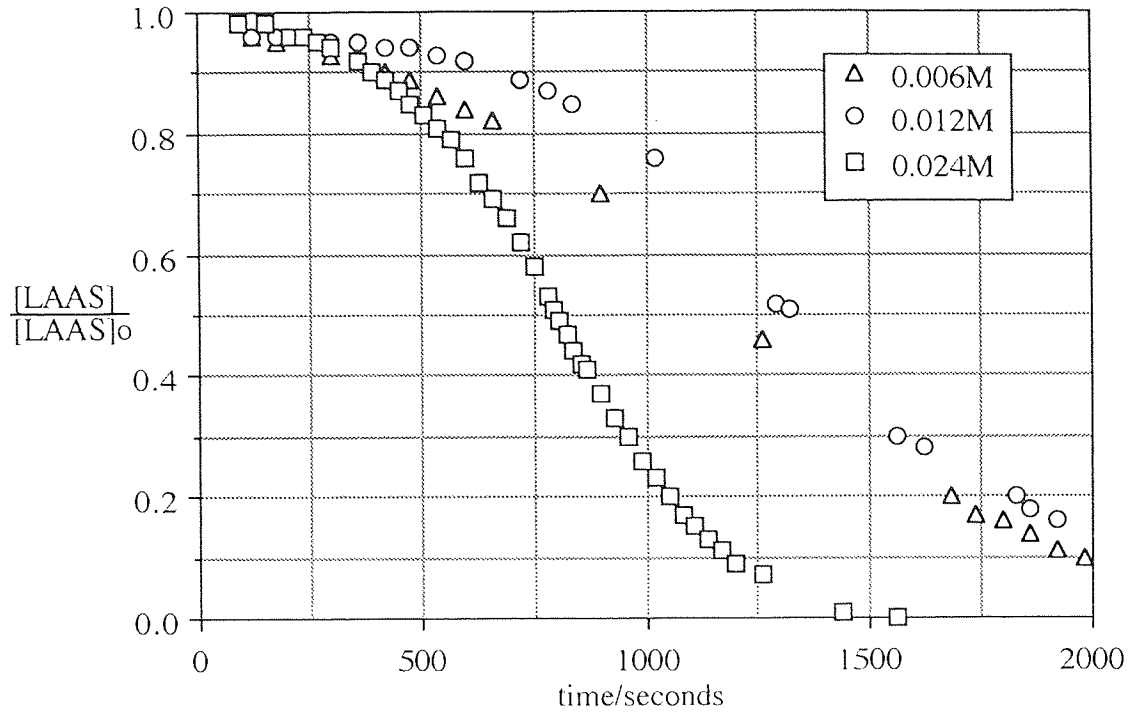

Figure 5.4 Decomposition of LAAS initiated by lithium *tert*-butoxide in nitrobenzene at 50.0°C - gas evolution graph.

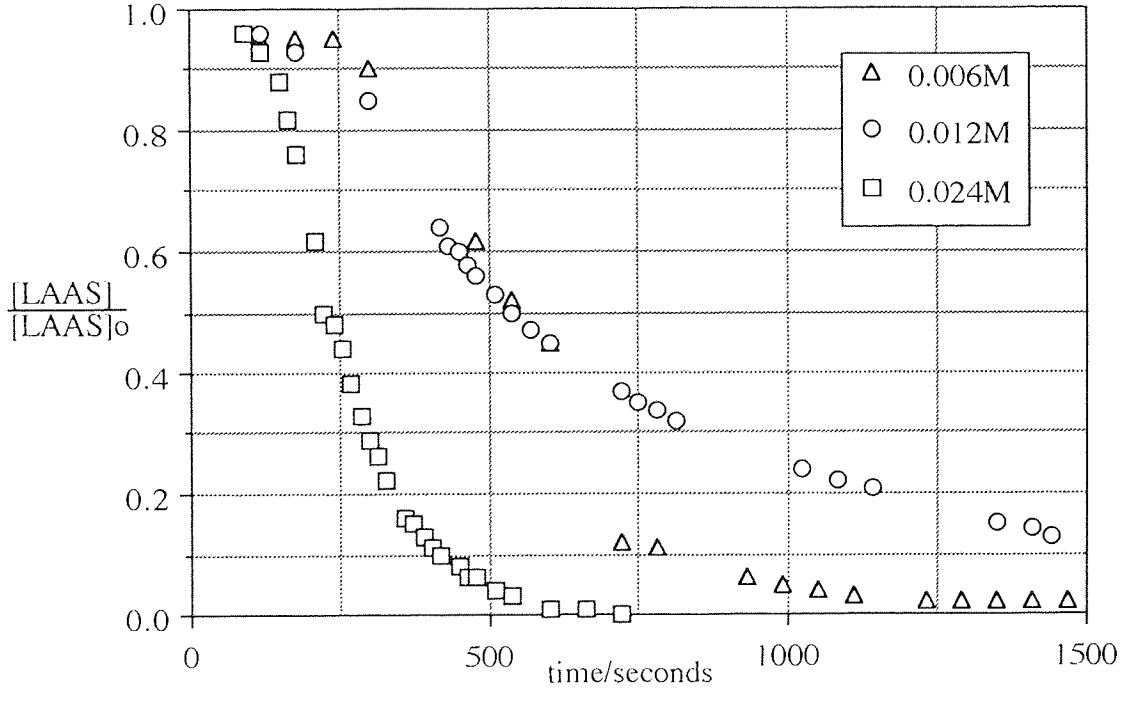

Figure 5.5 Decomposition of LAAS initiated by lithium *tert*-butoxide with crown ether in nitrobenzene at 50.0°C - gas evolution graph.

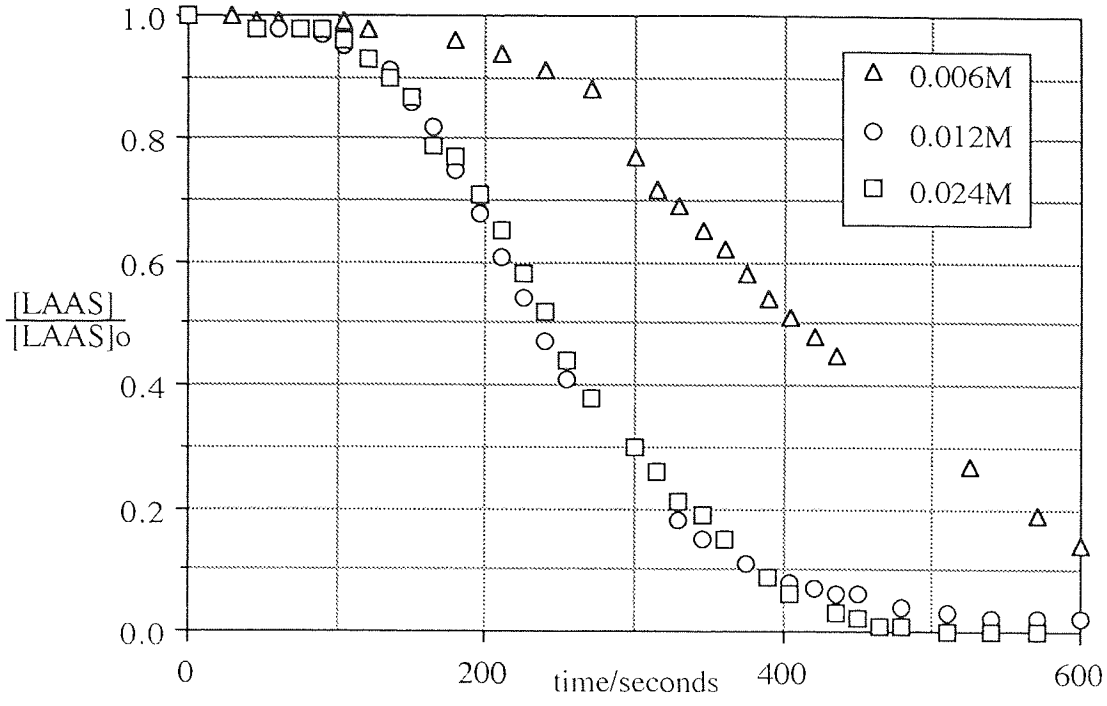

Figure 5.6 Decomposition of LAAS initiated by lithium *tert*-butoxide in nitrobenzene at 69.0°C - gas evolution graph.

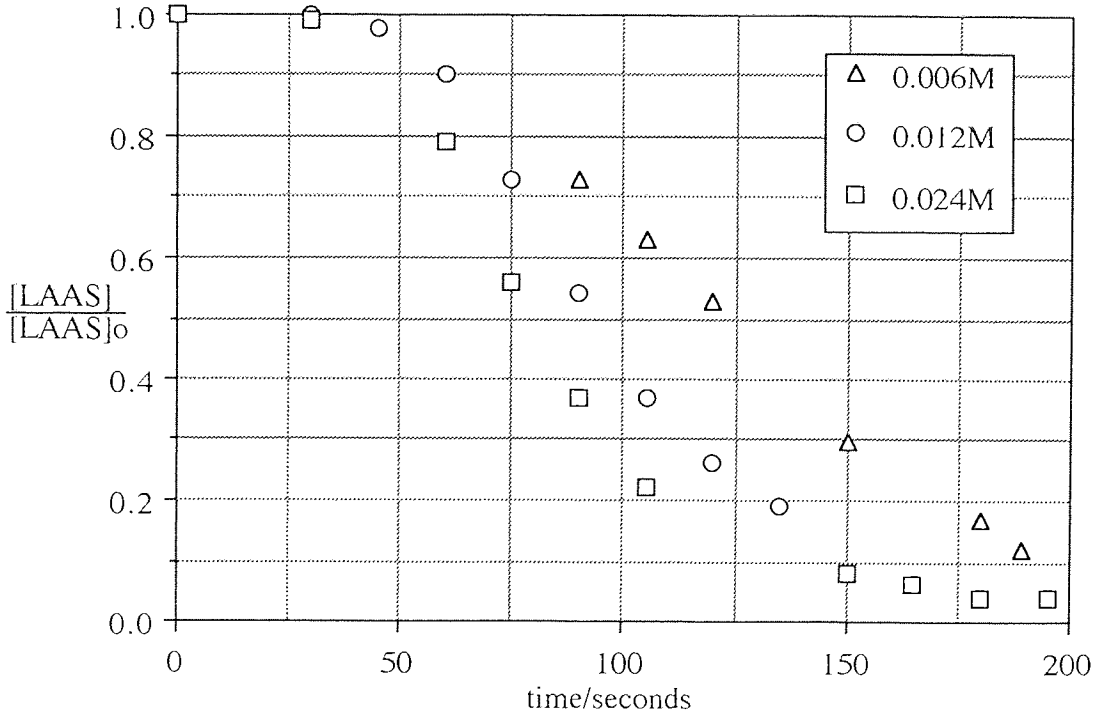

Figure 5.7 Decomposition of LAAS initiated by lithium *tert*-butoxide with crown ether in nitrobenzene at 69.0°C - gas evolution graph.

'Lines of best fit' were drawn by hand for the gas evolution graphs of each reaction. The half life of each reaction was determined by estimating the 'induction period', t_i, for each reaction from the graphs and subtracting this from the time required for the fractional monomer concentration to be reduced to half its original value. The rate constant of each experiment was then determined as described in section 2.3.1.2 and recorded in table 5.1.

Table 5.1 Decomposition of LAAS initiated by lithium *tert*-butoxide in nitrobenzene - kinetic data.

[LiOt-But]/ M	0.006	0.012	0.024	0.006	0.012	0.024
[CE]/ M	-	-	-	0.006	0.012	0.025
34.5 °C						
t_i /s	6400	2500	2200	1000	1000	600
half life/s	1280	740	1430	320	250	240
$k_1 \times 10^3/s^{-1}$	0.54	0.94	0.48	2.17	2.73	2.89
$k/l.mol^{-1}.s^{-1}$	0.09	0.08	0.02	0.36	0.23	0.12
50.0 °C						
induction period/s	800	900	600	300	400	180
t_i /s	370	320	200	250	140	50
$k_1 \times 10^3/s^{-1}$	1.87	2.17	3.40	2.75	4.95	12.83
$k/l.mol^{-1}.s^{-1}$	0.31	0.18	0.14	0.46	0.41	0.54
69.0 °C						
t_i /s	250	145	145	75	65	60
half-life/s	164	89	83	45	31	12
$k_1 \times 10^3/s^{-1}$	4.23	7.79	8.35	15.4	22.35	57.75
$k/l.mol^{-1}.s^{-1}$	0.70	0.65	0.35	2.57	1.86	2.40

(where $k_1 = 0.693/\text{half life}$, and $k = k_1/[\text{LiOt-But}]_o$).

5.1.2.2 GPC Analysis

The products of the experiments conducted at 34.5 and 50 °C were analysed by GPC in tetrahydrofuran as described in section 2.4.4. Table 5.2 shows the weight and number average molecular weights and polydispersities determined as polystyrene equivalents.

Table 5.2 Decomposition of LAAS initiated by lithium *tert*-butoxide in nitrobenzene - GPC analysis.

[LiOt-But]/M	0.006	0.012	0.024	0.006	0.012	0.024
[CE]/M	-	-	-	0.006	0.012	0.025
34.5 °C						
$\overline{M}_w$	3640	3590	3380	2860	2870	3310
$\overline{M}_n$	2560	2270	2340	1920	1820	2150
P_d	1.42	1.58	1.45	1.54	1.57	1.54
50°C						
$\overline{M}_w$	2710	3090	3400	3830	-	3670
$\overline{M}_n$	1790	1620	2290	2770	-	2530
P_d	1.51	1.90	1.49	1.38	-	1.45

5.1.3 Discussion

Figures 5.2 - 5.7 show the reaction profile characteristic of these reactions, i.e. a sigmoidal dependence of the pressure of sulphur dioxide upon time. It was considered that the initial 'induction period' might be due to the time required for the monomer solution to warm to the temperature of the water bath. In order to eliminate error from this source, the monomer was allowed to reach this temperature prior to injection into the reaction vessel. However, this did not affect the length of the induction period, as shown by a comparison of figures 5.2 - 5.7 with the results described in chapter 4.

This shape may be explained by the occurrence of a slow initial process followed by a rapid first order consumption of the monomer. The induction period may be due to the preferential reaction of initiator species with impurities. This would have the effect of slowing the rate of attack of initiator upon monomer until the concentration of the impurity is sufficiently reduced i.e. decomposition of LAAS begins to occur more rapidly as the impurity is consumed. However, while the impurity described in section 3.2 was subsequently found to be present at low concentrations in the monomer used for these experiments, it appears that the impurity is less reactive than the anhydrosulphite to alkoxides. When solutions of the products were examined by FTIR, the characteristic carbonyl absorption of the unusual impurity was observed at similar intensity to that of detected in the unreacted monomer solution. Similarly, during experiments followed using infra-red spectroscopy, no measurable decrease in the intensity of the impurity carbonyl absorption was observed.

Alternatively, the induction period may be attributed to a relatively slow initiation process involving attack of the alkoxide upon LAAS to create a more reactive propagation species. As the concentration of the propagation species builds up, the rate of monomer decomposition increases accordingly. Figures 5.8 - 5.10 show the effect of initiator concentration upon the length of this initial period.

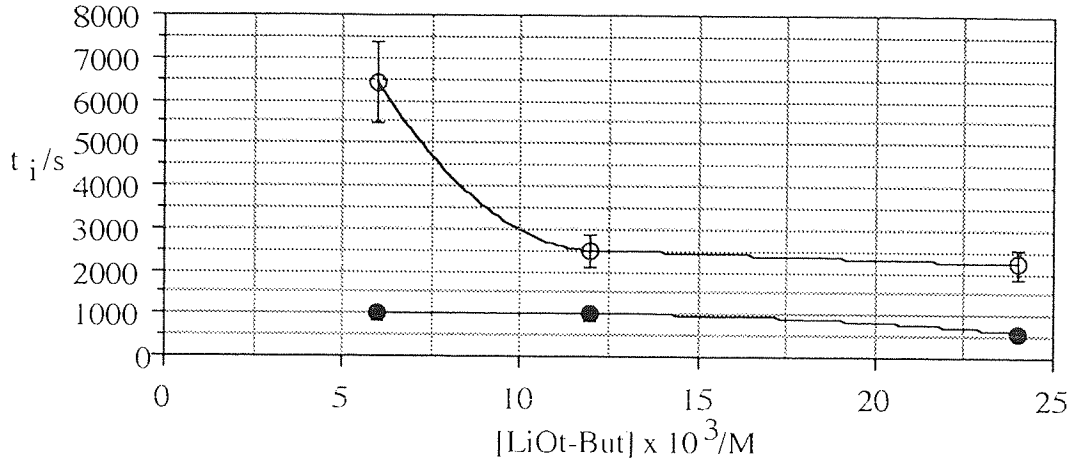

Figure 5.8 Effect of the concentration of lithium *tert*-butoxide, with (●), and without (○) crown ether, upon the length of induction period, (t_i), observed during the decomposition of LAAS in nitrobenzene at 34.5 °C.

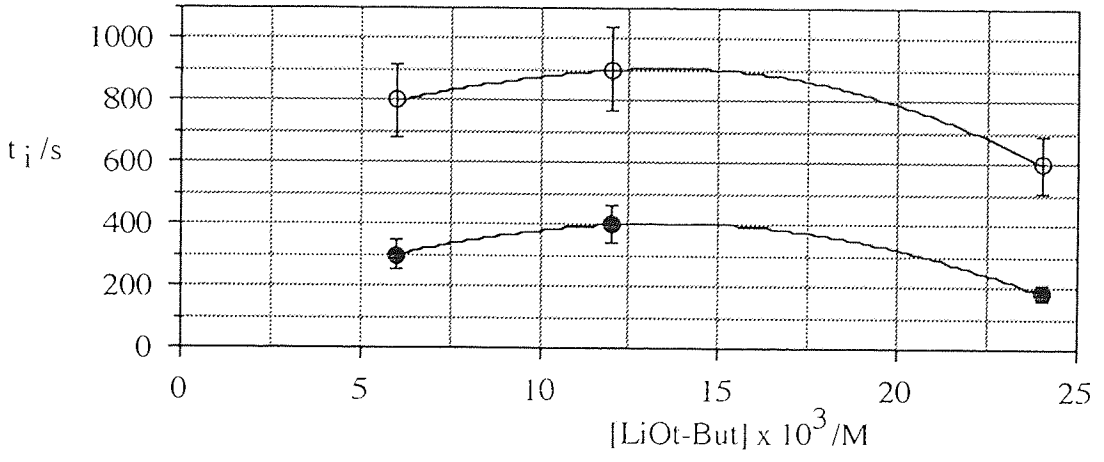

Figure 5.9 Effect of the concentration of lithium *tert*-butoxide, with (●), and without (○) upon the length of induction period, (t_i), observed during the decomposition of LAAS in nitrobenzene at 50.0°C.

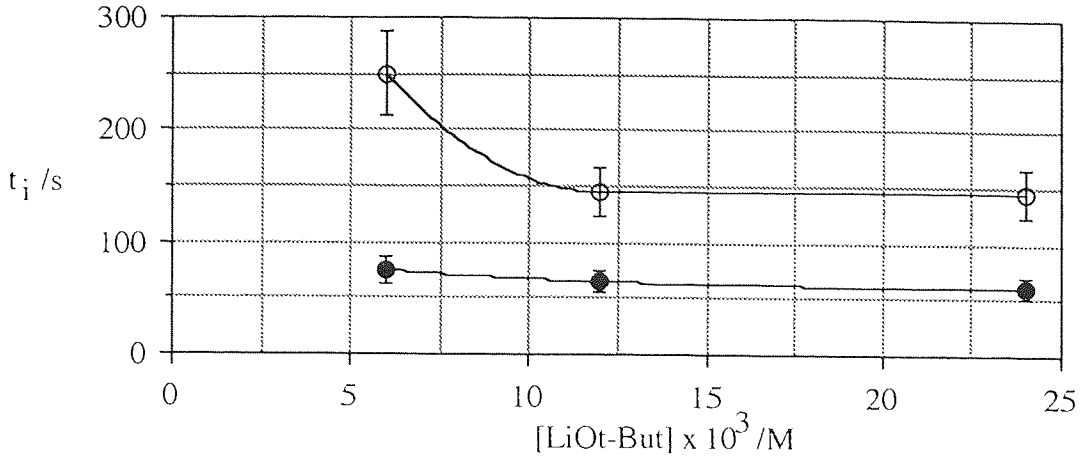

Figure 5.10 Effect of the concentration of lithium *tert*-butoxide, with (●), and without (○) crown ether, upon the length of induction period, (t_i), observed during the decomposition of LAAS in nitrobenzene at 69.0°C.

While the length of the induction period shows a tendency to decrease when higher concentrations of alkoxide are used, the presence of dibenzo-18-crown-6 has a more significant effect. A comparison of the lengths of the induction periods of reactions with and without crown ether present shows that the presence of crown ether in the initiator solution significantly reduces the length of this period.

It can be established that this reaction does not follow simple first or second order kinetics throughout since plots of $\ln([LAAS]/[LAAS]_0)$ against time, and $[LAAS]^{-1}$ against time are non-linear. However, if the rate constant, k_1 is calculated for each of the reactions and plotted against initiator concentration (as in figures 5.11-5.13), an imperfect dependence of rates of decomposition upon the concentration of lithium *tert*-butoxide can be seen. In the reactions where only lithium *tert*-butoxide was used, increasing the initiator concentration did not greatly increase the rate of monomer decomposition. However, when dibenzo-18-crown-6 was present, a more dramatic increase in the rate of decomposition was observed with increasing initiator concentration.

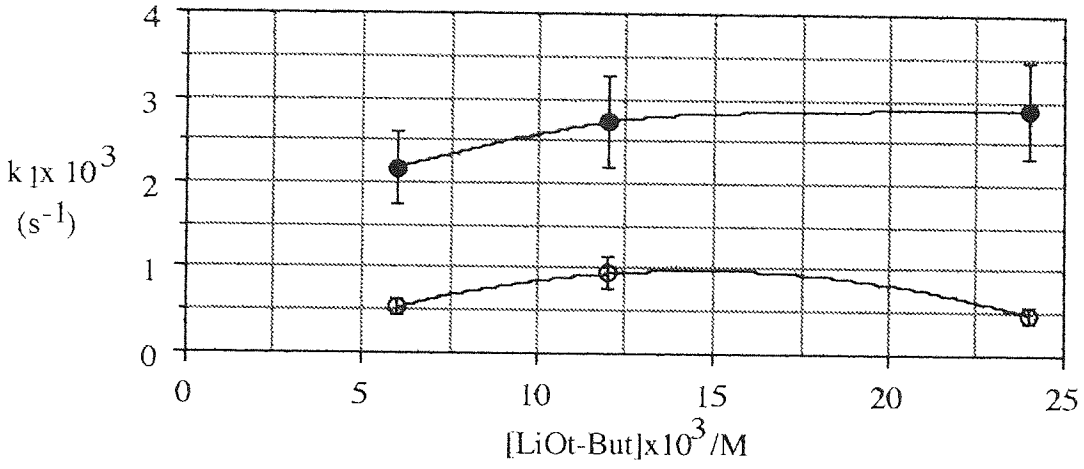

Figure 5.11 Effect of the concentration of lithium *tert*-butoxide, with (●), and without (○), crown ether, upon the rate constant, k_1 for the decomposition of LAAS in nitrobenzene at 34.5°C.

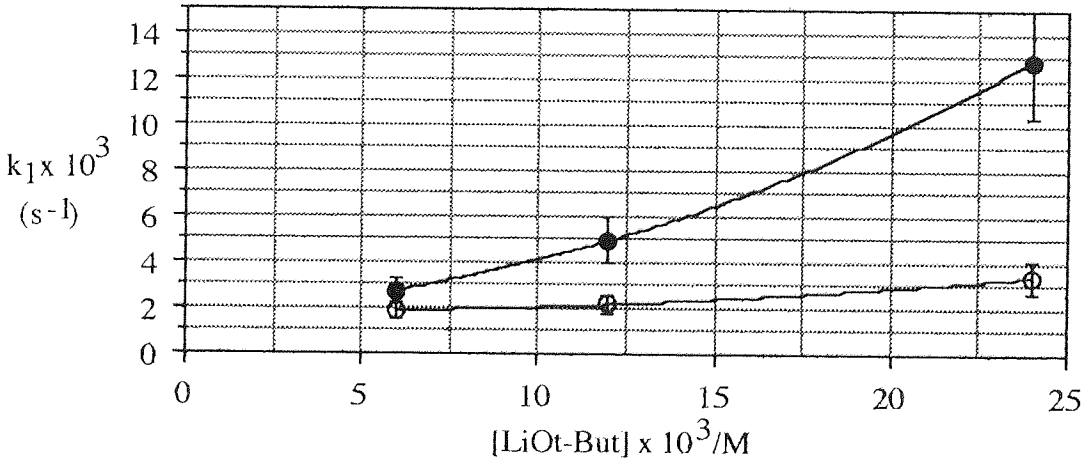

Figure 5.12 Effect of the concentration of lithium *tert*-butoxide, with (●), and without (○), crown ether, upon the rate constant, k_1 for the decomposition of LAAS in nitrobenzene at 50.0°C.

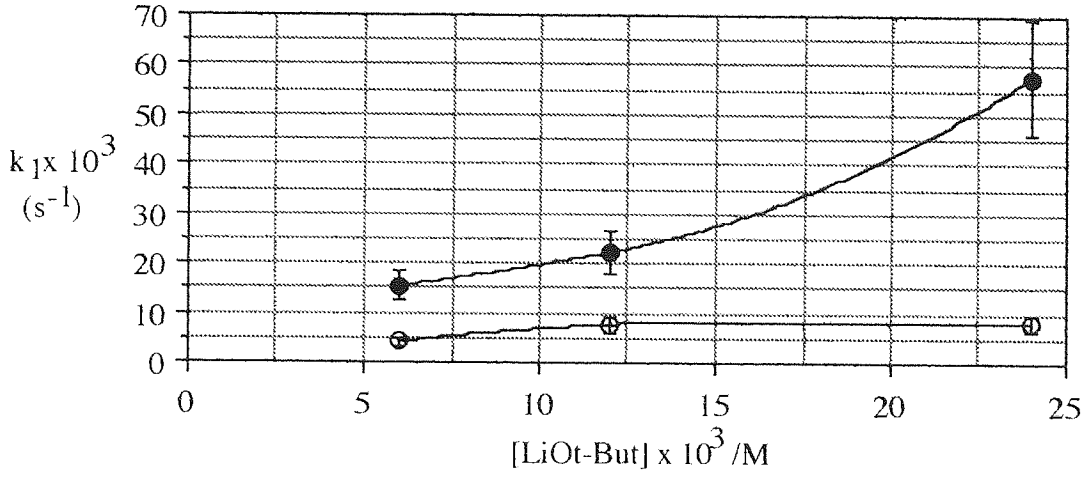

Figure 5.13 Effect of the concentration of lithium *tert*-butoxide, with (●), and without (○), crown ether, upon the rate constant, k_1 for the decomposition of LAAS in nitrobenzene at 69.0°C.

These results indicate that an increase in lithium *tert*-butoxide concentration does not significantly increase the rate of the rapid first order decomposition process unless crown ether is present. The presence of crown ether apparently has similar effects upon the slow initial process and the rapid decomposition process i.e. the presence of crown ether in the initiator solution causes the rate of reaction to be increased and the length of the induction period to be decreased. For the reactions performed at 50.0 °C, the presence of crown ether in the initiator solution increases the rate of polymerization by a greater factor at higher concentrations of initiator. The tendency for the effect of the crown ether to be more significant at higher concentrations of initiator may be explained by a consideration of the interaction of the dibenzo-18-crown-6 with alkali metal salts in solution.

This would tend to indicate that the propagating species can exist in more than one form. This is not unusual in ionic polymerizations where ion pair and free ionic species can exist in equilibrium, i.e. :-

$$P^-M^+ \rightleftharpoons P^- + M^+$$

The laws of equilibrium then dictate that :-

$$\left[P^-\right] = K^{\frac{1}{2}}.\left[P^-M^+\right]^{\frac{1}{2}}$$

and so the concentration of more reactive free ion increases only with square root of the concentration of initiator. It is believed that the presence of the crown ether forces the equilibrium to the right hand side and consequently a more dramatic effect of initiator concentration is observed.

The class of aromatic 'crown' ethers (so-called due to their shape) are neutral, colourless compounds which are themselves fairly soluble in aromatic solvents but have the useful property of being able to increase significantly the solubility of alkali metal salts by complexing with the metal cation. It is thought that the metal cation is accepted by the central hole in the crown ether, being located coplanar with, and equidistant from each oxygen atom. It is held there by the electrostatic attraction between its positive charge and the negative dipolar charge on each of the six oxygen atoms symmetrically arranged around it in the polyether ring (see figure 5.14).

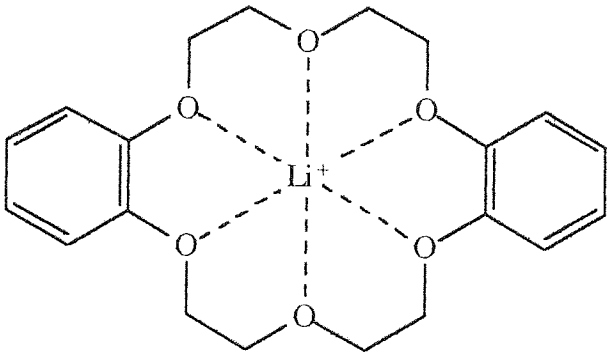

Figure 5.14 Structure of dibenzo-18-crown-6 complexed with lithium cation.

The relationship between the relative sizes of hole and cation is important due to the 'template' effect. The binding constant of crown ether and metal cation is highest when the closest 'fit' is obtained. The hole size of dibenzo-18-crown-6 is estimated as 2.6 - 3.2 Å while the ionic diameters of lithium and potassium cations are 1.52 and 2.76 Å, respectively.[91] Thus the crown ether should complex more effectively with lithium *tert*-butoxide than the potassium alkoxide. Lithium *tert*-butoxide was used in these studies rather than potassium since it was thought that the reaction of LAAS with the lithium alkoxide was slower and the effect of the crown ether might be more significant.

At higher concentrations, the initiator is less easily dissolved and the addition of solubising agent has a more dramatic effect. The crown ether increases the solubility of the initiator by co-ordinating with the lithium ion, thereby reducing the energy barrier for attack on the monomer by initiator and propagation species. This also has the effect of

increasing the concentration of initiator present in solution as more reactive dissociated species rather than aggregated dimers, etc. (see figure 5.15).

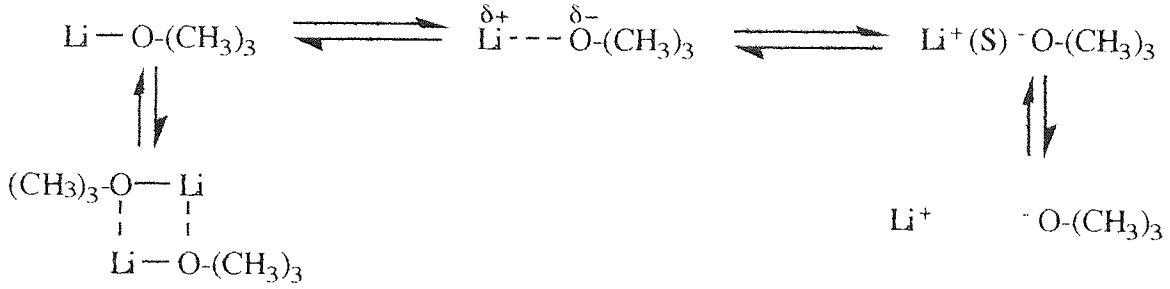

Figure 5.15 Structure of lithium *tert*-butoxide in solution.

The activation energies of the reactions both with and without dibenzo-18-crown-6, were determined by plotting ln(k) against reciprocal temperature (as shown in figure 5.16). The gradients of the lines were measured and their values fitted into the Arrhenius equation to give values for the activation energy (as described in section 2.3.1.2).

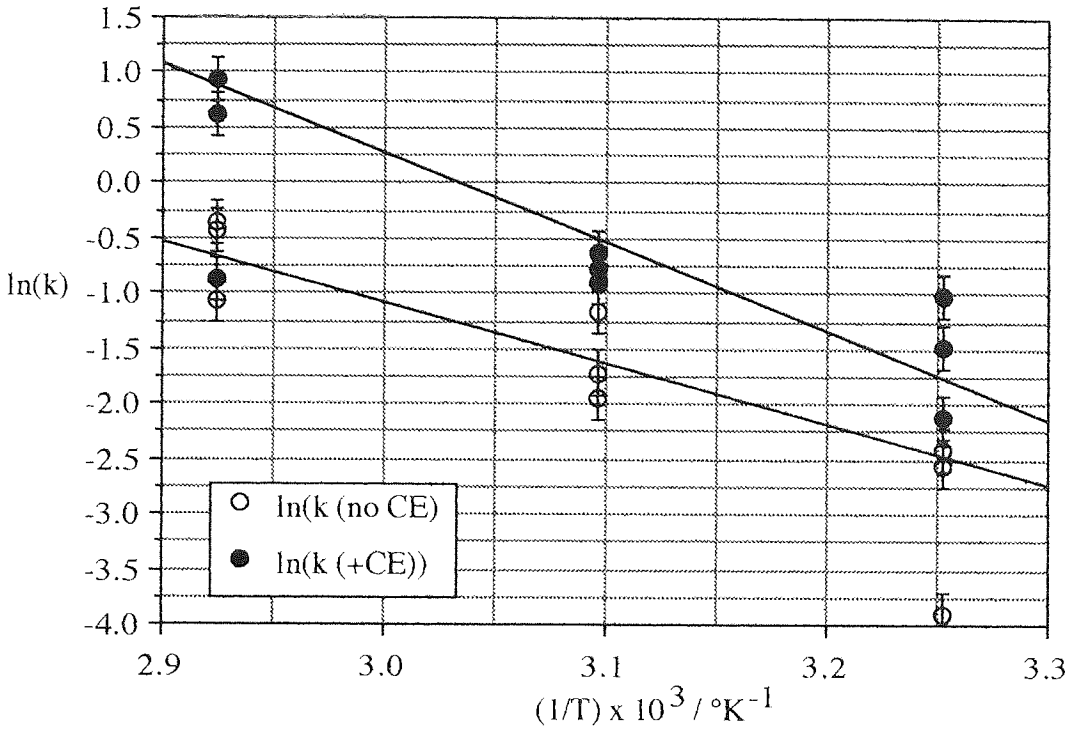

Figure 5.16 Graph of ln(k) plotted against 1/T for lithium *tert*-butoxide initiated decomposition of LAAS in nitrobenzene.

Activation energies were determined as:-

lithium *tert*-butoxide only:	54 ± 15 kJ.mole^{-1}
lithium *tert*-butoxide + dibenzo-18-crown-6:	52 ± 15 kJ.mole^{-1}

Since the addition of the crown ether to the initiator system appears to have the effect of increasing the rate of decomposition of LAAS it might be expected that the calculated activation energy for this reaction would be lower than that of the reaction initiated by lithium tert-butoxide alone. However, the values are very close and the error limits too great for any meaningful conclusions to be drawn. This is probably caused by variations in temperature occuring between the different experiments and other factors such as the presence of impurities.

In the potassium *tert*-butoxide-initiated polymerization of L,L-lactide in tetrahydrofuran the addition of dibenzo-18-crown-6 to the initiator system was found to have a narrowing effect upon the molecular weight distribution.[92] It is suggested that this is because the propagating species is less reactive when the counter-ion is complexed, causing a reduction in the extent of side-reactions. Given that, unlike anhydrosulphite polymerization, this reaction is reversible, it must be assumed that the stabilising effect of the crown ether is different in respect of the propagation and depropagation reactions. In the anhydrosulphite polymerization considered here, the molecular weights of the products are all relatively low, with number and weight average molecular weights ranging from 1600 to 2600 and 2700 to 3800, respectively. However, for all but one reaction, polydispersities are within the range 1.4 to 1.5, regardless of the presence of crown ether. Therefore, while the presence of dibenzo-18-crown-6 does not appear to affect the molecular weight distribution, molecular weights are independent of initiator concentration and temperature anyway, so this may not be significant.

It is possible that the presence of the impurity discussed in section 3.2 may have reduced the molecular weight distribution by termination of living chain ends. Alternatively, high molecular weight material may not be sufficiently soluble in tetrahydrofuran (the solvent used for GPC) for accurate results to be obtained. The technique may not be sensitive enough to distinguish between quantities of low molecular weight material with sufficient accuracy.

5.2 EFFECT OF MULTIPLE ADDITIONS OF MONOMER ON RATES OF REACTION

One of the most interesting characteristics of living anionic polymerizations is the fact that chain ends remain active even after all monomer present is consumed. This means that the subsequent addition of monomer will cause chain growth to continue. Experiments were performed using lithium *tert*-butoxide and its complex with dibenzo-18-crown-6 to decompose LAAS to find out whether initiator activity remained towards the end of the reaction.

5.2.1 Experimental

In two experiments using manometer vessels, as the reaction was observed to slow down, a further quantity of monomer was injected into the reaction vessel. In one experiment, 0.025 M lithium *tert*-butoxide was used to initiate decomposition of monomer. In another a 0.025 M solution of lithium *tert*-butoxide : dibenzo-18-crown-6 in a 1:1 molar ratio. Both reactions used dry nitrobenzene as solvent and LAAS which was free of all impurities.

Initiator solutions were injected into manometer vessels and the vessels placed in a water bath at 35.0 °C. After 30 minutes, the vessels were removed from the bath and 0.4 cm^3 of a 2.79 M solution of LAAS in nitrobenzene was injected. The vessels were agitated and replaced in the bath. The pressure of sulphur dioxide was recorded until the final slow phase was reached, at which point the vessels were removed from the bath, a further 0.4 cm^3 of monomer solution injected and the manometer readings recommenced. When the final phase was reached again, more monomer was again injected and readings continued.

The products were removed from the vessels and the analysed by FT-IR in order to confirm that no unreacted monomer remained. They were then purified as described previously and analysed by GPC in tetrahydrofuran.

5.2.2 Results

5.2.2.1 Gas Evolution Data

Figure 5.17 shows the pressure of sulphur dioxide evolved during the reactions as measured by the mercury manometer.

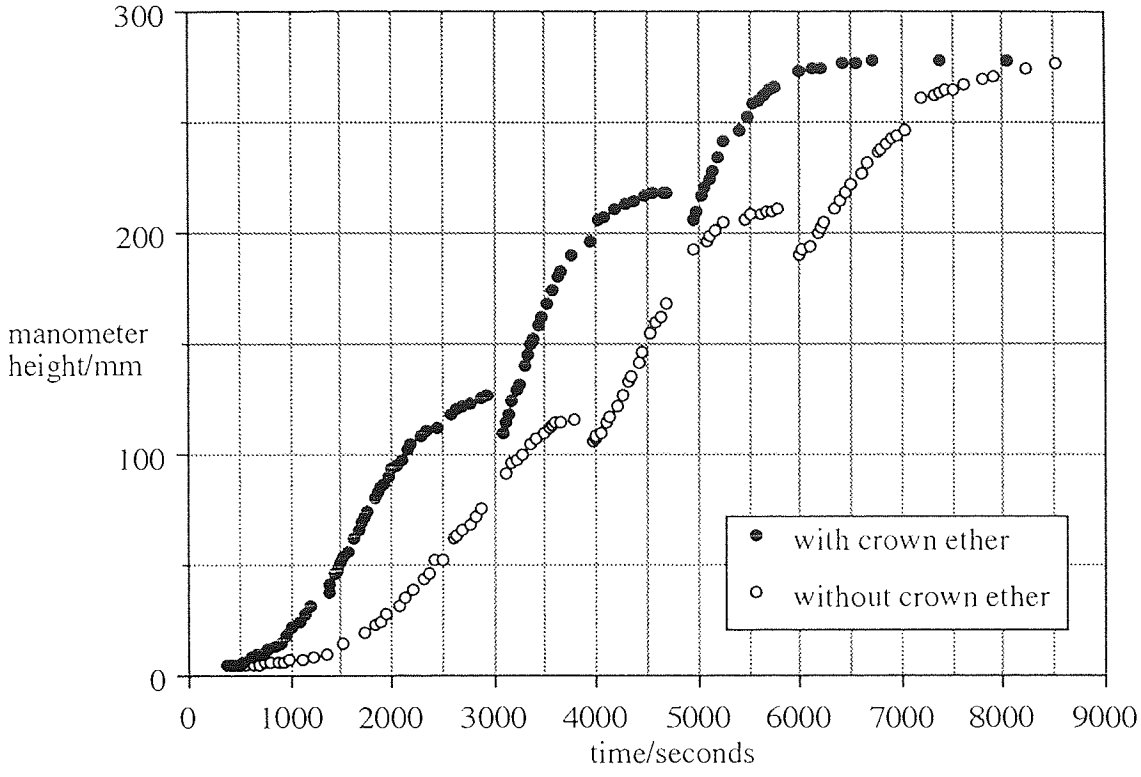

Figure 5.17 Effect of multiple additions of LAAS on rates of reaction - gas evolution graph.

5.2.2.2 GPC Analysis

Table 5.3 shows the results of GPC analysis of the end products, determined as polystyrene equivalents, for the two reactions.

Table 5.3 Multiple additions of LAAS - GPC analysis of end products.

Initiator system	[M]/[I]	$\overline{M}_w$	$\overline{M}_n$	P_d
Lithium *tert*-butoxide only	334	5810	3870	1.50
:Lithium *tert*-butoxide/crown ether	334	6200	4000	1.55

experiments, both with and without crown ether present, the addition of a quantity of monomer after gas evolution has slowed, causes rapid gas evolution to occur.

While the quantities of monomer added were identical, the maximum volume of gas evolved appears to decrease for each subsequent addition. The presence of unreacted monomer can be ruled out since FTIR analysis of the product solution showed that only polymer was present, and the addition of methanol at the end of the reaction caused no gas evolution. In fact, this effect may be explained by the solvation of the evolved gas in the greater volume of solvent present after addition of monomer. The slight drop in gas pressure associated with the addition of second and third quantities of monomer solution supports this conclusion.

The fact that no induction period is observed on addition of further quantities of monomer, would tend to support the idea that during the initial stages of reaction, initiator is slowly converted to more reactive propagating species.

If the induction period is due to the reaction of initiator with impurities then these impurities must be associated with the initiator rather than monomer solution. If impurities were present in the monomer solution, the further quantities of monomer added would only begin to decompose rapidly after these impurities were consumed.

The GPC analysis of the products of the two experiments shows that the presence of crown ether has no effect upon the molecular weights and polydispersities of the products.

5.3 EFFECT OF MULTIPLE ADDITIONS OF MONOMER ON MOLECULAR WEIGHT DISTRIBUTION OF PRODUCTS

Since it was not possible to take samples from the reaction mixture during the reaction, without disturbing the pressure of gas in the vessels, three experiments were performed in order to study the effect of multiple additions of monomer to lithium *tert*-butoxide on the molecular weights of the products.

5.3.1 Experimental

Three pressure monitoring reaction vessels marked A, B and C were used for this experiment. Each vessel was injected with a 0.053M solution containing a 1:1 molar ratio of lithium *tert*-butoxide : dibenzo-18-crown-6 in nitrobenzene. The reaction vessels were

then suspended in a water bath at 52.0 °C for 30 minutes. A 1.96 M solution of LAAS in nitrobenzene was also allowed to reach the bath temperature using the apparatus described in section 5.1. Vessel A was removed from the bath, 0.5 cm^3 of the monomer solution added, agitated and returned to the bath so that the pressure of evolved gas might be recorded. Measurements were made until gas evolution appeared to have stopped. This procedure was repeated for vessels B and C.

After gas evolution ceased, vessel A was removed from the bath, a second 0.5 cm^3 volume of monomer solution added, and measurements continued as before. This procedure was repeated for vessel B only.

Finally, the procedure was repeated for vessel A only, so that vessel A had received three injections of monomer, vessel B, two and vessel C, only one.

Samples of the product solutions were taken for analysis by FTIR spectroscopy, the reactions terminated and the products purified as described previously. The products were analysed by GPC in tetrahydrofuran.

5.3.2 Results

5.3.2.1 Gas Evolution Data

The pressures of gas evolved for each reaction were converted to fractional monomer remaining and plotted against time, as shown in figure 5.18.

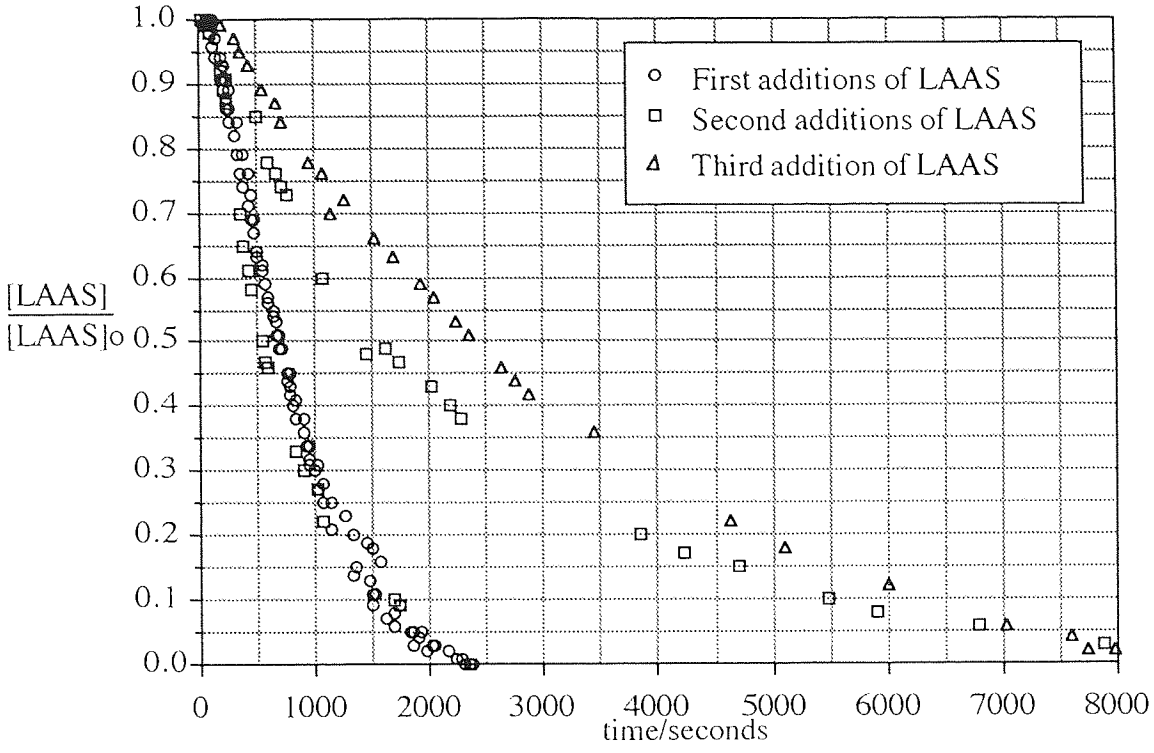

Figure 5.18 Effect of multiple additions of LAAS on molecular weight distributions of products - gas evolution graph.

5.3.2.3 GPC Analysis

The results of analysis by GPC for each of the three reaction products are recorded as polystyrene equivalents in table 5.4.

Table 5.4 Effect of multiple additions of LAAS on molecular weight distributions of products - GPC analysis.

Reaction	[LAAS]	[I]/M	[M]/[I]	$\overline{M}_w$	$\overline{M}_n$	Pd
A - 3 additions of monomer	1.47	0.007	218	3970	1880	2.08
B - 2 additions of monomer	1.31	0.009	145	3070	1650	1.86
C - 1 addition of monomer	0.98	0.014	75	570	360	1.60

Figure 5.19 shows the GPC traces of each reaction product superimposed in order to show differences in molecular weight distribution.

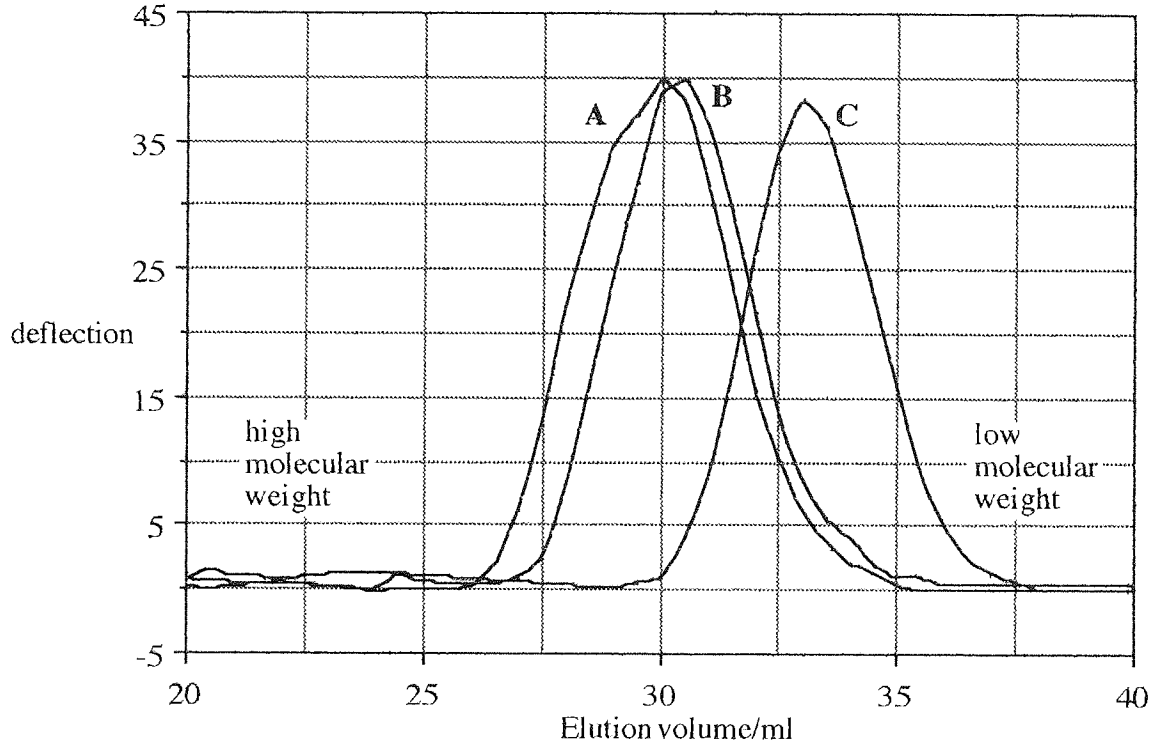

Figure 5.19 Effect of multiple additions of LAAS on molecular weight distributions of products - superimposed Gel Permeation Chromatographs.

5.3.3 Discussion

Obviously, with an experiment of this nature there is some potential for error due to variations in the concentration of reactants and reaction conditions. For experiment B the addition of a second quantity of monomer caused evolution of sulphur dioxide at a rate comparable with that of the first addition. In the case of experiment A, the second addition caused gas evolution at a slower rate and the third addition a slower rate still. However, the results do show that the addition of a second quantity of monomer causes a significant increase in the molecular weight of the products.

The situation is not so clear when a third quantity has been added since a less dramatic increase in molecular weight is observed. The molecular weight distribution is broadened by a high molecular weight 'shoulder'. This may be explained by the termination of some active chain ends so that the molecular weight of some of the product is fixed whilst the

remaining 'living' chains increase in length when more monomer is added. This would also be consistent with the slower monomer decomposition observed in reaction A.

Taken together, these results would seem to indicate that the reaction of lithium *tert*-butoxide with LAAS in nitrobenzene possesses some degree of 'living' character i.e. the propagating chain ends remain active even after all available monomer is consumed. When a similar experiment was performed with additional monomer added after 18 hours, no further gas evolution was observed. This may be because a slow termination of the living chain ends had occurred.

5.4 LITHIUM *tert*-BUTOXIDE INITIATED POLYMERIZATION OF LAAS USING DECALIN AS SOLVENT

Due to the limitations of the technique, the quantities of product derived from experiments using the mercury manometer vessels was small. In order to provide a larger sample of polymer for NMR spectral analysis, a polymerization was performed without monitoring the progress of the reaction.

5.4.1 Experimental

16.0 g of lactic acid anhydrosulphite (0.12 moles) was distilled into the vessel shown in figure 5.20 using micro-distillation apparatus.

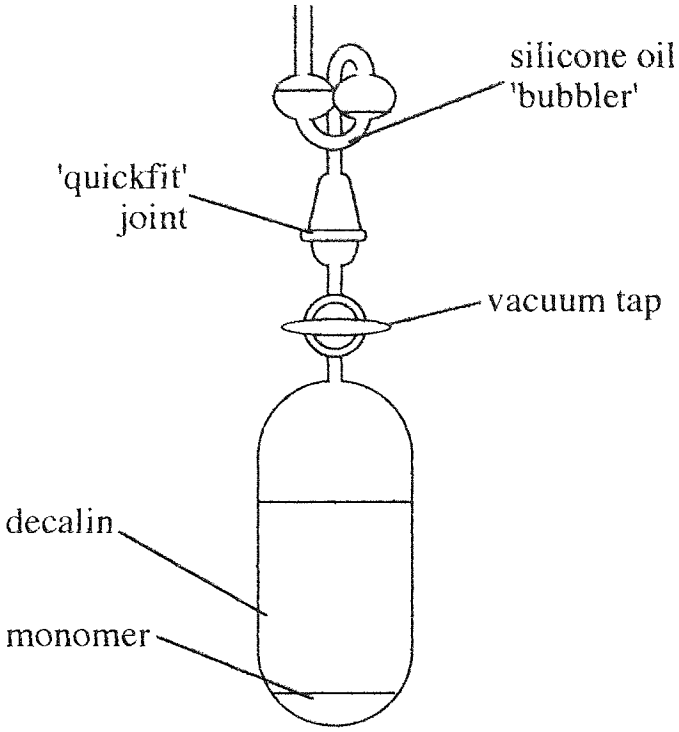

Figure 5.20 Polymerization vessel used for lithium*tert*-butoxide initiated polymerization of LAAS in decalin.

Approximately 100 cm^3 of dry decalin was distilled into the vessel from sodium metal under argon. The tap was closed and the vessel transferred to a dry box where25 cm^3 of a 0.05 M solution of lithium *tert*-butoxide in decalin was added and the bubbler fitted. The apparatus was agitatedin order to mix the solutions, removed from the dry box and suspended in a water bath at 40.0 °C. A rapid evolution of sulphur dioxide occurred initially but slowed over a periodof several hours until it stopped completely. The reaction was left for a total of 48 hours before methanol was injected.

Since the anhydrosulphite and product were insoluble in the solvent and remained at the bottom of the vessel, the bulk of thesolvent was removed by decantation and final traces evaporated under vacuum as described previously. The off-white powder remaining was analysed by ^1H and ^{13}C NMR. GPC analysis of the product was performed at Aston University and by RAPRA (see section 2.4.4).

5.4.2 Results

5.4.2.1 NMR Spectral Analysis

Figures 5.21 and 5.22, respectively show the ^{1}H and ^{13}C NMR spectra of the product.

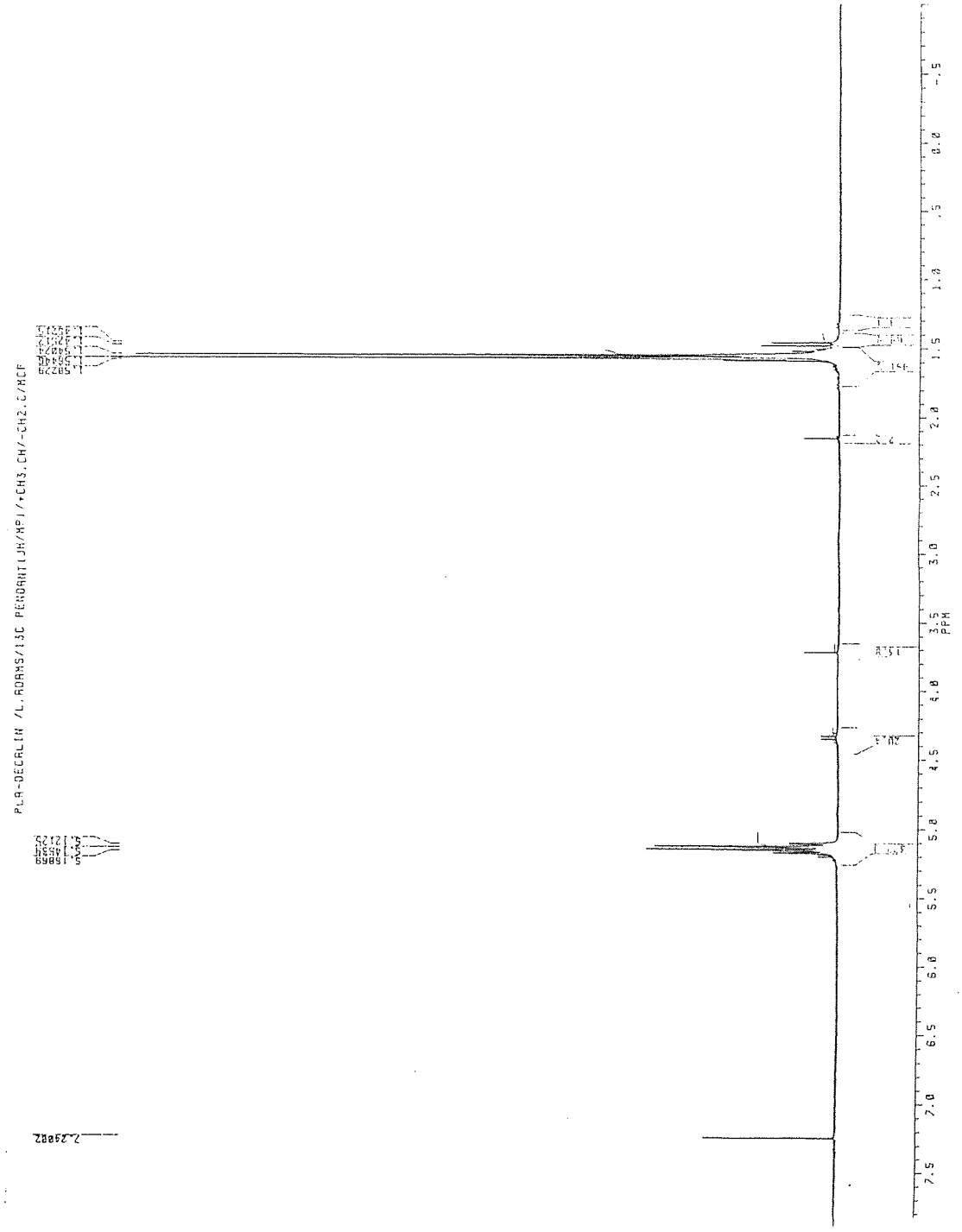

Figure 5.21 Product of lithium *tert*-butoxide initiated decomposition of LAAS in decalin - ^{1}H NMR spectrum.

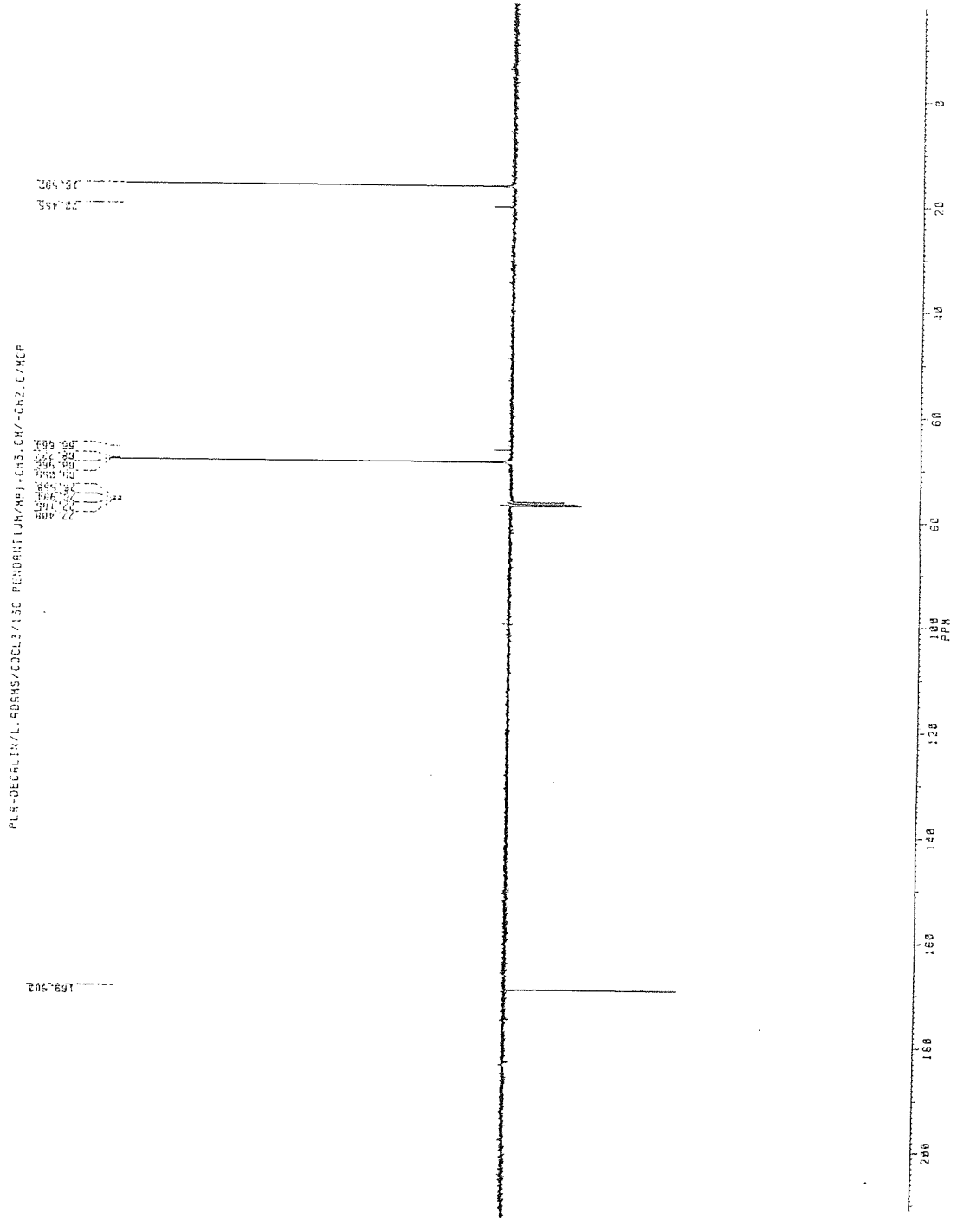

Figure 5.22 Product of lithium *tert*-butoxide initiated decomposition of LAAS in decalin - ^{13}C NMR spectrum.

Table 5.5 Product of lithium *tert*-butoxide initiated decomposition of LAAS in decalin - ^{1}H NMR peak table.

ppm	multiplicity	assignment	relative peak areas
1.54 - 1.56	doublet	**b**	3.0
5.02 - 5.25	quartet	**a**	1.0

Table 5.6 Product of lithium *tert*-butoxide initiated decomposition of LAAS in decalin - ^{13}C NMR peak table.

ppm	assignment	+/- intensity
16.59	**b**	11.9
68.97	**a**	12.6
169.6	**c**	-5.4

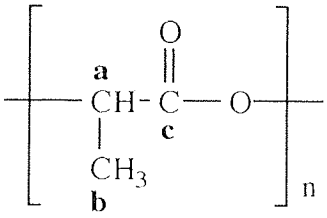

Figure 5.23 Key to NMR spectra of poly(lactic acid).

5.4.2.2 GPC Analysis

The results of GPC analysis of the products are recorded as poly(styrene) equivalents in table 5.7.

Table 5.7 Product of lithium *tert*-butoxide-initiated decomposition of LAAS in decalin - GPC analysis.

GPC	solvent	$\overline{M}_w$	$\overline{M}_n$	P_d
Aston	tetrahydrofuran	1770	1220	1.45
Rapra	dimethyl formamide	1900	1200	1.60

5.4.3 Discussion

In this experiment decalin, rather than nitrobenzene was used since lithium *tert*-butoxide is relatively soluble in decalin, yet the polymer is insoluble in this solvent. It was hoped that this would facilitate purification of the product. However, LAAS is also insoluble in decalin which may hinder smooth polymerization due to the additional barrier to reaction between the alkoxide and anhydrosulphite this creates. This may be the reason that the product was of low molecular weight, though the presence of trace moisture may have the same effect. The mechanism of the reaction of anhydrosulphites with alkoxides such as lithium *tert*-butoxide is discussed further in section 5.5.

5.5 MECHANISM OF LITHIUM *tert*-BUTOXIDE INITIATED POLYMERIZATION OF LAAS

The mechanism by which an anhydrosulphite reacts with an alkoxide is quite complex. Crowe studied the decomposition of dialkyl-substituted anhydrosulphites by lithium *tert*-butoxide using nitrobenzene and/or decalin as solvents. A mechanism, based upon the formation of a reactive intermediate which re-arranges to form two further intermediates, was suggested.[32]

This mechanism, shown in figure 5.24, involves two routes, both of which cause breakdown of the anhydrosulphite ring and expulsion of sulphur dioxide, but only one of which may lead to the formation of polymer. In both reaction pathways, the initial step is the rapid nucleophilic attack of the alkoxide upon the anhydrosulphite carbonyl, forming a charge transfer complex (A). It is possible for the charge transfer complex to rearrange in two ways, I and II.

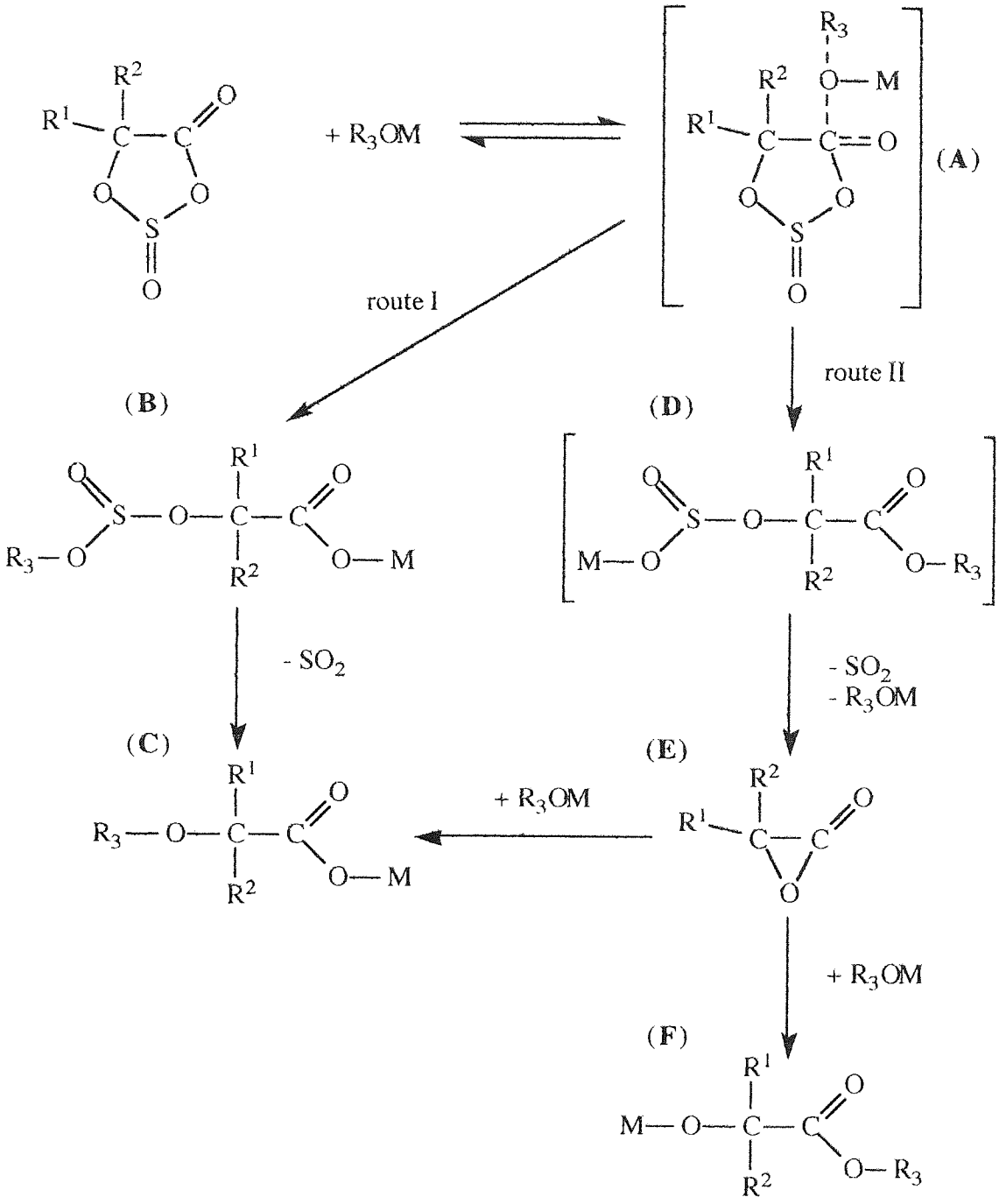

Figure 5.24 Modified reactive intermediate mechanism.

Route I involves the formation of a metal carboxylate (B) which decomposes to yield a carboxylate ester (C) and occurs slowly. In contrast, route II is relatively fast. Initially, the charge transfer complex (A) rearranges to form a second charge transfer complex (D) before breaking down in a reaction which releases sulphur dioxide, regenerates the alkoxide and yields an α-lactone (E). This short-lived species reacts rapidly with any nucleophiles present but if reaction is with the alkoxide initiator, there are two possible

products which may be formed. If nucleophilic attack occurs on the α-lactone's substituted carbon, the carboxylate ester (C) will be produced. If attack is upon the carbonyl carbon, an alkoxide (F) is the product. The alkoxide (F) is the propagating species which may go on to attack further anhydrosulphite molecules, though this is likely to occur rather more slowly than attack by the initiator alkoxide due to the reduced activity in the longer chain.

Crowe discards the possibility of alkoxide attack on the substituted carbon due to steric obstruction and the lack of nucleophilic character. While Crowe was studying the extreme case of di-substituted anhydrosulphites where the substituents were long alkyl chains, it is reasonable to assume that such a mechanism is relatively unlikely in the case of lactic acid anhydrosulphite for similar reasons.

5.6 POTASSIUM *tert*-BUTOXIDE INITIATED POLYMERIZATION OF LAAS

Since LAAS was successfully polymerized by potassium and lithium *tert*-butoxides in nitrobenzene, experiments were performed to determine whether polymerization would occur if a more volatile solvent was used. Tetrahydrofuran is, like nitrobenzene, a relatively polar solvent, but since it has a much lower boiling point, it is easily removed from the reaction products by evaporation.

5.6.1 Experimental

The rate of polymerization of lactic acid anhydrosulphite by potassium *tert*-butoxide was measured in tetrahydrofuran at room temperature and pressure using the calorimetric apparatus and techniques described in section 2.3.3. Re-distilled LAAS was injected into the vessel and a suitable volume of tetrahydrofuran added. A 1.0 M solution of potassium *tert*-butoxide in tetrahydrofuran was diluted to a concentration of 0.1 M in dry tetrahydrofuran and this weaker solution was used for initiation of polymerizations. The quantities of solvents and reactants injected were measured by recording the mass of syringes before and after injection.

5.6.2 Results

5.6.2.1 NMR Spectral Analysis

The ^{1}H and ^{13}C NMR spectra of the product are shown in figures 5.25 and 5.26, respectively. The corresponding peak data is recorded in tables 5.8 and 5.9. Refer to figure 5.23 for key.

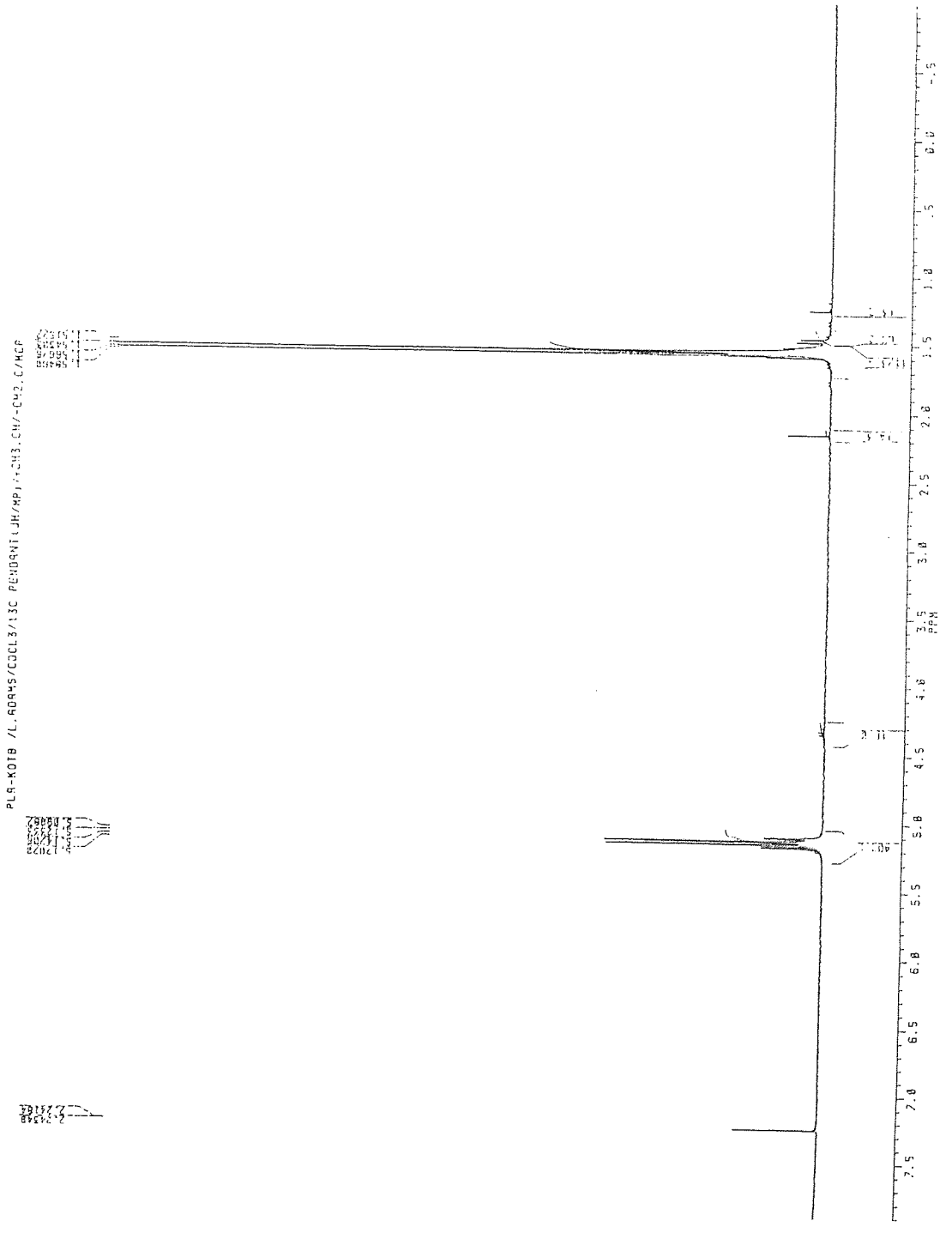

Figure 5.25 Product of potassium *tert*-butoxide initiated decomposition of LAAS - ^{1}H NMR spectrum.

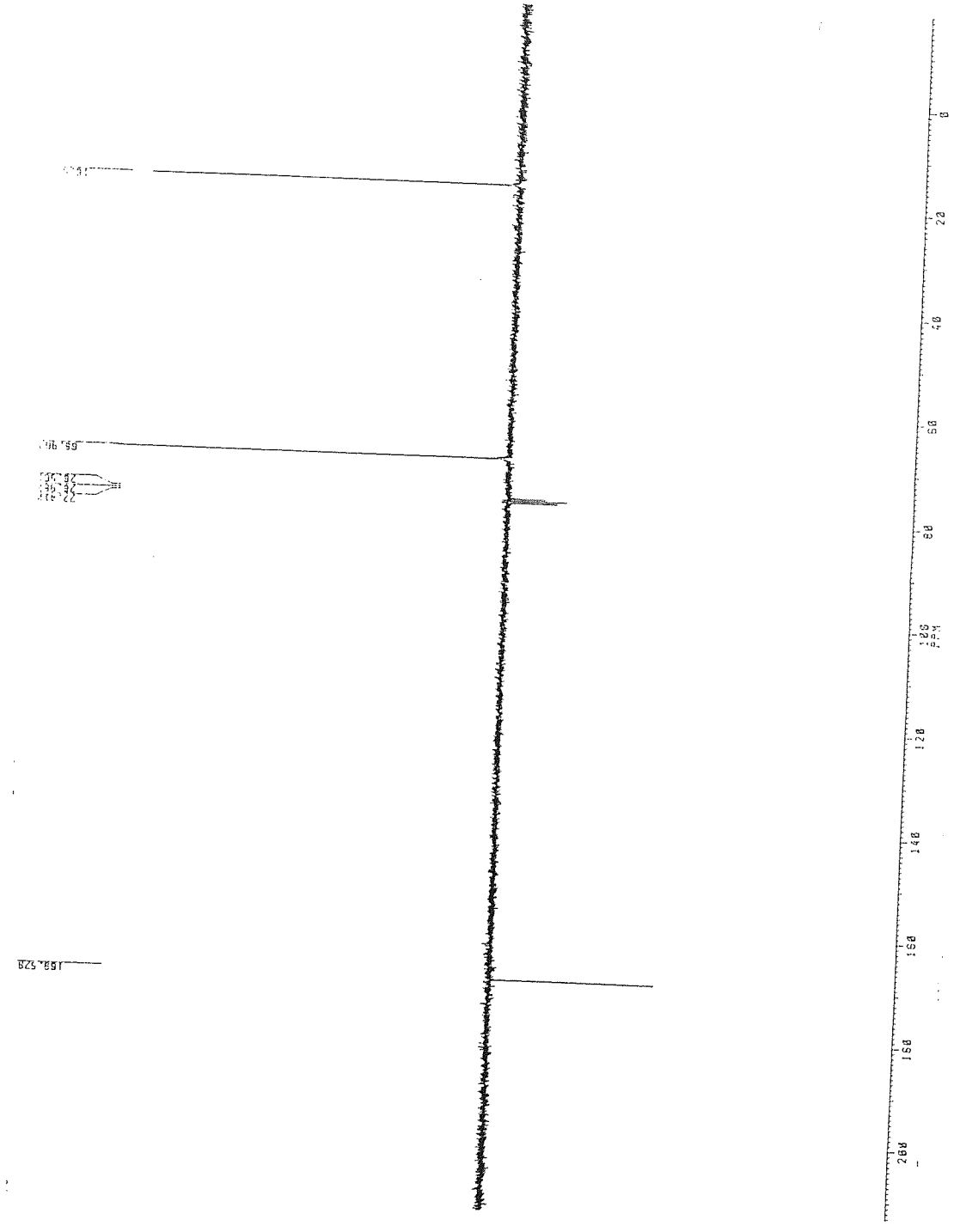

Figure 5.26 Product of potassium *tert*-butoxide initiated decomposition of LAAS - ^{13}C NMR spectrum.

Table 5.8 Product of potassium *tert*-butoxide initiated decomposition of LAAS - ^{1}H NMR peak table.

ppm	multiplicity	assignment	relative peak areas
1.52 - 1.59	doublet	**b**	2.9
5.04 - 5.28	quartet	**a**	1.0

Table 5.9 Product of potassium *tert*-butoxide initiated decomposition of LAAS - ^{13}C NMR peak table.

ppm	assignment	+/- intensity
16.60	**b**	11.3
69.00	**a**	12.1
169.60	**c**	-5.2

5.6.2.2 Calorimetric Data

The results of the experiments are recorded in table 5.10. The rate constant, k_1,for each of the experiments was determined from calorimetric data.

5.6.2.3 GPC Analysis

For these experiments, Gel Permeation Chromatography was performed in duplicate by RAPRA Technology Ltd using dimethyl-formamide as eluent. Number and weight average molecular weights are recorded in table 5.11 as the average of two GPC experiments and are poly(styrene) equivalents.

Table 5.11 Products of potassium *tert*-butoxide initiated decomposition of LAAS in tetrahydrofuran - GPC analysis.

[KOt-But] x10^{3}/ M	[LAAS]/M	[M] / [I]	$\overline{M}_w$	$\overline{M}_n$	P_d
7	2.65	379	12650	7450	1.7
15	2.53	169	11500	8250	1.4
30	2.84	95	9100	5900	1.6
6	1.34	220	15450	10620	1.5
12	1.28	107	12550	7870	1.6
24	1.36	57	10800	3435	3.2
30	1.25	42	4150	2830	1.5

5.6.3 Discussion

5.6.3 Discussion

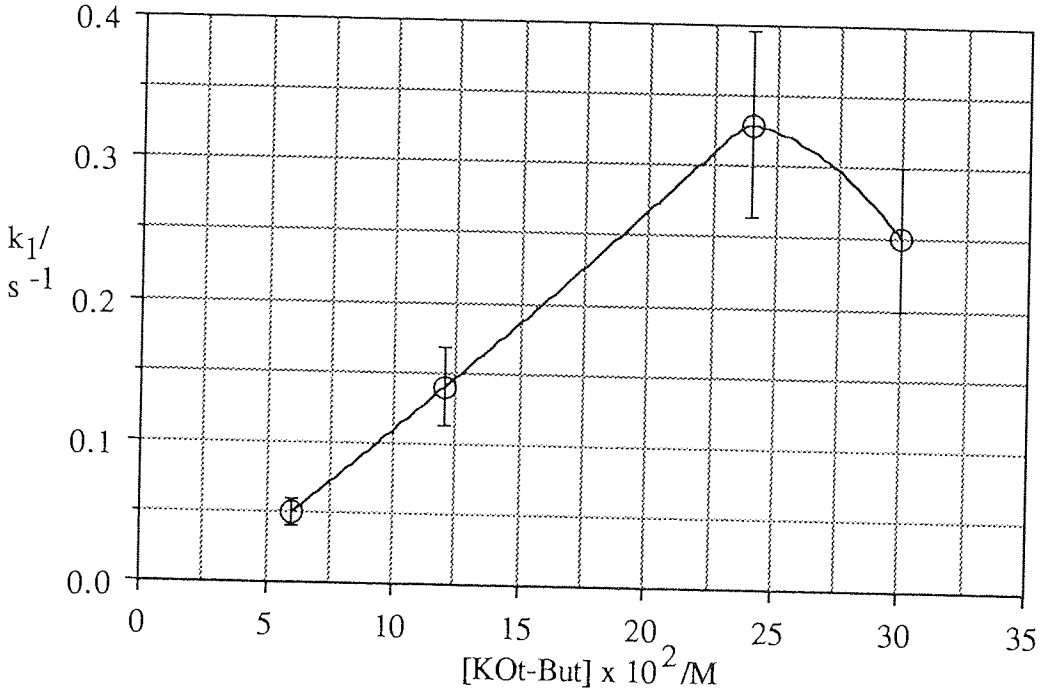

Figure 5.27 Effect of potassium *tert*-butoxide concentration on rate of decomposition of LAAS in tetrahydrofuran.

Molecular weights are generally higher than in nitrobenzene. If the number average molecular weight is plotted against the square root of [M]/[I], as shown in figure 5.28, a linear relationship is observed.

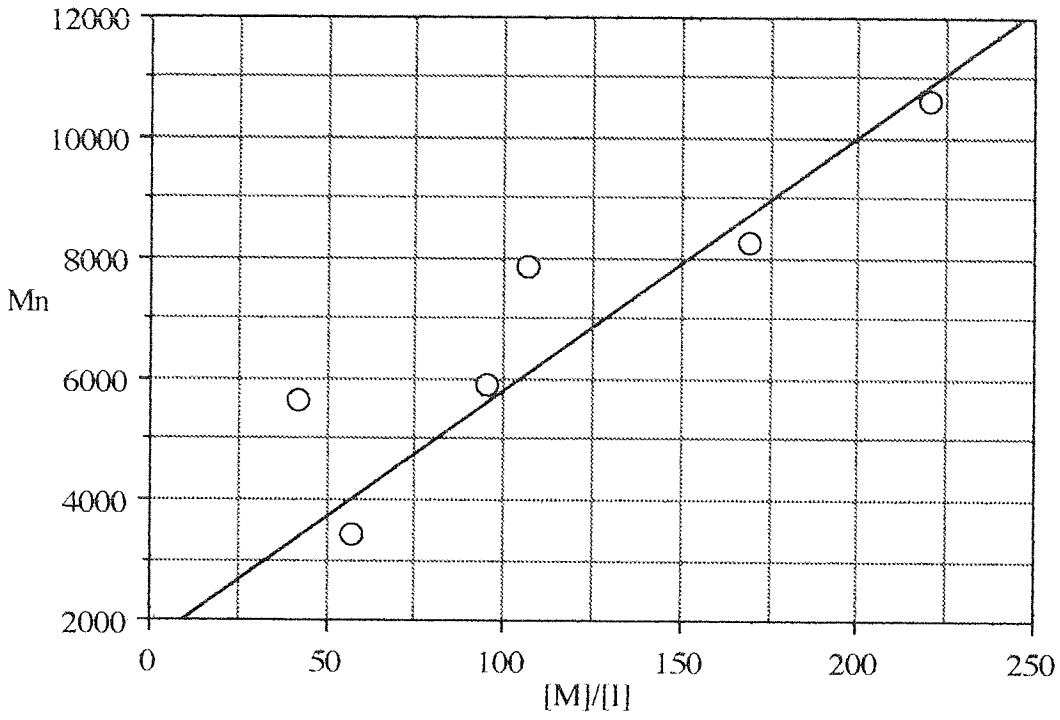

Figure 5.28 Potassium *tert*-butoxide initiated decomposition of LAAS in tetrahydrofuran - dependence of the number average molecular weight on [M]/[I].

5.7 EFFECTS OF REACTION CONDITIONS ON CRYSTALLINITY

A number of samples of poly(lactic acid) were prepared under different reaction conditions (different initiators and temperatures) and the crystallinity of the end products was estimated by means of X-ray crystallography.

5.7.1 Experimental

Samples of poly(lactic acid) were prepared by the polymerization of LAAS in tetrahydrofuran, initiated by potassium *tert*-butoxide at +25, -50 and -70 °C, and by *sec*-butyl lithium at 25 °C. The molecular weight distributions of the products were determined by GPC performed by RAPRA using dimethyl formamide as eluent.

A sample of the polymer prepared using potassium *tert*-butoxide at -70 °C was placed between acetate sheets in a Daniels melt press and subjected to 150 seconds pre-heating at 140 °C, pressed at 110 Kg/cm^2 pressure for 120 seconds before cooling to room temperature to yield a brittle, clear film.

A second sample of this polymer was solvent cast by allowing a 10 % solution of the polymer in chloroform to evaporate in a fume cupboard. This product was not a very strong film, being rather fragile and powdery.

X-ray crystallographic data was obtained using a 4-circle X-ray diffractometer (Enraf Nonius CAD-4). Only copper K_α radiation was used. The relative areas due to crystalline and amorphous material were calculated by cutting-out and weighing the areas on the graph paper representing them.[40]

5.7.2 Results

5.7.2.1 GPC Analysis

Table 5.12 shows the results of GPC analysis of the four products. Unfortunately it was not possible to analyse samples of the processed polymer as insufficient sample was available.

Table 5.12 Effect of reaction conditions on crystallinity - GPC analysis.

Initiator	reaction temp./°C	$\overline{M}_w$	$\overline{M}_n$	P_d
KOt-But	-50.0	12650	7450	1.70
KOt-But	-70.0	1800	1400	1.30
KOt-But	+25.0	3100	2100	1.50
s-BuLi	+25.0	8350	5700	1.45

(Note There was insufficient sample available for GPC analysis of processed samples).

5.7.2.2 X-Ray Crystallographic Analysis

Table 5.13 shows the percentage crystalline areas found in the various samples, as determined by X-ray crystallography. Unfortunately, there was insufficient sample to irradiate the melt pressed and solvent cast samples completely, therefore the results for these samples are not valid for direct comparisons.

Table 5.13 Effect of reaction conditions on crystallinity - X-ray crystallographic data.

Initiator	reaction temp./°C	processing	crystallinity/ %mole
KOt-But	+25.0	-	31.0
KOt-But	-50.0	-	32.9
KOt-But	-70.0	-	31.2
KOt-But	-70.0	solvent cast	*21.7*
KOt-But	-70.0	melt pressed	*5.0*
s-BuLi	+25.0	-	48.8

(Note. italicised values are not comparable due to insufficient sample).

5.7.3 Discussion

X-ray crystallography data shows that for the potassium *tert*-butoxide initiated polymerization of LAAS in tetrahydrofuran, the temperature at which the reaction is conducted has no effect upon the degree of crystallinity of the product. However, the product of the *sec*-butyl lithium-initiated reaction appears to be rather more crystalline in nature, indicating an initiator-specific effect. The reaction of LAAS with alkyl lithium initiators is discussed further in section 6.1.

CHAPTER SIX

COPOLYMERIZATION OF LACTIC ACID ANHYDROSULPHITE WITH STYRENE AND BUTADIENE INITIATED BY BUTYL LITHIUM

6.1 *sec*-BUTYL LITHIUM INITIATED POLYMERIZATION OF LAAS

Alkyl lithium compounds have been successfully used to initiate the polymerization of styrene and butadiene to living polymers. Experiments were performed to establish whether *sec*-butyl lithium would decompose LAAS to yield a polymeric product. It was hoped that this might lead to the production of co-polymers of poly(lactic acid) with non-biodegradable polymers. Such co-polymers might combine the biodegradation behaviour of poly(lactic acid) with the mechanical properties of other polymers.

6.1.1 Experimental

The rate of LAAS polymerization initiated by *sec*-butyl lithium was measured at room temperature and pressure for several reactions using the calorimetric apparatus described in section 2.3.3 . LAAS was injected into the reaction vessel and the required volume of dry tetrahydrofuran added. A 1.3 M solution of *sec*-butyl lithium in cyclohexane was diluted to 0.23 M using dry tetrahydrofuran and used immediately. This solution was injected into the reaction vessel and the chart recorder started. The reactions were very rapid with a white precipitate of poly(lactic acid) appearing almost immediately, accompanied by a sharp increase in temperature. After each reaction was complete, de-oxygenated methanol was injected and the product purified as described in section 5.6. The products were analysed by GPC.

6.1.2 Results

6.1.2.1 Calorimetric Data

Table 6.1 shows the rates of the reactions of *sec*-butyl lithium with LAAS as measured by calorimetry.

Table 6.1 *sec*-butyl lithium initiated decomposition of LAAS - calorimetric data.

[LAAS]/ mol.dm^{-1}	2.75	2.90	2.81
[*sec*-butyl lithium]/ mol.dm^{-1}	0.028	0.016	0.008
[LAAS]/[*sec*-butyl lithium]	98	181	351
Initial temperature/ °C	19.5	21.0	21.5
Final temperature/ °C	56.0	43.0	40.5
rate/ °C.s^{-1}	5.6	1.7	0.2
k_1/ dm^3.mol^{-1}.s^{-1}	0.422	0.224	0.030
k/ s^{-1}	15.07	14.00	3.75

$k = k_1$/[*sec*-butyl lithium]

6.1.2.2 GPC Analysis

The products were analysed by GPC at RAPRA using dimethyl formamide as eluent. Number and weight average molecular weights were then calculated as polystyrene equivalents as shown in table 6.2.

Table 6.2 Products of *sec*-butyl lithium initiated decomposition of LAAS - GPC analysis.

[LAAS]/ mol.dm^{-1}	2.75	2.90	2.81
[*sec*-butyl lithium]/ mol.dm^{-1}	0.028	0.016	0.008
[LAAS]/[*sec*-butyl lithium]	98	181	351
$\overline{M}_w$	15230	19970	20500
$\overline{M}_n$	10850	14500	14990
P_d	1.40	1.38	1.37

6.1.3 Discussion

Though only three experiments were performed, it is possible to make some observations about the polymerizations. The rate constant, k_1, and molecular weight of the product are both inversely proportional to the concentration of initiator, assuming monomer concentration is held constant. The reactions were rapid, and the reaction rates showed a strong dependence on initiator concentration. The dependence of rate constant, k_1, upon initiator concentration is shown in figure 6.1. The line of dependence does not pass

through the origin, which is probably due to the reaction of a proportion of the initiator with traces of moisture present in the reaction mixture.

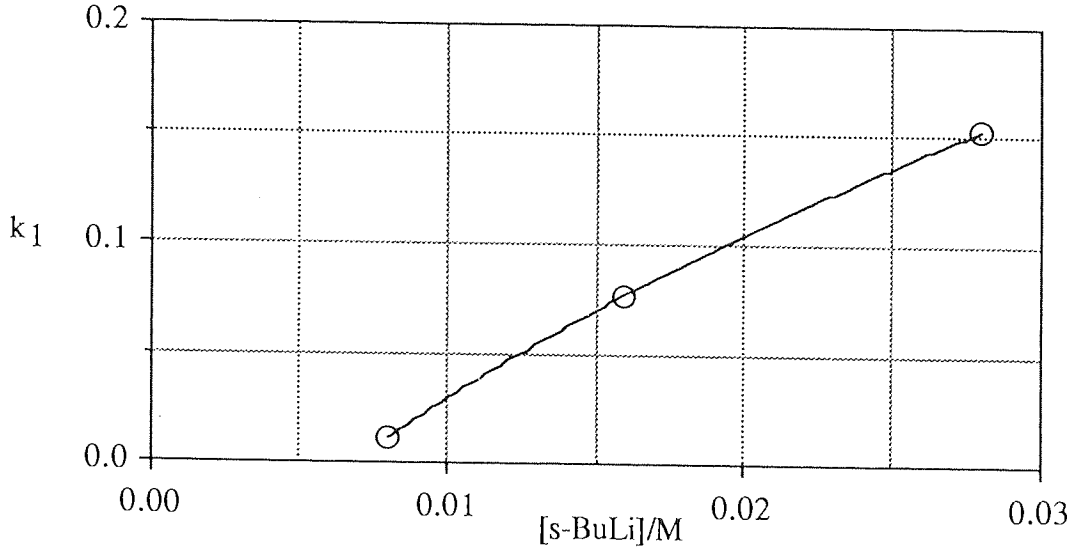

Figure 6.1 Effect of initiator concentration on the rate of *sec*-butyl lithium initiated decomposition of LAAS.

Figure 6.2 shows the number average molecular weights of the products plotted against the monomer : initiator molar ratio.

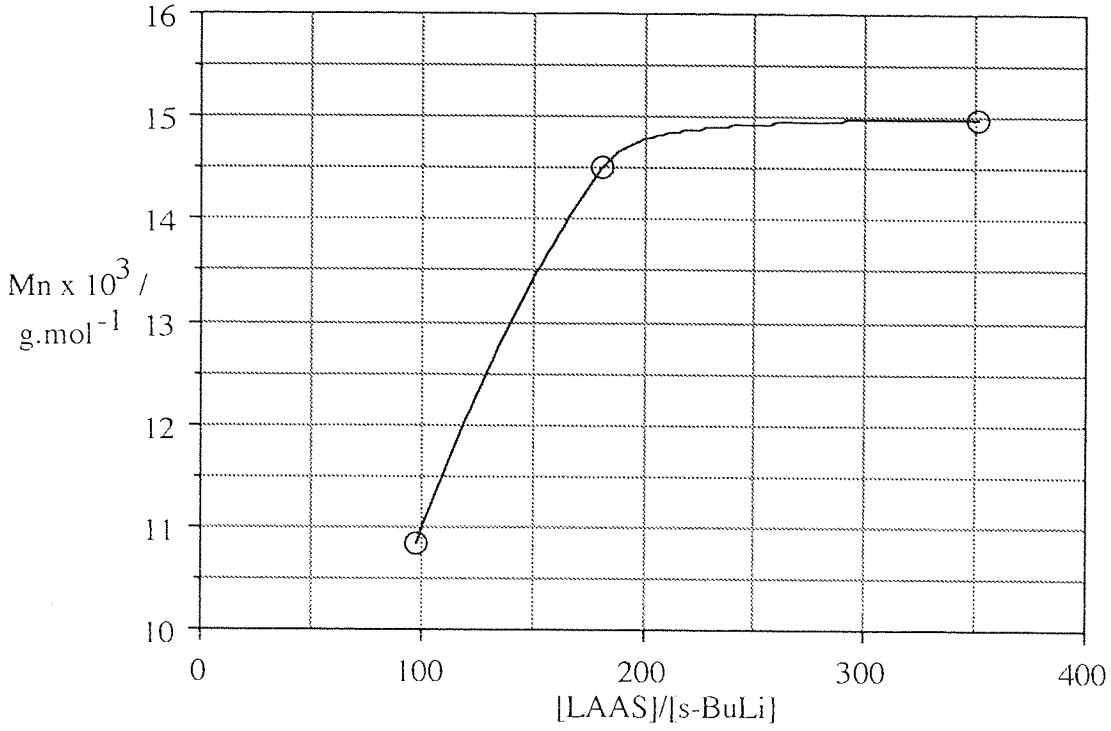

Figure 6.2 Effect of the monomer : initiator molar ratio upon the molecular weight of the products of *sec*-butyl lithium initiated decomposition of LAAS.

6.2 COPOLYMERIZATION OF LAAS WITH STYRENE

Since it was shown in section 6.1 that the polymerization of LAAS might be initiated by an alkyl lithium, experiments were performed in order to determine whether LAAS could be polymerized by polystyryl lithium.

6.2.1 Experimental

Polystyryl lithium (PSLi) was prepared by the reaction of styrene with *n*-butyl lithium in cyclohexane. Styrene was dried over calcium hydride and distilled into a suitable vessel using a vacuum line. Dry cyclohexane was distilled into the flask and the flask removed from the vacuum line whilst still evacuated. The vessel was cooled to -78 °C in a methanol/dry ice bath and filled with dry argon. *n*-butyl lithium solution was then injected in order to initiate polymerization. The reaction vessel was allowed to warm to room temperature, sealed and stored in a glove box until needed.

In a typical experiment to investigate the use of polystyryl lithium as an initiator for the polymerization of LAAS, a high molar ratio of LAAS to polystyryl lithium was used (88:1). 3.0 cm^3 of a 4.95 M solution of LAAS (0.015 moles) in tetrahydrofuran was injected into a polymerization vessel containing 1.0 cm^3 of 0.168 M polystyryl lithium solution (1.7 x 10^{-4} moles) in tetrahydrofuran, at 24 °C. The red polystyryl lithium solution began to bubble and become markedly more viscous, changing to an milky yellow and formation of a precipitate was observed. The evolution of gas ceased after approximately thirty seconds and when methanol was injected, no further evolution was observed. The solvent in the polymerization solution was allowed to evaporate overnight and the product was then dried under vacuum at 40 °C for 48 hours. 1.19 g of a fine white powder (95 % yield) was collected.

In the second experiment, a lower molar ratio of LAAS to polystyryl lithium was used (18:1). 3.03 g (0.023 moles) of LAAS was injected into a polymerization vessel containing 8.0cm^3 of 0.168M polystyryl lithium solution (1.3 x 10^{-3} moles) in tetrahydrofuran at 22.0°C. The second experiment yielded 1.50 g of a fine white powder (86 % yield).

The two products were analysed by FT-IR. The characteristic poly(lactic acid) carbonyl absorption at 1758 cm^{-1} was observed when the infra-red spectra of the products were obtained but no significant absorptions due to poly(styrene) could be seen. A sample of the polystyryl lithium solution was also taken, injected into methanol and dried, for comparison with the products. The products and polystyrene sample were analysed by ^1H and ^{13}C NMR and GPC.

6.2.2 Results

6.2.2.1 NMR Spectral Analysis

The ^1H and ^{13}C NMR spectra of the poly(styrene) sample and of the products of high and low [LAAS]:[PSLi] ratio experiments are shown in figures 6.3 and 6.4, 6.6 and 6.7, and 6.9 and 6.10, respectively. The corresponding peak tables are shown in tables 6.3 and 6.4, 6.5 and 6.6, and 6.7 and 6.8, respectively.

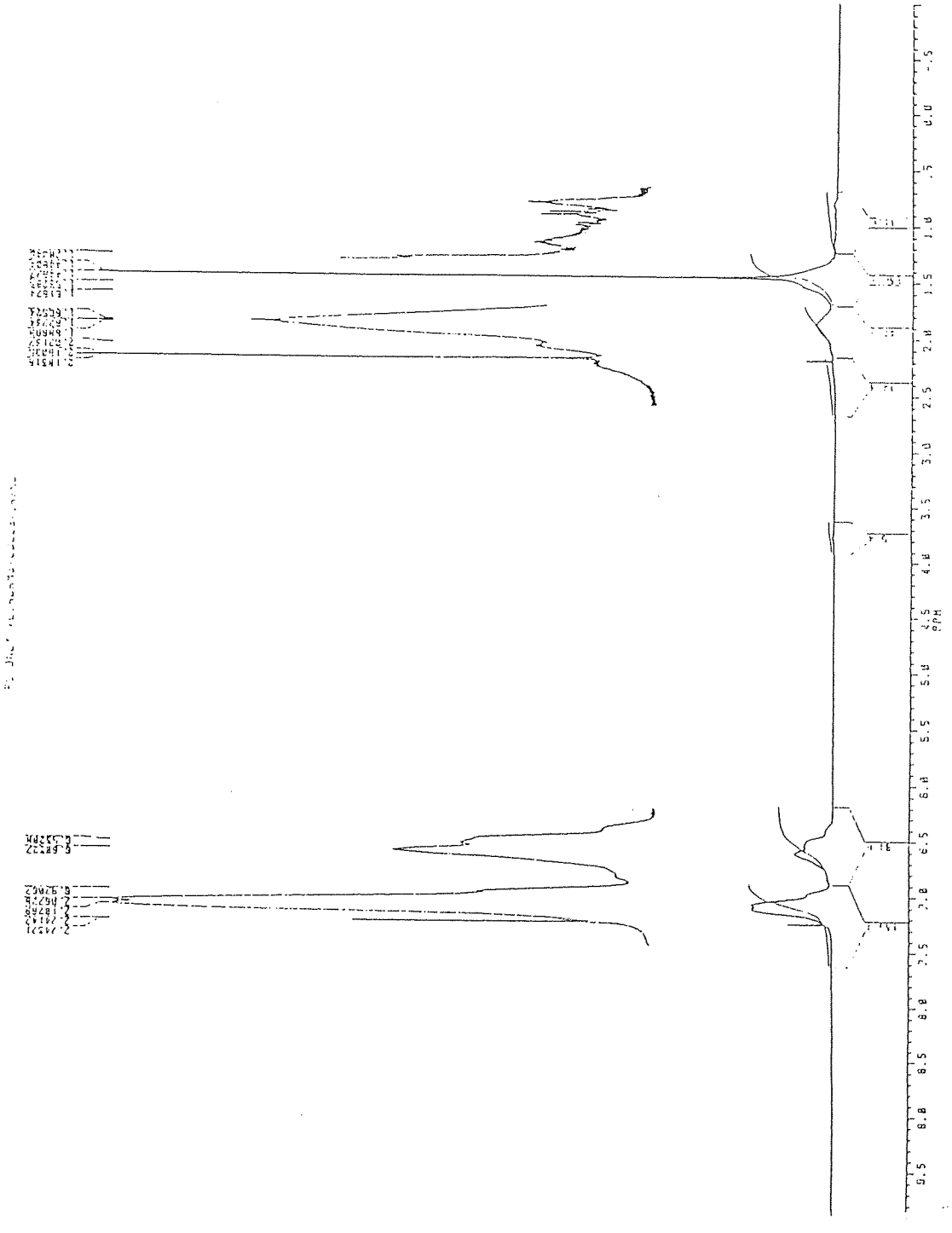

Figure 6.3 ^{1}H NMR spectrum of poly(styrene).

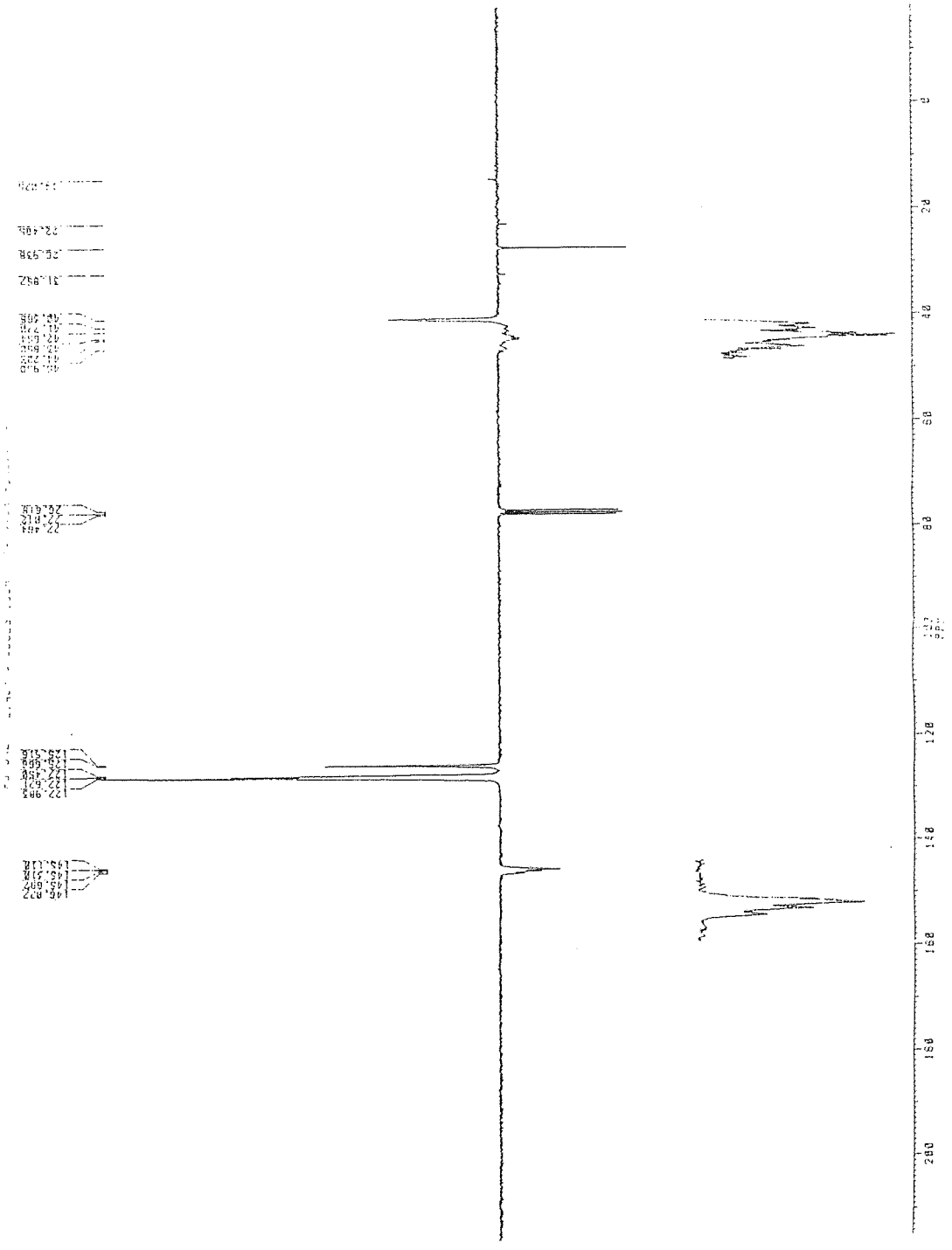

Figure 6.4 ^{13}C NMR spectrum of poly(styrene).

Table 6.3 ^{1}H NMR peak data for poly(styrene).

ppm	multiplicity	assignment	relative peak areas
1.23 - 1.70	sharp singlet	**e**	2.9
1.70 - 2.16	broad singlet	**d**	1.0
6.18 - 6.89	multiple	**g/h/i**	1.8
6.89 - 7.63	doublet ?	**g/h/i**	2.8

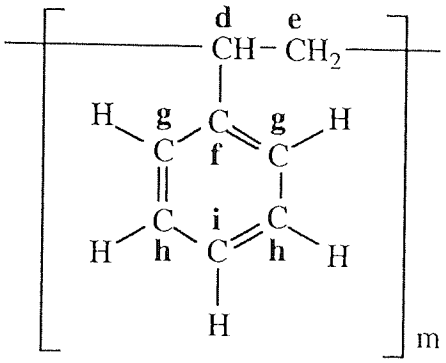

Figure 6.5 Key to NMR peak data for poly(styrene).

Table 6.4 ^{13}C NMR peak data for poly(styrene).

ppm	assignment	+/- intensity
26.94	**e**	- 4.1
40.37	**d**	+ 3.4
125.52 - 125.67	**g/h/i**	+ 3.2 ~ 5.3
127.45 - 127.98	**g/h/i**	+ 4.6 ~ 12.0
145.11 - 146.08	**f**	- 0.8 ~ 1.8

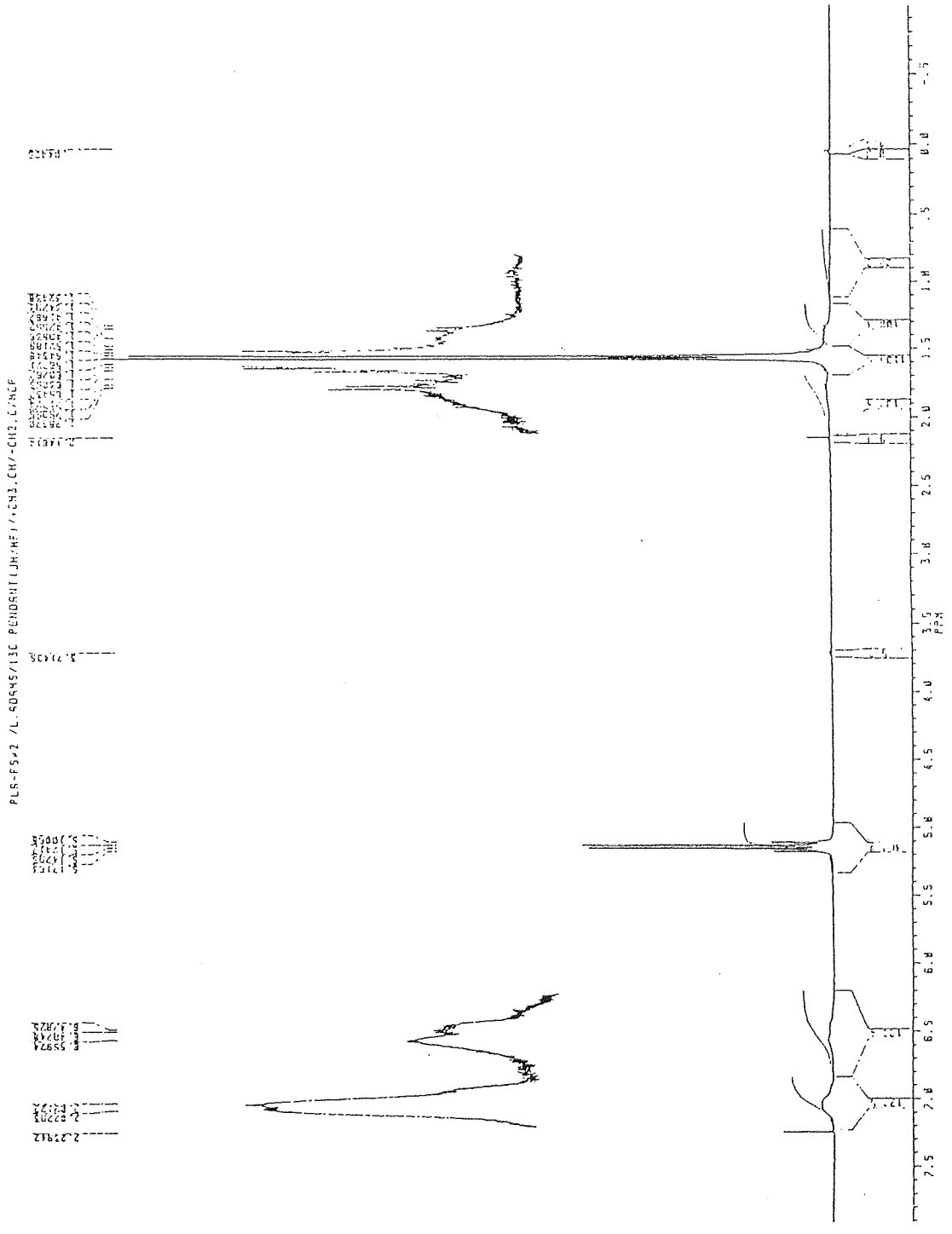

Figure 6.6 ^{1}H NMR spectrum of high ratio block poly(styrene-co-lactic acid) .

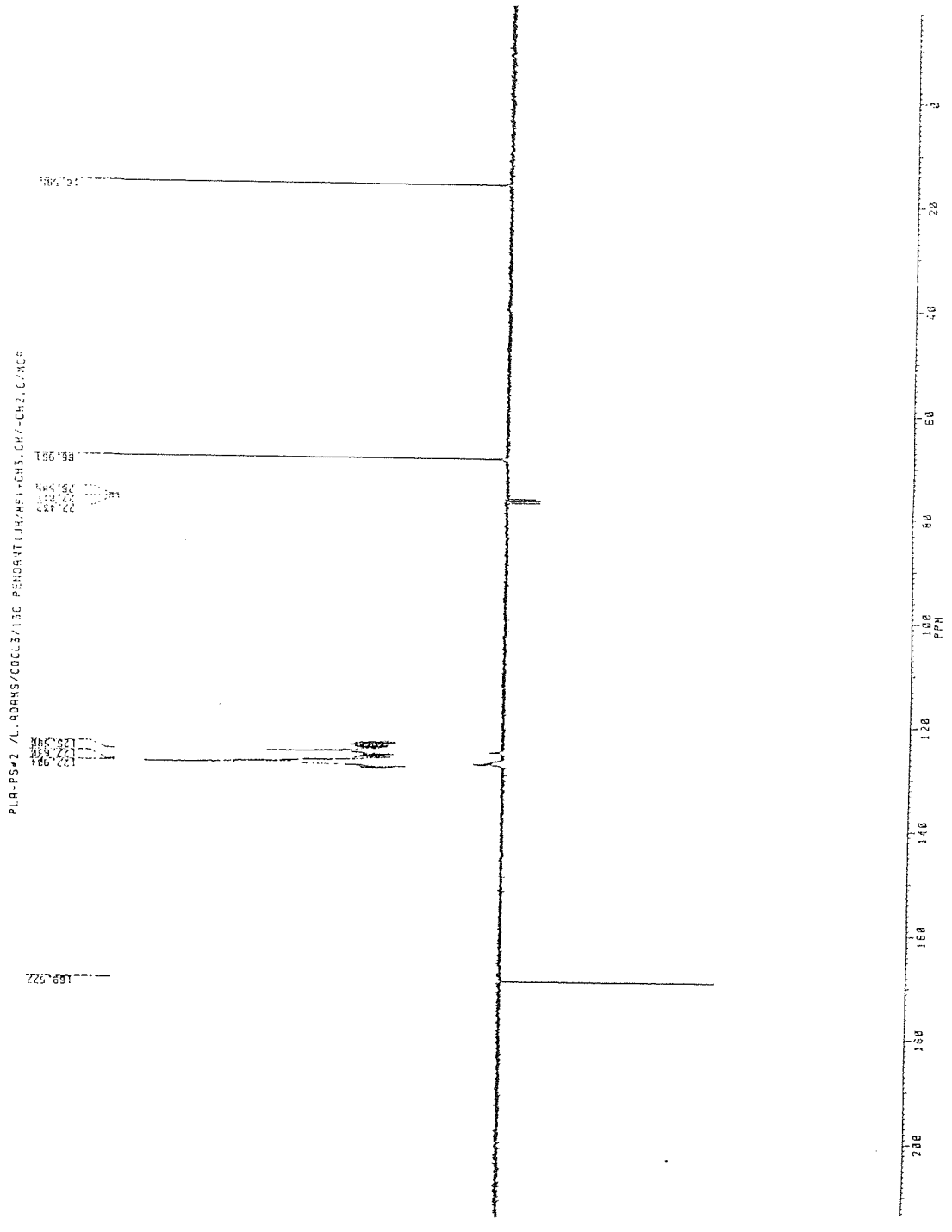

Figure 6.7 ^{13}C NMR spectrum of high ratio block poly(styrene-co-lactic acid).

Table 6.5 ^{1}H NMR peak data for high ratio block poly(styrene-co-lactic acid).

ppm	multiplicity	assignment	relative peak areas
1.47 - 1.68	doublet	**b**	9.1
4.95 - 5.319	quartet	**a**	3.0
6.19 - 6.82	broad	**g/h/i**	1.0
6.83 - 7.22	broad	**g/h/i**	5.7

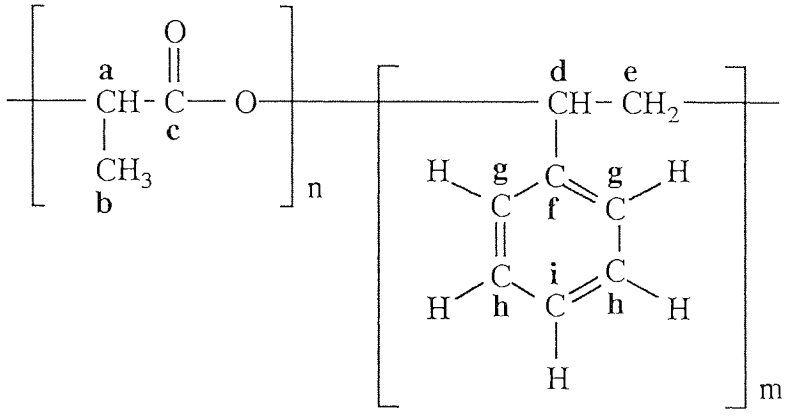

Figure 6.8 Key to NMR peak data for high ratio block poly(styrene-co-lactic acid).

Table 6.6 ^{13}C NMR peak data for high ratio block poly(styrene-co-lactic acid).

ppm	assignment	+/- intensity
16.60	**b**	+ 11.9
68.96	**a**	+ 12.3
125.59	**g/h/i**	+ 0.4
127.63 - 127.90	**g/h/i**	+ 0.6 ~ 0.9
169.58	**c**	- 6.6

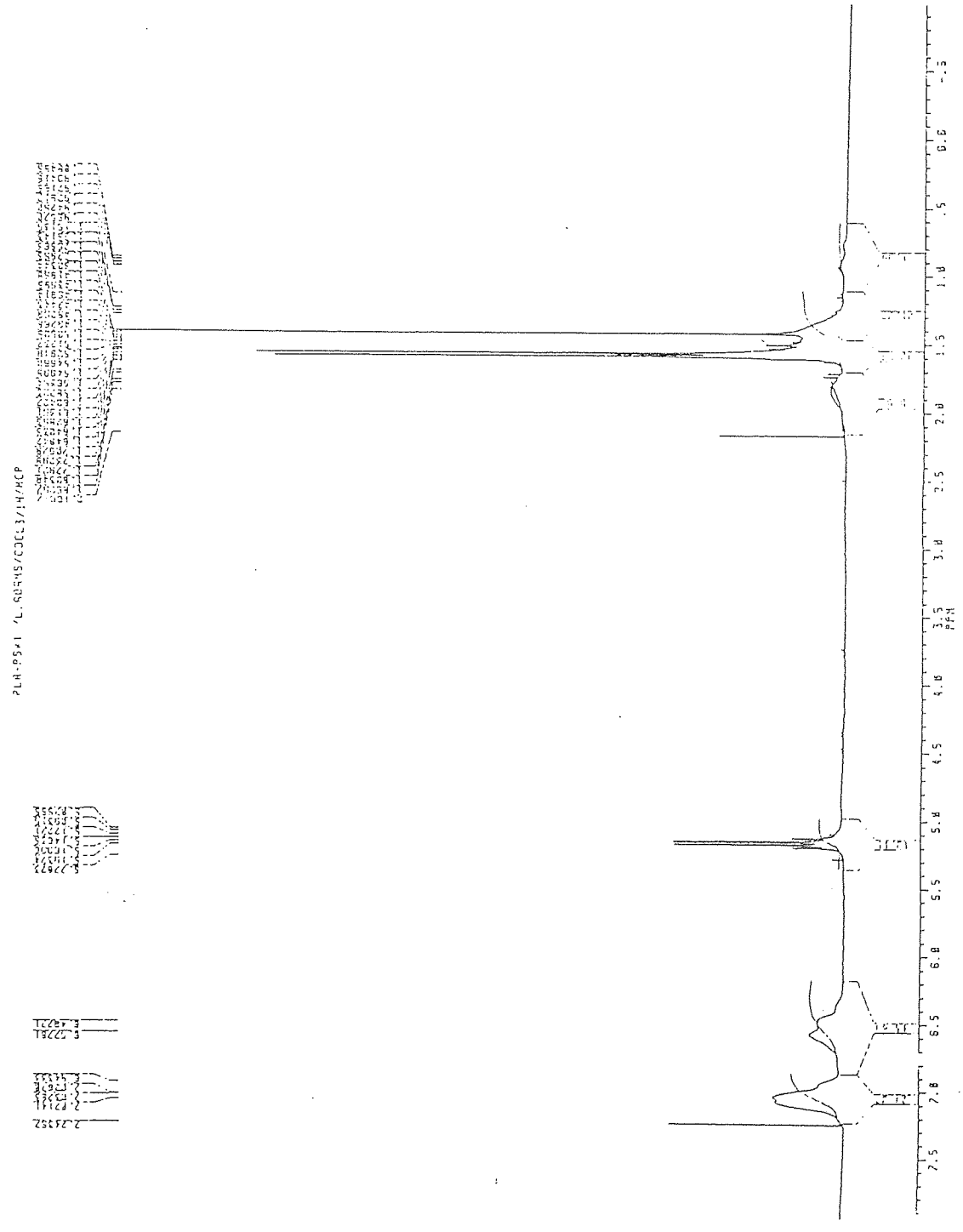

Figure 6.9 ^{1}H NMR spectrum of low ratio block poly(styrene-co-lactic acid).

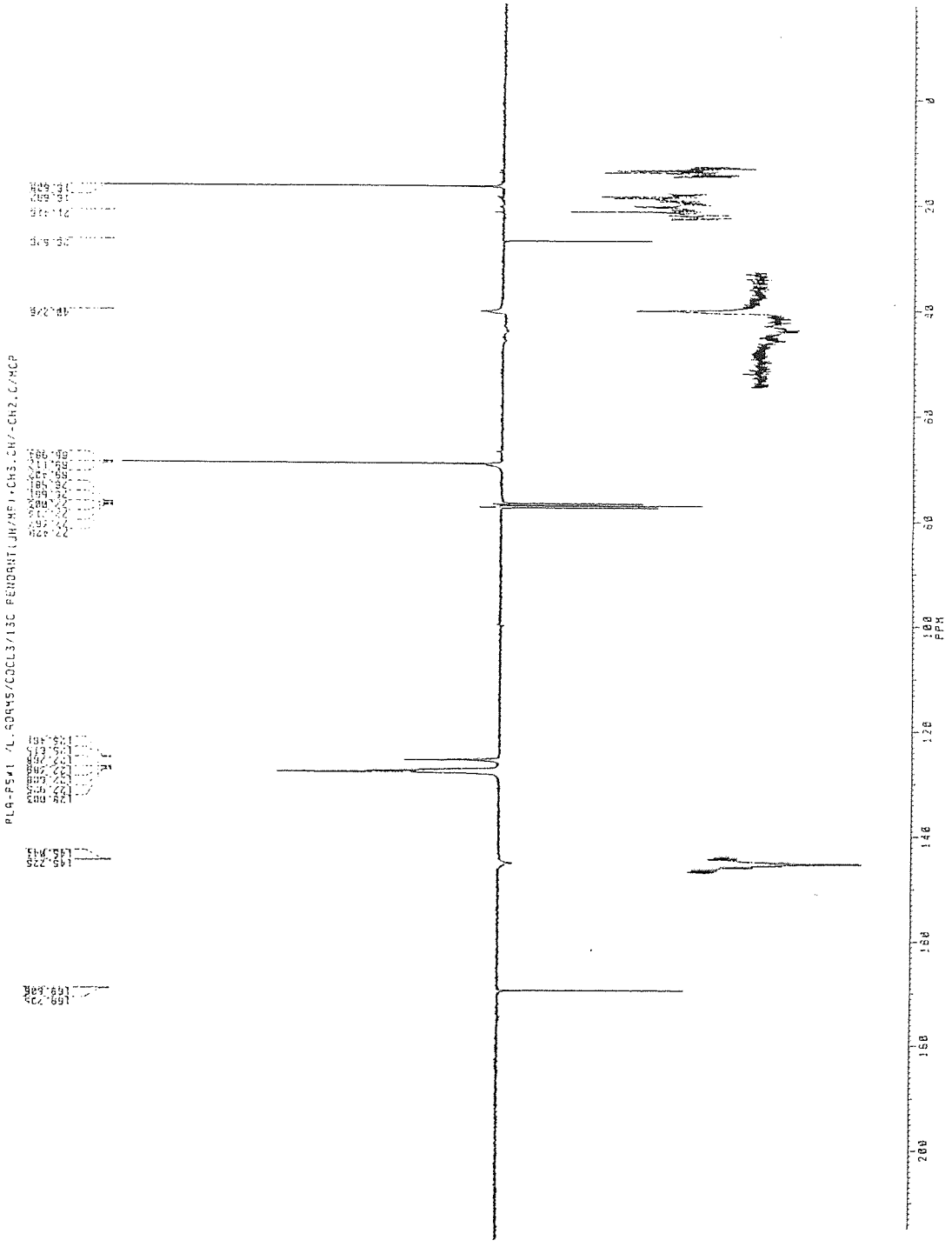

Figure 6.10 ^{13}C NMR spectrum of low ratio block poly(styrene-co-lactic acid).

Table 6.7 ^{1}H NMR peak data for low ratio block poly(styrene-co-lactic acid).

ppm	multiplicity	assignment	peak areas
1.09 - 1.45	sharp singlet	**e**	3.1
1.45 - 1.69	doublet	**b**	6.3
1.69 - 2.14	broad singlet ?	**d**	1.0
4.97 - 5.35	quartet	**a**	1.5
6.17 - 6.86	broad	**g/h/i**	2.1
6.86 - 7.23	broad	**g/h/i**	3.6

For key to tables 6.7 and 6.8, refer to figure 6.8.

Table 6.8 ^{13}C NMR peak data for low ratio block poly(styrene-co-lactic acid).

ppm	assignment	+/- intensity
16.61	**b**	+ 12.0
26.88	**d**	- 4.5
40.28	**e**	+ 0.7
68.98 - 69.40	**a**	+ 0.5 ~ 11.8
125.46 - 125.62	**g/h/i**	+ 1.6 ~ 3.0
127.27 - 128.00	**g/h/i**	+ 1.6 ~ 6.3
145.04 - 145.22	**f**	- 0.4
169.61 - 169.71	**c**	- 5.6

6.2.2.2 GPC Analysis

The products were analysed by GPC at RAPRA using dimethyl formamide as eluent. Table 6.9 shows the data obtained.

Table 6.9 Block copolymerization of LAAS and poly(styrene) - GPC analysis.

Polymer	[PLA]/[PS]	$\overline{M}_W$	$\overline{M}_n$	Pd
PS only	PS only	4800	2200	2.2
		4900	2300	2.1
high ratio	88	10300	4700	2.2
PLA-co-PS		10700	5000	2.2
low ratio	18	7600	2500	3.1
PLA-co-PS		7600	2400	3.2

6.2.2.3 DSC Analysis

The DSC trace for the product of the low [PLA]:[PS] ratio copolymerization is shown in figure 6.11. A highly endothermic melting transition occurs at 149 °C. This is likely to be due to crystalline poly(lactic acid).

The DSC trace of the low [PLA]:[PS] ratio product is shown in figure 6.12. A broad endothermic transition around 80 °C is seen. This is too low for poly(lactic acid) and is likely to be due to the poly(styrene) present, though the trace is less clear than that of the high [PLA]:[PS] ratio product.

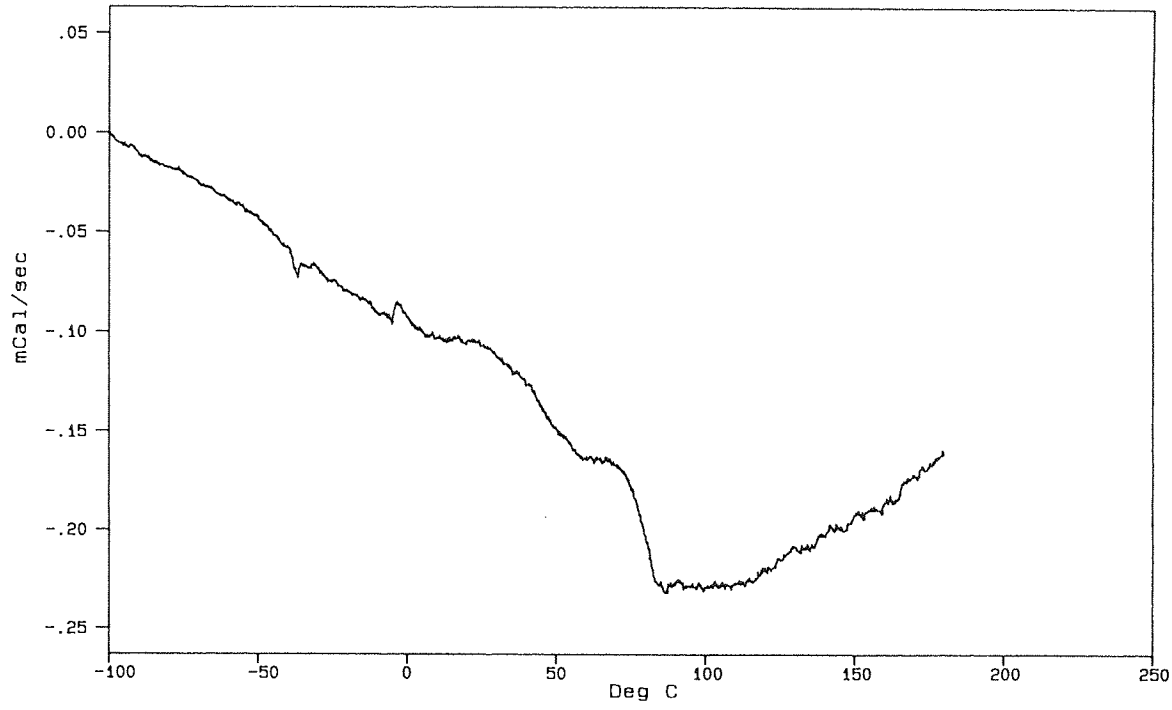

Figure 6.11 DSC trace of high ratio poly(styrene-co-lactic acid).

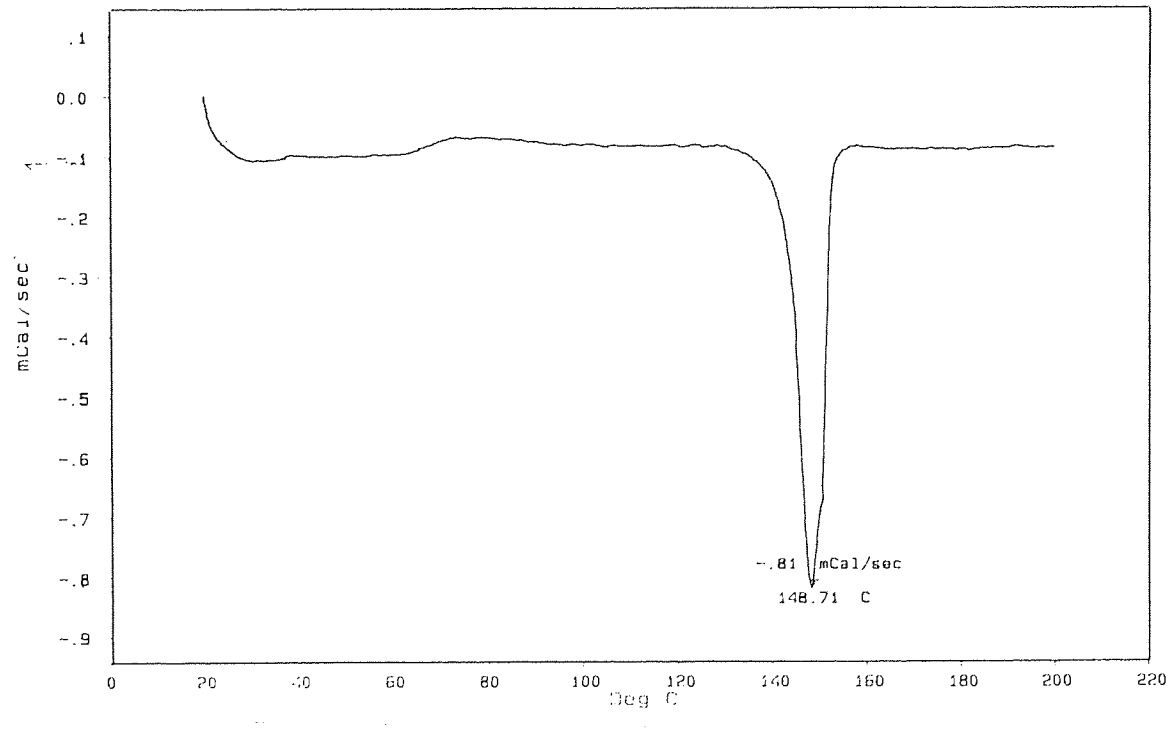

Figure 6.12 DSC trace of low ratio poly(styrene-co-lactic acid).

6.2.3 Discussion

The polystyryl lithium anion exhibits a distinctive red colour and in both experiments this was seen to disappear on contact with the anhydrosulphite, accompanied by the evolution of sulphur dioxide. These observations confirm the reaction of the polystyryl lithium with LAAS causing ring-opening and destruction of the polystyryl lithium anion.

From the ^1H NMR spectra, the composition of the average polymer chain may be calculated for both copolymers. The high ratio experiment (LAAS : polystyryl lithium ratio = 88:1) produced a product having a PLA :PS repeat unit ratio of 2.2:1. The low ratio experiment (LAAS : polystyryl lithium ratio = 18:1) produced a product having a PLA :PS repeat unit molar ratio of 1.6:1. The product ratios are clearly much lower than expected.

The GPC analysis indicates that the products are of higher molecular weight than that of the polystyrene derived from the polystyryl lithium initiator solution alone. This is indicative of the formation of a block copolymer.

6.3 BLOCK COPOLYMERIZATION OF LAAS WITH 1,3-BUTADIENE

Since 1,3-butadiene is similar to styrene in that it will undergo anionic polymerization, it was thought that polybutadienyl lithium might form co-polymers with LAAS. Poly(butadiene) is a rubber-like polymer at room temperature whereas poly(lactic acid) is an opaque solid. Therefore a copolymer based upon these might have physical properties which are distinct from the homo-polymers.

6.3.1 Experimental

1,3-butadiene was supplied by Aldrich, contained under pressure in a gas cylinder. The gas was collected for use in polymerization by means of the apparatus shown in figure 6.13. The manifold was evacuated by opening the main tap, A, and taps B and C. Taps D and E were then opened slowly and simultaneously so as to avoid disturbing the contents of the drying columns.

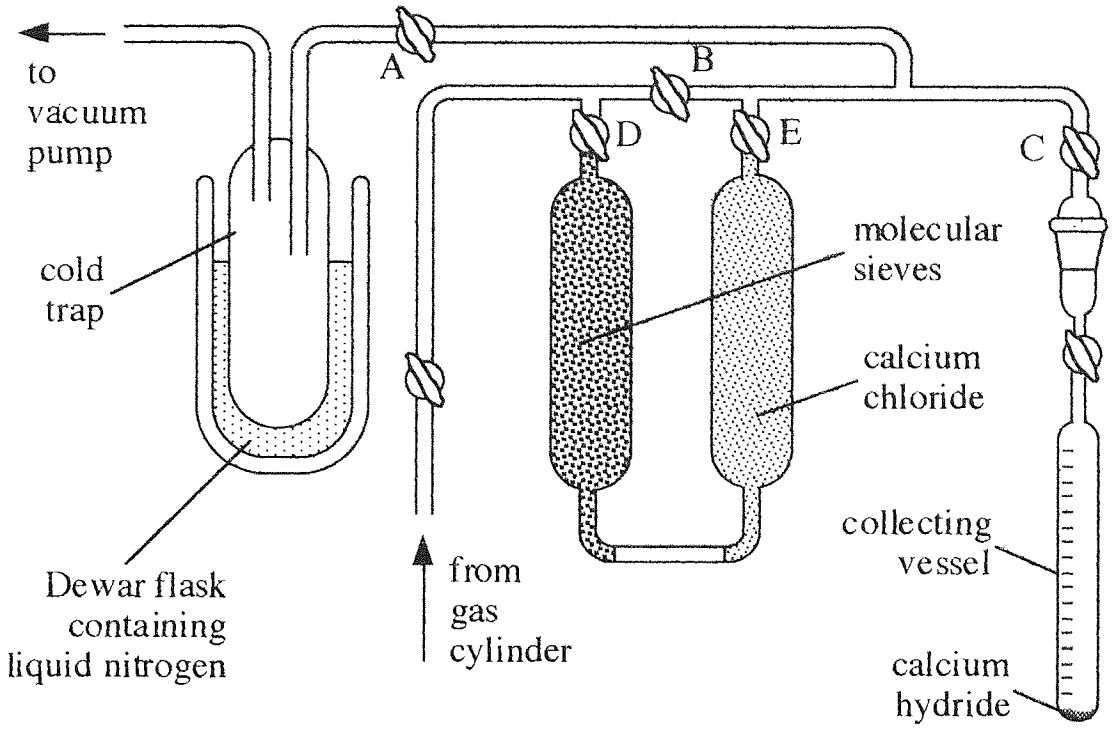

Figure 6.13 Collection of 1,3-butadiene.

The collecting vessel, containing a small quantity of calcium hydride, was secured to the manifold by means of a Delrin clip and cooled to -78 °C using a Dewar flask, containing dry ice and acetone. A 'hard' vacuum was allowed to develop over approximately 30 minutes and taps A and B were closed. The liquid nitrogen Dewar flask surrounding the vacuum pump solvent trap was removed and the vacuum pump was switched off. The cylinder valve was opened very slightly and the collecting vessel observed for signs of butadiene condensing. If after five minutes none was observed, the valve was opened a little more and observation continued. This process was repeated until a gentle rate of condensation was achieved. After around 15 cm^3 monomer was obtained, the cylinder valve, taps D and E, and the collecting vessel tap were closed. The system was then released to the atmosphere and the collecting vessel removed, still contained in the Dewar flask. A temperature of -78 °C was maintained by re-filling the flask with dry ice as was necessary, until the monomer was required for use in the experiment.

A suitable volume LAAS was re-distilled at reduced pressure into a 10 cm^3 round-bottomed flask using micro-distillation apparatus. The apparatus was released to atmospheric pressure with dry argon and fitted with a rubber septum. When required, the monomer was introduced to the polymerization vessel (a three-necked 250 cm^3 round-bottomed flask) using Schlenk techniques (as described in section 2.2.1.1). The

syringe was weighed directly before and after use so that the amount of monomer added might be calculated by difference.

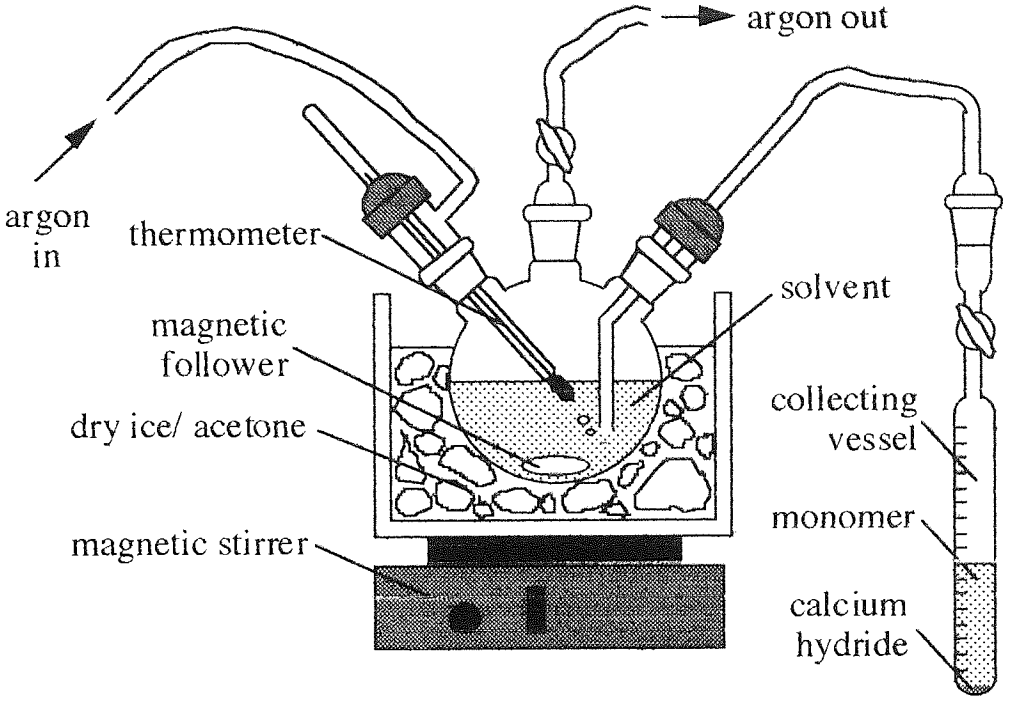

Figure 6.14 Butadiene polymerization vessel.

1,3-Butadiene was introduced to the polymerization vessel by means of the apparatus shown in figure 6.14. Prior to insertion of the glass tube, the collecting vessel was removed from the Dewar flask and its tap opened slightly, to release excess gas pressure (from hydrogen evolved during reaction of calcium hydride with residual moisture) and re-closed. The argon bubbler tap was then closed in order that the glass tube might be fitted to the flask with a flow of argon preventing ingress of atmospheric moisture. Once connected, the bubbler tap was re-opened and the flow of argon reduced to zero. The tap of the collecting vessel was opened slightly so that as 1,3-butadiene evaporated, the gas completely dissolved in the solvent. For this to occur, it was necessary for the tetrahydrofuran to be kept at -78 °C. To ensure that the rate of transfer was not too fast, the bubbler was monitored to see that no gas left the reaction vessel.

The required quantity of dry tetrahydrofuran was introduced into the reaction vessel by fractional distillation from sodium metal and benzophenone under argon (the first fraction was discarded). The reaction vessel was weighed before and after distillation so that the mass of tetrahydrofuran used might be calculated by difference.

It was possible to calculate the mass (and hence the number of moles) of 1,3-butadiene contained in the collecting vessel. The exact temperature in the Dewar flask was recorded and the volume of liquid in the collecting vessel measured (by means of graduations on the vessel wall). The mass of this volume of monomer at the temperature was then calculated by means of a density/temperature curve calculated from experimental data.[91]

Two reactions were performed under slightly different conditions. In the first copolymerization, neat anhydrosulphite was used and the reaction mixture was kept at -78 °C throughout the course of the reaction. In the second copolymerization, anhydrosulphite was added in solution and the reaction mixture allowed to warm to ambient temperature.

The reaction vessel was filled with 115 cm^3 of tetrahydrofuran and 15.0 cm^3 1,3-butadiene (0.21 moles) added at -78 °C using the techniques described in section 6.3. 1.4 cm^3 of a 2.5 M solution of *n*-butyl lithium (0.0035 moles) was then added, causing the reaction mixture to turn rapidly yellow, as is characteristic of butadiene polymerization.. After 55 minutes, an 8.0 cm^3 sample was taken and 3.96 g of LAAS (0.029 moles) dissolved in 25 cm^3 tetrahydrofuran, added, causing the yellow coloration to disappear. After a further 10 minutes, a second sample was taken but no gas evolution was observed. The bath surrounding the vessel was topped-up with dry ice and the reaction left to continue at -78 °C. After 18 hours, methanol was injected to terminate the reaction and solvent removed from the samples using a rotary evaporator.

Both the samples taken during polymerization yielded clear viscous liquids but the end product was clear waxy flakes which had an unusual 'nutty' odour unlike that of either poly(butadiene) or PLA.

In the second copolymerization, the reaction vessel was filled with 88.4 g of tetrahydrofuran (99.3 cm^3) and 16.0 cm^3 (11.9 g) 1,3-butadiene added at -78 °C. The addition of 2.0 cm^3 of a 2.5 M solution of *n*-butyl lithium (0.005 moles) caused the solution to turn a deep yellow-green. After one hour, the dry ice/acetone bath was removed and the temperature of the reaction mixture allowed to rise to 0 °C. After a further 30 minutes had elapsed, the temperature was allowed to rise to 25 °C and a sample was taken. No gas evolution was observed, indicating that no monomeric 1,3-butadiene remained. After one hour and 45 minutes had elapsed since injection of the initiator, 7.2 g (0.052 moles) of LAAS was added. The reaction mixture turned pale yellow and gas evolution was observed. After two and a half hours since initiation, a second sample was taken and the reaction mixture left to continue at room temperature, under a blanket of argon, for 18 hours. When methanol was then injected to terminate the reaction, the yellow coloration remained and solvent was removed from the samples using a rotary

evaporator. The end product was dissolved in tetrahydrofuran, precipitated in methanol and dried in a vacuum oven at 30 °C for 48 hours.

While the first sample taken was a sticky translucent white residue, the second sample appeared to be a mixture of a white, waxy solid and a sticky yellow material. The end product was an opaque putty-like material. The end products of both reactions were analysed by ^{13}C and ^{1}H NMR, DSC and GPC.

6.3.2 Results

6.3.2.1 NMR Spectral Analysis

The first sample was taken from the reaction vessel before addition of LAAS and thus only contained poly(1,3-butadiene). However, the structure of poly(1,3-butadiene) is not simple since addition may occur in a number of different ways resulting in the three possible repeat unit structures shown, along with PLA, in figure 6.15.

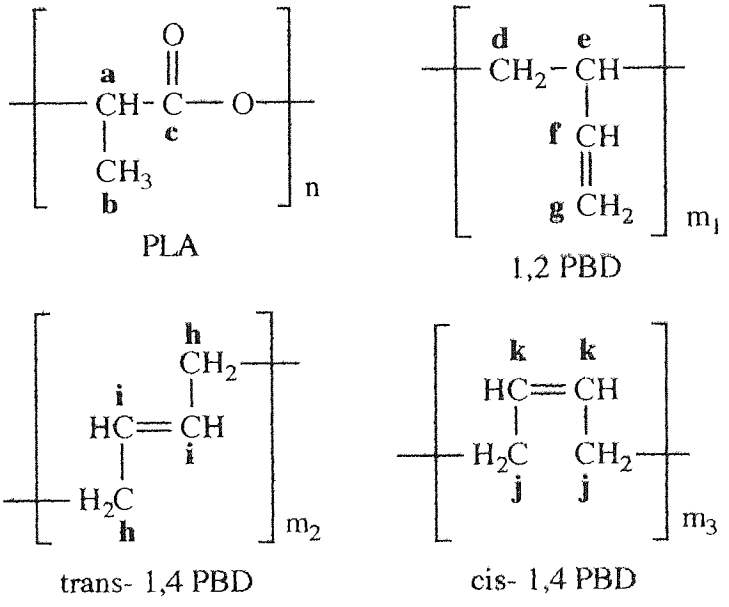

Figure 6.15 Isomeric repeat units of poly(1,3-butadiene).

The ^{1}H and ^{13}C NMR spectra and peak tables for the sample taken from copolymerization before addition of LAAS, i.e. poly(butadiene), are shown in figures 6.16 and 6.17, and tables 6.10 and 6.11, respectively.

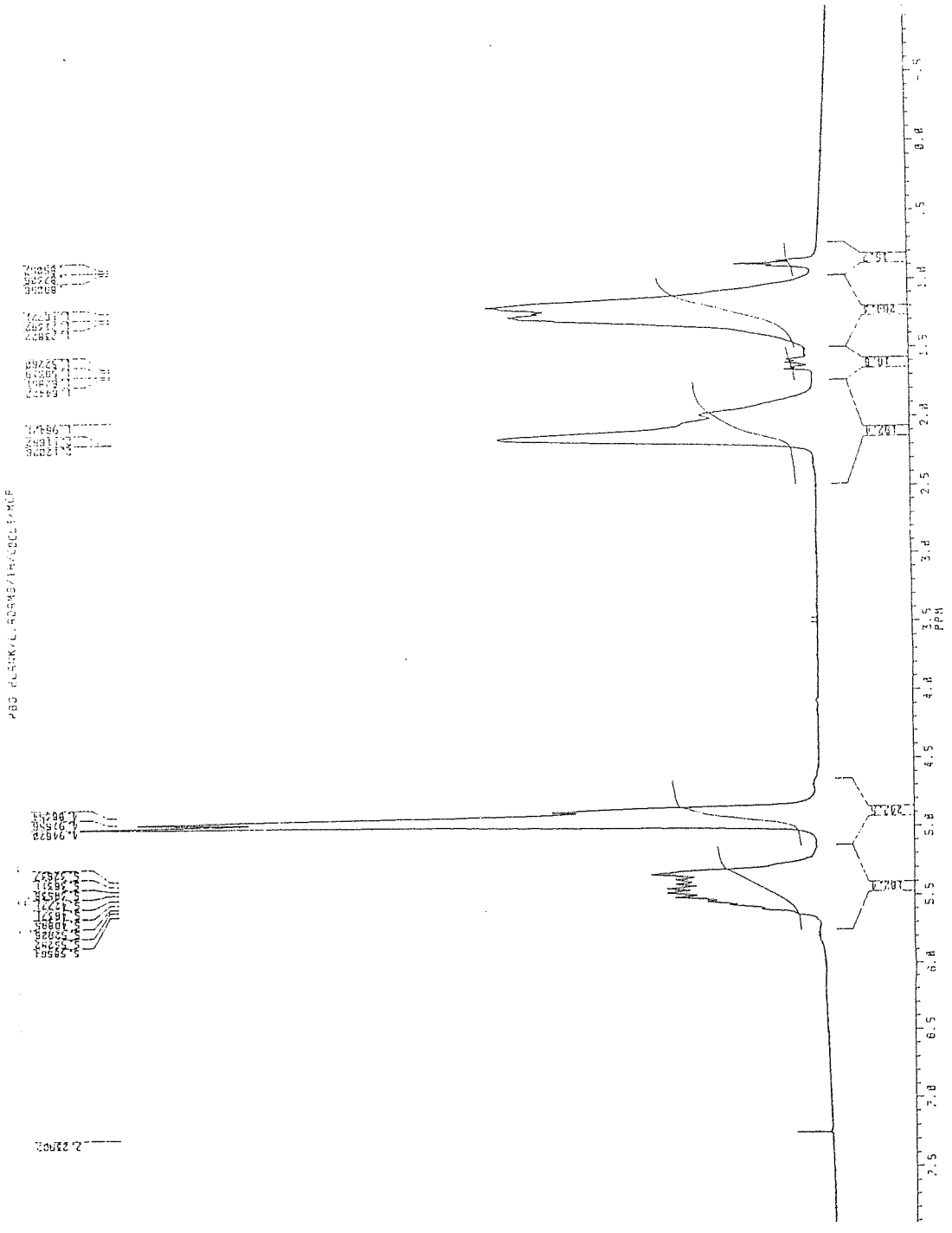

Figure 6.16 ^{1}H NMR spectrum of poly(1,3-butadiene).

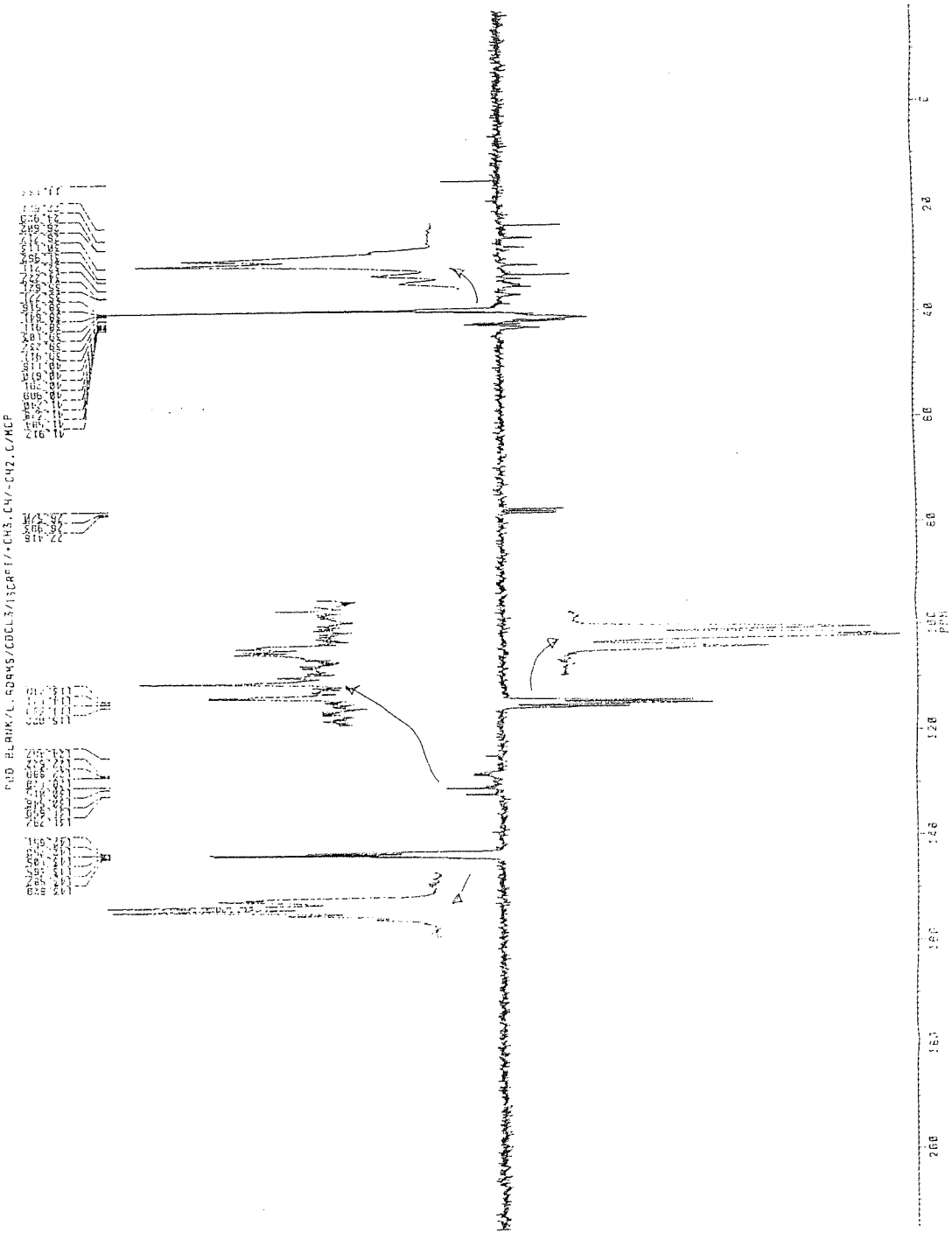

Figure 6.17 ^{13}C NMR spectrum of poly(1,3-butadiene).

Table 6.10 ^{1}H NMR peak data for poly(1,3-butadiene).

ppm	multiplicity	assignment	relative peak areas
1.17 - 1.24	broad doublet	**d**	1.6
1.97 - 2.12	broad singlets ?	**e/j/h**	1.2
4.96 - 4.95	doublet + singlet ?	**g/k**	1.5
5.32 - 5.59	complex	**f/i**	1.0

Though there may be some error in calculating peak areas for a complex spectrum (this is particularly true for polymer spectra, where many conformations are possible) it may be possible to determine the relative proportions of 1,2-, cis- 1,4- and trans- 1,4 repeat units present from the ^{1}H NMR spectral data. By doing this for the ^{1}H NMR spectrum of the poly(butadiene) sample it may be estimated that most of the poly(butadiene) repeat units are in the form of the 1,2- and trans-1,4- isomers, in the ratio 4:1, with a negligible quantity in the cis-1,4- form.

Table 6.11 ^{13}C NMR peak data for poly(1,3-butadiene).

ppm	assignment	+/- intensity
22.62 - 35.77	**h/j**	weak, negative
38.51 - 39.10	**e**	strong, positive
39.23 - 77.42	**d**	weak, negative
113.75 - 115.02	**g**	strong, negative
124.46 - 131.80	**i/k**	weak, positive
142.65 - 143.63	**f**	strong, positive

The ^{1}H and ^{13}C NMR spectra and peak tables for the product of the first block copolymerization are shown in figures 6.18 and 6.19, and tables 6.12 and 6.13, respectively.

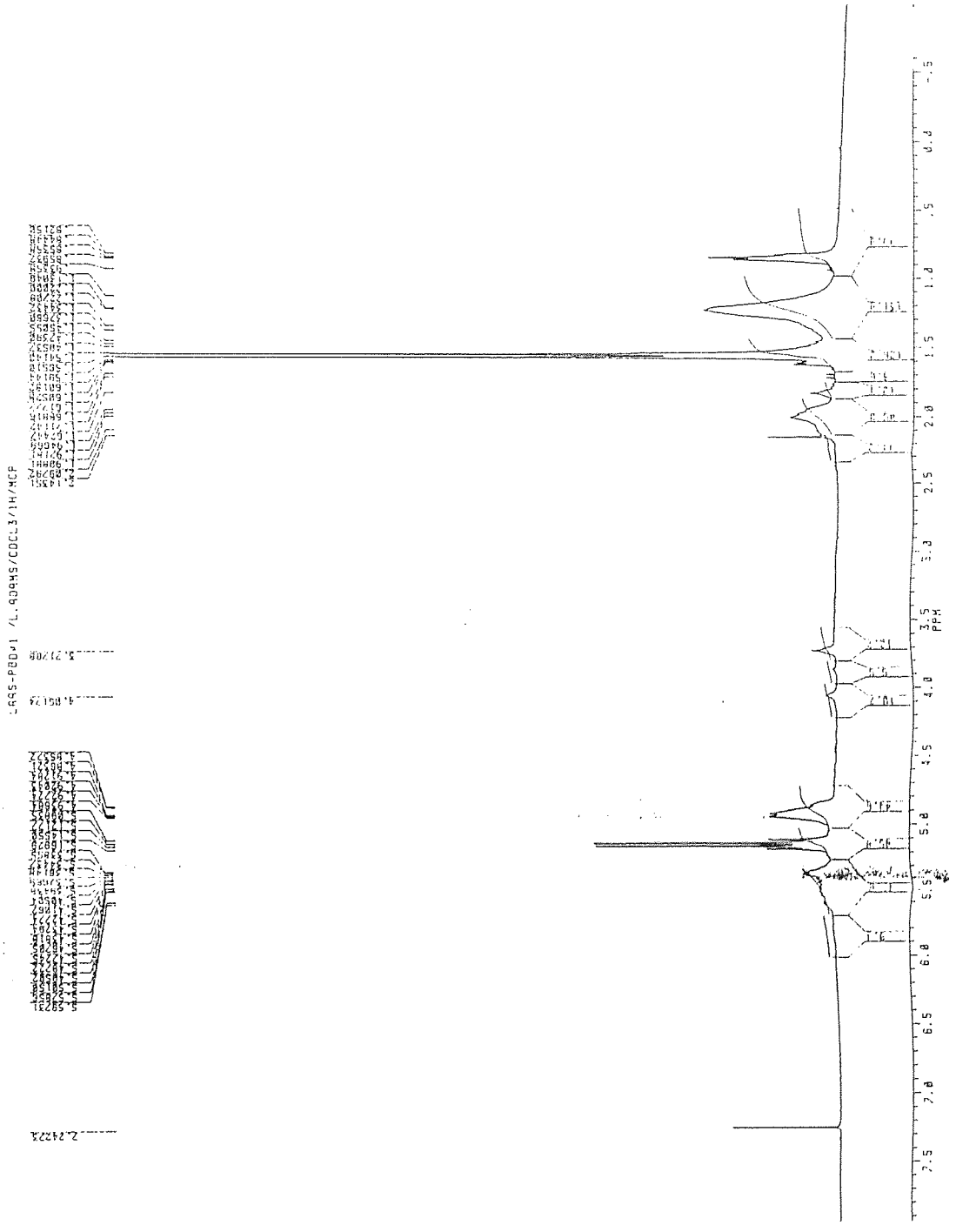

Figure 6.18 ^{1}H NMR spectrum of product of first block copolymerization of LAAS and 1,3-butadiene, initiated by *sec*-butyl lithium.

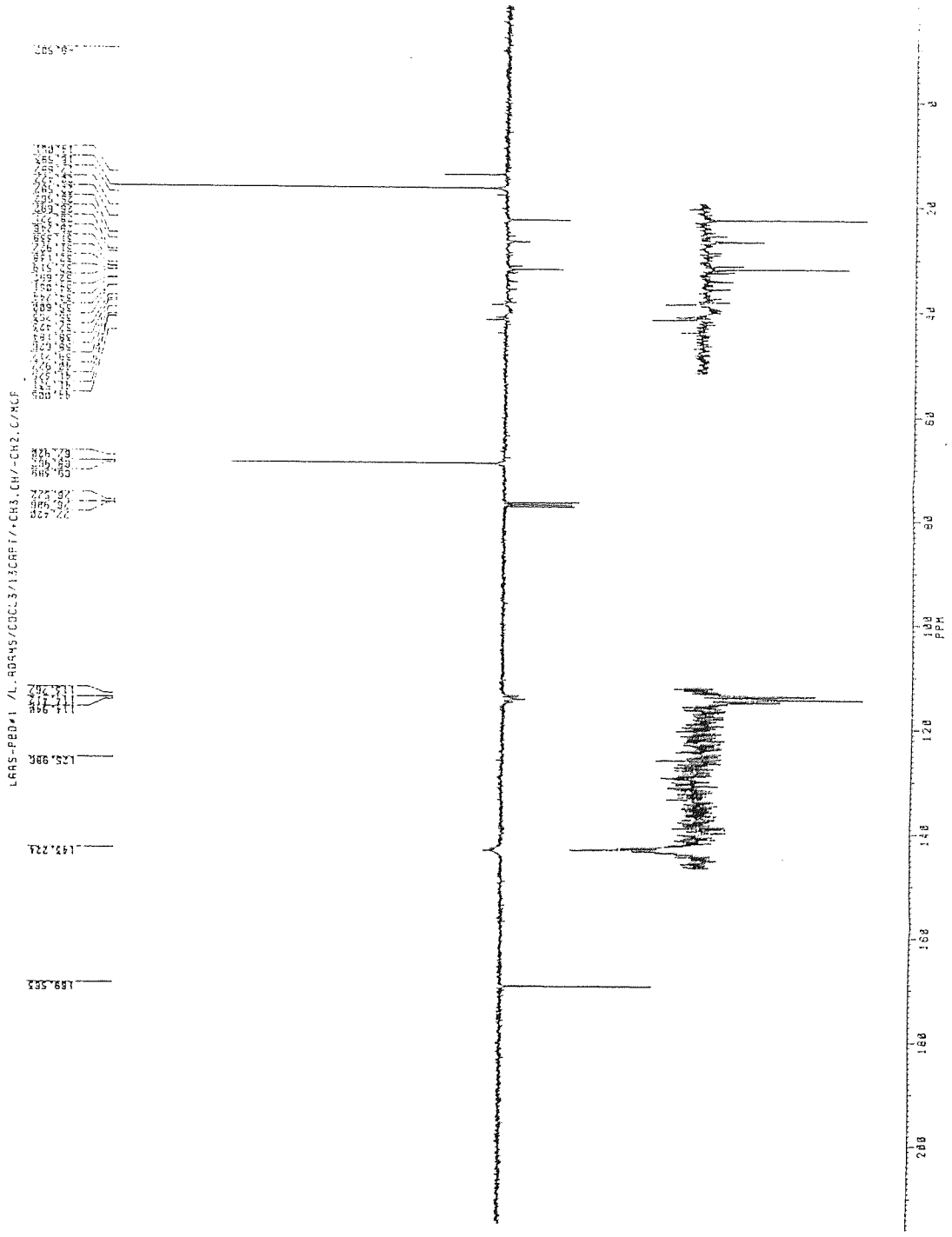

Figure 6.19 ^{13}C NMR spectrum of product of first block copolymerization of LAAS and 1,3-butadiene, initiated by *sec*-butyl lithium.

Table 6.12 ^{1}H NMR peak data for product of first block copolymerization of LAAS and 1,3-butadiene, initiated by *sec*-butyl lithium.

ppm	multiplicity	assignment	peak areas
0.98 - 1.43	broad singlet	**d**	3.0
1.43 - 1.67	doublet	**b**	2.8
1.86 - 2.13	complex	**e/j/h**	1.0
4.72 - 5.03	doublet + singlet ?	**g/k**	1.0
5.03 - 5.25	quartet	**a**	1.0
5.25 - 5.71	complex	**f/i**	1.1

The proportion of 1, 2-, cis- 1, 4- and trans- 1, 4 repeat units may be calculated algebraically using the peak area data. Although the algebraic calculation of the ratio of repeat units is not very revealing, it can be seen that an average chain is composed of 1, 2-poly(butadiene) and poly(lactic acid) in the ratio 1.6 : 1. The ^{1}H NMR spectrum also shows a number of other absorptions which may be due to repeat units at the junction between poly(lactic acid) and poly(butadiene) having a different chemical shift.

Table 6.13 ^{13}C NMR peak data for product of first block copolymerization of LAAS and 1,3-butadiene, initiated by *sec*-butyl lithium.

ppm	assignment	+/- intensity
16.59	**b**	12.0
22.59	**h/j**	-2.0
31.93	**e**	-1.8
68.96	**a**	8.4
113.7 - 114.9	**g**	-0.5 ~ -0.3
143.2	**f**	0.6
169.56	**c**	-4.6

The ^{1}H and ^{13}C NMR spectra and peak tables for the product of the second block copolymerization are shown in figures 6.20 and 6.21, and tables 6.14 and 6.15, respectively.

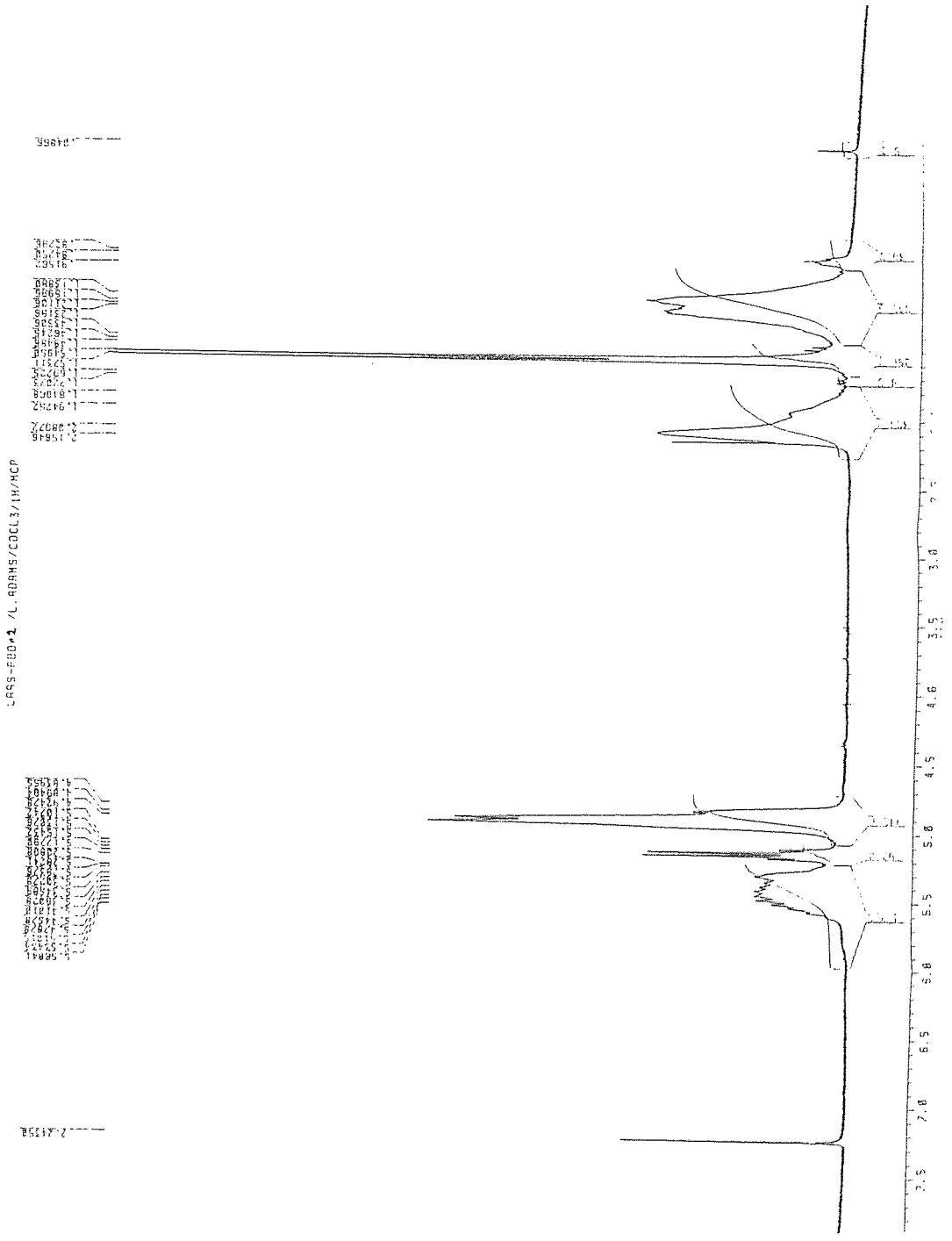

Figure 6.20 ^{1}H NMR spectrum of product of second block copolymerization of LAAS and 1,3-butadiene, initiated by *sec*-butyl lithium.

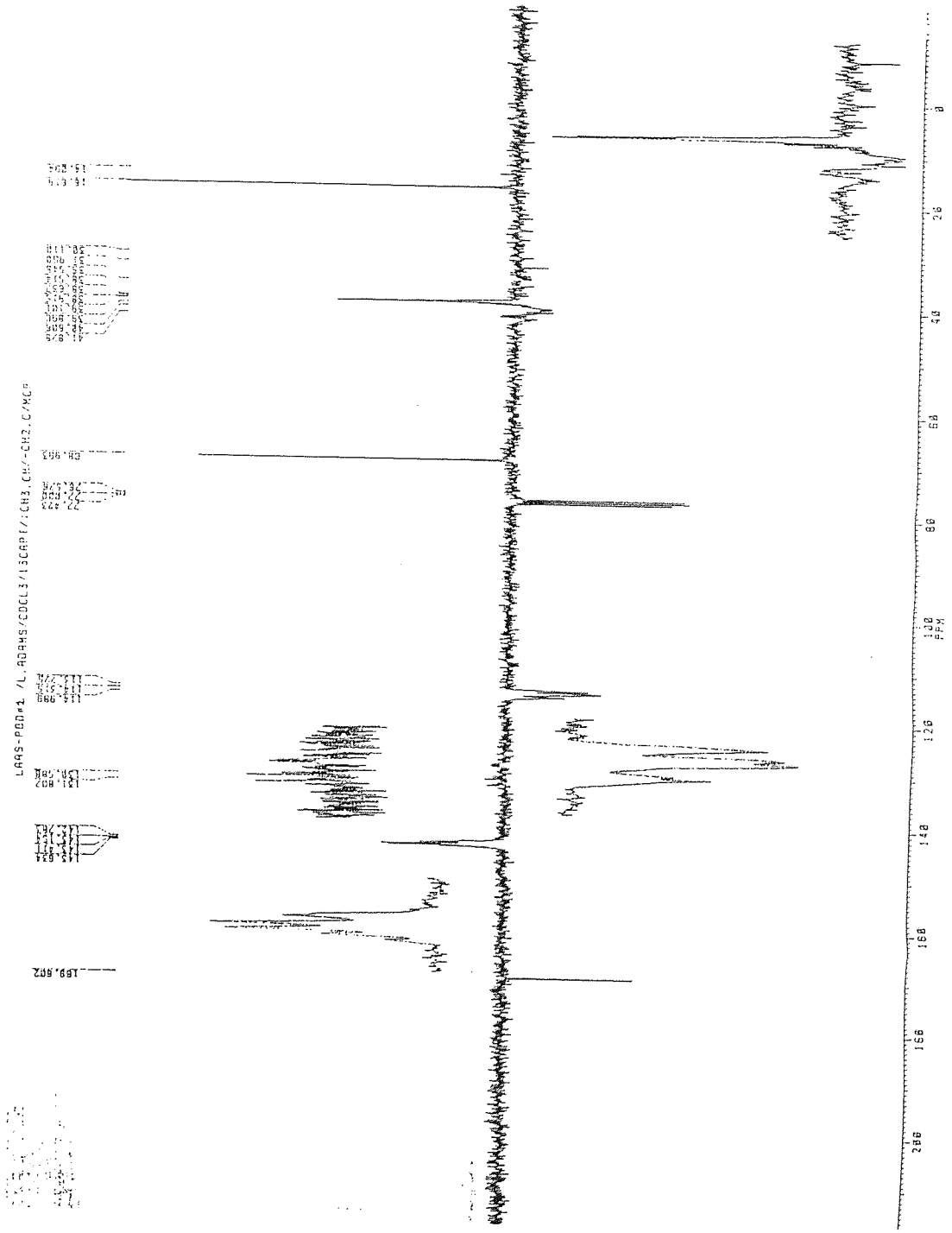

Figure 6.21 ^{13}C NMR spectrum of product of second block copolymerization of LAAS and 1,3-butadiene, initiated by *sec*-butyl lithium.

Table 6.14 ^{1}H NMR peak data for product of second block copolymerization of *sec*-butyl lithium initiated 1,3-butadiene and LAAS.

ppm	multiplicity	assignment	relative peak areas
0.91 - 1.45	broad doublet	**d**	13.6
1.45 - 1.67	doublet	**b**	7.3
1.75 - 2.27	broad & sharp peaks	**e/j/h**	8.9
4.71 - 5.07	doublet + ?	**g/k**	11.3
5.07 - 5.21	quartet	**a**	2.3
5.21-5.97	multiple	**f/i**	7.0

The ^{1}H NMR peak data was used to determine the ratio of poly(butadiene) : poly(lactic acid) as 2.8:1.

Table 6.15 ^{13}C NMR peak data for product of second block copolymerization of *sec*-butyl lithium initiated 1,3-butadiene and LAAS.

ppm	assignment	+/- intensity
16.62	**b**	+12.0
38.51 - 40.61	**e**	-1.19 ~ +5.0
68.99	**a**	+9.8
113.73 - 114.99	**g**	-2.5 ~ -1.8
142.78 - 143.63	**f**	+2.0 ~ 3.8
169.60	**c**	-4.1

6.3.2.2 GPC Analysis

The end products and samples taken during the copolymerizations were analysed using the GPC system at DRA, Fort Halstead, as described in section 2.4.4.

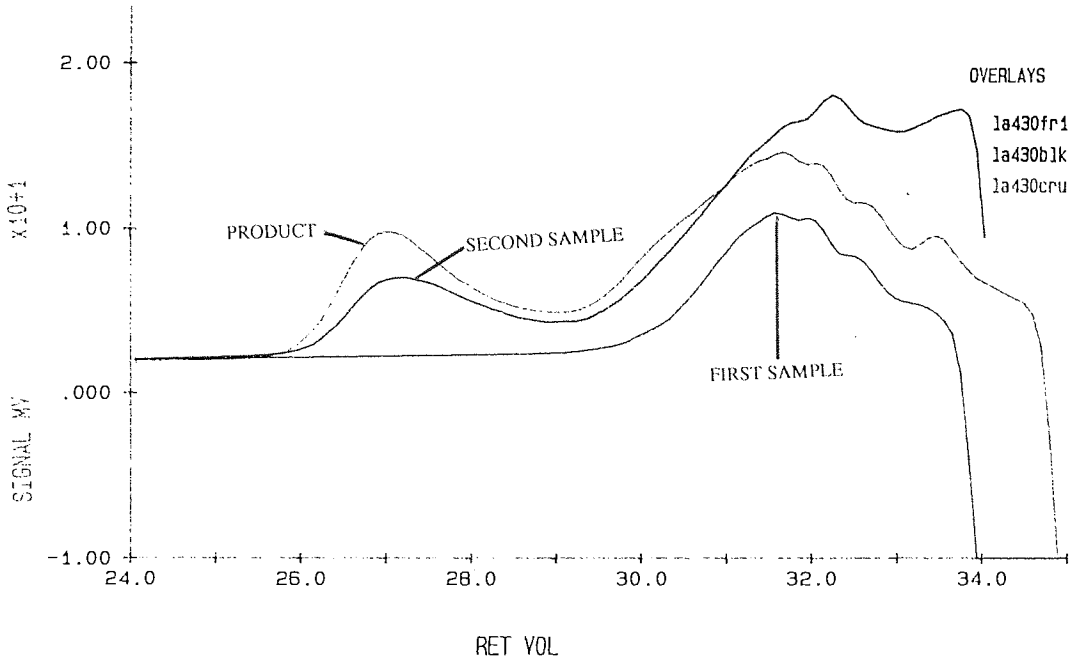

Figure 6.22 GPC of poly(1,3-butadiene-co-lactic acid) - first block copolymerization of *sec*-butyl lithium initiated 1,3-butadiene and LAAS.

The gel permeation chromatographs of the three samples taken during polymerization are superimposed in order to highlight changes in molecular weight distribution. The concentration chromatogram in figure 6.22 shows two peaks, with the peak of lower elution volume (and hence higher molecular weight) increasing over time relative to the higher elution volume peak. The GPC trace for the final product shows three peaks with the extra one at a higher elution volume.

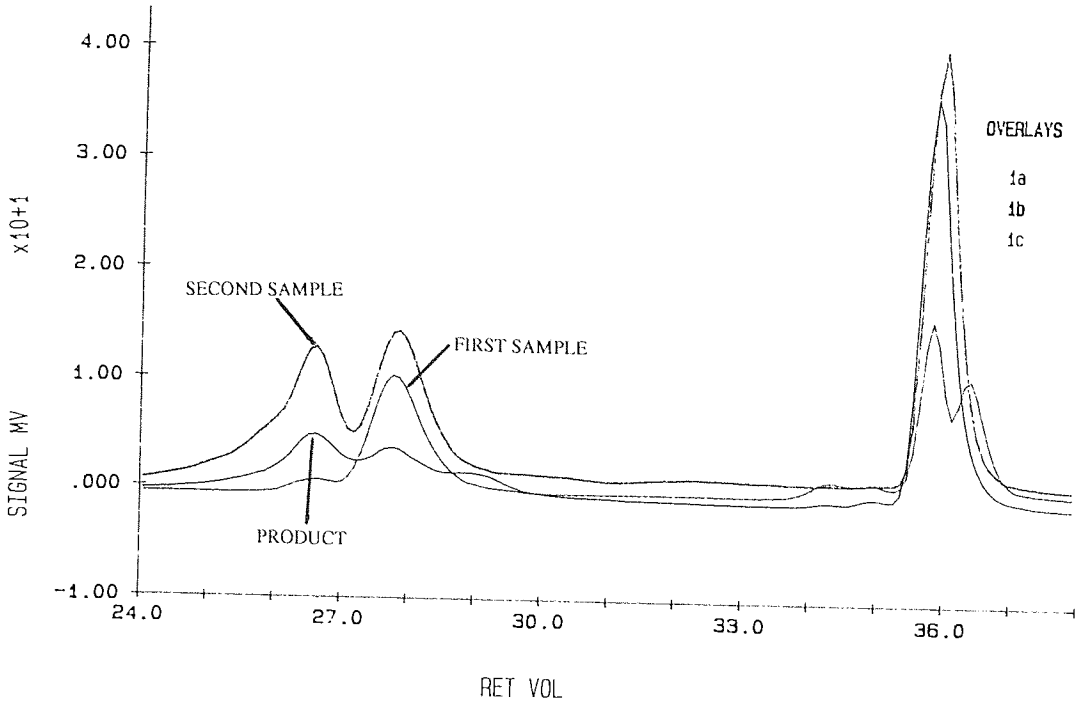

Figure 6.23 GPC of poly(1,3-butadiene-co-lactic acid) - second block copolymerization of *sec*-butyl lithium initiated 1,3-butadiene and LAAS.

Again, the GPC in figure 6.23 shows an increase in the intensity of the high molecular weight peak relative to that of the low molecular weight peak, as would be expected if block copolymerization had occurred.

6.3.2.3 DSC Analysis

The final product was analysed by DSC under the conditions described in section 2.4.5.

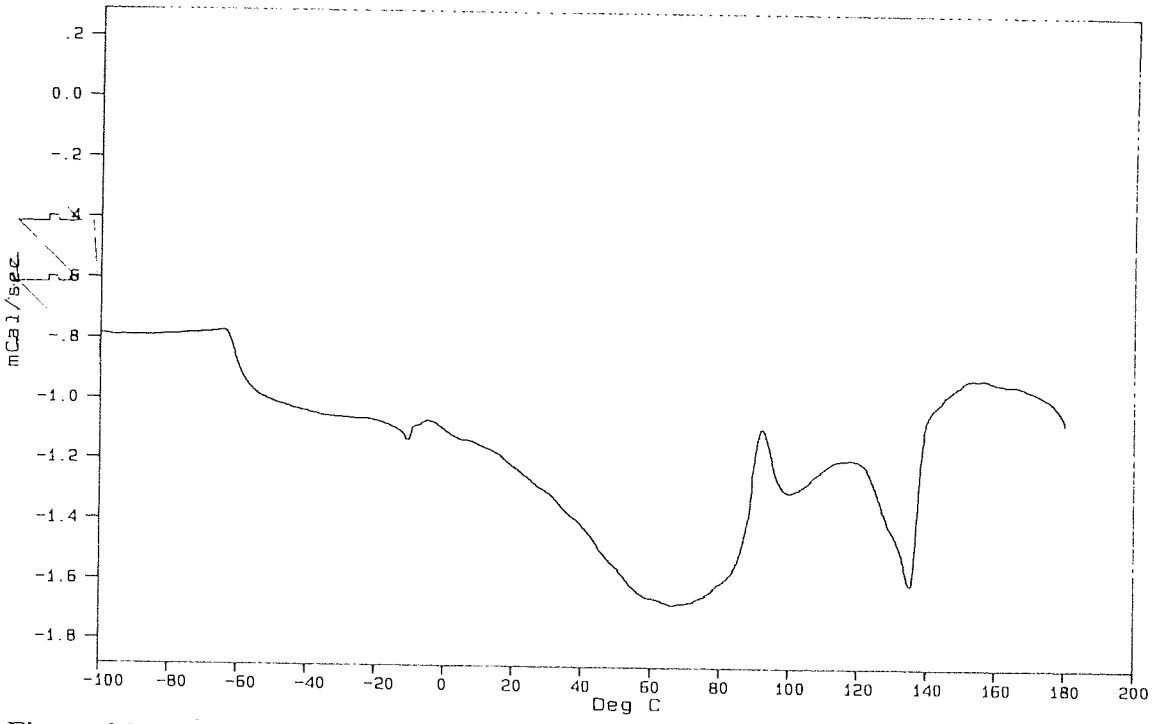

Figure 6.24 DSC for product of first *sec*-butyl lithium initiated block copolymerization of 1,3-butadiene and LAAS.

The DSC trace of the homo-polymeric poly(lactic acid) shows only one transition, an endothermic process occurring at 145 °C, while poly(butadiene) typically exhibits a transition at around -60 °C, the glass transition. The DSC of the copolymer, shown in figure 6.24, was run three times. The first two runs showing a broad endothermic transition around 40 - 90 °C due to evaporation of residual solvent. The final run shows a transition at -61 °C due to poly(butadiene), another at -10 °C, an exotherm at 92 °C and the typical poly(lactic acid) endotherm at 135 °C.

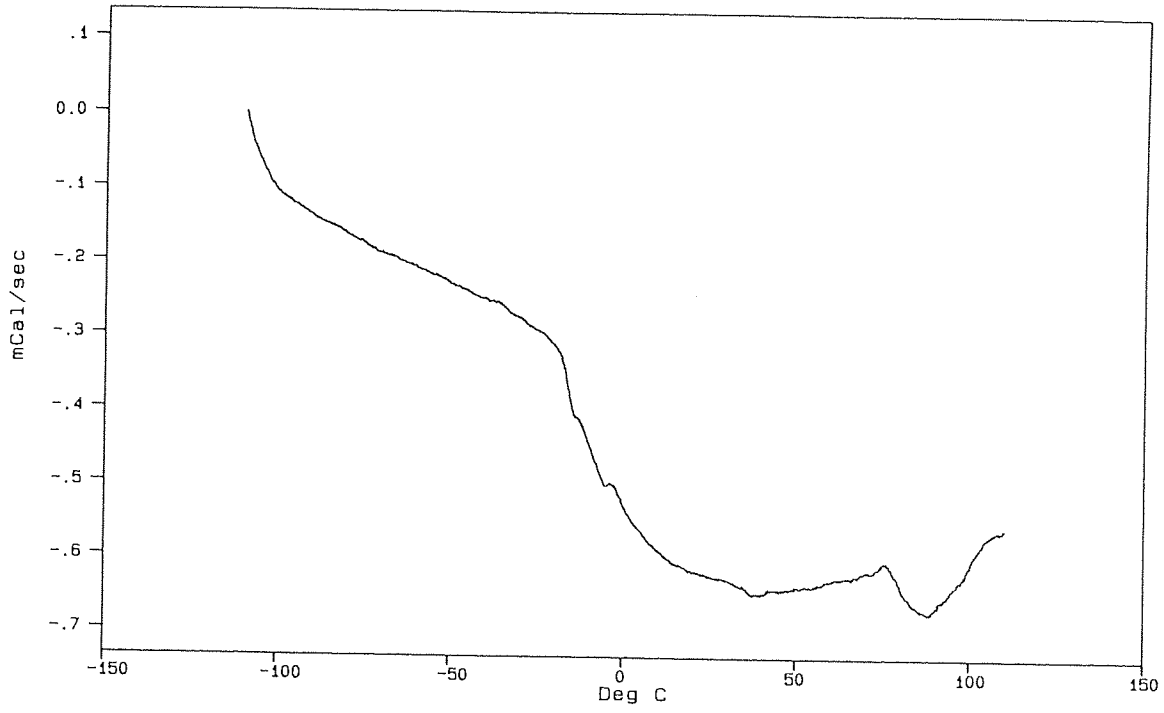

Figure 6.25 DSC for product of second *sec*-butyl lithium initiated block copolymerization of 1,3-butadiene and LAAS.

The DSC trace for the second polymerization, shown in figure 6.25, is unclear though there is a transition at around -60 °C, which is probably the poly(butadiene) glass transition, and an endothermic transition at around 130 °C, probably due to poly(lactic acid). The transition around 100 °C may be caused the presence of water.

6.3.3 Discussion

It seems likely that copolymer was formed as a result of living poly(1,3-butadiene) attacking the LAAS which was added. The product is significantly different in appearance to both poly(lactic acid) and poly(butadiene) homo-polymers. Evidence of the presence of poly(lactic acid) in the product is seen in the NMR and FT-IR spectra. Similarly, some features of the product DSC trace are not seen in the traces of the homo-polymers.

The polymerization of 1,3-butadiene is a strongly solvent-dependent process. In non-polar solvents, the anion exists as a σ-allyl structure, so that the negative charge is localised at the end carbon, as shown in figure 6.26. This means that attack upon monomer molecules tends to occur as a 1,4-addition, creating a polymer having an unsaturated back-bone. In a polar solvent, the anion will tend to exist as a π-allyl structure, so that the negative charge is de-localised, resulting in predominantly 1,2-

addition and hence a polymer chain having a saturated back-bone, with pendant vinyl groups.

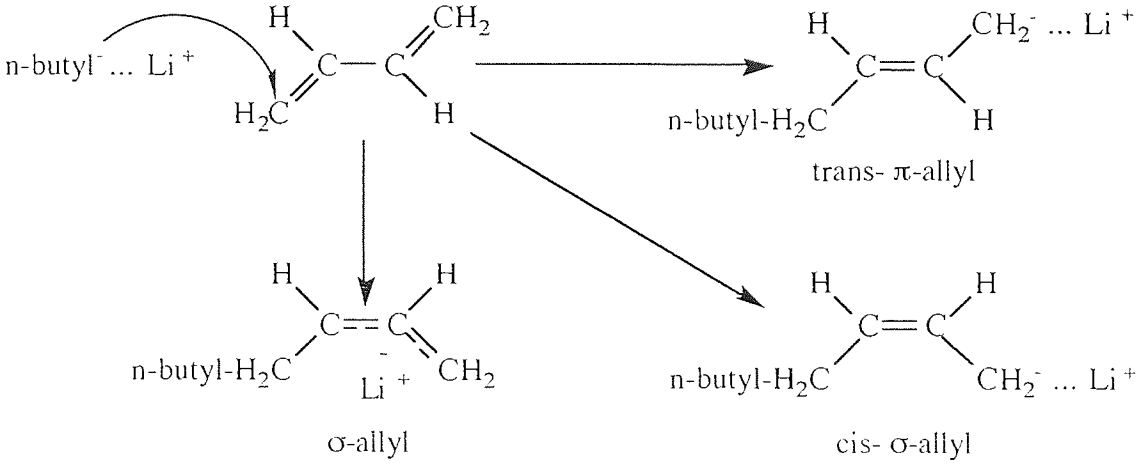

Figure 6.26 Initiation of 1,3-butadiene by butyl lithium.

While the ^1H NMR spectrum shows that both poly(lactic acid) and vinylic poly(butadiene) repeat units are present in the end product, further analysis of the spectra is difficult due to the overlap of a number of absorptions. The peak areas indicate that the proportion of end groups apparently increases during the course of polymerization (relative to the polymer chain repeat units). This may be explained by the nature of the initiator. *n*-butyl lithium tends to produce polymers having a higher polydispersity than *sec*-butyl lithium due to its relatively slow rate of initiation (compared to propagation, upon which the nature of alkyl group has no effect). If initiation was slow, then all available 1,3-butadiene may have been used up by the most reactive initiating species (i.e. those most completely ionised) before all *n*-butyl lithium was consumed. This would leave some initiator unreacted until poly(lactic acid) was added. In this situation, homo-poly(lactic acid) would be produced along with poly(lactic acid-co-butadiene).

6.4 RANDOM COPOLYMERIZATION OF LAAS WITH 1,3-BUTADIENE

6.4.1 Experimental

The reaction vessel was filled with 119.4 cm^3 of tetrahydrofuran and 22.0 cm^3 of 1,3-butadiene added (16.3 g) using the techniques described in section 6.3. 3.8 g of LAAS (0.028) was added, followed 30 minutes later by 3.4 cm^3 of a 2.5 M solution of *n*-butyl

lithium (0.0085 moles). On injection of initiator, the solution rapidly turned a deep yellow and some lumps of orange gel-like material appeared, accompanied by an apparent increase in viscosity. After one hour the coloration had faded to a pale yellow and a very fine suspension was visible in the reaction vessel. The dry ice/acetone bath was removed and the temperature of the reaction mixture allowed to rise to 0 °C. No gas evolution was observed, indicating that no monomeric 1,3-butadiene remained. After 30 minutes at 0 °C, a sample was taken. The temperature of the mixture was then allowed to rise to 25 °C, and a second sample was taken. The flow of argon was adjusted to provide a slow but steady flow and the reaction was left to continue at room temperature, overnight. The next morning, methanol was injected to terminate the reaction and solvent was removed from the samples using a rotary evaporator. The end product was found to be partially soluble in diethyl ether, so the fractions were separated by filtration. The samples were left in a fume cupboard overnight (in order to remove the solvent) and dried in a vacuum oven at 30 °C for 48 hours.

After the solvent was removed, both of the samples taken during the reaction yielded creamy yellow sticky material, though that from the second sample was rather more viscous. The end product was found to be only partially soluble in diethyl ether, the ether soluble fraction being a sticky orange-brown resin and the ether-insoluble fraction a sticky, opaque orange material. Both fractions were analysed by ^{1}H and ^{13}C NMR and all of the samples were analysed by GPC.

6.4.2 Results

6.4.2.1 NMR Spectral Analysis

Figures 6.29 and 6.30 and tables 6.16 and 6.17 show the ^{1}H and ^{13}C NMR spectra and peak data of the ether insoluble fraction of the product of the random copolymerization experiment.

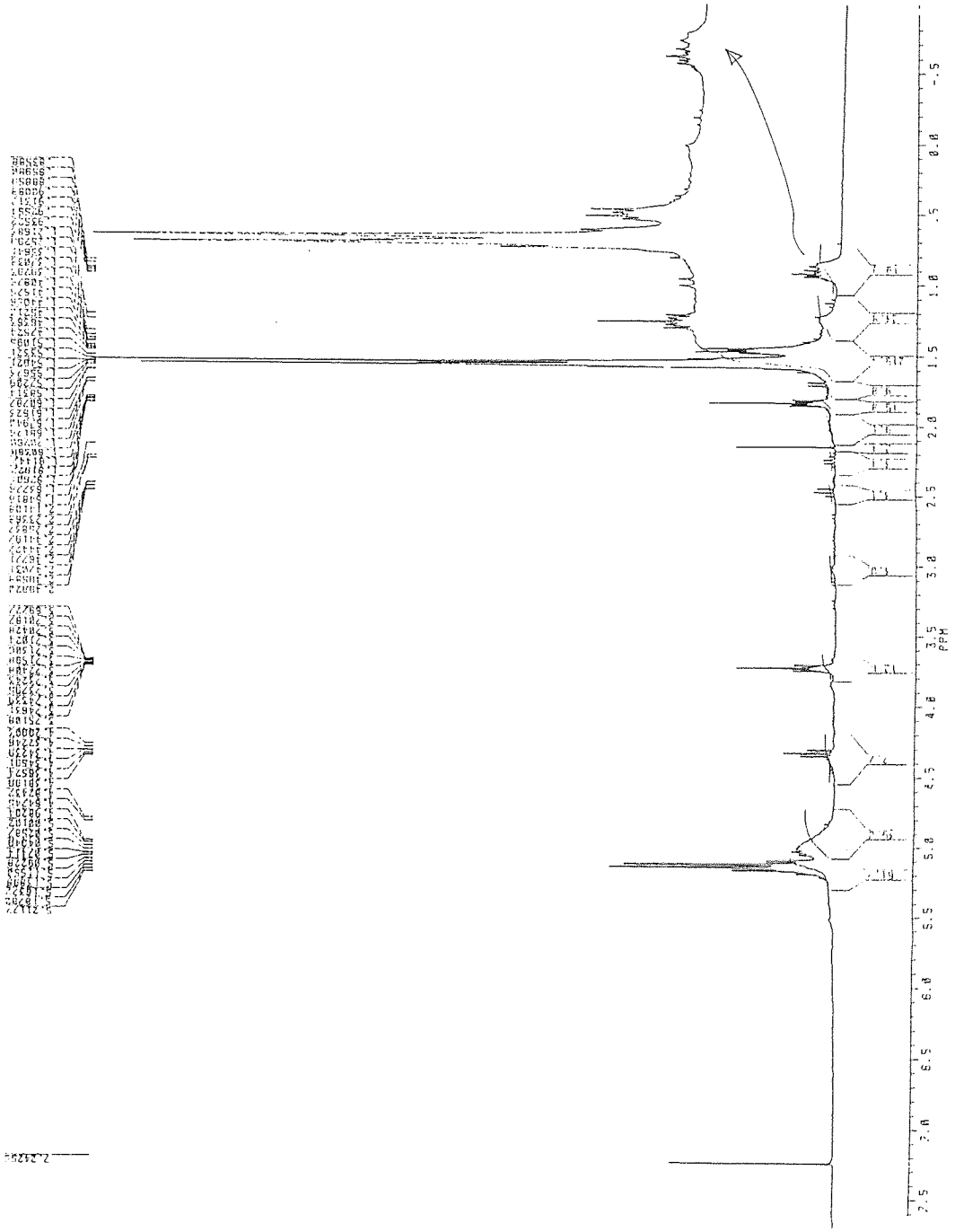

Figure 6.27 ^{1}H NMR spectrum of ether insoluble fraction of product of *sec*-butyl lithium initiated random copolymerization of LAAS and 1,3-butadiene.

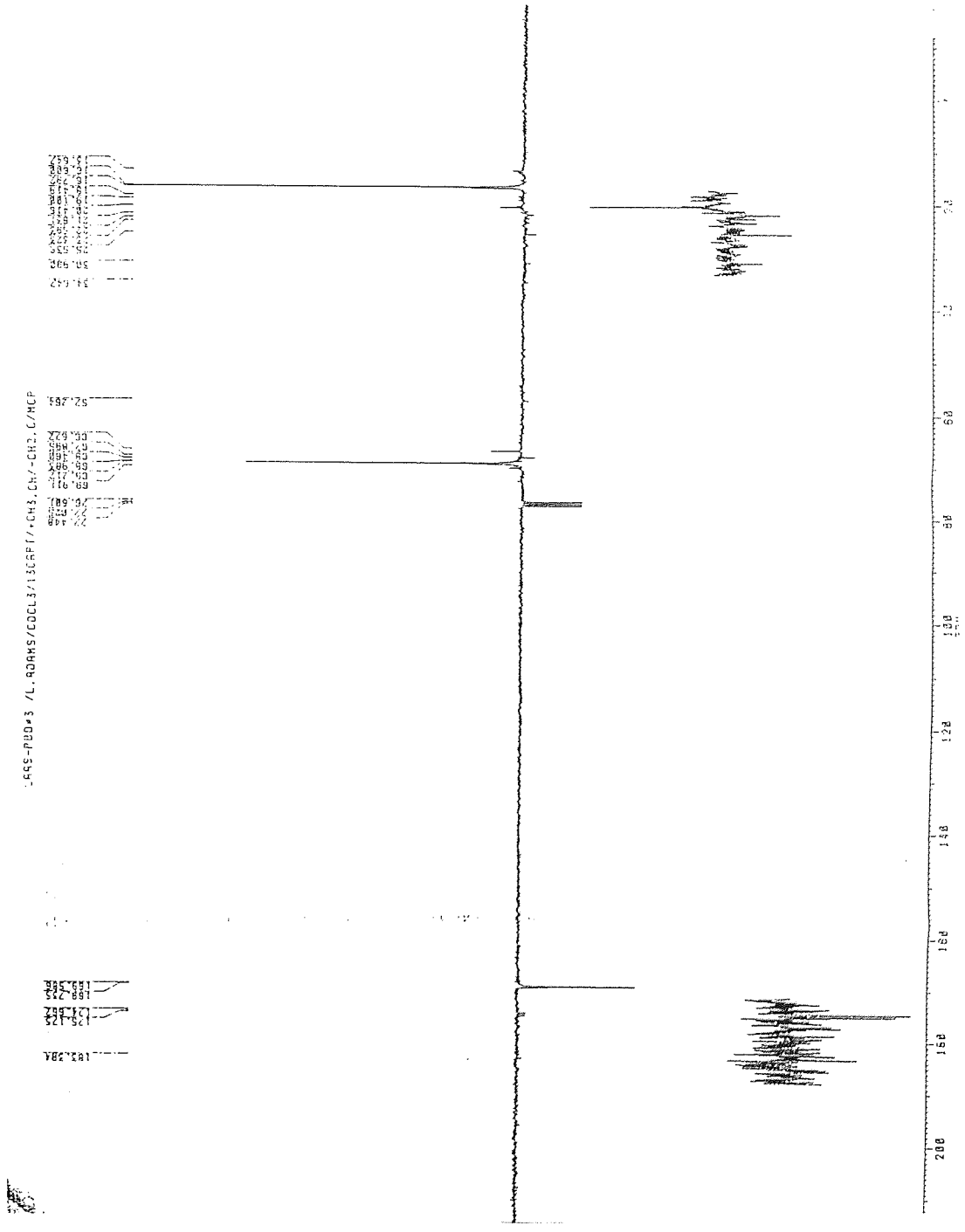

Figure 6.28 ^{13}C NMR spectrum of ether insoluble fraction of product of *sec*-butyl lithium initiated random copolymerization of LAAS and 1,3-butadiene.

Table 6.16 ^{1}H NMR peak data for ether insoluble fraction of product of *sec*-butyl lithium initiated random copolymerization of LAAS and 1,3-butadiene.

ppm	multiplicity	assignment	relative peak areas
1.06 - 1.38	complex	**d**	1.5
1.38 - 1.66	2 x doublets	**b** + ?	13.9
1.79 - 1.90	quintet	**e/j/h**	1.0
4.71 - 5.07	complex	**g/k**	2.5
5.07 - 5.29	quartet	**a**	3.9

The ^{1}H NMR spectrum of the ether insoluble fraction is complex but contains a high proportion of poly(lactic acid) repeat units. The ratio of poly(lactic acid) : poly(butadiene) may be estimated as being approximately 6:1. There is an extra doublet appearing close to the poly(lactic acid) methyl absorption. This may be due to the presence of poly(lactic acid) bonded to poly(butadiene) repeat units.

Table 6.17 ^{13}C NMR peak data for product of ether insoluble fraction of *sec*-butyl lithium initiated random copolymerization of LAAS and 1,3-butadiene.

ppm	assignment	+/- intensity
16.60	**b**	+12.1
68.98	**a**	+8.5
169.59	**c**	-3.6

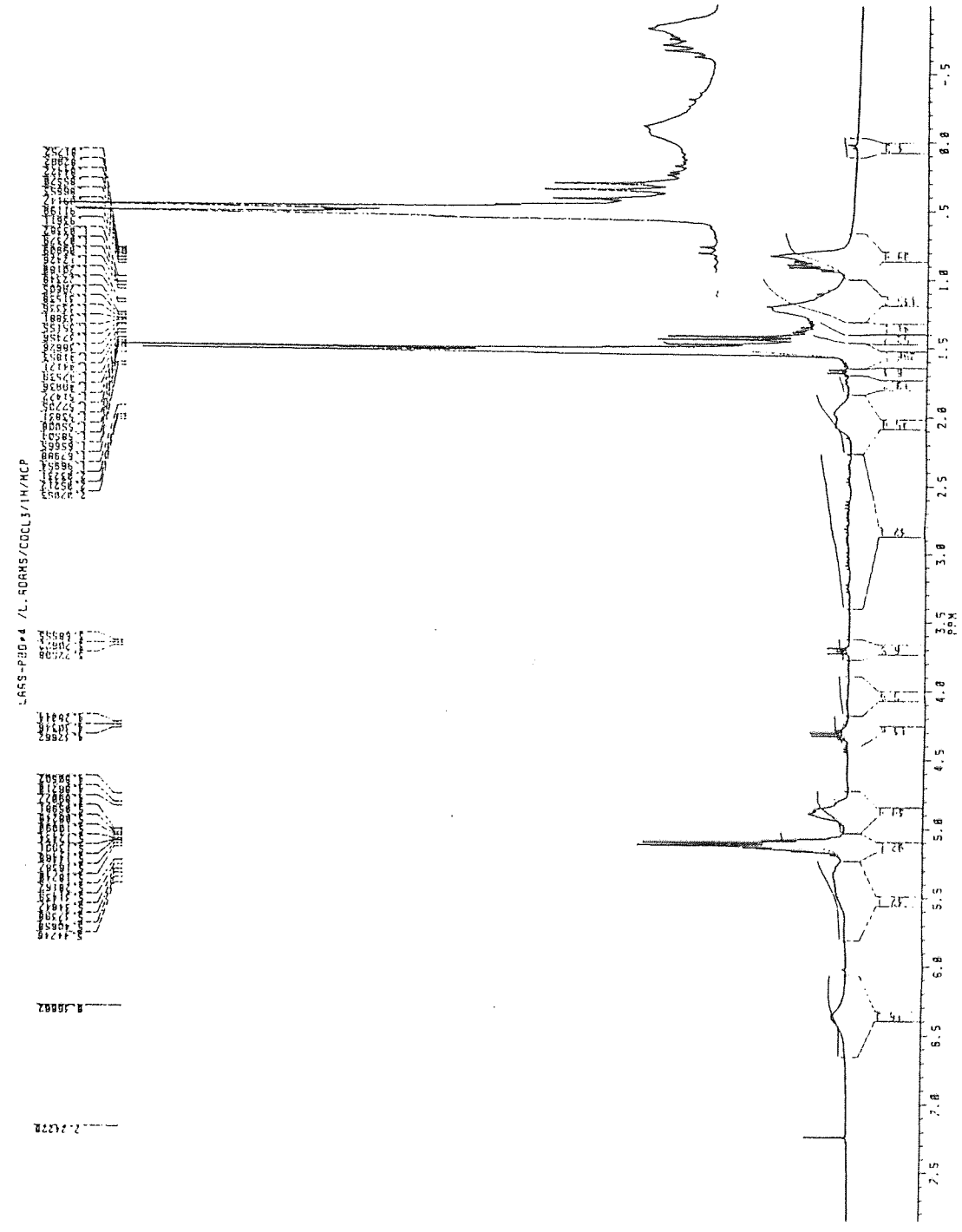

Figure 6.29 ^{1}H NMR spectrum of ether soluble fraction of product of *sec*-butyl lithium initiated random copolymerization of LAAS and 1,3-butadiene.

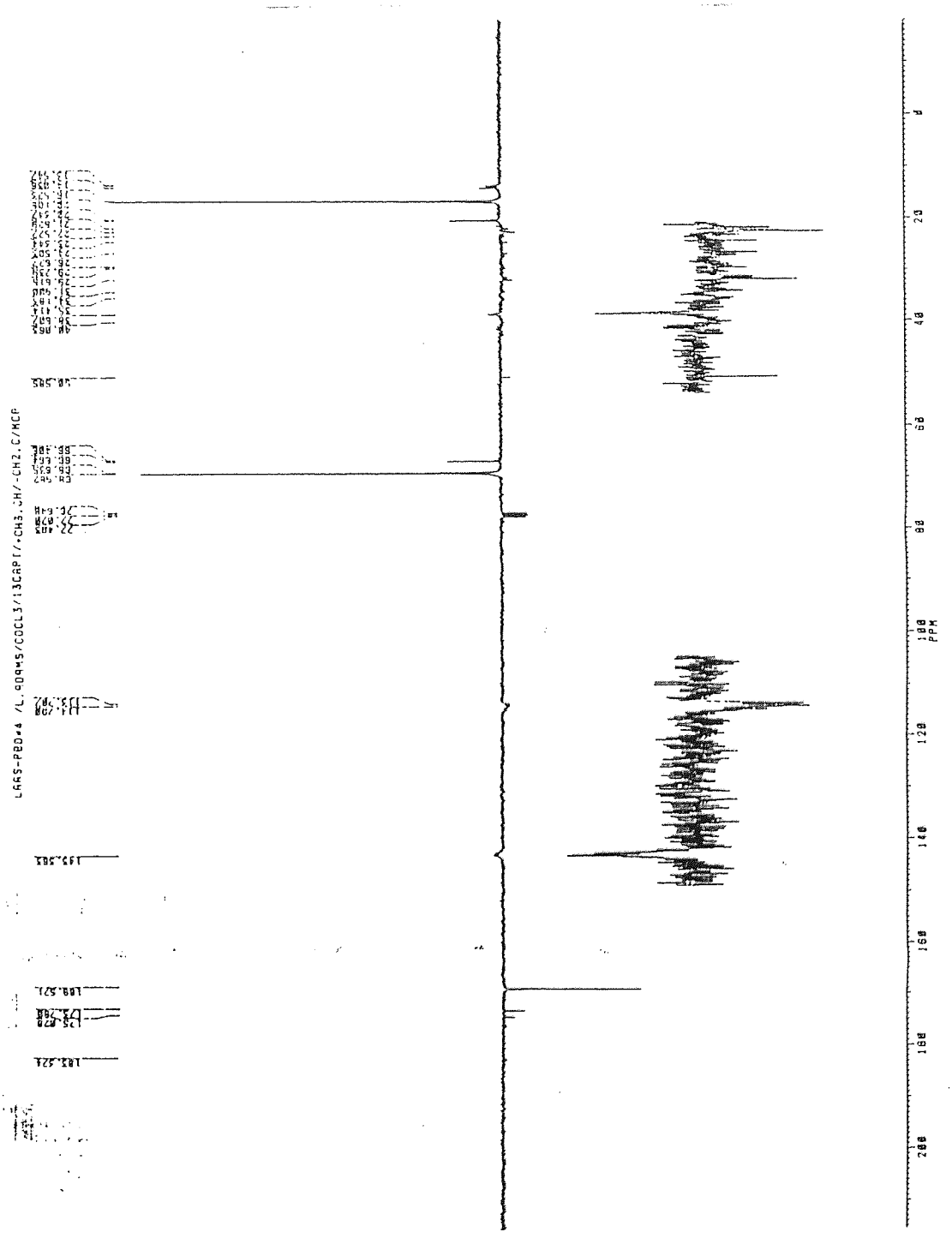

Figure 6.30 ^{13}C NMR spectrum of ether soluble fraction of product of *sec*-butyl lithium initiated random copolymerization of LAAS and 1,3-butadiene.

Table 6.18 ^{1}H NMR spectrum of ether soluble fraction of product of *sec*-butyl lithium initiated random copolymerization of LAAS and 1,3-butadiene.

ppm	multiplicity	assignment	relative peak areas
0.99 - 1.31	mutiplet	**d**	3.6
1.45 - 1.64	2 x doublets	**b** + ?	7.9
1.83 - 2.26	broad multiplet	**e/j/h**	1.2
4.71 - 5.02	broad multiplet	**g/k**	1.0
5.02 - 5.22	quartet	**a** + ?	2.6
5.22 - 5.80	broad	**f/i**	1.0

Though the spectrum is complex, with many absorptions overlapping, the ratio of poly(lactic acid) : poly(butadiene) repeat units may be estimated as 1.5:1. Again, there appears to be a second poly(lactic acid) methyl absorption.

Table 6.19 ^{13}C NMR peak data for ether soluble fraction of product of *sec*-butyl lithium initiated random copolymerization of LAAS and 1,3-butadiene.

ppm	assignment	+/- intensity
16.57	**b**	+12.0
68.98	**a**	+11.1
169.57	**c**	-4.3

6.4.2.2 GPC Analysis

The concentration gel permeation chromatograms of the end product fractions and two samples taken during the polymerization are shown superimposed in figure 6.31. The two samples taken during polymerization show only a single broad peak at high elution volume. The ether soluble product fraction however, shows two additional peaks at lower elution volumes. These peaks are also visible (though with much lower intensity) in the trace for the ether insoluble fraction.

Figure 6.31 Random copolymerization of LAAS and 1,3-butadiene, initiated by *sec*-butyl lithium - GPC analysis.

6.4.2.3 DSC Analysis

Figure 6.32 First sample taken from random copolymerization of LAAS and 1,3-butadiene, initiated by *sec*-butyl lithium - DSC analysis.

Figure 6.32, the DSC for the first sample, shows an endothermic transition around 120 °C, probably due to poly(lactic acid) but no indications of the presence of poly(butadiene).

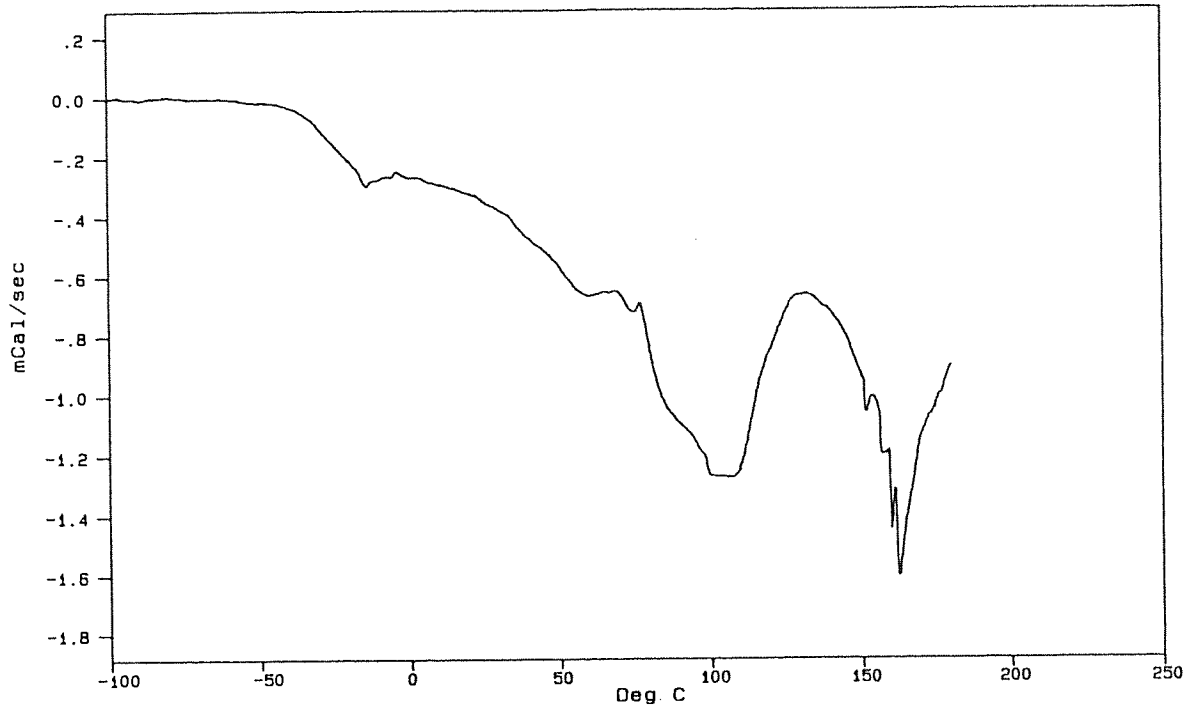

Figure 6.33 Second sample taken from random copolymerization of LAAS and 1,3-butadiene, initiated by *sec*-butyl lithium - DSC analysis.

The DSC for the second sample, shown in figure 6.33, shows the sharp melting transition at 160 - 170 °C characteristic of poly(lactic acid) and a transition at approximately -20 °C which may be due to poly(butadiene).

The DSCs of the two fractions of the end product were unclear with poor resolution.

6.4.3 Discussion

It appears that it may be possible to initiate the polymerization of lactic acid anhydrosulphite by means of 1,3-butadiene, but as to whether any copolymer is formed, the situation is unclear. The block copolymerization experiments appear to have been the most successful, with DSC and GPC results indicating the formation of copolymers. However, while the end products may have been different to the homopolymers in terms of physical appearance, this may have been due to a simple blending of the homopolymers. The random copolymerization experiment was less successful. While

NMR spectral analysis showed the presence of both poly(lactic acid) and poly(butadiene) repeat units, DSC results indicated that only poly(lactic acid) was present in the product. The appearance of the product also indicated that it was composed of two materials, an opaque solid and a clear, viscous liquid.

CHAPTER SEVEN

CONCLUSIONS AND SUGGESTIONS FOR FURTHER WORK

With regard to the synthesis and purification of anhydrosulphites, copper (I) and (II) oxides have been shown to provide more effective means of purifying lactic acid anhydrosulphite than either the use of silver (I) oxide or chromatographic methods for removal of chlorinated material. The chromatographic solvent systems and stationary phases considered here were unsuccessful in separating LAAS from impurities. While a more extensive survey might identify more suitable conditions for chromatographic purification, decomposition by the stationary phase must be avoided.

During some syntheses, a hitherto unknown impurity was isolated. The nature of this impurity has been investigated and it is suggested that its source was a contaminated batch of commercially prepared copper (II) lactate. Attempts were made to prepare the anhydrosulphite of gluconic acid, a 'sugar' acid. Although infra-red spectroscopy provided some evidence of success, the product was very difficult to purify due to the problems of removing parent acid and solvents, and the facile occurrence of the decomposition reaction. If the hydroxyl groups present in gluconic acid could be protected, perhaps by means of a silylating agent, synthesis of gluconic acid anhydrosulphite with a reasonable yield might be possible. However, the removal of protecting groups might be difficult to achieve without cleavage of the ring. It might be more fruitful to attempt the synthesis of simpler sugar acids.

Lithium and potassium alkoxides have been shown to be effective as initiators for the polymerization of lactic acid anhydrosulphite. The kinetics of the polymerization of lactic acid anhydrosulphite by lithium *tert*-butoxide in nitrobenzene, were studied in detail and the rates of the reaction were found to be strongly dependent upon the form of the initiator in solution. Highly concentrated solutions of initiator were less effective than would be expected, probably because much of the initiator was present as the less reactive covalent form or even undissolved solid. Though an induction period was observed, during which a relatively slow process occurred, the propagation reaction was probably first order with respect to monomer and initiator concentrations. The addition of a crown ether to the initiator solution was shown to decrease the length of the induction period, and increase the rate of polymerization, significantly. This was likely to be due to the crown ether co-ordinating to the alkali metal cation.

It was found that when the polymerization of lactic acid anhydrosulphite was initiated by potassium *tert*-butoxide in tetrahydrofuran at ambient temperatures and pressures, the products were of higher molecular weights than in nitrobenzene at low pressure and

elevated temperatures. The use of volatile solvents provided a more viable route to useful amounts of polymer. The technique of polymerization under an inert gas at atmospheric pressure was also used successfully for the *n*- and *sec*-butyl lithium initiated polymerization of lactic acid anhydrosulphite.

The addition of a crown ether to the initiator solution appears to have had no effect upon the polydispersity of the products of polymerization reactions initiated by lithium *tert*-butoxide in nitrobenzene. It would be interesting to study the effect of the addition of crown ether upon the reaction of lactic acid anhydrosulphite with potassium *tert*-butoxide in tetrahydrofuran, in terms of reaction rate and the nature of products, i.e. molecular weight distribution, polydispersity and crystallinity.

Attempts were made to co-polymerize lactic acid anhydrosulphite with styrene and 1,3-butadiene. Though random copolymerization of LAAS with butadiene was unsuccessful, GPC results appear to indicate that some block copolymers were formed. Further experiments in co-polymerization of α–anhydrosulphites with non-biodegradable polymers may produce co-polymers which blend easily with commodity plastics to produce materials with interesting bio-degradation behaviour.

Since the lactic acid anhydrosulphite polymer chain has no ultra-violet absorptions, co-polymerization with anhydrosulphites based on acids such as benzilic and mandelic would enable the molecular weight distribution of the products to be studied by means of gel permeation chromatography. The benzene ring contained in these monomers would make the corresponding polymers visible to a U.V. detector.

By adding lithium chloride to the butyl lithium initiator solution, it may be possible to make use of the 'common-ion' effect in order to narrow molecular weight distributions. The addition of a salt of the same metal as that of the initiator is thought to drive the initiator equilibrium over to right, i.e. the molar proportion of initiator existing as more dissociated species is increased.

The polymerization of lactic acid anhydrosulphite initiated by potassium *tert*-butoxide occurs rapidly at room temperature. If the reaction was slowed, by means of a reduction in either temperature or initiator concentration, so that conversion occurred at a more convenient pace, samples of the reaction mixture might be taken. The samples might then be weighed and molecular weight distributions determined. By this method, the kinetics of the reaction could be studied and, if X-ray data was obtained, the effects of temperature upon the crystallinity of the products determined.

So far, polymerizations of lactic acid anhydrosulphite, initiated by alkali metal alkoxides have only produced products of low molecular weight in comparison with those

produced by the thermal polymerization of the di-lactide, which are often in the order of 10^6. There are a number of strategies which may yield products of higher molecular weight. Reduction of the initiator concentration, while keeping the monomer concentration high is an obvious possibility, but the concentration of trace impurities may be a limiting factor. Such impurities may react with the propagating chain, terminating polymerization before all of the monomer is consumed, or a quantity of the initiator may be consumed by the impurities. This means that rigorous purification of solvents and reactants would be essential. An alternative method of increasing the molecular weight of products might be to steadily add monomer to the initiator solution, so that the concentration of monomer is kept high, thereby minimising the possibility of living chains ends reacting with impurities. By using a peristaltic pump to add the monomer, chain growth might be continued for an extended period.

REFERENCES

1 'Poly(l-lactide): a Long-term Degradation Study *in vivo* part III: Analytical Characterisation.' H.Pistner, D.R.Bendix, J.Muehling and J.F.Ruether, Biomaterials 14,(4), 291 - 298, (1993).

2 'Biocompatibility and Resorbability of a Poly(lactic acid) Membrane for a Periodontal Guided Tissue Regeneration.' P.Robert, J.Mauduit, R.M.Frank and M.Vert, Biomaterials 14 (5), 353 - 356, (1993).

3 'Thermal Oxidative Degradation of Poly(lactic acid) part I: Activation Energy of Thermal Degradation in Air.' M.C.Gupta and V.G.Deshmukh, Coll. and Polym. Sci. 260, 308 - 311, (1982).

4 'Biodegradability of a Hot-pressed Poly(lactic acid) Formulation with Controlled Release of LH-RH Agonist and its Pharmacological Influence on Rat Prostate.' M.Asano, M.Yoshida, I.Kaetsu, K.Imai, T.Mashimo, H.Yuasa, H.Yamanaka, K.Suzuki and I.Yamazaki, Makrom.Chem., Rapid Commun. 6, 509 - 513, (1985).

5 'Synthesis of High Molecular Weight Lactic Acid Polymers in the Solid State.' G.Perego, E.Albizzati (Himont Inc., USA) Eur.Pat.Appl. (1992).

6 'Synthesis, Application and Degradation of Poly(lactic acid).' Y.You, G.Lu, Y.Shen, Y.Yu and B.He, Zhongguo Shengwu Yixue Gongcheng Xuebao, 4(4), 244 - 248, (1985).

7 'Encyclopaedia of Polymer Science and Engineering (Volume 2)' 2nd Edition, Ed. H.F.Mark, N.M.Bikales, C.G.Overberger, G.Menges and J.I.Kroschwitz, John Wiley and Sons, Chichester, (1989).

8 'Preparation of High Molecular Weight Polyhydroxyacetic ester' C.E.Lowe (assignor to du Pont de Nemours and Co., Wilmington, Del.), U.S. patent 2,668,162, (1954).

9 'Action du Chlorure de Thionyle sur les Acides Alcools α.' E.E.Blaise and Mlle Montagne, Compt.rend. 174, 1553 - 1555, (1922).

10 'Polymer from α-Hydroxy Isobutyric Acid.' T.Alderson (assignor to du Pont), U.S. patent 2,811,511, (1957).

11 'Polyesters from the Anhydrosulphites of α-Hydroxy Acids.' J.B.Rose and C.K.Warren, J.Chem.Soc. 129, 791 - 792, (1965).

12 'Studies of the Reactions of the Anhydrosulphites of α-Hydroxy Carboxylic Acids. part II: Polymerisation of Glycollic and Lactic acid Anhydrosulphites' D.G.H.Ballard and B.J.Tighe J.Chem.Soc.(B), 976 - 980, (1967).

13 'The Use of Heterocyclic Monomers in the Preparation and Modification of Polymers.' S.Roy, PhD thesis, University of Aston in Birmingham, Birmingham. (1978).

14 'Polymers for Biodegradable Medical Devices (III): Polymerisation and Copolymerization of Cyclic Derivatives of Tartronic acid.' H.Al-Mesfer and B.J.Tighe, Biomaterials 8, 289 - 295, (1987).

15 'Studies of the Reactions of the Anhydrosulphites of α-Hydroxy Carboxylic Acids. part III: Purification and Polymerisation of Glycollic Acid Anhydrosulphite.' M.D.Thomas and B.J.Tighe, J.Chem.Soc. (B) 1039 - 1044, (1970).

16 'Studies of the Reactions of the Anhydrosulphites of α-Hydroxy Carboxylic Acids. part I: Polymerisation of Anhydrosulphite of α–Hydroxy Isobutyric Acid.' D.G.H.Ballard and B.J.Tighe, J.Chem.Soc. (B) 702 - 709, (1967).

17 'Studies of the Reactions of the Anhydrosulphites of α-Hydroxy Carboxylic Acids. part IX: Thermal Polymerisation of Anhydrosulphites of α-Hydroxy α-Methyl Carboxylic Acids.' A.J.Crowe and B.J.Tighe, Br.Polym.J., 6, 79 - 89, 1974.

18 'Studies of the Reactions of the Anhydrosulphites of α-Hydroxy Carboxylic Acids. part VII: Polymerisation of Anhydrosulphites Derived from Symmetrically-substituted α-Hydroxy acids.' G.P.Blackbourn and B.J.Tighe, J.Chem.Soc. (B), 1384 - 1390, (1971).

19 'Studies in Ring-opening Polymerisation III: 5-Methyl-5-propyl and 5-Methyl-5-isopropyl-1,3,2-dioxathiolan-4-one 2-oxide.' D.G.Pedley and B.J.Tighe, J.Polym.Sci. II, 779 - 788, (1973).

20 'Polymerization of α-Hydroxy Carboxylic Acid Anhydrosulfites by Tertiary Amines or Amides as Catalysts.' S.Inoue, K.Tsubaki, T.Tsuruta, Die Makrom.Chemie 125, 170 - 180, (1969).

21 'Thermal Decomposition of 5,5-(bis-chloromethyl)-1,3,2-dioxathiolan-4-one 2-oxide.' A.J.Crowe and B.J.Tighe, Chem. and Ind. 170 - 171, (1969).

22 'Studies of the Reactions of the Anhydrosulphites of α-Hydroxy Carboxylic Acids. part V: Thermal Decomposition of Benzilic and Mandelic Acid Anhydrosulphites.' B.W.Evans and B.J.Tighe, J.Chem.Soc. (B), 1049 - 1052, (1970).

23 'Studies of the Reactions of the Anhydrosulphites of α-Hydroxy Carboxylic Acids. part VIII: Polymerisation of Anhydrosulphites of α-Hydroxy-cycloalkanecarboxylic acids.' G.P.Blackbourn and B.J.Tighe, J.Chem.Soc. (Perkin transactions II) 1263 - 1268, (1972).

24 'Synthesis and Characterisation of Fluorine-containing Poly-α-esters II: Thermal and Hydroxyl-initiated Polymerisation of Pentafluorophenyl-substituted Anhydrosulphites and Anhydrocarboxylates of α-Hydroxycarboxylic Acids.' I.J.Smith and B.J.Tighe, Br.Polym.J. 7, 349 - 360, (1975).

25 'Studies of the reactions of the anhydrosulphites of α-hydroxy carboxylic acids. part VI: Anhydrosulphite Synthesis and Characterisation' G.P.Blackbourn and B.J.Tighe, J.Chem.Soc.(C), 257 - 259, (1971).

26 'Synthesis of Optically Active Polymers by Asymmetric Catalysts IX.(1). Asymmetric-selective Polymerisation of β-Chloro-α-hydroxy-α-methylpropionic acid Anhydrosulfite.' S.Inoue, K.Tsubaki and T.Tsuruta, Polymer letters 6, 733 - 736, (1968).

27 'Polymerization of α-Hydroxy-carboxylic acid Anhydrosulfites by Tertiary Amines or Amides as Catalysts.' S.Inoue, K.Tsubaki and T.Tsuruta, Die Makrom.Chemie 125, 170 - 180, (1969).

28 'Copolymerisation of α-Hydroxy-iso-butyric acid Anhydrosulfite with Vinyl Compounds.' S.Inoue, K.Tsubaki, T.Yamada and T.Tsuruta, Die Makrom.Chemie 125, 181 - 191, (1969).

29 'Polydepsipeptides I: Synthesis and Characterisation of Copolymers of α-Amino and α-Hydroxy Acids.' M.Goodman, C.Gilon, G.S.Kirschenbaum and Y.Knobler, Isr.J.Chem., 10(4), 876 - 79, (1972).

30 'Synthesis of Poly(depsi-peptides) by Ring-opening Polymerization.' J.Helder, F.E.Kohn, S.Sato, J.W.Van den Berg and J.Feijen, Adv.Biomater.6(Biol.Biomech.Perf.Biomater.), 245 - 250, (1986).

31 'New Polymer Syntheses 8. Synthesis and Polymerization of L-Lactic Acid O-Carboxyanhydride (5-methyl-dioxolan-2,4-dione).' H.R.Kricheldorf and J.M.Jonte Polym.Bull.(Berlin), 9(6 - 7), 276 - 283, (1983).

32 'Ring-opening Reactions of Some Di-alkyl Substituted 1,3,2-Dioxathiolan-4-one-2-oxides.' A.J.Crowe, PhD thesis, University of Aston in Birmingham, Birmingham, (1975).

33 'Polymerisation of Cyclic Derivatives of α-Hydroxy Acids.' H.A.Al-Mesfer, PhD thesis, University of Aston in Birmingham, Birmingham, (1981).

34 'Studies in Ring-opening - The Interactions of Some Cyclic Esters with a Bi-metallic Oxo-alkoxide.' W.A.Penny, PhD thesis, University of Aston in Birmingham, Birmingham, (1979).

35 'Thermodynamics of Polymerization of Cyclic Compounds by Ring Opening (II). Heterocyclic Compounds.' P.A.Small, Trans.Farad.Soc. 51, 1717, (1955).

36 'Polymerization of Cyclic Esters, Urethans, Ureas and Imides.' H.K.Hall and A.K.Schneider, J.Amer.Chem.Soc. 80, 6409 - 6412, (1958).

37 'Hydrolysis Rates and Mechanisms of Cyclic Monomers.' H.K.Hall, M.K.Brandt and R.M.Mason, J.Amer.Chem.Soc. 80, 6420 - 6427, (1958).

38 'Some Thermodynamic and Kinetic Aspects of Addition Polymerization.' F.S.Dainton and K.J.Ivin, Chem.Soc.Quart.Revs. 12, 61 - 90, (1958).

39 'Extrusion Reactions.' B.P.Stark and A.K.Duke, Pergamon press, London, (1967).

40 'Polymers: Chemistry and Physics of Modern Materials.' (2nd edition) J.M.G.Cowie, Blackie, Glasgow and London, (1991).

41 'The importance of Alkali Metallo-organic Compounds for Synthesis.' K.Ziegler, Angew.Chem. 49, 499 - 502, (1936).

42 'Carbanions, Living Polymers and Electron Transfer Processes.' M.Szwarc, Interscience Publishers Inc., London, (1968).

43 'The Covalent Nature of Alkali Metal Alkoxides.' M.S.Bains, Canadian J.Chem., 42, 945 - 946, (1964).

44 'The Mass Spectra of Lithiomethyl-trimethylsilane and Lithium *t*-butoxide.' G.E.Hartwell and T.L.Brown, Inorg.Chem. 5, 1257, (1966).

45 'Living Polymers and Mechanisms of Anionic Polymerization - Advances in Polymer Science 49.' M.Szwarc, Springer-Verlag, Berlin, Heidelberg and New York, (1983).

46 'Studies of the Reactions of the Anhydrosulphites of α-Hydroxy-carboxylic Acids. Part IV. Steric and Electronic Effects in the Reaction with Alcohols.' D.J.Fenn, M.D.Thomas and B.J.Tighe, J.Chem.Soc.(B) 1045 - 1048, (1970).

47 'Watch your Waste.' Open University/Dept. of the Environment, Community Education P934, Halstan and Co.Ltd, London, (1993).

48 'Having the Last Gas.' N.P.Freestone, P.S.Phillips and R.Hall, Chemistry in Britain 30(1), 48 - 50, (1994).

49 'Resorbable Materials of Poly(L-lactide).VI. Plates and Screws for Internal Fracture Fixation.' J.W.Leenslag, A.J.Jennings, R.R.M.Bos, F.R.Rozema and G.Boering, Biomaterials 8, 71 - 73, (1987).

50 'The Effect of an Intermedullary Self-re-inforced Poly-L-lactide (SR-PLLA) Implant on Growing Bone with Special Reference to Fixation Properties. An Experimental Study on Growing Rabbits.' H.Miettinen, E.A.Mäkelä, J.Vainio, P.Rokkanen and P.Törmälä, J.Biomater.Sci.Polym.Edn. 3(6), 443 - 450, (1992).

51 'Use of Supercritical Fluids to Obtain Porous Sponges of Biodegradable Polymers for Pharmaceutical Implants or Drug-delivery Systems.' R.De Ponti, C.Torricelli, A.Martini E.Lardini (Farmitalia Carlo Erba S.r.l), P.C.T.Int.Appl. (1991).

52 'Laminated Three-dimensional Foams for Use in Tissue Engineering.' A.G.Mikos, G.Sarakinos, S.M.Leite, J.P.Vacanti and R.Langer, Biomaterials 14 (5) 323 - 330, (1993).

53 'A Controlled, Sustained-release Delivery System for Treating Drug Dependency.' J.P.Kitchell, I.A.Muni and Y.N.Boyer (Dynagen Inc., USA.), P.C.T. Int.Appl., U.S.Patent 91-696637, (1992).

54 'Swelling Agent and Biodegradable Polymer Substances in Long-acting Pharmaceutical Granule Preparations.' T.Hata, A.Kagayama, S.Kimura, S.Ueda and S.Murata (Fujisawa Pharmaceutical Co., Ltd., Japan.), P.C.T. Int Appl. (1992).

55 'Biodegradable In-situ Forming Implants and Methods of Producing the Same.' R.L.Dunn, J.P.English, D.R.Cowsar and D.P.Vanderbilt, U.S.Patent 9219226, (1990).

56 'Biodegradable Implant Composites for Local Therapy.' I.Kaetsu, M.Yoshida, M.Asano, H.Yamanaka, K.Imai, H.Yuasa, T.Mashimo, K.Suzuki, R.Katakai and M.Oya, J.Controlled Release 6, 249 - 263, (1987).

57 'Bone-derived Growth Factor Release from Poly(α-hydroxy acid) Implants *in vitro*.' M.C.Meikle, W.Y.Mak, S.Papaioannou, E.H.Davies, N.Mordan and J.J.Reynolds, Biomaterials, 14(3), 177 - 183, (1993).

58 'Towards the Bionic Man: Current Trends in Development of Biomaterials.' B.J.Tighe, Int.Ind.Biotech. 78(7), 204 - 210, (1987).

59 'Biodegradable Polymers for Use in Surgery - Poly(glycolic)/poly(lactic acid) Homo and Copolymers: 2. *in vitro* degradation.' A.M.Reed and D.K.Gilding, Polymer 22, 494 - 498, (1981).

60 'Synthesis of Biodegradable Copoly(L-lactic acid/aromatic hydroxy acids) with Relatively Low Molecular Weight.' H.Fukuzaki, M.Yoshida, M.Asano, M.Kumakura, K.Imasaka, T.Nagai, T.Mashimo, H.Yuasa, K.Imai and H.Yamanaka, Eur.Polym.J., 26(12), 1273 - 1277, (1990).

61 'Synthesis and In-vitro Degradations of Low-molecular-weight Copolyesters Composed of L-Lactic Acid and Aromatic Hydroxy Acids.' K.Imasaka, T.Nagai, M.Yoshida, H.Fukuzaki, M.Asano and M.Kumakura, Makrom.Chem. 191(9), 2077 - 2082, (1990).

62 'Synthesis of Biodegradable Poly(L-lactic Acid-co-D,L-Mandelic Acid) with Relatively Low Molecular Weight.' H.Fukuzaki, Y.Aiba, M.Yoshida, M.Asano and M.Kumakura, Makrom.Chem. 190(10), 2407 - 2415, (1989).

63 'Biodegradable Polymer Blends for Drug Delivery.' A.J.Domb, M.Maniar and A.T.S.Haffer (Nova Pharmaceutical Corp., USA), P.C.T.Int.Appl. 9213567, (1992).

64 'Biodegradable Polymer Compositions.' O.Tawara, Jpn.Kokai Tokkyo Koho, Japan Pat. 04168149, (1990).

65 'Polyester Readily Hydrolyzable by Chymotrypsin.' I.Tabushi, H.Yamada, H.Masuzaki and J.Fusakawa, J.Polym.Sci. Polym.Lett.Edn. 13(8), 447 - 450, (1975).

66 'Radiation Effects on Poly(lactic acid).' M.C.Gupta and V.G.Deshmukh, Polymer 24, 827 - 830, (1983).

67 'Vogel's Textbook of practical Organic Chemistry.' 4th Edition, B.S.Furniss, A.J.Hannaford, V.Rogers, P.W.G.Smith and A.R.Tatchell, Longman, London and New York, (1978).

68 'The Manipulation of Air-sensitive Compounds.' D.F.Shriver, McGraw-Hill, USA, (1969).

69 'Spinning-band Fractionating Column.' R.G.Nester, U.S.Patent 2,712,520, (1955).

70 'Polymerization VII. The Polymerization of N-Carboxy-α-amino Acid Anhydrides.' Ballard and Bamford, Proc.Roy.Soc.(A) 223, 495 - 520, (1954).

71 'Some Aspects of the Synthesis and Polymerisation of 1,3,2-dioxathiolan-4-one-2-oxides.' G.P.Blackbourn, PhD thesis, University of Aston in Birmingham, Birmingham, (1970).

72 'Chemical Principles.', S.S.Zumdahl, 671 - 673, D.C.Heath and Co., Lexington, (1992).

73 'Metal Carbonyl Spectra.' P.S.Braterman, Academic Press, London, New York and San Francisco, (1975).

74 'The Ring-opening Polymerization of Ring Strained Cyclic Ethers.' D.P.S.Riat, PhD thesis, University of Aston in Birmingham, Birmingham, (1992).

75 'A New Versatile Apparatus for Measuring the Rates of Fast Liquid-Phase Reactions.' R.H.Biddulph and P.H.Plesch, Chem.Ind., 1482-1486, (1959).

76 'The Rapid Combustion Procedure.' G.Ingram, Mikrochimica Acta 1, 877 - 898, (1956).

77 'Studies of the Reactions of the Anhydrosulphites of α-Hydroxy Carboxylic Acids. part II: Polymerisation of Glycolic and Lactic Acid Anhydrosulphites.' D.G.H.Ballard and B.J.Tighe, J.Chem.Soc. (B), 976 - 980, (1967).

78 'Polylactide. II. Viscosity-Molecular Weight Relationships and Unperturbed Chain Dimensions.' A.Schindler and D.Harper, j.Biomater.Sci.Polymer Edn., 3, 6, 443 - 450, (1992).

79 'The Aldrich Library of FT-IR Spectra.' C.J.Pouchert, Aldrich Chemical Co. Inc., (1993).

80 'Polymerisation of Cyclic Derivatives of α-Hydroxy acids.' H.A.Al-Mesfer, PhD thesis, Aston University, 1981.

81 'The Infra-Red Spectra of Complex Molecules (2nd edn.)' L.J.Bellamy, Methuen and Co.Ltd., London, (1962).

82 'The Synthesis and Polymerisation of Glycollic Acid Anhydrosulphite.' M.D.Thomas, MSc. thesis, University of Aston in Birmingham, Birmingham, (1969)

83 'Experimental Organic Chemistry - Principles and Practice' L.M.Harwood and C.J.Moody, Blackwell Scientific publications, Oxford, (1990).

84 'The Design of Polymers for Contact Lens Applications' B.J.Tighe, Br.Polym.J. Sept. 71 - 76, (1976).

85 'Ring-opening Reactions of Some Di-alkyl Substituted 1,3,2-dioxathiolan-4-one-2-oxides.' A.J.Crowe, PhD thesis, University of Aston in Birmingham, Birmingham, (1975).

86 'Metal Alkoxides' D.C.Bradley, R.C.Mehrota and D.P.Gaur, Academic Press, London, (1978).,

87 'Macrocyclic Polyethers for Complexing Metals.' C.J.Pedersen, Aldrichchimica Acta 4, 1, 1 - 6, (1971).

88 'Crown Ether Chemistry: Principles and Applications' G.W.Gokel and H.Dupont Durst Aldrichchimica Acta, 9(1), 3, 3 - 12 (1976).

89 'Some Aspects of the Synthesis and Polymerisation of 1,3,2-dioxathiolan-4-one-2-oxides.' G.P.Blackbourn, PhD thesis, University of Aston in Birmingham, Birmingham, (1970).

90 'Qualitative Organic Analysis - Spectrochemical Techniques (2nd edn.)' W.Kemp, McGraw-Hill Book Co. (UK) Ltd., London, England, (1986).

91 'Chemistry of the Elements' N.N.Greenwood and A.Earnshaw, Pergamon Press, Oxford, (1984).

92 'Living Ring-opening Polymerization of L,L-lactide Initiated with Potassium *t*-butoxide and its 18-crown-6 complex' L.Sipos, M.Zsuga and T.Kelen, Polym.Bull. 27, 495 - 502, (1992).

93 Private Communication, N.Shepherd, DRA, Fort Halstead, Sevenoaks, Kent. (1993).